Published by
Nikolai Schubert

13th International Colloquium Fuels

Conventional and Future Energy for Automobiles

Narr Francke Attempto Verlag GmbH + Co. KG

13th International Colloquium FUELS
Conventional and Future Energy
for Automobiles
15th and 16th September 2021
Technische Akademie Esslingen

Narr Francke Attempto Verlag GmbH + Co. KG

Published by
Nikolai Schubert

13th International Colloquium Fuels – Conventional and Future Energy for Automobiles

Conference proceedings 2021

expert›

TAE Technische Akademie Esslingen
Ihr Partner für Weiterbildung

Narr Francke Attempto Verlag GmbH + Co. KG

Bibliografische Information der Deutschen Nationalbibliothek

Die Deutsche Nationalbibliothek verzeichnet diese Publikation in der Deutschen Nationalbibliografie; detaillierte bibliografische Daten sind im Internet über http://dnb.dnb.de abrufbar.

expert verlag GmbH

Dischingerweg 5 · D-72070 Tübingen
E-Mail: info@verlag.expert
Internet: www.expertverlag.de

Technische Akademie Esslingen e. V.
An der Akademie 5 · D-73760 Ostfildern
E-Mail: maschinenbau@tae.de
Internet: www.tae.de

Printed in Germany

ISBN 978-3-8169-3539-1 (Print)
ISBN 978-3-8169-8539-6 (ePDF)

Preface

With the signing of the Paris Agreement in December 2015 the United Nations explained their willingness to limit the GHG Emissions and contribute with measures against the global warming effect. In 2019 the European Commission proposed the Green Deal and thereof the target to be climate neutral in 2050.

On July 14, 2021, the President of the European Commission, Ursula von der Leyen, and Vice President Frans Timmermans, together with their fellow Commissioners Simson, Gentiloni, Vălean, Sinkevičius and Wojciechowski presented the so called “Fit-for-55” package, laying out the most ambitious draft of climate legislation ever launched globally. The impact of this draft EU legislation on the Transport Sector and Fuel Industry will be impressive.

With revised ETS regulation the EC is proposing that emissions from the current EU ETS sectors be reduced by 61% by 2030, compared to 2005 levels (= increase of 18% compared to the current -43%) and to increase the annual rate of reduction to 4,2% vs 2,2% so far. A separate new emissions trading system is set up for fuel distribution for road transport and buildings which will put a GHG cap on Fuel suppliers.

Renewable Energy Directive (RED III) will set an increased EU target to produce 40% of our energy from renewable sources by 2030, including specific targets for renewable energy use in transport (shift to GHG intensity reduction target of 13%),

Stronger CO2 emissions standards for cars and vans will accelerate the transition to zero-emission mobility by requiring average emissions of new cars to come down by 55% from 2030 and 100% from 2035 compared to 2021 levels. As a result, all new cars registered as of 2035 will be zero-emission and the combustion engine will probably not be any longer present in new cars.

Revised Alternative Fuels Infrastructure Regulation will require Member States to expand charging capacity in line with zero-emission car sales, and to install charging and fuelling points at regular intervals on major highways: every 60 kilometres for electric charging and every 150 kilometres for hydrogen refuelling.

ReFuelEU Aviation Initiative will oblige fuel suppliers to blend increasing levels of sustainable aviation fuels in jet fuel taken on-board at EU airports, including synthetic low carbon fuels, known as e-fuels.

FuelEU Maritime Initiative will stimulate the uptake of sustainable maritime fuels and zero-emission technologies by setting a maximum limit on the greenhouse gas content of energy used by ships calling at European ports.

Revision of the Energy Taxation Directive (ETD) proposes to align the taxation of energy products with EU energy and climate policies, promoting clean technologies and removing outdated exemptions (e.g. in aviation) and reduced rates that currently encourage the use of fossil fuels

In consequence the fossil-based energy system must transform into a climate neutral energy system with renewable and sustainable energy carriers. Research and development on alternative fuels and the realization of new production processes are ongoing to provide the technical solution. Energy and CO2 Taxation will provide the economic frame conditions for the introduction of such alternative fuel solutions. The alternative fuel solutions need to be backwards compatible for existing vehicle fleet and the new production technologies needs to be flexible for the production of sustainable Diesel and Gasoline Fuels as well as Jet (SAF) to justify the huge investment in those technologies.

The agenda of the 13th International Colloquium Fuels has been clearly focused on the latest developments with sustainable fuels research and the related production technologies in order to fully support the development into a sustainable Mobility. An impressive number of high-quality presentations were submitted and

Narr Francke Attempto Verlag GmbH + Co. KG

presented to the visitors of the colloquium. At this point I would like to express my special thanks to the authors and co-authors of this presentations. In this conference proceedings you will find all presentations of the 13th Colloquium.

We thank all visitors of the 13th International Colloquium Fuels for their participation and look forward to our next International Colloquium Fuels in Esslingen.

Best regards

Nikolai Schubert

Narr Francke Attempto Verlag GmbH + Co. KG

Table of contents

Narr Francke Attempto Verlag GmbH + Co. KG

Narr Francke Attempto Verlag GmbH + Co. KG

Appendix

* not available at the time of publication

Narr Francke Attempto Verlag GmbH + Co. KG

TAE Technische Akademie Esslingen
Ihr Partner für Weiterbildung

TOP ANBIETER FÜR WEITERBILDUNG 2021
FOCUS WEITERBILDUNGS-ANBIETER IM VERGLEICH
FOCUS-BUSINESS 03 | 2020

MASCHINENBAU, PRODUKTION UND FAHRZEUGTECHNIK

Besuchen Sie unsere Seminare, Lehrgänge und Fachtagungen.

Bis zu 70 % Förderung möglich!

ESF Chancen fördern
EUROPÄISCHER SOZIALFONDS IN BADEN-WÜRTTEMBERG
EUROPÄISCHE UNION

Ein Großteil unserer Seminare wird unterstützt durch das Ministerium für Wirtschaft, Arbeit und Tourismus Baden-Württemberg aus Mitteln des Europäischen Sozialfonds. Profitieren Sie von der ESF-Fachkursförderung und sichern Sie sich bis zu 70 % Zuschuss auf Ihre Teilnahmegebühr. Alle Infos zur Förderfähigkeit unter **www.tae.de/foerdermoeglichkeiten**

SEMINARE, LEHRGÄNGE, FACHTAGUNGEN

- Maschinenbau und Feinwerktechnik
- Fahrzeugtechnik
- Elemente, Maschinen und Anlagen
- Entwicklung und Konstruktion
- Werkstoffe und Betriebsstoffe
- Qualität, Mess- und Prüftechnik
- Verfahrens- und Oberflächentechnik, Korrosion
- Fertigungs- und Produktionstechnik
- Instandhaltung
- Betriebliche Organisation
- Arbeitssicherheit, Umwelt- und Strahlenschutz

Infos und Anmeldung: www.tae.de/go/maschbau

Narr Francke Attempto Verlag GmbH + Co. KG

Perspective of Renewable Fuels

Narr Francke Attempto Verlag GmbH + Co. KG

Refueling the Future? Perspectives of German Stakeholder Positioning towards Renewable Fuels

Dr. Dirk Scheer
KIT/ITAS, Karlsruhe, Germany

Lisa Schmieder
KIT/ITAS, Karlsruhe, Germany

Summery

Even if there is fundamental agreement between different stakeholders on the goal of the energy transition as a whole, regarding the Verkehrswende (transition in the transport sector) and in particular regarding refuels, stakeholders set their own and sometimes opposing accents in their positioning. This refers in the storytelling for example to divergent opinions about where and from which energy the synthetic fuels are made or which political framework and policy instruments are necessary for the diffusion of refuels in the market. Against this background, the aim of this analysis is to systematically identify, systemize and analyse the diversity of stakeholder perspectives in Germany using a document-based position analysis in order to provide the broadest possible range of (controversial) positions and evaluations on the refuels' future path. Based on a document analysis of 41 sources published by 17 stakeholders from the areas of economy (8), environment (3) and civil society (6) in the last ten years, we analyse commonalities and differences in the assessments of the refuels' path as well as the reasons behind it. The analysis was complemented by a Groupdelphi-Workshop with stakeholders. We thereon derive comprehensive narratives and conclusions regarding relevant dimensions such as the overall potential of refuels in the context of the energy transition, areas of application, type of energy production, timeline, possible trade-offs regarding water and land availability, political framework and others. The results may allow policy makers to recognize impending acceptance conflicts early on and to take appropriate planning, design, participative or communicative measures. The analysis presented here is part of a research project called refuels – rethinking fuels (https://www.refuels.de) funded by the State Government of and represents the first step of a broader stakeholder analysis.

1. Introduction

The transformation of the energy and transport system towards climate protection is a task for society as a whole, in which politics, business and society have to make contributions. In this context, there are sometimes very different assessments among the stakeholders about the design of the transformation and about promising and goal-oriented transformation paths. It can be assumed that the refuels route as a promising part of a transformation will be assessed very differently by different groups. It is therefore all the more important to investigate in advance which measures in which combination meet with the approval or rejection of stakeholder groups and what the reasons behind them are. Only in this way can impending conflicts of acceptance be recognised at an early stage and appropriate planning, design, participatory or communicative measures be taken.
Even if there is fundamental agreement among the various stakeholders on the direction of the energy transition with regard to climate protection, the actors set their own (and in some cases contradictory) accents in their positioning in some areas. This applies in particular to the "transport transition", which still has to be completed in large parts, and thus also to refuels routes. Against this background, the aim of this paper is to systematically record the diversity of stakeholder perspectives on synthetic fuels by means of a document-based position analysis in order to represent the broadest possible spectrum of (controversial) positions on and assessments of fuel routes. It is related to several working papers published in the reFuels project (www.refuels.de) ([26.]; [27.]; [28.]). This paper thus ties in with the existing state of research on the potential of synthetic fuels as well as attitudes and positions of social groups (e.g. [34.]; [21.]; [25.]).
This report summarises the results of the analysis. First, chapter 2 explains the method of the document analysis in more detail. Chapter 3 presents some results of the position analysis. Finally, Chapter 4 summarises the central results from a comparative perspective and draws conclusions.

Narr Francke Attempto Verlag GmbH + Co. KG

2. Methods

The position analysis of selected stakeholder documents was carried out methodically via desk research by first identifying documents published by stakeholder groups with reference to (synthetic) fuels. In a second step, an analysis tool was developed as a template ("association position profile"). Finally, the database was evaluated from a comparative perspective using the profiles1. The three methodological steps are briefly explained below.
A list of German associations from the fields of business, environment and civil society was compiled, as associations from these three areas are of great importance for the transport transition from an overall societal perspective. As a result, 21 organisations were identified across the three areas (cf. Table 1). The search for association-related documents (e.g. position papers, statements, working reports, etc.) resulted in statements with a positioning on the fuel route for 17 organisations. The search was carried out using the search term "fuels" on the websites of the organisations. As a result, 42 documents were available for further processing. Even if the table gives the impression of a numerical underweighting of environmental organisations (3) compared to business (8) and civil society (6), this distribution is not reflected in the results. The evaluation and presentation of results aims at an additive collection of arguments by associations without reporting frequencies. Each argument was included regardless of how often it was put forward by actors.

Table 1: Compilation of the organizations considered

Economy	
• VDA: German Association of the Automotive Industry • VDB: Association of the German Biofuel Industry • BEM: Federal Association eMobility | Electromobility • VDV: Association of German Transport Companies • BDEW: German Association of Energy and Water Industries	• bft/MEW: Federal Association of Independent Petrol Stations and Independent German Mineral Oil Traders • DBV: German Farmers' Association • BDI: Federation of German Industries • **Tankstellen-Interessenverband e.V.*
Environment	
• BUND: Federation for the Environment and Nature Conservation Germany • Greenpeace	• WWF: World Wide Fund For Nature • ** *Germanwatch* • *NABU: Nature and Biodiversity Conservation Union of Germany*
Society	
• Agora: Agora Transport Transition • vzbv: Federation of German Consumer Organisations • ADAC: German Automobile Club	• VCD: German Transport Club • IG Metall: Industrial Union of Metalworkers • KDA: Church Service in the World of Work • **German Caritas Association*
Explanation: * For associations marked with (*) and *in italics*, no independent documents on synthetic fuels were identified. They were therefore not included in the evaluation. ** On the part of the environmental associations, the position paper "Climate-friendly transport in Germany - setting the course for 2050" by the associations WWF, BUND, Germanwatch, NABU and the VCD was comprehensively included, which is summarised in the following analysis under WWF et al. 2014.	

3. Results

3.1 Positioning of stakeholders in the big picture

The overall view across all associations shows that the topic of "fuels" is firmly anchored in the German stakeholder discourse. All seventeen associations analysed have expressed and positioned themselves in one way or another on refuels (cf. Table 2).

This shows that alternative fuels (biogenic or electricity-based) are perceived as a possible building block of a transport turnaround and that an intensive discussion about the pros and cons of fuels is currently taking place between stakeholders.
Looking at the individual thematic lines, the following central results can be highlighted. All of the associations studied have taken a position via documents, whereby the clear majority have explicitly expressed themselves via statements, positions or position papers. Only three associations have implicitly positioned themselves on fuels (VDV, VCD, KDA). While the VDV as an association represents in particular the rail and bus-bound local passenger transport, the VCD focuses on the singular transport mode bicycle. The KDA, on the other hand, has no direct connection to mobility or the transport system. All associations, with the exception of the DBV, have taken a position on the transformation of transport and in some cases have set their own priorities, formulated goals and prioritised measures for a future transformation of transport. This shows that the topic of transport transition is now firmly anchored in the stakeholder discourse. The relevance of fuels is now also firmly integrated in the transport discourse. The clear majority of associations have issued assessments and statements on both biogenic and electricity-based fuels. For individual aspects of electricity-based fuels, there are differences between the individual stakeholder groups. The majority of associations from the economic sector have taken a very differentiated position on electricity-based fuels.
Only the VDV and the DBV are somewhat more reserved in their assessment. The majority of environmental and civil society associations, on the other hand, have a less comprehensive assessment of refuels. Civil society actors in particular (with the exception of Agora) only commented on individual aspects of refuels.

Narr Francke Attempto Verlag GmbH + Co. KG

Table 2: Overview of all stakeholders in the association position profile

	Economy								Environment			Civil society					
	VDA	VDB	BEM	BDEW	VDV	bft / MEW	DBV	BDI	BUND	Greenpeace	WWF	Agora	vzbv	ADAC	VCD	IG Metall	KDA
Chapter 3.1 "Positioning																	
• *Positioning (e = explicit, i = implicit)*	e	e	e	i	i	e	e	e	e	e	e	e	e	e	i	e	i
Chapter 3.2 "Transport turnaround																	
• *Understanding the transport turnaround*	✓	✓	✓	✓	✓	✓		✓	✓	✓	✓	✓	✓	✓	✓	✓	✓
Chapter 3.3 "Relevance of Fuels																	
• *Biogenic fuels assessment*	✓	✓			✓		✓	✓	✓		✓	✓	✓	✓	✓		
• *Assessment of synthetic fuels*	✓	✓	✓	✓	✓	✓		✓	✓	✓	✓	✓	✓	✓		✓	✓
• *Areas of application reFuels*	✓	✓		✓	✓		✓	✓	✓	✓	✓	✓	✓	✓		✓	✓
Chapter 3.4 "Aspects of Electricity-Based Fuels																	
• *Technology openness vs. selection*	✓	✓	✓	✓	✓	✓		✓				✓				✓	✓
• *Place of energy production + Relevance of imports*	✓	✓	✓	✓		✓	✓	✓	✓			✓					
• *Assessment of economic efficiency*	✓			✓		✓		✓		✓		✓	✓	✓			
• *Value reFuels for storage + flexibility*	✓	✓		✓		✓		✓	✓	✓	✓	✓	✓			✓	
• *Acceptance assessment*	✓	✓				✓		✓	✓			✓	✓	✓			
• *Sustainability assessment*	✓	✓	✓	✓		✓	✓	✓	✓	✓	✓	✓	✓	✓			
• *Role in securing the location*	✓					✓		✓								✓	
Chapter 3.5 "Political framework conditions																	
• *Political framework*	✓	✓	✓	✓	✓	✓	✓	✓	✓		✓	✓	✓			✓	✓

3.2 Spects of electricity-based fuels

3.2.1 Location of energy production and relevance of imports

In the discussion about electricity-based fuels, the location of production facilities plays a major role. Due to (absolute) cost advantages, foreign production capacities and corresponding imports of re-fuels are being discussed.

Trade associations such as the VDA see the renewable electricity volumes to be produced in Europe as sufficient to both produce renewable fuels and cover the direct electricity demand ([29.]. In addition, the existing infrastructure consisting of more than 14,000 public filling stations and the distribution systems of fuel retailers could continue to be used ([31.]), which would represent a cost advantage. According to the VDA, the production of the fuels would be possible in the long term and test plants exist ([29.]). Furthermore, according to the BDEW, there is the possibility of counteracting possible fluctuations by coupling renewable energy use with fuel production and thus making grid use more efficient ([6.]; [7.]).

From the MEW's point of view, the energy industry should be structured in a market economy ([22.]). A critical point of view is taken by the BEM, which sees refuels as a pretext to continue selling conventional passenger cars, regardless of energy production: "with the help of the permit, it is possible for conventional car manufacturers to keep their old products on offer and sell the engines with e-fuel admixtures as environmentally friendly." ([9.]). This is because by blending with refuels, combustion engines could be sold as "environmentally friendly" even though they are less efficient than battery-powered drives and also perform poorly in the energy balance ([9.]). VDV, DBV and BDI have not yet taken a position on the type and location of energy use and the import of electricity.

On the environmental side, BUND believes that water supply in warm but water-scarce areas should be considered, especially when importing refuels or renewable energy, and social-ecological land use should be ensured ([12.]). With the exception of Agora Verkehrswende, the civil society associations (ADAC, vzbv, VCD, IG Metall, KDA) did not make any statements on the location of fuel production or the relevance of electricity imports. Agora Verkehrswende ([4.]) assumes that the electricity required for the production of refuels or the refuels themselves would have to be imported. The joint study with Agora Energiewende ([5.]) also examines various scenarios with production sites in North Africa, the Middle East, Iceland (geothermal, hydropower) and Germany (wind offshore North Sea and Baltic Sea) with a view to costs, but does not take a position with regard to an optimal location.

3.2.2 Assessment of economic efficiency

The economic viability of refuels focuses in particular on the current and future costs of producing synthetic fuels. The economic viability of refuels is considered low by most industry associations due to efficiency disadvantages. The VDA and the BDI, for example, currently see no economic viability due to the lack of a technology-open political framework that enables and promotes investment in refuels technology ([29.]; [8.]). The VDA explicitly calls for investment security ([29.]). The MEW takes a different view, describing refuels as a win-win situation from an economic perspective ([24.]). According to this, the main advantages are climate neutrality, storability and use in conventional engines. According to the BDEW, cost efficiency and market-based approaches are the decisive criteria for setting up suitable climate protection instruments ([6.]). With regard to manufacturer costs, the VDA is aiming for a target cost level of around 1 euro per litre of diesel equivalent (currently around 4.50 euros per litre) ([29.]). From the MEW's point of view, refuels can be produced between 0.70 euros and 1.30 euros per litre in 2050, depending on location conditions ([23.]). The BDI ([8.]) also sees future production costs of around 1 euro per litre of diesel equivalent. No positioning on this point was identified by the VDB, BEM, VDV and DBV associations.

Greenpeace is the only environmental organisation to comment on the economic viability of the price development of refuels: "E-Fuels will be significantly more ex-

Narr Francke Attempto Verlag GmbH + Co. KG

pensive and less efficient in the long term" ([15.]). The remaining environmental organisations, such as WWF and BUND, did not provide any information on this point. Civil society associations, such as the vzbv and the ADAC, are critical of the economic viability ([33.]; [1.]; [2.]). They emphasise above all the current state of research, in which the electric drive has a head start over synthetic fuels ([33.]). In addition, e-cars are also ahead of re-fuels in terms of efficiency advantages and cost-effectiveness ([33.]; [2.]). Furthermore, there is a five- to six-fold higher energy demand compared to battery-electric cars with direct electricity use. Considering the costs, optimistic estimates exist that consider a price of 2.29 euros including taxes as possible ([1.]). Together with Agora Energiewende ([5.]), Agora Verkehrswende also examines the potential costs of synthetic fuels in detail in a study. These vary greatly depending on the point in time considered (2020, 2030, 2050) and the location of energy or fuel production (North Africa, Middle East, Iceland (geothermal, hydropower), Germany (wind offshore North Sea and Baltic Sea)). These vary between about 10 and up to more than 25 cents/kWh for 2020, between about 10 and 20 cents/kWh for 2030 and between about 8 and 15 cents/kWh for 2050 (assumed reference prices of a conventional fuel without distribution, levies/surcharges: premium petrol, 2020: 4.66 ct/kWh, 2030: 6.19 ct/kWh, 2050: 7.63 ct/kWh). Among other things, the study states that cost advantages are possible through the import of refuels. However, these in turn depend significantly on the development of investment costs for offshore wind energy.

3.2.3 Importance of refuels with regard to storage and flexibility

The role of refuels for the entire energy system is discussed in the discourse under the aspects of system efficiency, storage and flexibility. Some trade associations (VDA and VDB) see refuels as a chemical storage option for surplus electricity ([29.]; [30.]). According to the VDB, biorefineries can be used as inexpensive "long-term batteries" that also contribute to stabilising the electricity grid. Furthermore, refuels technology is a good way to use CO_2 from the air ([30.]). The argument of possible grid stabilisation is also shared by the BDEW, as PtX can additionally contribute to flexibilisation and security of supply in the energy sector ([6.]). The MEW also sees refuels as energy storage ([22.]; [23.]; [24.]). The BDI, on the other hand, sees the potential for long-term storage of renewable energy in the natural gas grid or in liquid fuel storage facilities. The possibility for decentralised reconversion into electricity in CHP plants should be given at best ([8.]). No positioning was identified by the associations BEM, VDV and DBV.
Environmental organisations (WWF, BUND, Greenpeace) also recognise the potential of using electricity surpluses in the sense of long-term storage for the production of synthetic fuels. At the same time, however, the WWF points out that electricity surpluses occur intermittently and electrolysers may only have low full-load hours, which in turn can lead to high costs ([35.]). For the civil society associations, the vzbv refers to refuels as a "relatively new energy storage system" in its documents, as does IG Metall in general "as a storage technology, without, however, taking a concrete position on this aspect ([33.]; [19.]). Agora Verkehrswende also addresses the aspect of electricity storage using PtX technologies, although it points to lower efficiencies. Furthermore, the operation of PtL plants in Germany via surplus electricity is not economical ([4.]). The ADAC and the VCD only address the aspect of storage in the context of electric vehicles; the KDA does not comment on this in its documents.

3.2.4 Acceptance assessment

Social acceptance for technologies and ultimately the purchase of electricity-based fuels by consumers at the filling station is crucial for the future role of refuels in the transport transition. Due to the relatively small structural changes that refuels entail, refuels will meet with high acceptance among consumers, according to the MEW ([24.]). For example, the use of the existing filling station infrastructure is seen as advantageous ([29.]; [31.]). Other trade associations such as BEM, BDEW, VDV and DBV do not take a position on this aspect in their documents. The BDI also does not make any specific statements on the acceptance of refuels, although it does state that refuels contribute to "increasing flexibility in the ramp-up of electrification and possible hedging through diversification when risks arise with regard to the expansion of the electricity grid/charging infrastructure, resource availability, customer acceptance, battery price development or recycling" ([8.]).
On the part of the environmental associations, the only position on social acceptance can be found in the BUND. For BUND, PtX materials are acceptable in terms of climate policy if only renewable energy is used in their production ([10.]). Greenpeace sees at least partial acceptance among the population. Based on a representative YouGov survey conducted on behalf of the Deutsche Presse-Agentur, more than half of the respondents see refuels as an alternative to electric cars ([17.]), but the price should not be too high: "For just under half of the respondents, so-called e-fuels produced with green electricity should cost less than 1.50 euros per litre. 28 percent would find 1.5 to 2 euros okay. This means that e-fuels should generally not cost much more than a litre of premium petrol, the price of which was 1.53 euros in May according to the Mineral Oil Association" ([17.]). The WWF and NABU have not provided any information on acceptance. A similar positioning to Greenpeace can be found at the ADAC. In the association's view, most customers would accept refuels, but only if the price is

Narr Francke Attempto Verlag GmbH + Co. KG

affordable, although there is generally a high ecological awareness ([1.]). In its documents, the vzbv calls for "political and technical options to be carefully weighed up and unacceptable side-effects to be ruled out before proceeding to implementation. Otherwise, there will be no acceptance for biofuels, also for ecological reasons ([32.])". The remaining civil society associations (including VCD, IG Metall and KDA) have not taken a position on the acceptance of synthetic fuels.

3.2.5 Role of securing Germany as a location for business and investment

From the point of view of industrial and economic policy, aspects of securing the location and value creation are important factors in securing prosperity.
With regard to the role of securing the location and value creation, the MEW sees at least part of the value creation in Germany as secured by means of refuels ([22.]). The BDI emphasises that know-how as well as jobs: "[...] in core European industrial technologies such as engines and gearboxes as well as in the energy and gas industry" ([8.]) should be secured. No positioning can be found in the documents of the trade associations VDB, BEM, BDEW, VDV and DBV. IG Metall points out that Germany should continue to serve as a development and production location for synthetic fuels and battery cells in line with industrial policy ([19.]).

3.2.6 Assessment of sustainability criteria

Sustainability on the three pillars of ecology, economy and social issues forms an important orientation for refuels as an umbrella concept.
On the part of the trade associations, there is agreement that refuels can make an important contribution to reducing greenhouse gas emissions and thus to achieving the Paris climate targets ([30.]; [9.]; [8.]; [22.]). In this context, both the VDA and the DBV mention that, on the one hand, sustainability criteria must exist for biogenic fuels so that there are "[...] no undesirable environmental impacts [...]" ([13.]). Among other things, ecological impacts are to be checked at regular intervals during the production of refuels. The DBV criticises the currently applied method of greenhouse gas accounting according to the so-called source accounting, in which emissions from raw material production in agriculture are accounted for and greenhouse gas avoidance is assigned to the transport sector.
The environmental associations demand the comprehensive inclusion of sustainability criteria in the production and use of refuels. From BUND's point of view, the water supply in warm and water-scarce areas in particular should be considered and further ensured. In addition, the association calls for social-ecological land use to be taken into account in the context of fuel production and for further work on sustainability criteria for PtX in the future ([10.]; [11.]; [12.]). Greenpeace ([16.]) also emphasises from a climate protection perspective that "synthetic (liquid) fuels [have] a worse efficiency than propulsion systems with hydrogen fuel cells. In this respect, it would be very welcome from a climate protection perspective that vehicle concepts with fuel cells for large cars and trucks or long distances become marketable as soon as possible." The vzbv points out that greenhouse gas neutrality of fuels can only be assumed if only renewable electricity is used. Agora Verkehrswende also notes that it must be ensured that the renewable electricity is generated from renewable energy so that the electricity-based fuels contribute to decarbonisation. It points out that the use of plant-based raw materials releases greenhouse gases and endangers animal and plant habitats ([3.]; [4.]). The ADAC emphasises that, from a sustainability perspective, refuels should be used in the existing fleet as soon as possible, as today's vehicles remain in the fleet for more than a decade ([1.]).

4. Conclusions

The analysis of stakeholder positions on refuels has shown that the issue of electricity-based fuels has been taken up by many associations in the fields of business, the environment and civil society – with quite different emphases and positioning. Fuels from renewable resources are discussed and evaluated by the associations in different thematic contexts. These range from a fundamental classification in the self-image of a transport turnaround to the differentiation of biogenic and electricity-based fuels to individual technical, economic, social and ecological aspects of electricity-based fuels. The positioning also focuses on the political framework conditions that are conducive to this.
In the overall view of the position analysis, three cross-stakeholder narratives can be synthesised, which take up the individual aspects mentioned above and condense them in their evaluation. These narratives serve as illustrative points of positioning in the current stakeholder discourse on refuels.
Narrative 1: refuels are crucial for the success of the transport transition
In view of the urgency of climate protection and thus the upcoming defossilisation of the transport sector, refuels – especially for the existing fleet, but also beyond – represent an immediately available solution using the existing infrastructure and are thus an important building block for achieving the climate targets. By dovetailing the two sectors of energy and transport, a significant contribution is made to grid stability, flexibility and security of supply in the energy system. In the process, refuels offer the possibility of storing surplus electricity in synthetic fuels until it is used, in the sense of a grid-stabilising and fluctuation-eliminating application. Refuels also ensure that at least part of the value creation remains in Germany and thus make a significant contribution to securing the loca-

Narr Francke Attempto Verlag GmbH + Co. KG

tion within the framework of the national transformation process. This concerns local value creation, know-how and job security, purchasing power and tax revenues. Within the framework of a technology-open approach, refuels should play out their potential for the transformation of transport. The acceptance of users will be crucial for the widespread use of synthetic fuels. The possibility of using the existing infrastructure, which does not require any significant changes in behaviour, favours this. In addition to the areas of application that are difficult to electrify (ship and aircraft), refuels are also seen as relevant for private transport in rural areas and for use in the existing fleet.

Narrative 2: refuels have potential – in transport modes without alternative and in compliance with sustainability criteria

In principle, there is potential for the use of synthetic fuels. While synthetic, electricity-based fuels are considered to contribute to the reduction of greenhouse gas emissions, it is important to phase out fuels from cultivated biomass by 2030. Refuels should only be used where no (direct electric) alternative is foreseeable, e.g. for use as a basic material in the chemical industry, as storage to ensure the stability of the energy supply or as an energy source in special transport sectors such as shipping and aviation. For the production of refuels, the use of CO_2 from the air is necessary for climate policy reasons (no fossil CO_2). Moreover, refuels are only acceptable in terms of climate policy if they are produced entirely on the basis of renewable energies. From a sustainability perspective, a complete phase-out of the use of cultivated biomass for road transport is necessary in the long term. With regard to biofuels, only those (of the second generation) that have no to little ecological impact are acceptable. The use of pesticides, fertilisers and the endangering of the food industry as well as rainforest deforestation must be avoided. In addition to electricity and CO_2, the production of re-fuels requires water. It must therefore be ensured, especially when importing refuels from water-scarce regions, that water availability is not impaired. The use of land for renewable energies must also take ecological and social aspects into account. The expansion of generation capacities for refuels does not make sense at the present time, but should take place after 2030 at the earliest, as the overall balance of electricity-based fuels is worse than that of conventional fuels due to the current CO_2 intensity of the electricity mix. The next few years should be used for further research and development in the field of refuels in order to then derive an appropriate path for the development of electricity-based fuels on the basis of sound knowledge and taking into account the development in the electricity sector.

Narrative 3: Transport transition as sustainable, affordable, safe and comfortable mobility – if refuels contribute to this, then yes!

From a climate policy perspective, there is an urgent need for action to tackle the transport turnaround. Sustainable, comfortable and affordable mobility that is accessible to all is the basis for welfare, quality of life and social participation. Especially from a social perspective, positive effects are expected from the transformation process, such as better air and higher quality of life in cities, less congestion on the roads, more space for urban culture, new jobs, etc. In order to achieve these goals, energy and resource consumption as well as greenhouse gas emissions must become significantly more expensive, while at the same time ensuring a social balance. It is therefore possible that a situation may arise in which CO_2-intensive mobility becomes so expensive for part of the population that some travels can no longer be afforded. For this reason, it is important to exclude or mitigate unacceptable side effects in the sense of mobility participation of the entire society and to enable all people – whether in the city or in the countryside – to have flexible mobility on foot, by bike, bus and train or with vehicles.

The development of refuels is currently at an early stage and is far from being commercially viable. Despite the general increase in ecological awareness, most users will only accept refuels at an adequate price. A relevant question will therefore be what taxes the state will impose on these fuels and how much fuel the cars consume in everyday use. In order to ensure openness to technology, politics must participate financially and at the same time create framework conditions for investment strategies that encourage investors and companies to invest in the development and production of refuels.

References

[1] ADAC (Allgemeiner Deutscher Automobil-Club) (2019): Synthetische Kraftstoffe – Energieträger der Zukunft?, o.O.

[2] ADAC (Allgemeiner Deutscher Automobil-Club) (o.J.): Elektromobilität voranbringen – Antriebsalternativen technologieneutral unterstützen, o.O.

[3] Agora Energiewende (2019): EU-wide innovation support is key to the success of electrolysis manufacturing in Europe, Berlin.

[4] Agora Verkehrswende (2017): Mit der Verkehrswende die Mobilität von morgen sichern: 12 Thesen zur Verkehrswende, Berlin.

[5] Agora Verkehrswende (2018): Klimaschutz im Verkehr: Maßnahmen zur Erreichung des Sektorziels 2030, Berlin.

[6] BDEW (Bundesverband der Energie- und Wasserwirtschaft) (2018a): Klimaschutz im Verkehrssektor – Bei-trag der Energiewirtschaft, Berlin.

[7] BDEW (Bundesverband der Energie- und Wasserwirtschaft) (2018b): EU-Paket für saubere Mobilität – „Clean Mobility Package III“, Berlin.

[8] BDI (Bundesverband der Deutschen Industrie) (2018): Positionspapier der deutschen Industrie zum Aufbau von Rahmenbedingungen für die e-

Narr Francke Attempto Verlag GmbH + Co. KG

fuels-Technologien. „e-fuels – jetzt handeln und Chancen nutzen“.
[9] BEM (Bundesverband eMobilität | Elektromobilität) (2019): Wahnsinn des Klimakabinetts: Verbrennungs-motoren sollen im Einsatz bleiben – CO²-Reduktion durch mehr Wasser- und Flächenverbrauch an-gestrebt, Berlin.
[10] BUND (Bund für Umwelt und Naturschutz Deutschland e.V.) (2019a): Schlussfolgerungen des BUND zum Impulspapier des Öko-Instituts „Kein Selbstläufer: Klimaschutz und Nachhaltigkeit durch PtX“, o.O.
[11] BUND (Bund für Umwelt und Naturschutz Deutschland e.V.) (2019b): Kein Selbstläufer: Klimaschutz und Nachhaltigkeit durch PtX: Diskussion der Anforderungen und erste Ansätze für Nachweiskriterien für eine klimafreundliche und nachhaltige Produktion von PtX-Stoffen (Impulspapier im Auftrag des BUND im Rahmen des Kopernikus-Vorhabens „P2X“), Berlin.
[12] BUND (Bund für Umwelt und Naturschutz Deutschland e.V.) (2019d): Power-to-X ist nicht per se klima-freundlich und ohne Nachhaltigkeitsregeln potentiell schädlich (Gemeinsame Pressemitteilung von BUND und WWF), o.O.
[13] DBV (Deutscher Bauernverband) (2019b): KLIMASTRATEGIE 2.0 des Deutschen Bauernverbandes, Berlin.
[14] Deutsche Energie-Agentur (dena) & Ludwig Bölkow Systemtechnik (LBST) (2017): E-Fuels Studie - Das Potenzial strombasierter Kraftstoffe für einen klimaneutralen Verkehr in der EU: Zusammenfassung (Ein Gutachten von LBST und dena im Auftrag von VDA), o. O.
[15] Greenpeace (2019a): Der Beitrag von synthetischen Kraftstoffen zur Verkehrswende: Optionen und Priori-täten (Kurzstudie im Auftrag von Greenpeace Deutschland), o.O.
[16] Greenpeace (2019b): Greenpeace-Studie: Synthetische Kraftstoffe für Pkw zu teuer und ineffizient, o.O.
[17] Greenpeace (2019c): Grüner Treibstoff ja, aber bitte ohne viel Extrakosten, Berlin.
[18] Greenpeace (2019d): Greenpeace- Studie: Strombasierte Kraftstoffe können Klimalücke im Verkehr nicht schließen: Verkehrsministerium überschätzt CO_2-Einsparpotenzial von E-Fuels deutlich, Berlin.
[19] IG Metall (Industriegewerkschaft Metall) (2019b): Antrag L1.001: Leitantrag 1 Aktionsprogramm zur Mobilitäts- und Energiewende, o.O.
[20] IG Metall (Industriegewerkschaft Metall) (2019c): Neue Autos braucht das Land, o.O.
[21] Kasten, Peter; Kühnel, Sven (2019): Positionen zur Nutzung strombasierter Flüssigkraftstoffe (efuels) im Verkehr, Berlin.
[22] MEW (Mittelständische Energiewirtschaft Deutschland)/ bft (Bundesverband Freier Tankstellen) (2017): Kein AUS für den Verbrennungsmotor – Mit E-Fuels alle Vorteile für die Klimawende nutzen, Bonn.
[23] MEW (Mittelständische Energiewirtschaft Deutschland)/ bft (Bundesverband Freier Tankstellen) (2018): Prognos-Studie zu neuen flüssigen Energieträgern: E-Fuels sichern das Erreichen der Klimaziele, Bonn.
[24] MEW (Mittelständische Energiewirtschaft Deutschland)/ bft (Bundesverband Freier Tankstellen) (2019): Überzeugungsarbeit für die Zukunft flüssiger Kraftstoffe, Bonn.
[25] NPM-AG2 (Nationale Plattform Zukunft der Mobilität, Arbeitsgruppe 2 „Alternative Antriebe und Kraftstoffe für nachhaltige Mobilität“) (2019): Elektromobilität, Brennstoffzelle, alternative Kraftstoffe: Einsatzmöglichkeiten aus technologischer Sicht, herausgegeben vom Bundesministerium für Verkehr und digitale Infrastruktur, Berlin.
[26] Scheer, D.; Nabitz, L.; Narasinghe, N. (2021): refuels im Stakeholder-Diskurs: Eine Positionsanalyse von Verbänden aus Wirtschaft, Umwelt und Zivilgesellschaft, Working Paper refuels 01 (KIT-ITAS), Karlsruhe
[27] Scheer, D.; Schmieder, L.; Pfeiffer, J. (2021): Gesellschaftliche Implikationen von rege-nerativen Kraftstoffen im Expertendiskurs, Working Paper refuels 03 (KIT-ITAS), Karls-ruhe
[28] Schmieder, L.; Scheer, D. (2021): Regenerative Kraftstoffe im System betrachtet: Zur Rolle von refuels in Energiesystemanalysen, Working Paper refuels 02 (KIT-ITAS), Karlsruhe
[29] VDA (Verband der Automobilindustrie) (2017): Mehr Klimaschutz durch eine bessere und umfassendere CO_2-Regulierung: Position zur CO_2-Regulierung Pkw post 2020, Berlin.
[30] VDB (Verband der Deutschen Biokraftstoffindustrie) (2019): Allianz für grüne Kraftstoffe: Klimaziele im Verkehr sind nur mit CO_2-armen Kraftstoffen zu erreichen (Gemeinsame Erklärung der Verbände BDBe, DVFG, MEW, MVaK, MWV, UFOP, UNITI und VDB), Berlin.
[31] VDB (Verband der Deutschen Biokraftstoffindustrie) (o.J.): Klimaschutz mit nachhaltigen regenerativen Kraftstoffen: Bestehende nachhaltige Optionen zur Treibhausgasminderung im Verkehr nutzen, neue Technologien gezielt fördern (Ein Positionspapier vom Bundesverband der Deutschen Bioethanolwirtschaft e.V. (BDBe), Biotechnologie-Industrie-Organisation Deutschland e.V. (Bio-Deutschland) Clariant, Deutscher Bauernverband e.V. (DBV), Mittelstandsverband abfallbasierter Kraftstoffe e.V. (MVaK), Novozymes, Scania Union zur Förderung von Öl- und Proteinpflanzen e.V. (UFOP), UNITI Bundesverband mittelständischer Mineralölunternehmen e.V., UPM, Verband

Narr Francke Attempto Verlag GmbH + Co. KG

der Automobilindustrie e.V. (VDA), Verband der Deutschen Biokraftstoffindustrie e.V. (VDB)), o.O.

[32] vzbv (Verbraucherzentrale Bundesverband) (2011): E 10-Debakel: Ursachen und Auswege (Hintergrundpapier zu „Benzingipfel“ am 8. März 2011 im Bundeswirtschaftsministerium), Berlin.

[33] vzbv (Verbraucherzentrale Bundesverband) (2018): Kraftstoffverbrauch von Autos senken: Klima schützen, Verbraucher entlasten (Stellungnahme des Verbraucherzentrale Bundesverbands zum Vorschlag der Europäischen Kommission für eine Verordnung zu den CO_2-Flottengrenzwerten von Personenkraftwagen), Berlin.

[34] WD (Wissenschaftliche Dienste des Deutschen Bundestages) (2018): E-Fuels, WD 5 - 3000 - 008/18, Berlin.

[35] WWF (World Wide Fund For Nature), BUND (Deutschland Bund für Umwelt und Naturschutz Deutschland), Germanwatch, NABU (Naturschutzbund Deutschland), VCD (Verkehrsclub Deutschland (2014): Klimafreundlicher Verkehr in Deutschland: Weichenstellung bis 2050, o.O.

Narr Francke Attempto Verlag GmbH + Co. KG

GHG Emissions and Primary Energy Demand of Vehicle Fleets Based on Dynamic LCA Methodology – Introduction of Electric Vehicles in Austria 2010 – 2050

Gerfried Jungmeier
JOANNEUM RESEARCH – Institute for Climate, Energy and Society (LIFE), Graz, Austria

Summary

The environmental effect of electric vehicles can only be assessed based on life cycle assessment (LCA) covering production, operation and end of life treatment. Since 2011 in the Technical Collaboration Program (TCP) on "Hybrid & Electric Vehicles" (HEV) of the International Energy Agency (IEA) with 20 participating countries an expert group develops and applies LCA methodology to estimate the environmental effects of the increasing electric vehicle (EV) fleet globally.
Since 2014, IEA HEV Task 30 estimates the LCA based environmental effects of the worldwide EV fleet in 40 countries. In the LCA of these vehicles using the different national framework conditions, the environmental effects are estimated by assessing the possible ranges of GHG emissions, acidification, ozone formation, PM emissions and primary energy consumption in comparison to conventional ICE vehicles. Now this approach was further developed to a dynamic LCA by taking the time depending effects of the BEV fleet introduction and the parallel increasing supply of renewable electricity into consideration.
To illustrate the timing of the environmental effects in a dynamic LCA perspective the case of Austria shows that the additional renewable electricity generation increased between 0.2 up to 2.2 TWh per year up to 2020. The annual GHG emissions due to the installation of new renewable electricity generation plants in Austria were between 100,000 up to 800,000 t CO_2-eq per from 2005 to 2020. Due to the dynamic LCA approach, the GHG emissions of the construction of renewable electricity generation plants before 2005 are not considered in the years from 2005 onwards, only the GHG emissions of operating the plants for maintenance and the fuel supply for bioenergy are included. The GHG emissions of renewable electricity generation in Austria in existing and newly installed power plants are in the range between 8 to 33 g CO_2-eq/kWh, whereas the GHG emissions of the additionally installed renewable electricity generation is between 31 and 250 CO_2-eq/kWh.
The BEV introduction in Austria started in 2010 and the annually registered BEV increased significantly to 16,000 new BEVs in 2020. The BEV fleet increased up to 46,000 BEVs in 2020, and consumes 142 GWh electricity, which is 1.1% of the additional renewable electricity generated since 2010. The GHG emissions of the BEV introduction since 2010 in Austria are calculated by considering the GHG emissions of the production from the annually new registered BEV and the operation of the BEV fleet by taking the substituted conventional ICE vehicles into account. In 2020, the GHG emissions of producing the newly registered 16,000 BEV are 167,000 t CO_2-eq and the GHG emissions of the BEV fleet operation of 45,000 vehicles with renewable electricity are 3,000 t CO_2-eq. Assuming each BEV substitutes for an ICE, 16,000 newly registered conventional ICE vehicle were substituted in 2020 avoiding GHG emissions from their production of 96,000 t CO_2-eq and avoiding GHG emissions of 94,000 t CO_2-eq in the ICE fleet operation of 45,000 conventional ICE vehicles. Therefore, in 2020 the BEV fleet in Austria emitted 170,000 t CO_2-eq and avoided 190,000 t CO_2-eq from substituting conventional ICE vehicles, which results in an overall GHG reduction of 20,000 t CO_2-eq in 2020.
In a next step this methodology is applied in scenarios up to 2050 to reach a climate neutral Austrian transport sector and to identify its necessary framework conditions.

1. Introduction

The environmental effect of electric vehicles can only be assessed based on life cycle assessment (LCA) covering production, operation and end of life treatment. Since 2011 in the Technical Collaboration Program (TCP) on "Hybrid & Electric Vehicles" (HEV) of the International Energy Agency (IEA) with 20 participating countries an expert group develops and applies LCA methodology to estimate the environmental effects of the increasing electric vehicle (EV) fleet globally [1, 2, 5].

Narr Francke Attempto Verlag GmbH + Co. KG

Since 2014, IEA HEV Task 30 estimates the LCA based environmental effects of the worldwide EV fleet in 40 countries. In the LCA of these vehicles using the different national framework conditions, the environmental effects are estimated by assessing the possible ranges of GHG emissions, acidification, ozone formation, PM emissions and primary energy consumption in comparison to conventional ICE vehicles [3, 4, 6, 7].
The environmental assessment of the global EV fleet based on LCA compared to the substituted conventional ICE vehicles leads to the following key issues:

- The environmental effects depend on the national framework condition, e.g., national grid electricity generation mix.
- The broad range of possible environ]mental effects is caused by the:
  - emissions of the national electricity production and distribution,
  - electricity consumption of EVs at charging point, and
  - fuel consumption of substituted conventional ICE vehicles.
- The highest environmental benefits can be reached by using additional installed renewable electricity, which is synchronized with the charging of the EVs.
- The adequate loading strategies for EVs to integrate additional renewable electricity effectively will create further significant environmental benefits.

Now this approach was further developed to a dynamic LCA by taking the time depending effects of the BEV fleet introduction and the parallel increasing supply of renewable electricity into consideration.

2. Issues on dynamic LCA of vehicle fleet

Issues on dynamic LCA, e.g. annual environmental effects, become relevant for the rapidly increasing of EV-fleets combined with an additional generation of renewable electricity. For this, the Task identified the following relevant methodological aspects:

1. timing of environmental effects in the three lifecycle phases,
2. timing of environmental effects of increasing supply of renewable electricity,
3. timing of environmental effects of EVs using increasing supply of renewable electricity, and
4. substitution effects and timing of environmental effects of EVs substituting for ICE vehicles.

The possible environmental effects of a system occur at different times during their lifetime. In LCA, the environmental effects are analysed for the three phases separately – production (for vehicles) or construction (for power plants), operation and end of life – over the whole lifetime of a system. Then the cumulated environmental effects over the lifetime are allocated to the service provided by the system during the operation phase, which is the functional unit in LCA, e.g. per kilometre driven for vehicles and kWh generated for power plants. Therefore, the functional unit gives the average environmental effects over lifetime by allocating the environmental effects for production and end of life over the lifetime to the service provided independent of the time when they occur.
Another approach considered in the Task is to reflect and keep the time depending course of the environmental effects in the life cycle and compare the absolute cumulated environmental effects in a dynamic LCA.
In Figure 1, the possible courses of the cumulated environmental effects of three systems in their lifetime are shown for the three phases – production, operation and end of life. All the three systems – A, B and C - have the same lifetime and provide the same service but the courses of the environmental effects are quite different. The system A has low environmental effects in the production/construction phase but high effects during the operation/use phase and again low effects in the end of life phase. While system B has very high effects in the production phase, very low further effects in the operation phase and declining environmental effects in the end of life phase due to the recycling of materials and a credit given for the supply of secondary materials for substituting primary material. The system C has lower effects in production/construction phase than system B and no further effects during the operation phase, but significantly declining environmental effects in the end of life phase, which is due to the reuse of certain parts, facilities or materials for other further purposes.
Considering the total cumulated environmental effects system C has the lowest and system A the highest effects in their lifetime. However, additionally it can be analysed at which time in the lifecycle the system C has lower cumulated environmental effects compared to the other systems. At t_1 system C has lower cumulated environmental effects than system A; at the time t_2 system B has lower cumulated effects than system A.
This timing of the environmental effects becomes more relevant in future, when new innovative systems substitute for conventional systems to reduce the overall environmental effects. However, it might take some time until the real reduction of environmental effects takes place by the new innovative system. This aspect becomes more and more relevant in the context e.g. of the global necessary reduction of GHG emissions with increasing energy efficiency and renewable energy. Therefore, in dynamic LCA the course of the cumulated environmental effects have to be considered and addressed more adequately.

Narr Francke Attempto Verlag GmbH + Co. KG

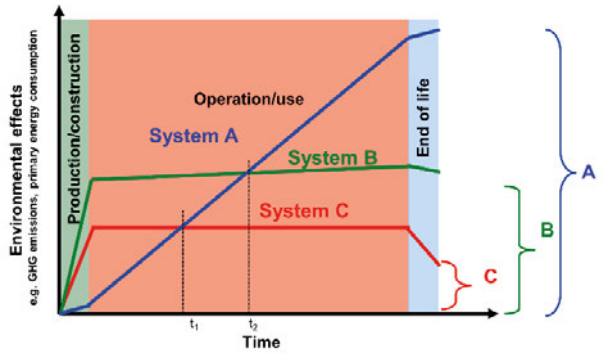

Figure 1: Timing of cumulated environmental effects of three systems with the same lifetime

In Figure 2, the timing of environmental effects of a BEV using renewable electricity substituting an ICE vehicle is shown. In total over the lifetime the BEV has lower environmental effects e.g. GHG emissions than the ICE. Due to the higher environmental effects from production of the BEV the environmental effects are higher in the beginning, but after about 3 years the environmental benefits of substituting ICE vehicles starts. An additional effect is that due to the rebound effect not each electric driven kilometre might substitute a fossil fuel driven kilometre. Therefore, the substitution rate might be lower than 100%. In the example below, the timing of environmental effects is shown for a substitution rate of 80% and 100%. Additionally, if the timing effects are analysed for a rapid annual increase of BEV the annual environmental effect might still be higher than the substituted ICE vehicles. So depending on the annual growing size of the BEV fleet it might take some time until the overall annual environmental effects decline by substitution of ICE vehicles.

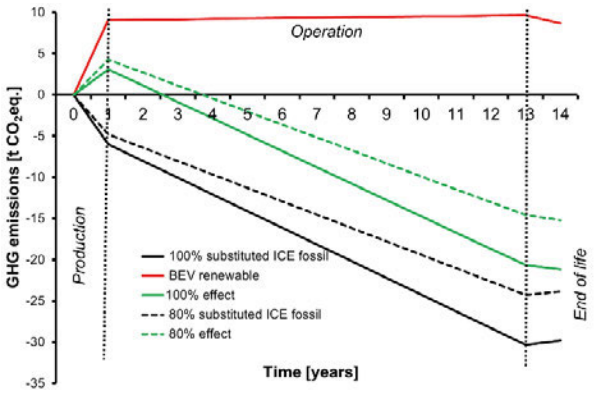

Figure 2: Timing of environmental effects of a BEV using renewable electricity substituting an ICE vehicle

3. LCA of supplying additional renewable electricity – Example Austria

It is relevant to analyse and assess the environmental effect of the increasing production of renewable electricity generation and its use, e.g. in BEV. The environmental effects, e.g., GHG emissions, of electricity from hydro, wind and solar power plants mainly occur in the construction and the end of life phases. In most countries, there are huge investments in new facilities to generate additional renewable electricity. Related to these investments significant environmental effects are taking place with these investments, but the substitution of conventional electricity generation will lead to a reduction of environmental effects in the coming years.
To illustrate the timing of the environmental effects in a dynamic LCA perspective the following example of Austria of increasing the renewable electricity generation is described. The additional renewable electricity generation in Austria increased between 0.2 up to 2.2 TWh per year from 2005 up to 2020. In Figure 3, the total renewable electricity generation in Austria is shown from 2005 to 2020. Already in 2004 about 40 TWh renewable electricity was generated mainly in hydro power plants. Over the years, the generation from renewable electricity increased from 41 TWh in 2005 up to 57 TWh in 2020 significantly. The share of renewable electricity in the Austrian grid mix (incl. imports) increased from about 60% in 2005 up to 75% in 2020.

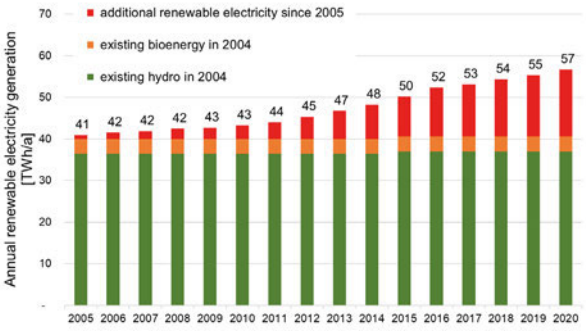

Figure 3: Renewable electricity generation in Austria (references are given in working document)

The annual GHG emissions due to the installation of new renewable electricity generation plants in Austria were between 100,000 up to 800,000 t CO_2-eq per from 2005 to 2020, depending on the annual installed generation capacity and the type of renewable energy. E.g. the installation of a power plant to generate 1 GWh annually of PV with about 1,400 to 1,600 t CO_2-eq has significantly higher GHG emissions than hydro and wind with about 250 – 600 t CO_2-eq.
The combination of the annual GHG emissions and the additional electricity generation gives the specific GHG emissions of renewable electricity generation in Austria (Figure 4), on one hand the GHG emissions of the additional installed renewable electricity generation and on the other hand of the total renewable electricity mix in Austria. Due to the chosen dynamic LCA approach here, the GHG emissions of the construction of renewable electricity generation plants before 2005 are not considered in the years from 2005 onwards, only the relatively low GHG emissions of operating the plants for maintenance and the fuel

Narr Francke Attempto Verlag GmbH + Co. KG

supply for bioenergy are included. So the GHG emissions of renewable electricity generation in Austria in existing (before 2005) and newly installed power plants (since 2005) are in the range between 8 to 33 g CO_2-eq/kWh, whereas the GHG emissions of the additionally installed renewable electricity generation is between 31 and 250 CO_2-eq/kWh between 2005 and 2020.

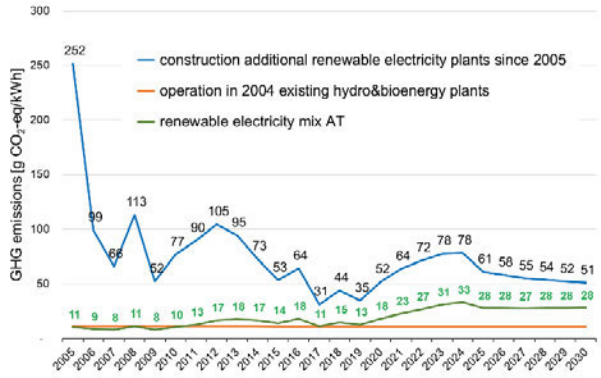

Figure 4: GHG emissions of renewable electricity generation in Austria

4. GHG emissions of BEV introduction in Austria

The introduction of BEV in Austria started in 2010. Additionally, also PHEV were introduced, which are not considered here. The annually registered BEV increased significantly and reached nearly 16,000 new BEVs in 2020. The BEV fleet increased up to about 46,000 BEVs in 2020. The rapid increase of the BEV fleet in Austria was stimulated by public funding of up to € 6,000 for the investment and the charging stations. If the supply of renewable electricity for the operation of the BEV is guaranteed by a corresponding electricity purchase contract. Assuming an electricity demand of about 0.22 kWh/km (incl. heating, cooling and auxiliaries) and 10% grid and charging losses the additional renewable electricity demand for the operation of the BEV fleet increased from 0.3 GWh in 2010 up to 142 GWh in 2020. Considering the increased renewable electricity generation since 2010 in Austria the demand to operate the BEV fleet is in a range of 0.1 to 1.1% of the additional renewable electricity generated since 2010. Concluding, also in this system perspective it is evident that the Austrian BEV fleet is operated on renewable electricity, while the increasing demand for electricity is met with increasing supply of renewable electricity.

Considering the course of the annual GHG emissions of the renewable electricity generation in Austria the GHG emissions of the operations of the BEV fleet in Austria are calculated using the GHG emission (2010 – 2020) between 10 to 18 g CO_2-eq/kWh. The GHG emissions of BEV fleet operation using the renewable electricity mix in Austria are in average between 2.5 to 4.5 g CO_2-eq/km without considering maintenance and spare parts. Therefore, in average between 2010 and 2020 the GHG emissions of a BEV operating in Austria are about 3.6 g CO_2-eq/km.

In addition, the GHG emissions from the production of the new registered BEV are calculated in an LCA perspective. The average GHG emissions of the global battery production has decreased from about 100 kg CO_2-eq per kWh battery capacity in 2010 to about 70 kg CO_2-eq/kWh. At the same time the battery capacity of a new BEV in Austria increase from about 30 kWh in 2010 to about 65 kWh in 2020 in average, due to the lower battery costs and the demand for higher driving ranges. Therefore, the production of a new BEV between 2010 and 2020 causes GHG emissions between 8.5 up to 10.5 t CO_2-eq. In comparison, the production of a conventional new ICE vehicle causes about 6 t CO_2-eq. However, the operation of a conventional substituted ICE vehicle has GHG emissions of about 145 g CO_2-eq/km with an average fuel consumption of about 0.52 kWh/km.

The GHG emissions of the BEV introduction since 2010 in Austria are calculated by considering the GHG emissions of the production from the annually new registered BEV and the operation of the BEV fleet by taking the substituted conventional ICE vehicles into account.

In Figure 5, the change of GHG emissions of the BEV fleet substituting an ICE fleet in Austria are shown. In 2020, the GHG emissions of the production of the newly registered 16,000 BEV are about 167,000 t CO_2-eq and the GHG emissions of the BEV fleet operation of about 45,000 vehicles with renewable electricity are about 3,000 t CO_2-eq.

Assuming each BEV substitutes for an ICE, about 16,000 newly registered conventional ICE vehicle were substituted in 2020 avoiding GHG emissions from their production of about 96,000 t CO_2-eq and avoiding GHG emissions of about 94,000 t CO_2-eq in the ICE fleet operation of about 45,000 conventional ICE vehicles. Therefore, in 2020 the BEV fleet in Austria emitted about 170,000 t CO_2-eq and avoided about 190,000 t CO_2-eq from substituting conventional ICE vehicles, which results in an overall GHG saving in 2020 of about 20,000 t CO_2-eq.

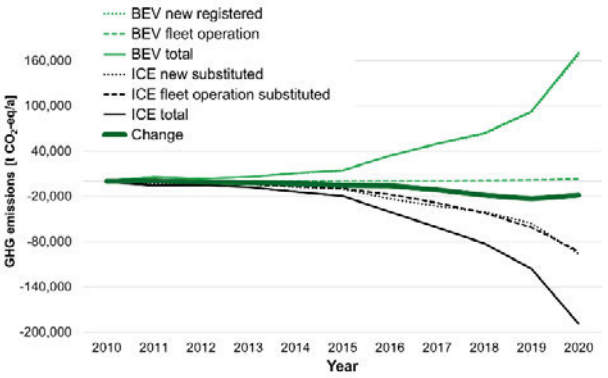

Figure 5: Change of GHG emissions of BEV fleet substituting ICE fleets in Austria

Narr Francke Attempto Verlag GmbH + Co. KG

5. Conclusions and outlook

Timing of environmental effects in LCA of EVs production-operation-end-of-life phases becomes relevant in the transition time of

- strong BEV introduction in combination with a
- strong increase of additional renewable electricity generation and
- improvement of battery production technologies.

Within the framework of LCA a methodology is developed and applied to the annual environmental effects of an increasing BEV fleet and substitution of ICE vehicles by considering the annual environmental effects of

- New vehicle production
- Supply of renewable electricity from existing and new power plant
- Substituted operation of ICE vehicles and
- End of life of old vehicles.

In a next step this methodology is applied in scenarios up to 2050 to reach a climate neutral Austrian transport sector and to identify its necessary framework conditions.

References

[1] Jungmeier Gerfried, Dunn Jennifer B, Elgowainy Amgad, Gaines Linda, Ehrenberger Simone, Doruk Enver Özdemir, Widmer Rolf: Key Issues in Life Cycle Assessment of Electric Vehicles - Findings in the International Energy Agency (IEA) on Hybrid and Electric Vehicles (HEV) (EVS27, 2013)

[2] Jungmeier Gerfried, Dunn Jennifer B, Elgowainy Amgad, Gaines Linda, Ehrenberger Simone, Doruk Enver Özdemir, Widmer Rolf: Life cycle assessment of electric vehicles – Key issues of Task 19 of the International Energy Agency (IEA) on Hybrid and Electric Vehicles (HEV), TRA 2014

[3] Gerfried Jungmeier, Jenifer Dunn, Amgad Elgowainy, Simone Ehrenberger, Rolf Widmer: Estimated Environmental Effects of the Worldwide Electric Vehicle Fleet – A Life Cycle Assessment in Task 19 of the International Energy Agency (IEA) on Hybrid and Electric Vehicles (HEV), , Conference Proceedings, EEVC 2015 - European Battery, Hybrid and Fuel Cell Electric Vehicle Congress, Brussels, Belgium, 2 – 4. December 2015

[4] Gerfried Jungmeier, Jennifer B. Dunn, Amgad Elgowainy, Linda Gaines, Martin Beermann, Simone Ehrenberger, Rolf Widmer: Life-cycle Based Environmental Effects of 1.5 Mio. Electric Vehicles on the Road in 35 Countries – Facts & Figures from the IEA Technical Cooperation Program on Hybrid & Electric Vehicles (EVS 30, 2017)

[5] Gerfried Jungmeier, Amgad A. Elgowainy, Simone Ehrenberger, Gabriela Benveniste Pérez, Pierre-Olivier Roye, Lim Ocktaeck: Water Issues and Electric Vehicles - Key Aspects and Examples in Life Cycle Assessment (EVS 31, 2018)

[6] Gerfried Jungmeier, Amgad A. Elgowainy, Simone Ehrenberger, Gabriela Benveniste Pérez, Pierre-Olivier Roye, Lim Ocktaeck: LCA Based Estimation of Environmental Effects of the Global Electric Vehicles Fleet – Facts & Figures from the IEA Technology Collaboration Program on Hybrid & Electric Vehicles, Transport Research Arena TRA 2018 in Wien, 16-19 April 2018

[7] Gerfried Jungmeier, Lorenza Canella, Jarod C. Kelly, Amgad A. Elgowainy, Simone Ehrenberger, Deidre Wolff: Evaluation of the Environmental Benefits of the Global EV-Fleet in 38 Countries – A LCA Based Estimation in IEA HEV (EVS 32, 2019)

Acknowledgement

The work of the Austrian participation in IEA HEV Task 30 (2018 – 2022) is financed by the Austrian Climate and Energy Fund and the FFG

Narr Francke Attempto Verlag GmbH + Co. KG

Renewable Fuels Production

Narr Francke Attempto Verlag GmbH + Co. KG

BMWi project ”Solare Kraftstoffe“ – Technical Fuel Assessment

Samuel Schlichting
German Aerospace Center (DLR), Institute of Combustion Technology, Stuttgart, Germany
samuel.schlichting@dlr.de

Julia Zinsmeister
German Aerospace Center (DLR), Institute of Combustion Technology, Stuttgart, Germany

Michael Storch
Robert Bosch GmbH, Powertrain Solutions, Stuttgart, Germany

Matthias Mansbart
Robert Bosch GmbH, Powertrain Solutions, Stuttgart, Germany

Uwe Bauder
German Aerospace Center (DLR), Institute of Combustion Technology, Stuttgart, Germany

Clemens Hall
German Aerospace Center (DLR), Institute of Combustion Technology, Stuttgart, Germany

Corina Janzer
German Aerospace Center (DLR), Institute of Combustion Technology, Stuttgart, Germany

Nathalie Monnerie
German Aerospace Center (DLR), Institute of Future Fuels, Koeln, Germany

Torsten Methling
German Aerospace Center (DLR), Institute of Combustion Technology, Stuttgart, Germany

Patrick Oßwald
German Aerospace Center (DLR), Institute of Combustion Technology, Stuttgart, Germany

Markus Köhler
German Aerospace Center (DLR), Institute of Combustion Technology, Stuttgart, Germany

Uwe Riedel
German Aerospace Center (DLR), Institute of Low-Carbon Industrial Processes, Cottbus, Germany

Summary

Sustainably produced drop-in fuels offer great potential for reducing greenhouse gases in the transport sector, and the possibility of using existing infrastructures facilitates a quick implementation into the transportation system. Hence, drop-in fuels are the only option that can address the existing vehicle fleet. Nevertheless, renewable fuels have to be economically competitive and comply with technical specifications.
An intriguing concept are solar-thermal produced renewable drop-in fuel components for gasoline engine with time horizon up to 2030. The techno-economic consideration and the studies of technical fuel assessment for selected solar fuels are activities embedded in the BMWi funded project “Solare Kraftstoffe”.
The goal is the identification of optimized, low-pollutant, synthetic fuel components as well as the evaluation of the engine performance including pollutant behavior. Therefore, chemical analytic experiments, engine tests and the development of a digital platform for the model-based assessment and optimization of fuels are carried out and presented here.

Narr Francke Attempto Verlag GmbH + Co. KG

1. Introduction

Since the transport sector accounts for a large proportion of the global greenhouse gas emissions, it is important to implement new technologies with the potential to reduce greenhouse gas emissions. Besides of battery electric vehicles and vehicles powered by renewable hydrogen, sustainably produced synthetic fuels offer great potential for reducing greenhouse gases in the transportation system. The introduction of renewable synthetic fuels enables a quick reduction of emissions and offers striking benefits: use of existing vehicle fleet, reduction of emissions and compatibility with existing infrastructure Other notable benefits are the high energy density as well as the fast refueling.

Synthetic fuels open up the chance to not only mimic existing fossil-based fuels, but make them even better in terms of performance The optimization of the fuel's composition via fuel design allows the enhancement of the performance and the pollutant behavior can be reduced compared to non-synthetic fuels e.g. by reduction of heavy aromatic components (Wiese et al. [1]). For a successful implementation, renewable fuels have to be economically competitive and comply with technical specifications.

Within the project "Solare Kraftstoffe" funded by the Bundesministerium für Wirtschaft und Energie (BMWi), the entire process, starting from CO_2 and H_2O as the feedstock and ending with the combustion in the engine, is investigated and schematically illustrated in Figure 1.

For the production of the synthesis gas, the use of concentrated solar power (CSP) in a two-stage thermochemical cycle is being investigated. This technology is particularly attractive for regions with high solar irradiation. Monnerie et al. [2] studies the application of the thermochemical cycle for the production of methanol as an alternative fuel, also considering techno-economic aspects. The actual principle of operation of the two-stage thermochemical cycle for splitting CO_2 and water using metal oxides to produce syngas is discussed in detail by Lu et al [3]. For improved efficiency, Rosenstiel et al [4] describes CSP power plants with the possibility of thermal energy storage (TES) in combination with photovoltaics (PV). In the following we will focus on the downstream challenge, i.e. application and optimization of a gasoline product suitable to be produced in a solar process.

For the application in gasoline engines, fuels need to fulfil the current valid fuel standard, which is EN 228 [5] for Europe. This standard restricts certain fuel properties (e.g. density, boiling behavior) and fuel components especially the maximum concentration of oxygenated components (e.g. ethanol, ethers). Within the EN 228 standard, the admixture of renewable synthetic components is possible, as long as the final blend has standard-compliant properties. These fuel mixtures can be denoted as drop-in renewable fuels.

The fuel candidates selected in this study use different renewable blending components and compositions for exploring the EN 228 limits. All selected fuels (listed in Table 1) are liquid gasolines for spark-ignition engines which comply with the standard EN 228 with the exception of E30, containing 30 vol.% of ethanol, where the volumetric ethanol content was increased above the allowed 10% according to EN 228.

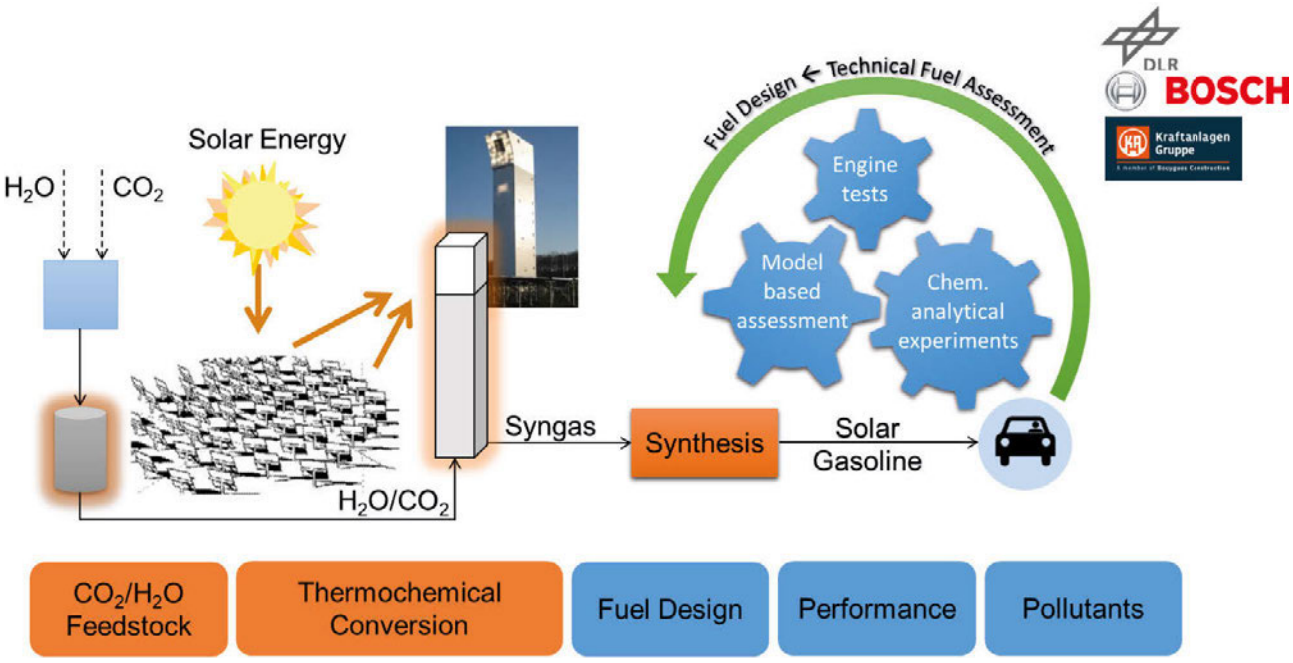

Figure 1: Illustration of the complete solar fuel process. The present work is focused on the marked downstream processes.

Narr Francke Attempto Verlag GmbH + Co. KG

Table 1

Specification (EN 228 limit)	abbrevation	EN 228
Fuel blend with max. ETBE-concentration (22%v/v)	ETBEmax	✓
Fuel blend with max MTBE-concentration (20%v/v)	MTBEmax	✓
Fuel blend with max. isobutanol-concentration (14.5%v/v)	iBuOHmax	✓
Fuel blend with max. „Renewable“-concentration: FT_Surrogat (18%v/v) and ETBE (22%v/v), enriched additionally with iso-oktane (23%v/v)	ReMax	✓
Fuel blend with ETBE (22%v/v) and FT_Surrogat (20%v/v)	FT20-ETBE	✓
Fuel blend with MTBE (20%v/v) and FT_Surrogat (18%v/v)	FT18-MTBE	✓
Fuel blend with EtOH (30%v/v), exceed the standard	E30	×

The focus of this work is the technical evaluation of the fuel list above. The work is experimental as numerical likewise. The physical-chemical properties of the liquid fuels are to be analyzed and fundamental combustion properties will be determined. Investigations of the combustion chemistry from a molecular point of view were performed in an atmospheric laminar flow reactor (ALFR) system, which allows tracing the formation and destruction of most of the important combustion intermediates in great detail. In addition, engine tests are carried out, where fuel effects were evaluated on combustion behavior, criteria pollutant emissions and calibration neutrality. In this paper an overview of the engine measurement procedure is given. Furthermore, an exemplary result of injector coking endurance run is presented and discussed. A digital platform for the model-based assessment and optimization of fuels is also to be developed as part of this work. This platform includes the training and application of machine-learning models for the prediction of certain fuel properties. An important part of this project is also to gain an understanding of the relationship between the chemical composition and the resulting ignition delay time and the octane number. Therefore, a quasi-dimensional model approach was developed to predict the octane number through the simulation of ignition delay times by using chemical kinetic mechanisms.

2. Fuels

The study focuses on liquid drop-in fuels which are compliant to the current EN 228 standard and may be produced from a solar route. This approach ensures the usage of the fuels in new and stock vehicles as well as the fuel supply infrastructure, which can lead to prompt CO_2 reduction in the current vehicle fleet. The renewable components where chosen according to potential near time availability with the target by 2030. The matrix of the chosen drop-in fuel candidates is listed in Table 1.

The fuels were designed in order to maximize the renewable content with renewable drop-in blend components. The fossil base fuel quality was adjusted for each fuel candidate in order to meet the EN 228 limits. For the gasoline blends ETBEmax and MTBEmax the maximum content of ethyl tert-butyl ether (ETBE), and methyl tert-butyl ether (MTBE), respectively, was achieved. For iBuOHmax the maximum possible Isobutanol content was chosen. FT18-MTBE and FT20-ETBE include maximum MTBE and ETBE amounts and furthermore a Fischer-Tropsch surrogate was added to maximum possible amount, which could be achieved within EN 228. ReMax contains 63% of possible renewable components which compose of isooctane, FT-surrogate and ETBE. In addition, a near drop-in fuel candidate E30 was chosen. This candidate does not meet the EN 228, but should be tested in order to see effects of a potential higher ethanol content on series calibrated engine combustion and emission behavior. The renewable test fuels were blended by the supplier Coryton and do not contain any additives. As reference fuel a EU5 certification fuel (Bosch EU5 Cert) was used. The fuel list and the blend shares can be found in Table 1and the key properties of the fuels are listed in Table 2.

3. Technical Fuel Assessment Approach

3.1 Assessment of the fuels using the SimFuel platform

The SimFuel platform connects distributed models and combines them with datasets and knowledge to gain additional insight. The two main application areas are the holistic assessment and optimization of fuels in an interdisciplinary and complex context. The platform also supports the development of models by providing massive data for the validation of models and the training of Machine Learning (ML) models [6]. .

Narr Francke Attempto Verlag GmbH + Co. KG

Table 2: Relevant key fuel properties

Fuel	Bosch EU5 Cert	ETBE max	MTBE max	iBuOH max	ReMax	FT20-ETBE	FT18-MTBE	E30
RON [-] [a]	96.8	97.4	98.3	98.8	98	97.4	97.5	103.3
MON [-] [a]	87.0	86.0	87.5	87.1	88.9	86.8	86.1	88.6
Density @15°C [kg/m³] [a]	748.2	754.9	755.8	757.1	730.7	765.2	764.7	741.5
Vol. lower heating value [MJ/l] [a]	31.43	30.97	31.1	31.01	30.62	31.37	31.27	28.41
DVPE @37.8 °C [kPa] [a]	58.8	58.8	58.5	58.1	57.6	55.3	59.0	101.9
E70 [%v/v] [a]	32.2	29.7	39.2	29.8	22.5	20.0	32.4	41.7
E150 [%v/v] [a]	82.7	79.9	82.3	78.2	88.4	81.9	82.3	92.8
FBP [°C] [a]	201.5	197.3	197.9	195.1	197.4	196.2	196.2	199.6
C9/C9+aromatic [%v/v] [a]	17.5	16.5	16.2	16.1	11.1	17.2	16.8	1.7
Ethanol [%v/v] [a]	4.8	0.4	0.1	0.1	0.3	0.4	0.1	29.2
Aromatic [%v/v] [a]	32.8	30.8	31.8	31.4	11.3	30.3	33.2	19.2
Olefins [%v/v] [a]	8.2	7.8	6.9	7.7	4.0	6.9	7.2	14.9
C [%-m/m] [a]	84.81	83.20	83.21	83.12	81.88	83.37	83.55	75.54
H [%-m/m] [a]	13.43	13.17	13.13	13.27	14.45	13.02	12.85	13.59
O [%-m/m] [a]	1.76	3.63	3.66	3.61	3.68	3.61	3.60	10.87
a Measurement resource: Coryton, England								

The platform was originally developed for aviation fuels, but is currently extended to other sectors including road transport. It consists of four main components: databases, models, a distributed model environment and the human-in-the-loop concept.

The databases consist of composition, property and performance values of conventional fuels, synthetic fuels and blends as well as of over 5300 single compounds and their properties. A visualization of the pure compounds in the database is given in Figure 2, as scatter plot of quantitative structural components of the molecules, reduced to two dimensions with a dimension reduction algorithm. The datasets are systematically used to assess new fuels as well as to create new ML models or validate physical based models.

Those models are used to predict unknown properties or performance metrics of the fuels. Model types include correlations as well as physical based and ML based property and performance models. If the models have a quantified predictive capability [7] they can play an important role for the pre-screening of fuels [8].

The distributed model environment allows the connection of distributed models from partners to perform a completely digital multidisciplinary assessment and optimization across institutions, operating system and other boundaries. The Remote Component Environment (RCE) software [9] is used, which handles the secure data transfer from and to the models including a rights management.

The human-in-the-loop concept finally captures the implicit knowledge of experts by providing interactive visualization of the relevant data and model predictions enriched with reference data as well as e.g. the appropriate specification limits. Hence, the human-in-the-loop concept integrates the platform into real world decision making.

Results

Fuels for road transport significantly differ from aviation fuels, e.g. in terms of hydrocarbon families present in the composition, where oxygen containing compounds are not allowed in aviation. Hence, the models as well as the single compound database had to be extended to include those additional families and molecules. Also, the fuel database hat to be extended to contain enough diesel and especially gasoline fuels not only for use as a reference (range of experience) when assessing new synthetic fuels, but also for training and validation of the property models.

First machine learning models for density and motor octane number (MON) were trained directly on the composition data as input and show good predictive capability with an accuracy of 0.1% for the density at 15°C and 0.5% for MON, respectively.

Narr Francke Attempto Verlag GmbH + Co. KG

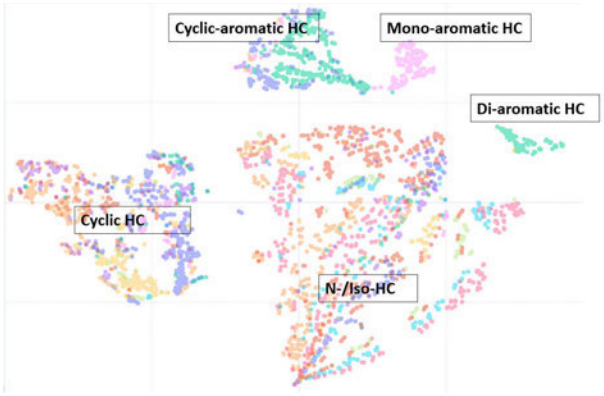

Figure 2: Visualization of single compound database (dimensionality reduction). Colors indicate the 60 different hydrocarbon families.

However, since the training data was limited to conventional crude oil based gasoline, the applicability to synthetic fuels is not directly given. Hence, new machine learning models are under development, which are not trained on the fuels composition, but on all single components from the single component database, which may sum up to a fuel.

3.2 When the composition of the synthetic fuels from Table 1 is available, the models will predict relevant properties. These properties will then be visualized together with measured data in the context of relevant specification limits and real fuel data of conventional fuels as an indicator for the range of experience to support the technical fuel assessment of the fuels.

2-Zone-Cylinder-Model

Sustainably produced synthetic fuels offer a great possibility for decarbonizing the public transport. In addition, a further option for reducing CO_2 emissions through an increase of the compression ratio, which results in a better thermodynamic efficiency. However, the limiting factor hereby is the fuel itself, which tends to uncontrolled self-ignition, also called engine knock, since increasing the compression ratio leads to higher temperatures and pressures in the cylinder.

The resistance of the fuel against uncontrolled self-ignition is given by the octane number (ON), which can be basically derived through a comparison between the knocking behavior of the fuel and the knocking behavior of a primary reference fuel (PRF). A PRF is a blend of *iso*-octane and n-heptane, where its composition, the volume fraction of *iso*-octane, respectively, determines the octane number.

Experimental measurement of the ON. The experimental determination of the octane number is carried out in a single cylinder Cooperative Fuel Research (CFR) engine. This purpose build engine features a variable compression ratio which allows to adjust the in-cylinder conditions to the point, where the fuel starts to self-ignite. If the fuel has the same knocking behavior as the PRF, the fuel's octane number corresponds to the composition of the PRF. The exact boundary conditions for the experiment are set in the ASTM D2699 [10] for the research octane number (RON) and in the ASTM D2700 [11] for the motor octane number (MON).

Motivation for modelling the ON. The fuel quantities required for the experimental tests make preliminary parameter studies very cost-intensive, which is why numerical methods are being developed. In literature there are various approaches specified. There are empirical models, like the one introduced by Morgan et al. [12], as well as machine learning models based on experimental data.

A different approach is to use chemical kinetic models to determine the octane number through the well-known correlation to ignition delay times. With this method, there are different options for the spatial resolution of the combustion chamber or the cylinder, respectively. The easiest modelling-approach is to assume the cylinder as a zero-dimensional reactor with fixed motor related boundary conditions [13]. This simple approach supports the applications of detailed chemical kinetic mechanisms and a correlation between the simulated ignition delay times and the octane number can be evolved. Studies carried out by Badra et al. [13] show promising results.

Nevertheless, the zero-dimensional approach comes with some simplifications. One quite significant drawback is the absence of the burned gas, which takes a significant role during the compression of the unburned fuel-air mixture.

Computational fluid dynamics (CFD) simulations provide a very good spatial resolutions of the cylinder and offer separate consideration of different gas states. The better physical modeling leads to higher computational costs and make the application of detailed chemical mechanisms unfeasible.

To overcome this, within the project ”Solare Kraftstoffe” a quasi-dimensional approach is chosen, in which the cylinder is divided into two different zones, a burned and an unburned one. This separate reflection of the burned and unburned gas enables the model to replicate the impact of the burned gas on the compression with a moderate increase in computational cost compared to the zero-dimensional approach.

Modelling approach

The idea behind the 2-zone-cylinder model, is to reproduce the experimental procedure for deriving the octane number and provide engine related boundary conditions for chemical kinetic simulations. For the modelling of the combustion, the gasoline surrogate mechanism from the Lawrence Livermore National Laboratory [14] is used.

In the first step, the model searches in an iterative process for the compression ratio leading to self-ignition of the unburned fuel air mixture. Subsequently, the obtained critical compression ratio can be related to the octane number. Applying these two steps on a set of PRFs results in a clear correlation between the critical compression ratio and the octane number. During the simulation, an engine cycle is simulated from the time when the inlet valve closes on to the opening of the outlet valve.

Narr Francke Attempto Verlag GmbH + Co. KG

Figure 3 visualize the structure of the model. The burned and the unburned zone in the cylinder are each represented by homogeneous zero-dimensional reactor. The volumes are time depended functions and are defined by the CFR-engine's piston stroke under RON conditions. Both reactors are linked through a pressure conditions which ensures the same pressures in both zones.
The flame front is modeled through mass transfer from the unburned to the burned zone. The actual mass flow, the burning rate, respectively, is calculated via Vibes Burning Law [15]. The heat flux into the reservoir with the burned gas, shown in Figure 3, equals the compression work of the piston into the system and is necessary to fulfill the energy conservation. Lacking a real radial spatial resolution of the combustion chamber, no direct possibility is given to model a temperature profile with dropping temperatures near the wall. To overcome this issue, the adiabatic core hypothesis is applied and the wall heat losses are modeled through an isentropic expansion. This method is commonly used for the simulation of rapid compression machines [16].

Validation and first results

With the implemented model, the critical compression ratio of fuels can be derived, provided that all included species occur in the chemical-kinetic mechanism and are validated.
Table 3 lists already simulated fuel blends with known octane numbers from the literature. The octane number of the PRFs can be determined from their composition. If the simulated critical compression ratios of the fuels are linked to their octane numbers, a clear correlation of both quantities becomes visible as illustrated Figure 4-left. The PRFs data set is used to derive a correlation visualized by the black line in Figure 4-left.
The derived correlation between the critical compression ratio of the PRF blends and the octane number can now be used to calculate octane numbers for the other datasets.

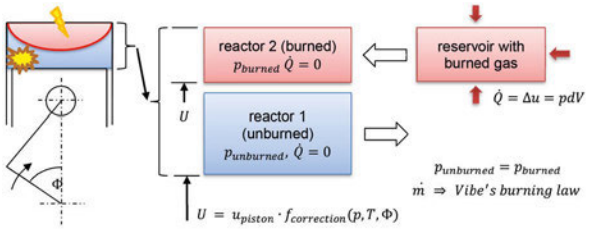

Figure 3: Schematic view of a cylinder during the compression cycle with spreading flame front and the 2-Zone-Cylinder-Model visualizing the two homogeneous reactors for the burned and the unburned zone plus the reservoir for the unburned gas.

Table 3: Collection of relevant fuel-blends with known octane number from literature.

Fuel	Composition	Source ON
PRF (primary reference fuel)	iso-octane, n-heptane	blending ratio
TRF (toluene reference fuel)	iso-octane, n-heptane and toluene	[12]
PRF + ethanol	PRF91 + ethanol	[17]
TRF91-15 + ethanol	TRF mit 15 vol.% toluene + ethanol	[17]
TRF91-30 + ethanol	TRF mit 30 vol.% toluene + ethanol	[17]
TRF91-45 + ethanol	TRF mit 45 vol.% toluene + ethanol	[17]

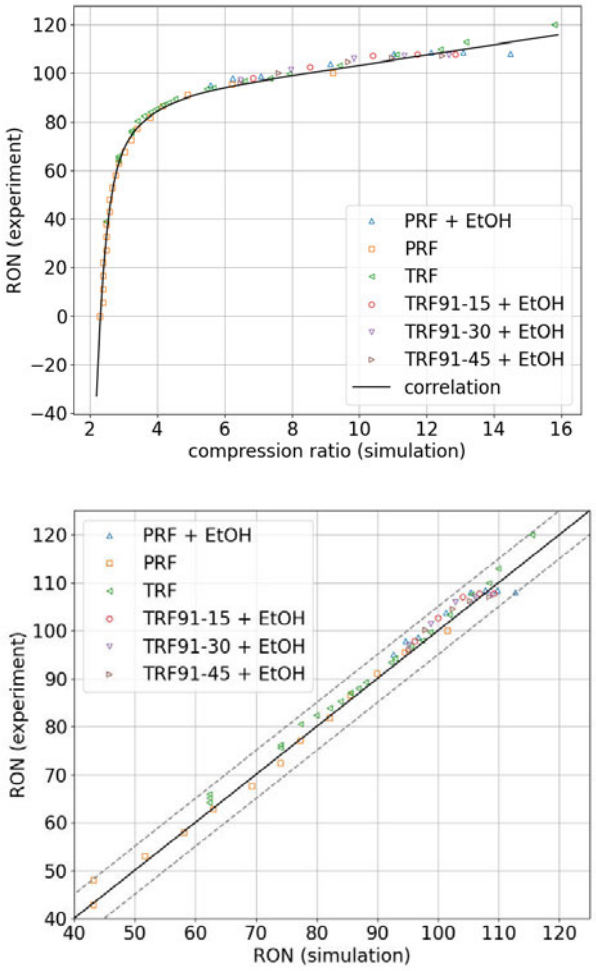

Figure 4: Modelling results of the 2-Zone-Cylinder-model. Left: comparison between the experimental derived octane number and the simulated critical compression ratio, the black line visualizes the derived correlation.

Narr Francke Attempto Verlag GmbH + Co. KG

Right: experimental derived octane number vs. the octane number calculated using the correlation.

Figure 4-right shows the comparison between the experimental derived octane numbers from the literature and the calculated ones. The results are found to deviate less than 5 octane numbers compared to the actual values. The current results confirm the promising approach for deriving the octane number. For the application of the method to all relevant fuels listed in Table 1 within the project “Solare Kraftstoffe”, the chemical kinetic mechanism has to be extended to include the species ETBE, MTBE and isobutanol. Further, an optimization of the implementation of the combustion rate is considered. This will enable a better representation of the fuel-specific influence on the combustion process.

3.3 Flow reactor experiments

Approach

To study technical fuels' combustion chemistry reactor-experiments were performed at DLR's atmospheric high-temperature laminar flow reactor (ALFR) coupled with molecular-beam mass spectrometry (MBMS) detection. Instrumentation and design as well as experimental methodology are described in high detail in Oßwald et al. [18]. Thus, the experimental approach is only briefly summarized below.

In DLR's ALFR fuel oxidation, from fuel consumption over intermediate species pool, to final combustion products can be examined in the homogeneous gas phase. The pre-evaporated and premixed fuel is fed to the reactor in high argon dilution (Ar > 99%) including oxygen as oxidizer. Examinations where performed from intermediate to high temperature regime (8001200 K) for lean and slightly-rich equivalence ratios ($\phi = 0.8$ and 1.2) and air-fuel ratios ($\lambda = 1.25$ and 0.83), respectively. Depending on the temperature, residence times are about 2 s. Flow rates are controlled by precise Coriolis mass flow controllers (MFC). *In-situ* sampling is performed by means of a quartz nozzle/skimmer differential pumping system, where the gas probe is transferred to a molecular-beam and further reactions are prevented. Finally, soft electron ionization (EI; actual energy 11.5 eV) is applied and the individual combustion species are detected in a time-of-flight mass spectrometer (TOF-MS). Note that there is no isomer-specific differentiation here. Data evaluation and quantification is processed according to [18, 19].

Results

Figure 5 shows a general mass spectrum for mass to charge ratios (m/z) up to 200 u of the oxidation of the reference gasoline Bosch EU5 Cert under lean conditions ($\lambda = 1.25$) for highly reactive temperature (T = 1057 K). The temperature has been chosen in a way to ensure that most of the fuel molecules have already been consumed and a large number of important combustion intermediates have relatively high concentrations. Each mass peak corresponds to one or more partially oxygenated hydrocarbons. We observed intermediate species within a broad mass range from low molecular-weight aliphatic species up to high molecular-weight species such as polycyclic aromatic hydrocarbons (PAHs). Based on the high mass resolution (R = 3000 [18]) separation of species with the same nominal mass is possible, which is shown in Figure 5insert for m/z = 42 u. Here, ketene (C_2H_2O) is properly separated from propene (C_3H_6). Selected detailed speciation data of some major species, key intermediates, and aromatic soot precursors are presented and discussed below of fuel oxidation under lean conditions ($\lambda = 1.25$).

Major species. Oxidative reactivity of the fuels can be examined by following the species profiles of major species shown in Figure 6 where the mole fractions of O_2 and H_2O under lean air-fuel ratios ($\lambda = 1.25$) are plotted as a function of the gas temperature. Overall, the comparison of the gasoline blends compliant with standard EN 228 shows very similar species profiles in quality and quantity and thus, similar combustion behavior within experimental uncertainty can be stated. Only the non-standard-compliant fuel candidate E30 shows a deviating behavior. With regard to the water profile (Figure 6bottom), H_2O is already formed at lower temperature in higher amounts than for oxidation of the other blends. The higher reactivity of E30 can be attributed to a high volume fraction φ_i of ethanol (φ_{EtOH} =30 %v/v) and the associated higher oxygen content w_O (w_O = 10.9 %m/m) [20]. Thus, most small carbonyl compounds are also formed earlier and a broader species profile emerges, as shown in Figure 7top/left for formaldehyde (CH_2O).

Key intermediate. We chose species with maximum mole fractions > 10 ppm as key intermediates. This includes small paraffins like methane (CH_4), and ethane (C_2H_6), as well as small olefins like ethylene (C_2H_4), propene (C_3H_6), butadiene (C_4H_6), and butene (C_4H_8), and small alkynes such as propyne/allene (C_3H_4), which are known to be part of the PAH building block. Furthermore, we observed oxygenated key intermediates like formaldehyde (CH_2O) and ketene (C_2H_2O). Exemplary we discuss formaldehyde as a representative for oxygenated key intermediates in the following. In Figure 7top the species profiles of formaldehyde and maximum mole fractions for fuel oxidation under lean conditions ($\lambda = 1.25$) are presented and compared to the fuel's oxygen content. It is known that a higher oxygen content in the system favors the formation of oxygenated combustion intermediates [20, 21]. The reference gasoline Bosch EU5 Cert with the lowest oxygen content (w_O = 1.8 %m/m) exhibits one of the lowest CH_2O-concentrations and the gasoline blend E30 with the highest oxygen content (w_O = 10.9 %m/m) has one of the highest concentrations in CH_2O. Looking at the group of standard-compliant gasoline blends, with approximately the same oxygen content ($w_O \approx 3.6$ %m/m) it becomes clear, that not only the fuels' oxygen content can be decisive for the formaldehyde formation. For example, MTBEmax (w_O = 3.7 %m/m), in which the fuel oxygen is bound in methyl tert-butyl ether (MTBE; $C_5H_{12}O$) yields a higher formaldehyde concentration than the ETBEmax (w_O = 3.6 %m/m), in which ethyl tert-butyl ether (ETBE; $C_6H_{14}O$) is the oxygenated fuel additive.

Narr Francke Attempto Verlag GmbH + Co. KG

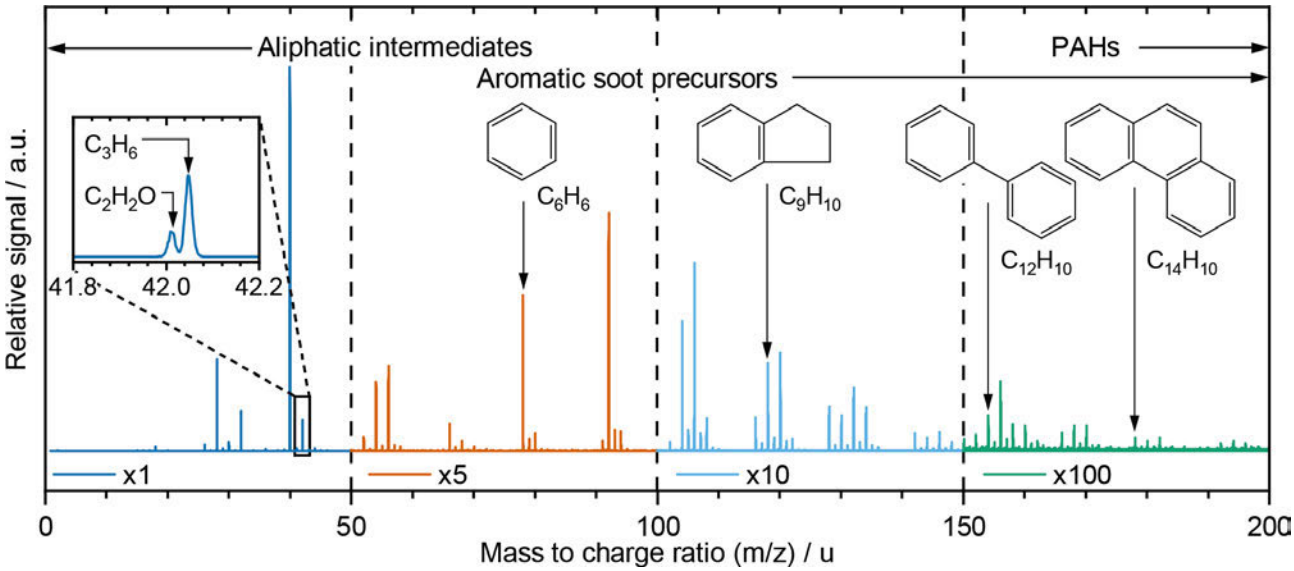

Figure 5: Mass spectrum of Bosch EU5 Cert oxidation under lean condition (λ = 1.25) at highly reactive temperature (T = 1057 K), selected aromatic soot precursors are marked. Insert: Separation on nominal mass m/z = 42.

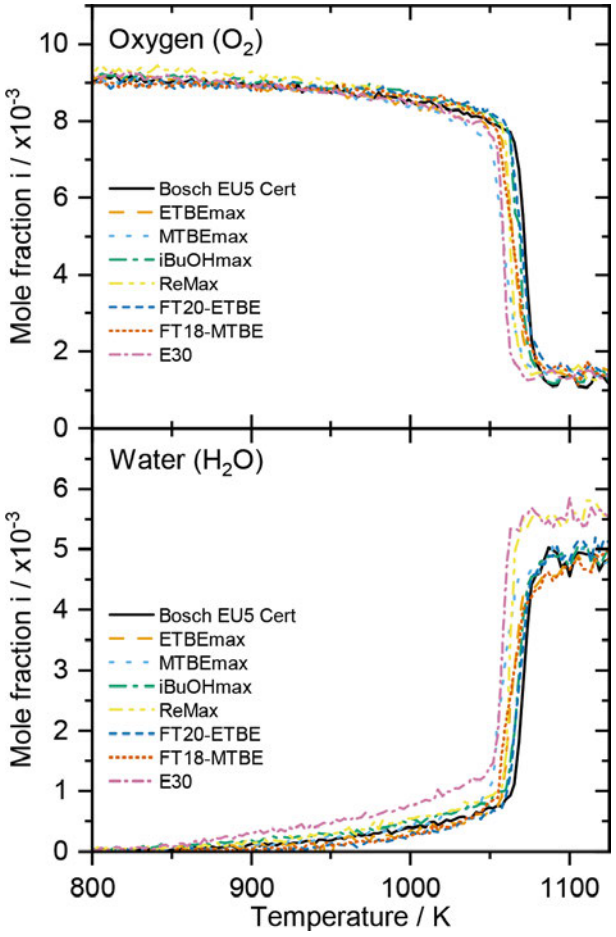

Figure 6: Mole fractions of selected major species (O_2 and H_2O) of fuel oxidation under lean condition (λ = 1.25) plotted as function of the gas temperature.

The highest CH_2O amount within this fuel group is reached by the gasoline blend ReMax (w_O = 3.7 %m/m), although also ETBE is the primary oxygen carrier as for the blend ETBEmax. This is where the different composition of each base gasoline used for fuel blending comes into play. In contrast to the other standard-compliant blends, ReMax has a relatively low aromatic volume fraction ($\varphi_{Arom.}$ = 11.3 %v/v) and also a decreased volumetric content of olefins (φ_{Olefin} = 4.0 %v/v). Overall, the maximum CH_2O concentration increases as follows: Bosch EU5 Cert ≈ FT20-ETBE < ETBEmax < iBuOHmax < FT18-MTBE < MTBEmax < ReMax ≈ E30. It could be stated, that not only the fuels oxygen content but also the molecular structure of the oxygenated blending component and the fuel itself play an important role in formation processes of oxygenated combustion intermediates.

Aromatic soot precursors. Benzene is considered a flagship aromatic soot precursor. The formation reaction of the first aromatic ring structure is strongly dependent on the fuel-specific intermediate pool, which result from fuel degradation [22]. In addition to mono-aromatics, PAHs play a crucial precursor role in soot formation [23-25]. Generally, aromatics are used as octane boosters and are therefore present in high proportions in standard-compliant gasolines, with up to 35 %v/v permitted according to EN 228 [5]. Peak position of selected aromatic soot precursors and PAHs are marked in the mass spectrum of reference gasoline Bosch EU5 Cert oxidation in Figure 7, namely benzene (C_6H_6), indane (C_9H_{10}), biphenyl/acenaphthene ($C_{12}H_{10}$), and phenanthrene/anthracene ($C_{14}H_{10}$). These species occur almost exclusively as intermediates in the oxidization of the fuels under consideration and are therefore particularly suitable for investigating the combustion reaction process. This does not apply to toluene and naphthalene, for example, as these are already contained in high percentages in the fuels themselves. In the

Narr Francke Attempto Verlag GmbH + Co. KG

following we discuss the experimental data of benzene as typical representative of the aromatic soot precursors.

The benzene species profiles and maximum mole fractions for fuel oxidation under lean conditions ($\lambda = 1.25$) are shown in Figure 7bottom in comparison to the hydrogen content of the fuels. For non-oxygenated technical fuels, like kerosene or diesel, the benzene concentration formed during fuel oxidation correlates well with fuels hydrogen content w_H [26-28]. In H/C-fuel systems, a low hydrogen content promotes benzene formation. In addition, it is known that the aromatic content of the fuel has a major impact on the aromatic intermediate species pool, as fuel's aromatics can skip decomposition and act directly as soot precursors [24, 25].

As expected, the standard-compliant gasoline blend ReMax with the highest hydrogen content (w_H = 14.4 %m/m) and the lowest aromatics volume fraction ($\varphi_{Arom.}$ = 11.3 %v/v) shows the lowest benzene concentration within the fuel series studied. The second lowest C_6H_6 maximum mole fraction is reached by the non-standard-compliant blend E30 with reduced volume fraction of aromatics ($\varphi_{Arom.}$ = 19.2 %v/v). The hydrogen content of E30 (w_H = 13.5 %m/m), on the other hand, is nearly as high as that of the reference gasoline Bosch EU5 Cert (w_H = 13.4 %m/m), which has one of the highest benzene concentrations. Consequently, the correlation between fuels hydrogen content and benzene formation seems to fail for C/H/O-fuel-systems. Moreover, it seems to be not sufficient to consider only the aromatic concentration in the fuel. Thus, the gasoline blend FT18-MTBE with the highest aromatics content ($\varphi_{Arom.}$ = 33.2 %v/v) and the lowest hydrogen content (w_H = 12.9 %m/m) is only in the middle range of the high-aromatic fuel blends in terms of maximum mole fraction of benzene. Therefore, the fuels molecular structure also be considered for the soot precursor chemistry, including the oxygen in the fuel.

Overall, based on the flow reactor study, it can be assumed that the standard-compliant fuel candidate ReMax and the near drop-in gasoline blend E30 have a lower tendency to form soot in the engine operation, than the other investigated fuels. Note, that the observed benzene reduction for these fuels cannot be transferred directly into real engine emissions, thus other fuel properties like vaporization behavior matter too. However, a relative soot reduction should be visible.

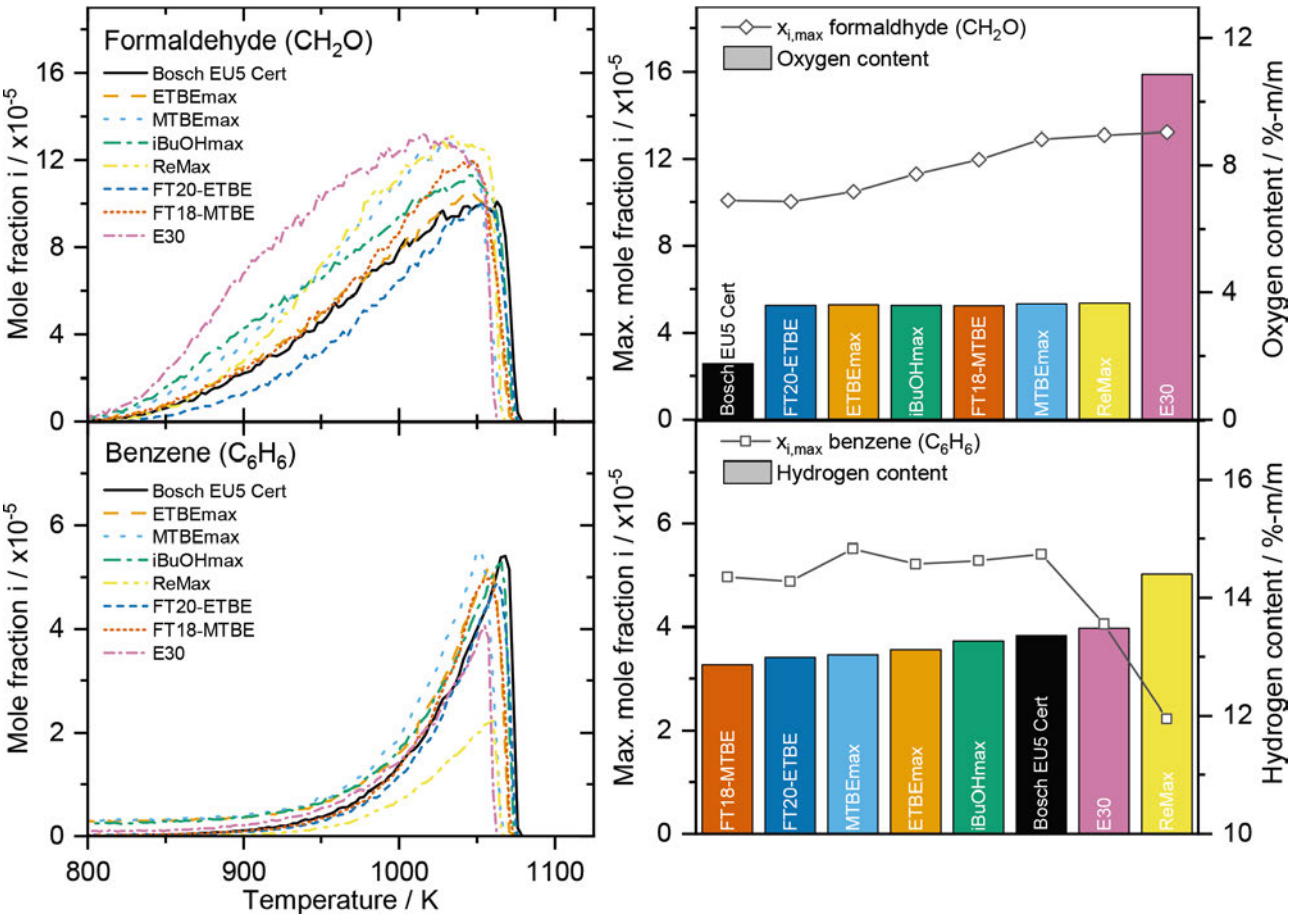

Figure 7: Left: Mole fractions of formaldehyde (CH_2O) as representative for oxygenated key intermediates and benzene (C_6H_6) as representative for aromatic soot precursors of fuel oxidation under lean condition ($\lambda = 1.25$) plotted as function of the gas temperature. Right: Measured peak mole fraction of the respective combustion intermediate (lines, left axis) compared to the fuel's oxygen content or hydrogen content (bars, right axis).

Narr Francke Attempto Verlag GmbH + Co. KG

3.4 Engine test

The renewable fuel candidates were evaluated using a production calibrated turbo charged gasoline direct injection engine with 4 cylinders (in-line), a displacement volume of 2 liters and a central mounted Bosch high-pressure-injector (Bosch Hochdruckeinspritzventil, HDEV 6). The system fuel pressure is 350 bar. Fuel effects were evaluated on calibration robustness, combustion characteristics and criteria pollutant emissions.
Engine test bench includes an engine dynamometer with external controllable coolant, fuel, air and intercooler temperatures. Engine oil temperature is not controlled. This temperature results from constant coolant temperature and specific load. In-cylinder pressures were measured by piezoelectric pressure transducers (Kistler 6041B). Gaseous and particulate emissions were measured using a Horiba Mexxa 7100 and a Horiba SPSC 2100 respectively.

Measurement program
The Bosch renewable fuel evaluation program includes mixture formation measurements in a spray test chamber as well engine measurements. For the engine fuel investigation, a special test approach was developed containing engine map evaluation at cold and warm conditions, an injector coking drift run, fuel knocking behavior at full load conditions, transient operation as well as special engine operation modes e.g. catalyst heating and EGR variation. In order to evaluate the calibration neutrality of the fuel candidates, for all operating points mainly the series calibration data was used. However, in some program points, the calibration robustness was tested e.g. by SOI sweeps at different engine loads. Also, an engine oil dilution test is assessed at cold start conditions. In Table 4 the fuel evaluation program is listed including engine operating points and measurement conditions.

Table 4: Spray and engine evaluation program

Program	Details and Conditions
Spray measurements Evaluation of mixture formation behavior @ spray chamber test bench under engine relevant conditions	
Endurance run: PN drift of injector/engine	2000 rpm / medium load for 14h at 200 bar and 4h at 350 bar @ warm engine
Engine out emissions, fuel consumption, combustion parameters	Engine map at 1000/2000/4000/6000 rpm, idle → full load @warm engine Engine map at 1000/2000/4000/6000 rpm, Idle → full load @cold engine
Calibration robustness	Start of injection (SOI) sweeps, 1500 rpm, low medium and full load @warm engine
Engine knocking	1500/2000/3000/4000/5000/6000 rpm, full load, ignition angle sweep @warm engine
Transient operation	Load step at 1500 rpm, low load → full load @cold engine
Catalyst heating	Catalyst heating operating point incl. ignition angle sweep @cold engine
Internal EGR variation	1500 rpm, low load, variation of exhaust valve timing @cold engine
Oil dilution	1500rpm medium load, medium engine coolant temperature

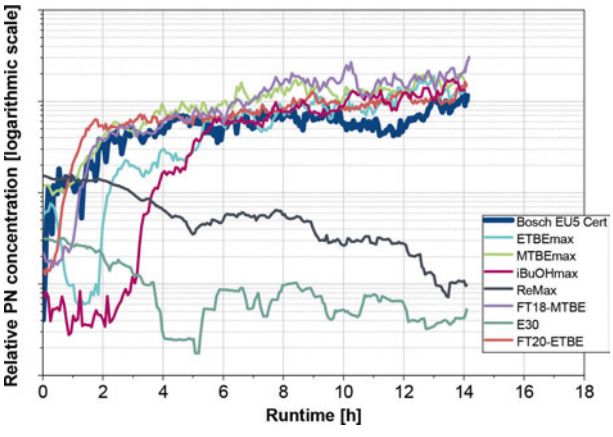

Figure 8: 14 hours PN endurance run results for 200 bar rail pressure and all tested renewable fuel candidates.

Results engine measurement program
For this paper, only the results of the particle number (PN) drift run at 2000 rpm and warm engine are exemplary presented and discussed. The main operating parameters of the engine map are listed in Table 5. The aim of

Narr Francke Attempto Verlag GmbH + Co. KG

the drift endurance run is, to see if a fuel candidate tends to injector coking and subsequent temporal PN drift. In order to provoke this behavior, the system pressure is reduced from 350 bar to 200 bar. Before start of the drift run, the injector tips were cleaned. Thereafter, the engine was stationary operated at 2000 rpm and 10 bar Break mean effective pressure (BMEP) for 14 h. If a fuel tends to injector drift the PN concentration will increase and stabilize at high PN emission level during the drift run time. In Figure 8 the results of the 14 h drift run are shown for all tested fuel candidates.
It can be seen that all fuels except of ReMax and E30 show significant PN drift after minimum of 6 hours. At this point in time a similar high steady level of PN concentration is reached. After the drift run the injectors were removed and the injector tips were imaged. The results are shown in Figure 9.

Table 5: Endurance run operating conditions

Parameter	Unit	Value
Speed	rpm	2000
Load BMEP (Break mean effective pressure)	bar	10
Rail pressure	bar	200 / 350
Runtime	h	14 / 4
Temperature Coolant	°C	90
Temperature engine oil	°C	95
SOI	°CA	Fuel specific optimization for low PN emission: Bosch EU5 Cert: 320 / 320 ETBEmax: 320 / 310 MTBEmax: 320 / 310 iBuOHmax: 300 / 310 ReMax: 310 / 300 FT20-ETBE: 300 / 300 FT18-MTBE: 320 / 310 E30: 300 / 290
Ignition angle	°CA	Optimized for MFB50 (50% mass fraction burned) at 8°CA

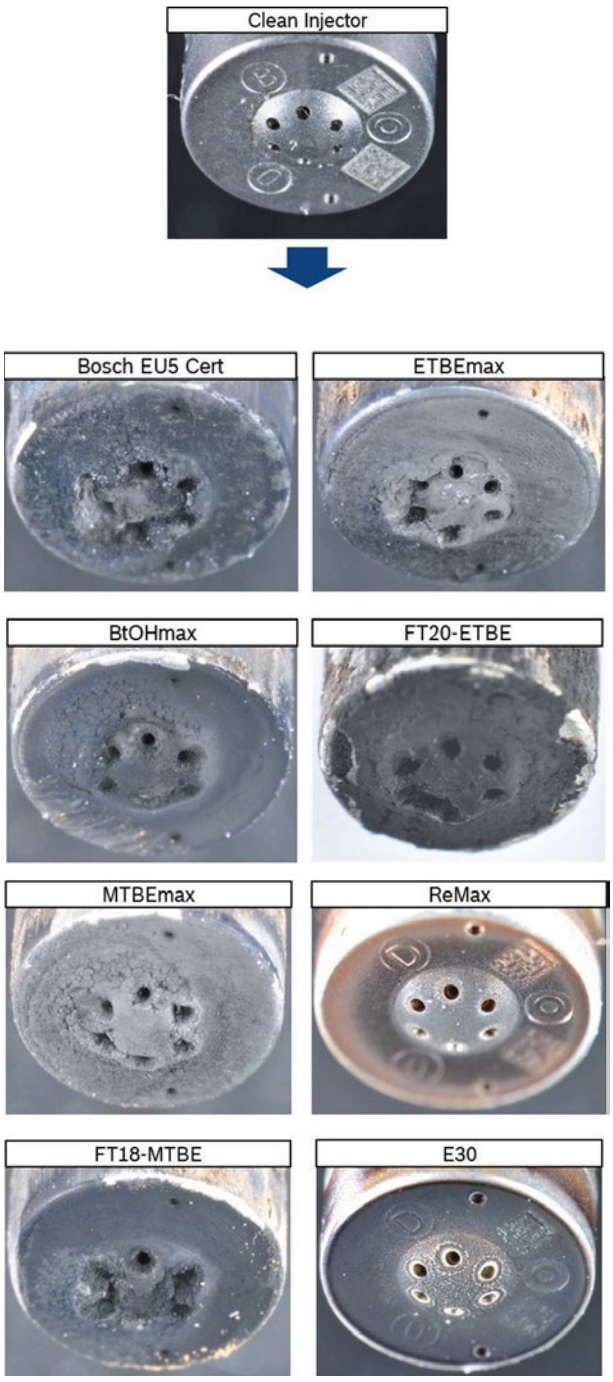

Figure 9: Images of injector tip after 14 h endurance run for all tested fuels including an example image of a clean injector tip at the top row before the endurance run.

Narr Francke Attempto Verlag GmbH + Co. KG

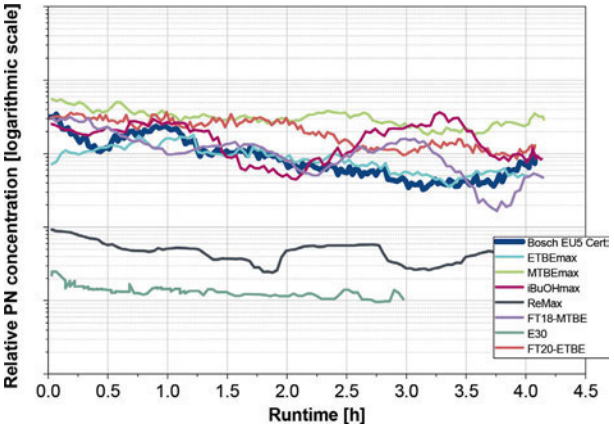

Figure 10: 2 hours PN stabilization run results for 350 bar rail pressure and all tested renewable fuel candidates

The reason for this fuel drift behavior may be ascribed to the volumetric concentration of heavy aromatics with carbon chain lengths equal and greater than 9 atoms (C9/C9+ aromatics). E30 and ReMax exhibit lowest C9/C9+ aromatic content in comparison to the other fuel candidates. The mechanisms and the effect of gasoline fuel properties on emission behavior for the injector drift run where investigated in Wiese et al. [1] and Fatouraie et al. [29].

All fuel candidates except of ReMax and E30 show significant injector deposits at the injector tip (see Figure 9). ReMax and E30 are free of deposits. The images prove the emission test results of the PN concentration drift in Figure 8.

After the 14 hours drift run the injectors were rebuild and a stabilization run for 2 hours at system pressure (350 bar) followed. The purpose of this measurement was to see how the fuels behave at series calibration and if the fuels may show a cleaning behavior by decreasing PN concentration.

For the coked and drifted injectors, a slight decrease in PN concentration can be measured. After 1 h the PN emission level slightly decreases. The injectors which did not show coking (E30 and ReMax) have a lower stable PN concentration level.

It can be concluded that, although the fuel candidates ETBEmax, MTBEmax, IBuOHmax, FT18-MTBE and FT20-ETBE show significant injector drift, the PN emission behavior is in the same order of magnitude as for the reference fuel Bosch EU5 Cert, which can be seen as a bad case market fuel. Moreover, the content of heavy aromatics of the fuel is connected to the fossil base fuel and not to the renewable fuel component. So, the behavior of PN drift is not directly influenced by the renewable blend component. As seen in the homogeneous gas phase experiments (Chapter 3.3) the ReMax fuel exhibits the lowest amount of soot precursor intermediates. For ReMax with high renewable share (e.g. isooctane, ETBE and FT surrogate) the fossil fuel components are diluted enough to reduce C9/C9+ aromatics. A similar reason could be quoted for E30 where Ethanol states the dilution blend component.

Moreover, from the study of Wiese et al. [1], it is known, that by additivities of detergents, the PN drift of the fuel can be reduced. This could be possible measure for such fuel candidates, which show high coking tendency.

Conclusions

This paper provides an overview of the status of the work being done as part of the BMWi-funded project “Solare Kraftstoffe” to evaluate synthetic fuels that can be produced sustainably via a solar powered, thermal conversion route. All the fuels considered, with the exception of the E30 blend, are compatible with the EN 228 standard and can be quickly established on the market with the existing fleet of vehicles.

In order to evaluate the synthetic fuels and to identify particularly suitable fuel components for improving the fuel properties in terms of combustion and emission behavior, model-based methods were used as well as analytical tests and experiments on the engine were carried out.

DLR’s SimFuel platform, originally developed for aviation fuels, was extended to the application of transportation fuels. Based on the detailed fuel’s composition further properties of the fuel could be predicted. New machine learning models are currently being developed, which are trained on single components and fuels. These models then can also predict unknown complex fuels (e.g. renewable gasoline), for which not yet enough training data exists.

Provided that the detailed composition of the fuel candidates in “Solare Kraftstoffe” is available, as it can be analysed e.g. by two-dimensional gas chromatography (GCxGC), properties of these real fuels can be predicted and then visualized and assessed in context to the range of experience using the SimFuel platform.

To evaluate the octane number of the fuels as well as to identify especially suitable fuel compositions the 2-Zone-Cylinder-Model was developed. The model provides engine related boundary conditions combined with reaction models for the numerical estimation of octane numbers. First numerical predictions of the research octane numbers by the model are in good agreement with experimental data. In the next step, the chemical kinetic mechanism has to be extended and validated, in order to be able to simulate all fuel components, which are important within the project.

The analytical research in the flow reactor shows that the standard-compliant fuel candidate ReMax and the close drop-in gasoline blend E30 have a lower tendency to form soot during engine operation than the other fuels.

It must be noted, however, that the observed benzene reduction for these fuels cannot be directly extrapolated to real engine emissions, as other physical fuel properties such as evaporation behavior also influence emissions.

Despite the highly idealized boundary conditions of the analytical study, they confirm the particle number tests

Narr Francke Attempto Verlag GmbH + Co. KG

carried out on a turbo charged gasoline direct injection engine. The evaluations of the PN concentration in an endurance run where injector drift was provoked at medium load condition show that both the E30 and the ReMax exhibit significantly reduced particulate number emissions and no injector coking in comparison to the other fuel candidates. Both results can mainly be attributed to the reduced amount of heavy aromatic components in the fossil base fuel because of the high share of renewable components with low sooting tendency.

References

[1] W. Wiese, C. Laidig and E. Schünemann, “Effects of Fuel Composition, Additives and Injection Parameters on Particulate Formation of Gasoline DI Engines,” *Wiener Motorensymposium,* 2018.

[2] N. Monnerie, P. G. Gan, M. Roeb and C. Sattler, “Methanol production using hydrogen from concentrated solar energy,” *International Journal of Hydrogen Energy,* vol. 45, p. 26117–26125, 10 2020.

[3] Y. Lu, L. Zhu, C. Agrafiotis, J. Vieten, M. Roeb and C. Sattler, “Solar fuels production: Two-step thermochemical cycles with cerium-based oxides,” *Progress in Energy and Combustion Science,* vol. 75, p. 100785, 11 2019.

[4] A. Rosenstiel, N. Monnerie, J. Dersch, M. Roeb, R. Pitz-Paal and C. Sattler, “Electrochemical Hydrogen Production Powered by PV/CSP Hybrid Power Plants: A Modelling Approach for Cost Optimal System Design,” *Energies,* vol. 14, p. 3437, 6 2021.

[5] *DIN EN 228:2017-08, Kraftstoffe – Unverbleite Ottokraftstoffe – Anforderungen und Prüfverfahren.*

[6] C. Hall, B. Rauch, U. Bauder, P. Le Clercq and M. Aigner, “Application of Machine Learning algorithms for the prediction of fuel properties in comparison with state of the art physical models,” *16th International Conference on Stability, Handling and Use of Liquid Fuels,* 2019.

[7] C. Hall, B. Rauch, U. Bauder, P. L. Clercq and M. Aigner, “Predictive Capability Assessment of Probabilistic Machine Learning Models for Density Prediction of Conventional and Synthetic Jet Fuels,” *Energy & Fuels,* vol. 35, p. 2520–2530, 1 2021.

[8] J. Heyne, B. Rauch, P. L. Clercq and M. Colket, “Sustainable aviation fuel prescreening tools and procedures,” *Fuel,* vol. 290, p. 120004, 4 2021.

[9] B. Boden, J. Flink, R. Mischke, K. Schaffert, A. Weinert, A. Wohlan and et al., “Distributed Multidisciplinary Optimization and Collaborative Process Development Using RCE,” *AIAA Aviation 2019 Forum. American Institute of Aeronautics and Astronautics,* 2019.

[10] *ASTM Interanational, Standard test method for research octane number of spark-ignition engine fuel, ASTM D2699-11, 2011.*

[11] *ASTM International, Standard test method for motor octane number of spark-ignition engine fuel, ASTM D2700-11, 2011.*

[12] N. Morgan, A. Smallbone, A. Bhave, M. Kraft, R. Cracknell and G. Kalghatgi, “Mapping surrogate gasoline compositions into RON/MON space,” *Combustion and Flame,* vol. 157, p. 1122–1131, 6 2010.

[13] J. A. Badra, N. Bokhumseen, N. Mulla, S. M. Sarathy, A. Farooq, G. Kalghatgi and P. Gaillard, “A methodology to relate octane numbers of binary and ternary n-heptane, iso-octane and toluene mixtures with simulated ignition delay times,” *Fuel,* vol. 160, p. 458–469, 11 2015.

[14] M. Mehl, W. J. Pitz, C. K. Westbrook and H. J. Curran, “Kinetic modeling of gasoline surrogate components and mixtures under engine conditions,” *Proceedings of the Combustion Institute,* vol. 33, p. 193–200, 2011.

[15] S. Verhelst and C. G. W. Sheppard, “Multi-zone thermodynamic modelling of spark-ignition engine combustion – An overview,” *Energy Conversion and Management,* vol. 50, p. 1326–1335, 5 2009.

[16] G. Mittal and C. Sung*, “A rapid compression machine for chemical kinetics studies at elevated pressures and temperatures,” *Combustion Science and Technology,* vol. 179, p. 497–530, 3 2007.

[17] T. M. Foong, *On the Autoignition of Ethanol/GasolineBlends in Spark-Ignition Engines,* PhD thesis, Department of Mechanical Engineering, The University of Melbourne, 2013.

[18] P. Oßwald and M. Köhler, “An atmospheric pressure high-temperature laminar flow reactor for investigation of combustion and related gas phase reaction systems,” *Review of Scientific Instruments,* vol. 86, p. 105109, 10 2015.

[19] F. Herrmann, P. Oßwald and K. Kohse-Höinghaus, “Mass spectrometric investigation of the low-temperature dimethyl ether oxidation in an atmospheric pressure laminar flow reactor,” *Proceedings of the Combustion Institute,* vol. 34, p. 771–778, 1 2013.

[20] S. M. Sarathy, P. Oßwald, N. Hansen and K. Kohse-Höinghaus, “Alcohol combustion chemistry,” *Progress in Energy and Combustion Science,* vol. 44, p. 40–102, 10 2014.

[21] K. Kohse-Höinghaus, “A new era for combustion research,” *Pure and Applied Chemistry,* vol. 91, p. 271–288, 1 2019.

[22] L. Ruwe, K. Moshammer, N. Hansen and K. Kohse-Höinghaus, “Influences of the molecular fuel structure on combustion reactions towards soot precursors in selected alkane and alkene flames,” *Physical Chemistry Chemical Physics,* vol. 20, p. 10780–10795, 2018.

[23] H. F. Calcote and D. M. Manos, “Effect of molecular structure on incipient soot formation,” *Combustion and Flame,* vol. 49, p. 289–304, 1 1983.

Narr Francke Attempto Verlag GmbH + Co. KG

[24] M. Frenklach, “Reaction mechanism of soot formation in flames,” *Physical Chemistry Chemical Physics,* vol. 4, p. 2028–2037, 2 2002.

[25] H. Richter and J. B. Howard, “Formation of polycyclic aromatic hydrocarbons and their growth to soot—a review of chemical reaction pathways,” *Progress in Energy and Combustion Science,* vol. 26, p. 565–608, 8 2000.

[26] P. Oßwald, J. Zinsmeister, T. Kathrotia, M. Alves-Fortunato, V. Burger and R. Westhuizen, “Combustion kinetics of alternative jet fuels, Part-I: Experimental flow reactor study,” *Fuel (in press),* 2021.

[27] T. Kathrotia, P. Oßwald, C. Naumann, S. Richter and M. Köhler, “Combustion kinetics of alternative jet fuels, Part-II: Reaction model for fuel surrogate,” *Fuel (in press),* 2021.

[28] T. Kathrotia, P. Oßwald, J. Zinsmeister, T. Methling and M. Köhler, “Combustion kinetics of alternative jet fuels, Part-III: Fuel modeling and surrogate strategy,” *Fuel (in press),* 2021.

[29] M. Fatouraie, M. Frommherz, M. Mosburger, E. Chapman, S. Li, R. McCormick and G. Fioroni, “Investigation of the Impact of Fuel Properties on Particulate Number Emission of a Modern Gasoline Direct Injection Engine,” *SAE Technical Paper 2018-01-0358,* 4 2018.

Narr Francke Attempto Verlag GmbH + Co. KG

Latest developments in modular Power-to-X technologies in INERATEC´s micro-structured reactor technology

Dr. Tim Böltken
INERATEC

1. Introduction

The European Union has not only been striving to reduce their carbon footprint since the Paris Agreement in 2015, but ever since the efforts have been intensified significantly. Amongst others, this led to the European Green Deal, which had been announced in 2019 by the European Commission and is currently being implemented[1]. Strong efforts have been taken, especially in the last years, to overcome the dependency from fossil resources in all sectors. While the energy sector has made significant advances in the installation of renewable sources and minimizing the CO_2 emission, the transportation sector still has a long way to go. Currently, there is an intense and in parts very lobby-driven political discussion on the right direction for the transport sector to turn to in order to minimize CO_2 emissions in the upcoming years and to reach the climate goals set on an international and also a national level in various countries. At a first glance, battery-driven cars might seem to be the preferred solution for urban traffic due to their superior efficiency in utilization of the renewable electricity. On the other hand, there are still unanswered questions like the availability of suitable charging infrastructure or the environmental footprint of the battery production. One aspect further ignored in this discussion is also that renewable energy sources, such as wind or solar, are highly volatile not only on minute or hour scale but also on a daily and seasonal scale. Downturns of wind on weekly basis can occur several times throughout a year.
Renewable carbon-based fuels produced from renewable energy, so called e-Fuels, on the other hand could be utilized instantly in the available infrastructure for distribution and also in the current car fleets. They could help to overcome these power fluctuations while being produced only in times of energy availability. Despite lower well-to-wheel efficiency, e-Fuels have significant advantages when it comes to accessing renewable energy in remote locations, so called Power-to-X sweet spots[2]. Even if the above-described challenges of electric mobility can be solved, there are still important sectors that will most presumably rely on carbon-based fuels also on the mid- and long-term. These sectors are aviation, long distance heavy-duty and maritime transport. Carbon based fuels, like Diesel or kerosene outmatch solid-state batteries or hydrogen fuel cell technology in terms of available energy density of the fuel by orders of magnitude[3]. That is why carbon-based fuels will play an important role also in the long-term future in the named sectors.
There are various candidates for the described e-Fuels, like Methanol (MeOH), Dimethylether (DME), Oxymethylene ethers (OME), Synthetic natural gas (SNG) or Fischer-Tropsch-based (FT) hydrocarbons[4]. Of course, in the production of all of these e-Fuels, one needs to make sure that the carbon feed is originating from an unavoidable CO_2 or renewable source (originating from biomass or air). Power to produce these e-Fuels via power-to-x technologies (PtX) should as well come from renewable sources to generate the hydrogen via electrolysis. Therefore, the costs for these e-Fuels currently cannot be considered equal or even lower than their fossil-based counterparts. Probably the most interesting e-Fuels, especially in short-term, are FT-based fuels. Those are chemically similar to current fuels like Diesel or kerosene but contain no hetero-atoms which generate poisonous emission and can additionally be tuned to combust even cleaner than fossil fuels. Therefore, these e-fuels could directly be handled in the existing infrastructure and used in the available engines and turbines. Of course, this might require adaptions in the legal framework but in contrary to other e-Fuels it does not require to install a completely new infrastructure-network.
INERATEC GmbH, a spin-off from the Karlsruhe Institute for Technology, has developed an innovative Power-to-X (PtX) technology that can produce FT-based fuels and MeOH efficiently and load-flexible. The modular approach renders INERATEC´s application an ideal fit for the upcoming challenges of future energy systems, like volatile energy availability or decentralized production of electricity.

[1] Communication from the Commission to the European Parliament, the European Council, the Council, the European Economic and Social Committee and the Committee of the Regions — The European Green Deal (COM(2019) 640 final, 11.12.2019)
[2] THE CONCEPT OF EFFICIENCY IN THE GERMAN CLIMATE POLICY DEBATE ON ROAD TRANSPORT, Frontier Economics, November 2020
[3] STATUS UND PERSPEKTIVENFLÜSSIGER ENERGIETRÄGER INDER ENERGIEWENDE, Prognos, May 2018
[4] P. D. Lund et al., Review of energy system flexibility measures to enable high levels of variable renewable electricity, Renewable and Sustainable Energy Reviews 45 (2015), 785–807

Narr Francke Attempto Verlag GmbH + Co. KG

2. Innovative chemical Reactor technology and scale-up

The above-mentioned Fischer-Tropsch synthesis is the conversion of syngas, a mixture of CO and H_2, into long-chain hydrocarbons, usually facilitated by a heterogeneous catalyst. The technology has been available since the first half of the 20th century and is widely applied in large scale production plants all over the world. Up to date, the technology is mainly used to produce liquid hydrocarbons from coal or methane via the so-called Gas-to-liquid process and is conducted in large scale fixed bed or bubble column reactors. These reactors follow the classical economy of scale, with improved efficiencies at very large scales. However, these reactor concepts are dependent on a continuous and large stream of gas supply and therefore hardly fit the above-described volatility of a renewable energy system.

One possible solution for the integration of the FT-process into a renewable energy system is the application of novel reactor concepts[5]. Based on research work at the Institute for Micro Process Engineering (IMVT) at KIT, INERATEC has developed a reactor technology that is easily scalable and suitable for the described flexible applications. The technology is based on microstructured reactors. The reactors are equipped with an innovative evaporation cooling in intermediate inside layers, which enables the plants to operate exothermic reactions under stable conditions[6,7]. The current commercially available generation of such reactors can be seen in Figure 1.

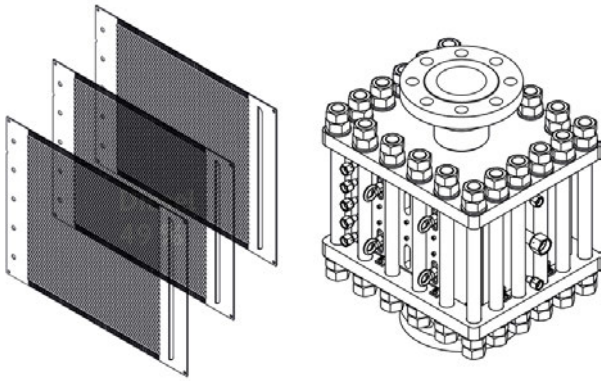

Figure 1: Rendering of INERATEC´s current commercially available reactor generation

Over the last decade, the reactor technology has been scaled up from laboratory scale to a size of 6 barrels per day per reactors of production capacity by KIT and INERATEC. This equals a scaling factor of more than 30.000, as can be seen from Figure 2.

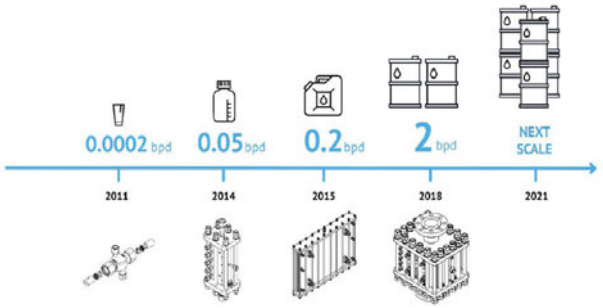

Figure 2: Reactor upscaling timeline

Together with the available advances in automation, which the whole process industry has made over the last couple of years, this opens the possibility to modularize the FT-process. This means that a number of individual FT-modules, that contain all necessary process units, like gas conditioning, one or multiple serial or parallel reactors and product handling, can be produced and combined again on next higher level of modularization in serial or parallel. This allows to establish FT processes that are customized towards the individual customer´s requirements. For example, in biomass-derived syngas (from gasification processes), inert gases like nitrogen might be contained in the feed-gas stream. In such a case it might be of interest to implement a 2-stage process rather than a 1-stage process to obtain near full conversion without inert accumulation while recycling unconverted feed. Both stages could be set up from a multitude of FT-modules with numerous FT-reactors each.

Several reactors in each stage or multiple modules offer another dimension of load flexibility as it is possible to operate the synthesis in only a reduced number of reactors or modules and leave the others in standby. Beyond load flexibility the modularization on reactor or module scale might be very useful for maintenance or other services, for which in other cases a complete plant would need to be shut down. On the contrast, the modular plant could then be operated at least in parts while other sections are in refurbishment. Furthermore, it is possible to foster ramp up of production capacity on availability of the renewable source, installing one plant unit at a time and therefore increasing production capacity. Schematically, one can see such the different operational modes in Figure 3.

[5] Leviness, Steve & Tonkovich, A & Jarosch, Kai & Fitzgerald, Sean & Yang, Bin & Mcdaniel, Jeff. (2011). Improved Fischer-Tropsch Economics Enabled by Microchannel Technology.

[6] M. Belimov, D. Metzger, P. Pfeifer, On the temperature control in a microstructured packed bed reactor for methanation of CO/CO2 mixtures, AIChE J. 63(2017) 120-129

[7] P. Piermartini, T. Boeltken, M. Selinsek, P. Pfeifer, Influence of channel geometry on Fischer-Tropsch synthesis in microstructured reactors, Chemical Engineering Journal 313 (2017) 328-335

Narr Francke Attempto Verlag GmbH + Co. KG

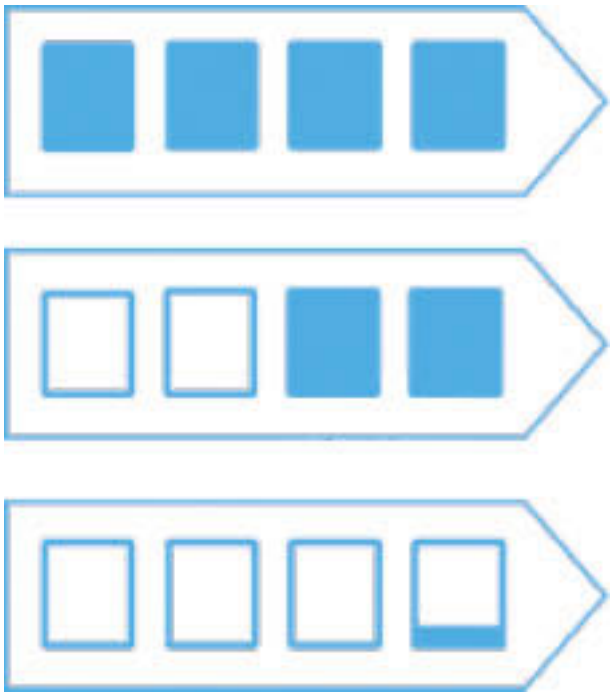

Figure 3: Operational modes of the modular concept

Going from bottom to top, the production capacity starts off very low at approx. 5 % of the maximum capacity. This can be realized by only one reactor module, which not even needs to be operated at full load. Increasing the production capacity to 50% would then require 2 modules fully operated. Increasing capacity 100% would in this case require two more modules to be operated at full load. The above-described reactor and core process development has been achieved in the two EU-funded research project COMSYN[8] and FLEXCHX[9]. Both projects focused on the utilization of biomass for sector coupling and the flexible (day-wise and seasonal) application of FT synthesis for the chemical storage of energy.

3. Plant scale-up and numbering-up

This modular approach will be basis for the plant scale-up of the company in the near- and mid-term future following a 3-dimensional numbering-up strategy. In the first dimension, the number of reaction plates per reactors are multiplied by increasing the reactor volume. Secondly, the number of reactors per module will be increased, which leads to an increase of the overall production capacity per module. And thirdly the number of modules can be multiplied to match the requirements of the customer site and the available feed streams, without significant re-engineering to be necessary. This way, plant volumes between 50 t/a and 35.000 t/a will be reachable by 2025 (see Figure 4)

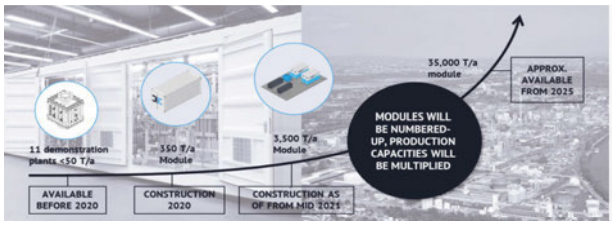

Figure 4: Plant Scale-Up concept

4. Feedstocks and FT-Products

One feature that makes the FT synthesis so extraordinarily interesting, especially for sector coupling, is the large adaptability towards feedstock. As an example, the syngas used in FT can be biomass-derived, in which case one would speak of biomass-to-liquid (BtL) process. Another possibility is to employ hydrogen, which has been generated via electrolysis together with CO_2. In addition, the source for CO_2 is neither pre-defined. This means it could be provided from a biogas-source or from an industrial exhaust but also from ambient air. Together with partners in various research project, national and international, INERATEC has developed and applied various BtL and PtL value chains.
In the REDIFUEL project, just like in the forementioned projects COMSYN and FLEXCHX, biomass is used as feedstock but this time the process is designed to produce high-performance fuels[10]. For this purpose, INERATEC´s FT-reactor is equipped with a specially designed catalyst and produces crude which can be converted to the desired fuels via hydroformylation. Another example for BtL is currently under investigation in the EU-funded project GLAMOUR. Here glycerol, which currently is a mostly unused by-product from the biodiesel production, is used as very cheap feedstock for the production of renewable maritime and aviation fuels. INERATEC is evaluating novel 3D-printed reactor designs against their established technology and will elaborate in the course of the project a possible upscaling route for the process[11].
A completely different use case is the integration of the FT synthesis into industrial waste gas streams, and the direct utilization of CO_2 to produce chemicals. This process has been investigated and technically proven in the ICO2CHEM project, together with international partners[12]. During the project, a demonstration plant has been engineered and implemented at the industrial site of the partner InfraServ Höchst. It was shown that it is possible to produce high quality waxes from the utilized exhaust gases. Consequently, this project laid the basis for the upcoming integration of PtL-technologies at various industrial sites. This includes chemical plants but also production sites for cement or steel. The latter two in-

8https://www.comsynproject.eu/
9 http://www.flexchx.eu/
10 https://redifuel.eu/
11 https://www.glamour-project.eu/
12 https://www.spire2030.eu/ICO2CHEM

Narr Francke Attempto Verlag GmbH + Co. KG

dustries intrinsically produce CO_2 as part of their process and have an accordingly high urge to find solutions for the utilization of their waste streams. As shown, modular PtL-technologies can provide such solutions.
In a future energy system, point sources of CO_2, like the beforementioned steel and cement plants, will be very scarce and therefore not sufficient to satisfy the demand for carbon sources. Hence, the capture of CO_2 from ambient air will become more and more important for future applications. The integration of such a direct air capture together with an innovative co-electrolysis has already been shown in a world-first demonstration plant back in 2019 in the German Kopernikus project P2X. A picture of the plant can be found in Figure 5.

Figure 5: World-first demonstration plant for the integration of direct air capture, co-electrolysis and Fischer-Tropsch-synthesis

All these project results show how flexible INERATEC´s FT reactors are in the various PtL and BtL processes and that many feedstocks can be used for the process. Interestingly, the FT synthesis in microstructured reactors is at least as flexible with respect to the downstream side. With the process being an a-priori undirected chain growth mechanism, which is dependent on the process conditions, it is relatively simple to adapt the product spectrum to the customers´ requirements. Very short chain products, like gasoline or even gaseous hydrocarbons can, in principle, be as well produced as long chain waxes for fine chemical applications. The product distribution usually follows the Anderson-Schulz-Flory (ASF) distribution, given by the equation

$$w_n = n(1-\alpha)^2\alpha^{n-1}$$

,where w_n is the mass content of the product, α is the chain growth probability and n is the specific chain length. With α being a constant that is (given a fixed catalyst) directly dependent on the process conditions – mainly space velocity, temperature and pressure – the ASF distribution is easily adaptable by these parameters. It needs to be pointed out here, while there are limits to the product distribution selection and side products cannot be excluded completely, it is still possible to adapt the process in a wide range. This has been proven for INERATECs microstructured FT-reactor technology in a number of projects. As mentioned before, in the ICO2CHEM project, long chain waxes, that could be introduced into chemical production lines, were produced. Simultaneously, INERATEC is working together with partners in the EU-funded project KEROGREEN[13] and the project by the German Federal Ministry of Economic Affairs and Energy PowerFuel[14] on the development of drop-in renewable jet-fuel alternatives. Results indicated that the FT-products can come close to the relevant ASTM-norms and suitable refining procedures can be implemented also on a modular level. Depending on the future regulatory framework, product upgrading might even be possible without the need for a complex infrastructure of a large-scale refinery. Another product, INERATEC has successfully developed is drop-in ready Diesel. Alongside gasoline pre-cursors this is under investigation in the reFuels project together with a number of car manufacturers. Finally, it needs to be stated that the microstructured reactor technology of course can also be used for other exothermic reactions, like MeOH-synthesis – which is, as stated above, another path for PtX. This reaction pathway is investigated in the German national research project E[4]MeWi[15].

5. Summary and Outlook

Modular FT-technology has made significant advances over the last couple of years. The technology is ready to be spread out on an industrial level and INERATEC is taking steps towards this roll-out. An important step on this path will be the realization of the newly acquired EIC Accelerator project IMPOWER2X. INERATEC will use this project to prepare a serial production for the reactor modules and chemical plant units. Such a serial production can reduce the CAPEX for new plants significantly, as it reduces the individualizing efforts for the PtX-plants. The individual process units of the plant will be re-engineered and standardized to suit the modular concept and to be producible in a serial production line. Furthermore, the complete company will undergo a re-structurization procedure with the overarching goal to effectively implement the serial production on al organizational levels. Finally, INERATEC will be able to "produce chemical plants like cars": modular products manufactured on a serial production line with the possibility to individualise them with very little effort towards the needs of the customers.
This enables INERATEC not only to be supplier of plants for customers but will render the company towards a provider of fuel. For this case INERATEC implements an offtake business model in which the company identifies

[13] https://www.kerogreen.eu/
[14] https://www.elab2.kit.edu/powerfuel.php
[15] https://www.e4mewi.de/

Narr Francke Attempto Verlag GmbH + Co. KG

interesting locations for PtX plants and sells the produced fuels to customers directly, opening novel customer groups who would not consider operating chemical plants themselves.

Acknowledgements

[1] This work has received funding from the European Union's Horizon 2020 research and innovation programme under grant agreement No 884197 (GLAMOUR), 817612 (COMSYN), 768543 (ICO2CHEM), 763909 (KEROGREEN), 763919 (FLEXCHX), 817612 (REDIFUEL) and 970564 (IMPOWER2X). Further funding from the Federal Ministry of Economic Affairs and Energy (BMWi) and the Federal Ministry of Education and Research is highly acknowledged in the framework of the projects PowerFuel (03EIV071A), E4MeWi (03EI3035C), and Kopernikus P2X Phase I (03SFK2D1) and II (03SFK2D1-2).

Narr Francke Attempto Verlag GmbH + Co. KG

Outline of a 10,000 t/a PtL plant: Technological Assessment and Upscale-Study

Thorsten Jänisch
German Aerospace Center – Institute of Combustion Technology, Stuttgart, Germany

Ulf Neuling
Hamburg University of Technology – Institute of Environmental Technology and Energy Economics, Hamburg, Germany

Fabian Carels
Hamburg University of Technology – Institute of Environmental Technology and Energy Economics, Hamburg, Germany

Manfred Aigner
German Aerospace Center – Institute of Combustion Technology, Stuttgart, Germany

Martin Kaltschmitt
Hamburg University of Technology – Institute of Environmental Technology and Energy Economics, Hamburg, Germany

Uwe Gaudig
John Brown Voest GmbH, Leipzig, Germany

Summary

To mitigate climate change there is a strong need to reduce CO_2 emissions in the transport sector. Synthetic fuels from power-to-Liquid (PtL) pathways are a promising strategy, especially for sectors that are challenging to electrify. In this contribution, the outline of a 10.000 t/a PtL plant is presented. Therefore, the needed technology steps - H_2 and CO_2 supply, synthesis gas formation, fuel synthesis, and downstream/refining - were identified and different options were evaluated. With regard to the technology selection, certain general assumptions were taken into consideration, such as the TRL, the robustness of the technologies and their commercial availability. Amine scrubbing from biogenic sources was chosen for CO_2 capture. For H_2 production PEM and alkali electrolysis were assessed as best options. For synthesis gas production the reverse water gas shift (RWGS) reaction is the most promising technology, while for fuel synthesis, a Co-catalyzed low temperature Fischer-Tropsch reaction was selected. For refining of the FT-crude to fuels compliant with the given standards, hydrocracking, hydrogenation, isomerization and distillation were identified as necessary steps.

1. Introduction

Due to the progressing climate change, mankind has to solve the great challenge of transforming its industrial processes as well as the transport, heat, and energy sector towards climate neutrality. Among others, the goal for the German transport sector is a complete defossilization, ergo a transformation away from crude oil towards renewable sources and CO_2 neutrality. While in Germany the industry could already reduce their greenhouse gas (GHG) emissions by 31 - 33 % compared to 1990, there is no noteworthy GHG emission reduction in the German transport sector (i.e. road traffic, aviation, and shipping) [1]. To reach the climate goals of the German government, a fast action is necessary to reduce the CO_2 emissions in short-time. Especially, as the German government is even encouraging their aims for GHG emission reduction in this sector from 42 % [2] to 48 % [3] until 2030, compared to 1990. The replacement of fossil-based gasoline, diesel, and kerosene by PtL fuels is a good option to achieve this fast GHG emission reduction. If PtL fuels are produced from green hydrogen and CO_2 from the atmosphere or from point or biogenic sources, such as biogas or bioethanol plants, they combust CO_2 neutral. Even if the Well-to-Wheel efficiency with 13 % is low (69 % e-mobility) [4], PtL fuels have the great advantage that they can be used as direct replacement in the existing car, truck, aircraft or ship fleet (drop-in fuels) or with minor reconstructions (near-drop-in fuels), as they are chemically identical or similar to fossil-based fuels.

Narr Francke Attempto Verlag GmbH + Co. KG

As such they can be used in the existing fuelling infrastructure [5]. Because of their good gravimetric and high volumetric energy density [6], PtL fuels are a promising strategy, especially for sectors that are challenging to electrify, like long-haul air transport, marine applications or long-distance haulage. As a sufficient replacement of the existing car fleet to fuel cell or electric vehicles until 2030 is not to expect, PtL fuels could also play a key role in road transport as an intermediate solution for CO_2 emission reduction.

Currently several research projects are conducted, addressing the production of PtL fuels, e.g. the Kopernikus project P2X [7], the PtM Miniplant in Freiburg (Germany) [8] and the C^3-Mobility project [9]. But the scales are still quite far off from industrial scale. In some cases, like in P2X, decentralized production approaches are investigated. Larger PtL plants for centralized production are in planning at the moment, e.g. in Frankfurt-Höchst (Germany) with a capacity of 3,500 t/a e-fuel [10] or the Haru Oni project in Chile with about 130,000 l/a e-gasoline at the beginning [11].

This contribution presents the conceptual outline of a first of its kind 10,000 t/a demonstration PtL plant, based on a study conducted for the German Federal Ministry for Transport and Digital Infrastructure (BMVI). If built, the main goal is to gain experience with regard to process integration and optimization as well as to lay the foundation for a potential later scale up to commercial plant size, which would be in the order of at least 100,000 t/a. The PtL plant features a modular design, allowing single components of the process chain to be exchanged with other technologies at a later stage. Water electrolysis is used to produce H_2 from renewable energy, while CO_2 can stem from point sources or direct air capture. Syngas is generated via a reverse water gas shift reaction (RWGS) or a Co-Electrolysis. For the synthesis step a Fischer-Tropsch process and the methanol/DME based route are considered. The upgrading of the received intermediate (i.e. syncrude or methanol/DME) to standard conform fuels is achieved via a varying combination of refining steps, e. g. hydrocracking, hydrogenation, isomerization, and distillation. In the following sections the different technology options for each process step are referred to as "technology blocks".

A technical evaluation of the different technologies for each block, based on literature review and in-house expert judgement, was performed with respect to the technological readiness level (TRL), the scalability, conformity, integrability into the PtL plant, specific energy demand and costs, as well as accruing waste streams and byproducts. Based on this technology screening, the most promising technologies for the 10,000 t/a PtL plant were selected. Special focus is dedicated to the connection of the different technology components. Based on these results a selection of mature and robust technologies for this first of its kind plant is presented. Furthermore, highly innovative but yet not sufficiently developed components for the 10,000 t/a PtL plant were identified and will be further investigated in a parallel construction of a smaller research plant (scale: <1 % of demo plant).

2. Evaluation method

In the following section the evaluation method for the different technologies is described. Six criteria were defined. As first criterion the "accordance with the goal of the PtL concept", ergo the feasibility for a discontinuous operation with renewable (fluctuating) electrical energy was assessed. Second, the technical readiness of the technology for its application in a 10,000 t/a PtL plant was evaluated, based on the investigated TRL of the desired technology as well as on the availability of the technology in the desired scale and potential scaling problems. The third criterion was the specific energy (electric and thermal energy) and reactant demand, based per kg product. The fourth criterion was the possibility of integrating the desired technology into the PtL plant energy management and the possibility of connecting the technology to upstream, reaction, and downstream steps for the production of a fuel compliant with given standards (i.e. process integration). The fifth point was the formation of by- and waste products, and the last point the specific costs per kg product for the specific technology.

The needed information for evaluating the different technology blocks related to these criteria were obtained from literature research and in-house expert judgement. If one or more of these points were not applicable for a technology block, they were excluded from the evaluation.

An evaluation system from 0 points "unsuitable" to 5 points "very good" was defined and each technology was rated quantitatively, based on the results of the literature research and in-house expert knowledge, per criterion and then compared to competing technologies within a technology block (cf. Fig. 1). Finally, the average points of the technologies were compared. Thereby, the selection of mature and robust technologies for each process step, resp. technology block, for the initial equipment of the 10,000 t/a PtL plant was performed.

Very good	good	medium	low	very low	unsuitable
5	4	3	2	1	0

Fig. 1: Evaluation system for the different technology blocks

Afterwards a first interconnected process layout based on the selected technologies including all utility units, material flows and peripheral systems was developed.

Technologies that were not chosen for the initial equipment but have a high innovation potential were considered for a smaller research plant (scale: <1% of demo plant). The layout of the research plant was conceived in parallel but is not within the scope of this contribution. Main goal of the research plant is to further investigate these high potential technologies separately as well as in

Narr Francke Attempto Verlag GmbH + Co. KG

line with other technology steps in terms of an optimized process integration to develop them for later use in the 10,000 t/a plant.

3. Results and discussion

3.1 H_2 production

For H_2 production five different technologies were identified as potentially interesting for the 10,000 t/a PtL plant. The alkaline electrolysis (AEL), the proton exchange membrane electrolysis (PEMEL), the high temperature electrolysis (SOEL), methane pyrolysis, and steam reforming in combination with carbon dioxide capture and storage (CCS). Through literature research results, in-house expert knowledge and physical-chemical calculations, the electric and thermal energy demand, the TRL level, operation temperature, further reactant and product streams as well as the ramp-up time from standby, the H_2 purity and the specific H_2 costs per kg were investigated. The results are shown in Table 1.

Based on these values the evaluation shown in Table 2 was performed. Steam reforming with CCS is not in accordance with the PtL concept, as it cannot directly implement renewable electricity as main source of energy. Additionally, steam reforming is available on industrial scale, but the necessary CCS infrastructure does not yet exist in Germany. Thus, steam reforming with CCS is not a suitable option for the 10,000 t/a PtL plant, even if the specific energy demand is low (no electric and low thermal energy demand), the only used additional reactant besides methane is water and the H_2 production costs are low. Also, methane pyrolysis is no option for the PtL plant, due to its low technological readiness and its specific energy demand. As byproduct carbon black is formed that has to be separated and used, except by total oxidation, which would again result in significant CO_2 emissions. The specific H_2 costs would be in the same region as for steam reforming, but additional gas cleaning would be necessary. During methane pyrolysis, there would be an option for the direct formation of synthesis gas (CO, H_2) by partial oxidation of the carbon black. Thereby, and by the low H_2 costs, methane pyrolysis can become an interesting technology after further investigation, using biogas as green methane source.

Thus, the remaining technology is the water electrolysis, for which the before mentioned three options were evaluated. The AEL is the highest developed technology, followed by the PEMEL. SOEL is still at demonstration level. Even if the SOEL has a higher thermal energy demand, due to the reaction temperature of 550 to 850 °C, its electric energy demand is lower. While heat can be provided from the exothermic Fischer-Tropsch reaction, for example, electricity has to be produced in a renewable manner. This is a great advantage, leading to a better ranking of the SOEL compared to AEL and PEMEL, for the criterion of "Integration in the PtL system", where

Table 1: Process data for H2 production [Investigated using in-house expert knowledge and literature]; LHV: Lower heating value; CCS: Carbon dioxide capture and storage; *Calculated with an electricity rate of 7 ct/kWh, 7000 Full load hour/a and literature values for CAPEX & OPEX; References: [12-19].

	Energy demand [kWh/kg H_2]			TRL	Temperature	Reactant demand	Ramp-up time from standby (cold)	Product gas quality	Specific costs [€/kg H_2]
	el.	therm.	chem.						
Alkaline electrolysis (AEL)	54	0.15	-	9	60 - 80 °C	Water: 12 kg/kg H_2 Byproduct: O_2	1 - 2 h	H_2-purity 99 - 99.8 %	4.5 - 5.2*
Proton exchange membrane electrolysis (PEMEL)	58	0.35	-	7 - 8	50 - 80 °C	Water: 12 kg/kg H_2 Byproduct: O_2	5 - 10 min	H_2-purity >99.99 %	5.5 - 6.3*
High temperature electrolysis (SOEL)	41	9.37	-	6	550 - 850 °C	Water (vapor): 12 kg/kg H_2 Byproduct: O_2	Several hours	H_2-purity 99.8 %; Synthesis gas formation possible (Co-Electrolysis)	~5*
Methane pyrolysis	9.5	-	62.5 (CH_4, LHV)	5 - 6	800 - 2000 °C	Byproduct: C (carbon black)	-	Gas cleaning necessary; Synthesis gas formation possible	2.5 - 3
Steam reforming (with CCS)	-	0.5-0.58	46.7 (CH_4, LHV)	9	820 - 880 °C	Water: 7.5 - 15 kg/kg H_2 Exhaust: CO_2	-	Synthesis gas formation possible	2 - 2.5

Narr Francke Attempto Verlag GmbH + Co. KG

Table 2: Evaluation of the different H_2 production technologies; CCS: Carbon dioxide capture and storage.

	In accordance with the goal of the PtL-concept	Technological readiness	Specific energy and reactant demand	Integration in the PtL system	By-/Waste products	Specific costs	ø
AEL	4	5	3	3	5	3	3.8
PEMEL	5	4	2	3	5	2	3.5
SOEL	3	2	4	4	4	3	3.3
Methane pyrolysis	1	1	1	4	3	4	2.3
Steam reforming (+ CCS)	0	5	5	5	1	5	3.5

PEMEL and AEL are evaluated equally, and for the criterion "specific energy and reactant demand". Regarding PEMEL and AEL, the AEL was ranked higher according to the latter criterion. As reactant for all three electrolysis technologies, only water is needed, while oxygen is formed as byproduct. The latter can be sold to improve the business plan of the plant. The H_2 is gained in very high purity >99.8 %, but the H_2 price with 4.5 (AEL) to 6.3 €/kg (PEMEL) is comparatively high. For the 10.000 t/a plant, the AEL needs to be upscaled to about 30 MW. Thanks to its high TRL, this upscaling is not critical. For PEMEL a numbering up of smaller modules would lead to the 30 MW requirement. For PEMEL Iridium (Ir) is needed as raw material for the electrodes, which might be critical for a state-of-the-art use of PEMEL, especially for its use in various industrial PtL plants. Even if a numbering up to 30 MW for SOEL would be possible, the complex technology, a challenging heat management as well as occurring degradation make the SOEL not suitable for the initial equipment for the first of its kind 10,000 t/a PtL plant. However, it is an interesting technology for the future and the research plant. Thus, for H_2 production in the 10,000 t/a PtL plant, the best options are AEL and PEMEL, which are ranked nearly equally to one another and show low upscale and operational problems. Therefore, both technologies shall be used in the PtL plant.

3.2 CO_2 capture

For CO_2 separation, seven technology options were investigated for CO_2 exploitation from two different sources. First, the membrane separation, water washing, amine scrubbing, and pressure swing adsorption for CO_2 separation form biogenic point sources, such as digester gases (e.g. biogas plant or bioethanol plant). Second, the high temperature aqueous solution DAC (direct air capture), the low temperature DAC with temperature swing adsorption, and the low temperature DAC with moisture swing adsorption for CO_2 separation from the atmosphere. Via in-house expert knowledge, physical-chemical calculations, and literature research the energy demands, the TRL levels, the CO_2 purity, the specific CO_2 costs, the requisite auxiliary materials, as well as waste/byproducts were investigated (cf. Table 3). The evaluation of the technologies according to the defined criteria (cf. Chapter 2) is shown in Table 4. The three direct air capture (DAC) methods fit optimal to the PtL concept, as CO_2 from the atmosphere is used, thus being more flexible than biogenic CO_2 capture which has to rely on the operation of a biogas or bioethanol plant. But the DAC methods are of much lower technical readiness than the methods for separation from biogenic digester gases. The highest TRL has the low temperature DAC with temperature swing adsorption (TRL 8) and would be thereby the only possible DAC option for a 10,000 t/a PtL plant. But the CO_2 costs are very high (155 €/t_{CO2} compared to 50 - 100 €/t_{CO2}) as well as the energy demand, that is much higher than for the CO_2 separation from biogenic sources. Therefore, the low temperature DAC with temperature swing adsorption is a promising option for CO_2 exploitation from air, but it has to be further investigated (lower energy demand, lower price, higher TRL, etc.) before it is applicable for large PtL plants and will only be considered for the research plant.
Thus, for the 10.000 t/a PtL plant a biogenic CO_2 source, e.g. a biogas or bioethanol plant, must be chosen. The technological readiness is fairly developed for all methods shown (TRL 9), except the membrane separation (TRL 6-8), which makes scaling up difficult and eliminates this technology as an option for the 10.000 t/a PtL plant. Water washing, amine scrubbing, and pressure swing adsorption can be scaled without problems to 10.000 t/a fuel scale, but with water washing a very impure CO_2 is obtained (14 - 22 vol%), which makes this technology not applicable. Pressure swing adsorption and amine scrubbing can both be used for the 10.000 t/a PtL plant. In the end, amine scrubbing was chosen, as higher CO_2 purities are obtained along with the lowest CO_2 costs.

3.3 Synthesis gas formation

The next step in the PtL process is the formation of synthesis gas (CO, H_2) (syngas) from H_2 and CO_2. For this process, four technologies were considered: water electrolysis, e.g. AEL, in combination with a reverse water gas shift reaction (RWGS), co-electrolysis, dry biogas reforming and autothermal reforming of FT-tail gas. The investigated data, based on literature research, in-house expert knowledge, and physical-chemical calculations, includes the necessary reactants, the energy demand, the TRL, and the residue/waste products (cf. Table 5). The evaluation according to Chapter 2 is shown in Table 6.
The co-electrolysis is suitable for the Fischer-Tropsch (FT) route, as it directly converts CO_2 and H_2O to syn-

Narr Francke Attempto Verlag GmbH + Co. KG

thesis gas; however, it does not fit for methanol synthesis from CO_2 and H_2. The "AEL plus RWGS" process fit for both cases: for FT-synthesis, AEL and RWGS are put in line; for methanol synthesis, the RWGS is bypassed.
Co-electrolysis could possibly be scaled up to the desired scale by numbering up, but with a low TRL of 4, many difficulties must still be faced (e.g. membrane stability or degradation), while for RWGS, with a TRL of 6 the technology is more mature. Scaling up to the 10,000 t/a scale should, therefore, be possible. The biggest problem appears to be a CO_2 neutral heat supply, as the energy demand is quite high, even a bit higher than for co-electrolysis. As compared to co-electrolysis for syngas formation with AEL + RWGS, two reaction steps are needed instead of one. The "integration into the PtL system" is thereby ranked higher for co-electrolysis.
Waste products of AEL + RWGS are O_2 and H_2O. The first can be sold and the latter used in the AEL again. Also, for the co-electrolysis, the byproduct is O_2.
The "autothermal reforming of FT-tail gas" is a commercially available option, but for its application a tail gas must already exist. Thus, this reaction is an option for tail gas recycling and thereby for process optimization, but not for main synthesis gas production. Also, the dry reforming of methane and CO_2 is an interesting option for synthesis gas production, but, since the methane from biogas plants is mostly used in other ways (e.g. power generation), the methane from the biogas plant is limited. Thus, grey methane from natural gas would be needed, making it incompatible with a green PtL plant. Additionally, no renewable electricity would be intro-

Table 3: Process data for CO_2 capture [Investigated using in-house expert knowledge and literature]; DAC: Direct air capture; References: [20-30].

		Energy demand [kWh/kg CO_2]		TRL	Purity CO_2 [vol%]	Spec. CO_2 costs [€/t CO_2]	Auxiliary material	Waste/ Byproducts
		el.	therm.					
Biogenic digester gas	Membrane separation	0.34	-	6 - 8	75	~95	-	-
	Water washing	0.2	-	9	14 - 22	*No utilizable CO_2*	Additive absorbents	Waste water
	Amine scrubbing	0.01	0.63 (120 - 140 °C)	9	90 - 99.9	50 - 75	Treated absorbent	Used absorbent
	Pressure swing adsorption	0.2	-	9	87 - 99.9	~100	Adsorbent	Used adsorbent
Atmosphere	High temperature aqueous solution DAC	1.5 - 1.8	-	6	~97 %	186	Potassium hydroxide, Water (4.7 l/kg CO_2), Calcium carbonate	Waste water $CaCO_3$
	Low temperature DAC with temperature swing adsorption	0.3 - 0.65	1.5 - 2.0 (100 °C)	8	>99.9 %	155	Amine based sorbent	Waste Water
	Low temperature DAC with moisture swing adsorption	0.3	-	5	n.s.	144	n.s.	n.s.

Table 4: Evaluation of the different CO_2 capture technologies; DAC: Direct air capture; *No data available.

		In accordance with the goal of the PtL-concept	Techno-logical readiness	Specific energy and reactant demand	Integration in the PtL system	By-/Waste products	Specific costs	Ø
Biogenic digester gas	Membrane separation	4	3	3	2	5	4	3.5
	Water washing	4	5	4	0	3	0	2.7
	Amine scrubbing	4	5	3	5	3	5	4.2
	Pressure swing adsorption	4	5	4	3	3	4	3.8
Atmosphere	High temperature aqueous solution DAC	5	2	1	2	2	1	2.2
	Low temperature DAC with temperature swing adsorption	3	4	2	5	4	2	3.3
	Low temperature DAC with moisture swing adsorption	5	0	3	*	*	2	2.5

Narr Francke Attempto Verlag GmbH + Co. KG

duced into the system. Thus, as the most suitable option for synthesis gas generation, a coupling of water electrolysis (e.g. AEL) and RWGS was chosen for the initial equipment of the 10,000 t/a PtL plant. The co-electrolysis will be closer investigated at the research plant.

3.4 Fischer-Tropsch synthesis

After synthesis gas formation comes the synthesis step. One very promising option for producing PtL fuels is the Fischer-Tropsch synthesis (FTS).
Three different process ways were examined: the low temperature FTS with Fe-catalyst, the low temperature FTS with Co-catalyst, and the high temperature FTS with Fe-catalyst. The investigated process data are shown in Table 7: CO and H_2 demand, investment (invest) costs, TRL, reaction temperature, residue/waste products and syncrude composition. Table 8 shows the evaluation of these values. Easy to see is that the high temperature FTS is not suitable for a PtL plant, as the main products are short chain hydrocarbons with a chain length from C1 - C4 (57 %), which is even too small for gasoline. With the low temperature FTS, the formed chain length is longer: 45 % waxes (>C22) and 42 % hydrocarbons with a chain length between C5-C22 are obtained by Co-catalyzed FTS; 50 % waxes (>C22) and 32 % hydrocarbons between C5 and C22 are obtained for the Fe-catalyzed FTS, depending on the chosen process conditions.
In both cases, scaling up is not the problem to solve, but rather the scaling down to 10,000 t/a fuel scale, as FTS is used in the industry in large scales for years, like the Sasol process [31] or the Pearl GTL process from Shell [32]. The core challenge is to run the FTS with acceptable costs in this small scale. The needed scale for the 10,000 t/a PtL plant is not available on the market and must, therefore, be developed. One core challenge of the FTS is its bad performance to load flexible operation. This problem has to be solved for the desired PtL plant either by optimizing the FTS synthesis to work with fluctuating reactant input, or by installing a synthesis gas buffer to compensate the fluctuation. As reactor, a tube bundle reactor or microstructure reactors with fixed catalyst beds can be used. Microstructure reactors have the benefit of well controlled heat development, but for a 10,000 t/a fuel scale, a huge number of reactors would be needed. Therefore, for the 10,000 t/a plant, a tube bundle reactor shall be used.
For low temperature FTS, the Co-catalyzed route was chosen, as it has a slightly lower reactant (CO, H_2) demand and has a slightly higher yield in hydrocarbons with chain lengths ≥C5 (87 % to 82 %).

3.5 Downstream/ Refining of FT syncrude

After the FTS, a crude mixture of alkanes, alkenes, alcohols, and other organic compounds with different chain lengths are obtained, denoted as FT-crude or syncrude. This syncrude cannot be used as fuel immediately, but must be processed in several downstream/refining process steps (cf. Table 9). As those processes are mandatory to fulfill the given fuel specifications, no eva-

Table 5: Process data for synthesis gas (syngas) formation [Investigated via in-house expert knowledge and literature]; LT: Low temperature; *Assumed syngas composition: H_2/CO = 2/1; **Assumed syngas composition: H_2/CO = 1/1; References: [33-44].

		Reactants	Energy demand		Reactant demand	TRL	Residues/ Waste products
			el.	therm.			
LT electrolysis + RWGS	AEL	H_2O	54 kWh/kg H_2	0.15 kWh/kg H_2	12 kg H_2O/kg H_2	9	~8 kg O_2/kg H_2
	RWGS	$H_2 + CO_2$	-	0.4 - 0.5 kWh/kg CO at 700 - 1000 °C	~0.07 kg H_2/kg CO ~1.6 - 1.7 kg CO_2/kg CO	6	~0.65 kg H_2O/kg CO
	Overall process	$H_2O + CO_2$	~10 kWh/ kg syngas*	~0.47 kWh/ kg syngas*	~1.5 kg H_2O/kg syngas* ~1.5 kg CO_2/kg syngas*	6	1 kg O_2/kg syngas* 0.57 kg H_2O/kg syngas*
Co-electrolysis		$H_2O + CO_2$	~8.8 kWh/ kg syngas*	0.75 - 1 kWh/ kg syngas*	~1.6 kg CO_2/kg syngas* ~1.2 kg H_2O/kg syngas*	4	O_2 Waste heat (550 - 850 °C)
Dry biogas reforming		Biogas	Methane demand: 0.3 kg/kg CO		~0.75 kg CO_2/kg syngas** ~0.28 kg CH_4/kg syngas **	5 - 6	-
Autothermal reforming of FT-tail gas		FT-tail gas	-	-	~0.4 - 0.6 kg CH_4/kg syngas* ~0.25 kg O_2/kg syngas* ~0.875 kg H_2O/kg syngas* ~0.17 kg CO_2/kg syngas*	9	-

Narr Francke Attempto Verlag GmbH + Co. KG

Table 6: Evaluation of the different synthesis gas formation technologies; LT: Low temperature; †Data availability not sufficient for qualitative comparison.

	In accordance with the goal of the PtL-concept	Techno-logical readiness	Specific energy and reactant demand	Integration in the PtL system	By-/Waste products	Specific costs†	Ø
LT electrolysis + RWGS	4	3	3	4	5		3.8
Co-electrolysis	3	0	4	5	5		3.4
Dry biogas reforming	0	3	5	3	4		3.0
Autothermal reforming of FT-tail gas	3	5	5	5	4		4.4

Table 7: Process data for Fischer-Tropsch synthesis (FTS) [Investigated using in-house expert knowledge and literature]; HC: Hydrocarbons, References: [12; 33; 45-47].

	CO demand [kg CO/kg syncrude]	H_2 demand [kg H_2/kg syncrude]	Invest costs [k€/MW]	TRL	Temperature	Residues/ Waste products	Syncrude-composition
Low temperature FTS with Fe-catalyst	2.3 - 2.5	~0.17	450 - 725 Cheap catalyst	9	220 - 230 °C	Waste water, Tail gas	~50 % Waxes (>C22) ~32 % HC C5-C22 ~18 % HC C1-C4
Low temperature FTS with Co-catalyst	2.2 - 2.4	~0.16	450 - 725 Expensive catalyst	9	220 - 230 °C	Waste water, Tail gas	~45 % Waxes (>C22) ~42 % HC C5-C22 ~13 % HC C1-C4
High temperature FTS with Fe-catalyst	4.5 - 4.7	~0.33	500 - 800 Cheap catalyst	9	320 - 340 °C	Waste water, Tail gas	<3 % Waxes (>C22) ~40 % HC C5-C22 ~57 % HC C1-C4

Table 8: Evaluation of the different Fischer-Tropsch synthesis (FTS) technologies; *Criterion not evaluated, as not meaningful for this process step.

	In accordance with the goal of the PtL-concept*	Techno-logical readiness	Specific energy and reactant demand	Integration in the PtL system	By-/Waste products	Specific costs	Ø
Low temperature FTS with Fe-catalyst		5	4	4	4	5	4.4
Low temperature FTS with Co-catalyst		5	5	5	4	4	4.6
High temperature FTS with Fe-catalyst		5	2	1	2	4	2.8

Narr Francke Attempto Verlag GmbH + Co. KG

luation of the specific technologies was carried out.
Essential for the refining of the FT-crude is the hydrocracking that cleaves long chain hydrocarbons (e.g. waxes (>C22)) to the desired chain length. For kerosene the range of C9 - C17 and for diesel the range of C9 - C22 is desired. Nevertheless, it is not possible to crack the crude to only one fraction, so that always several fractions are obtained, e.g. gasoline (C5 - C11) and kerosene. Furthermore, through the addition of hydrogen, double bonds can be hydrogenated and alkenes are converted to alkanes. Organic acids, aldehydes and alcohols in the crude are also reduced to alkanes. If after hydrocracking alkenes or alcohols remain in the cracked crude, or if the original FT-crude should not be cracked, an (additional) hydrogenation is necessary to reduce all oxygen compounds and unsaturated compounds to alkanes. Afterwards an isomerization is needed to branch the alkanes and to adjust the desired i-alkane/n-alkane ratio. Hydrogenation and isomerization can be performed in parallel in one process step.
Afterwards several distillations are necessary to obtain the desired fuel fractions, which must be compliant with the given standards. For synthetic kerosene, the ASTM 7566 is applicable, for Diesel the DIN EN 590 and for gasoline the DIN EN 228.

3.6 Methanol (MeOH) synthesis and further processing to fuels

Methanol can be produced via two processes. Directly from CO_2 and H_2 or from synthesis gas (CO, H_2). The first process has the benefit, that CO_2 must not be converted to CO by means of co-electrolysis or RWGS. Thus, energy could be saved by avoiding the high temperatures for these applications (550 - 1000 °C).
The investigated data for these two methods are shown in Table 10 and the evaluation according to Chapter 2 is shown in Table 11.
For the second process, in this study an RWGS was combined with the methanol synthesis from synthesis gas. In this case, the technological readiness of the direct methanol synthesis from CO_2 is a bit higher (TRL 6 - 8) than for the synthesis gas synthesis (TRL 6), due to the required RWGS. Both processes have similar reactant (CO_2, H_2) as well as similar energy demands (electric and thermal), as long as for the synthesis gas based process the waste heat and heat demand are optimally integrated. In both cases, due to the exothermic methanol synthesis, waste heat is produced, which can be used in an integrated manner in the PtL plant to cover other heat demands. In both cases, the specific investment costs are very high (5500 and 6300 - 6670 €/(kg MeOH/h)). For both processes waste water is produced, which can be reused in the electrolysis after purification. For the direct methanol synthesis, exhaust gases like methane and CO are formed. Regarding these arguments, the direct methanol synthesis from CO_2 and H_2 is the more promising option. However, the further processing of the methanol to fuels is challenging (cf. Table 12). While Methanol-to-Gasoline (MtG) is well known, and scaling up to the 10,000 t/a scale would be possible by numbering up, this technology is not conducive if kerosene is the target product. Therefore, the Methanol-to-Jet (MtJ) process must be applied, which is still being researched on lab scale (TRL 4 - 5). According to the alcohol-to-jet process, also for MtJ the three reaction steps dehydration (Methanol-to-olefins (MtO)), oligomerization and hydrogenation are under investigation [58], but problems occur producing sufficiently long enough chain length (>C6), even if the individual process steps are well understood. As the main focus of this PtL plant is kerosene production, the methanol route (methanol synthesis + MtJ) will be further considered at the smaller research plant. However, it is not a suitable option for the 10,000 t/a PtL plant. Thus, the FT-route was selected for the demonstration plant.

Table 9: Downstream methods for FT-crude (syncrude) refining to fuels [Investigated via in-house expert knowledge and literature]; References: [48-57].

	TRL	Function	Usage	Energy demand [kWh/kg jet fuel]		H_2 demand [kg/kg jet fuel]
				electric	thermal	
Hydrocracking	9	Catalytic conversion of long chain hydrocarbons to shorter hydrocarbons and hydrogenation of double bonds, alcohols, etc.	• Cracking of FT-product to the desired chain length distribution (solid waxes to liquid products) • Conversion of alkenes, alcohols, etc. to alkanes	0.01 (wax pumps)	-0.1 (exotherm)	for FT-waxes: 0.05 - 0.15
Hydrogenation	9	Hydrogenation of double bonds, alcohols, etc.	Conversion of alkenes, alcohols, etc. to alkanes	-	(exotherm)	0.03
Isomerization	9	Catalytic conversion of linear alkanes and alkenes to branched alkanes and alkenes.	Optimizing of freezing point	-	0.1 (reactant heating)	0.05

3.7 DME synthesis

A third alternative to FTS and the methanol route is the dimethyl ether (DME) synthesis. DME can be produced

Narr Francke Attempto Verlag GmbH + Co. KG

via three ways. By dehydration of methanol, from synthesis gas or directly from CO_2 and H_2. The investigated process parameters are shown in Table 13, and the evaluation in Table 14. For DME synthesis from methanol, the methanol must first be formed from CO_2 and H_2. This reaction also limits the TRL of this process to 6 to 8. TRL 6 is reached for the synthesis gas DME synthesis, as the synthesis gas has to be formed before by a co-electrolysis or, as in this study, with a RWGS limiting the TRL. On the other side, the direct synthesis of DME from CO_2 and H_2 has an even lower TRL of 4 - 5. The reactant demand (CO_2, H_2) is quite similar for direct and syngas synthesis and higher for synthesis based on methanol. The excess heat is nearly equal for all three methods, if the heat integration is optimum for DME from synthesis gas (-0.6 - -0.8 kWh/kg DME). The excess heat can be used as heat source for other process steps. For the DME from methanol route, additional electric energy is needed (methanol synthesis). However, the specific DME investment costs are, as for methanol synthesis, very high (7900 - 9460 €/(kg DME/h)). As a residue, waste water is formed for all DME synthesis routes, which can be reused in the electrolysis. For synthesis via methanol additional exhaust gas is produced during methanol synthesis (CO, CH_4) and for syngas-DME synthesis additional CO_2.
The workup to fuels would be identical to the methanol route, MtG or MtJ, and would face the same problems.
Thus, no reaction route is particularly promising for the 10,000 t/a PtL plant. Furthermore, DME is an intermediate product of the MtG and MtJ process [59] and is produced during the methanol route. While the methanol route will become part of the research plant, the DME route will not be considered at all.

3.8 Initial equipment of the 10,000 t/a PtL plant

After the evaluation of the single technology steps for the 10,000 t/a PtL plant, the best technologies steps were combined within a PtL process.
For water electrolysis two technologies were chosen, AEL and PEMEL, which will produce H_2 in equal amounts (50 % each). CO_2 will be obtained from biogenic digestor gases (biogas plants or bioethanol plants) via amine scrubbing, while the synthesis gas formation will be performed by RWGS. As fuel synthesis step, the

Table 10: Process data for methanol synthesis [Investigated via in-house expert knowledge and literature]; MeOH: Methanol; References: [26; 45; 60-67].

		Reactant demand			TRL	Energy demand		Specific investment costs	Residues/ Waste products
		H_2	CO_2	CO		electric	thermal		
Methanol from CO_2 & H_2		~0.2 [kg/kg MeOH]	1.4 - 1.5 [kg/kg MeOH]	-	6 - 8	0.11 - 0.17 [kWh/kg MeOH]	~-0.4 [kWh/kg MeOH] (210 - 300 °C)	~5,500 [€/(kg MeOH/h)]	Waste water (0.57 kg/kg MeOH) Exhaust gas, e.g. CO & CH_4 (0.91 kg/kg MeOH)
Methanol from CO & H_2	RWGS	~0.07 [kg/kg CO]	1.6 - 1.7 [kg/kg CO]	-	6	-	0.4 - 0.5 [kWh/kg CO] with 700 - 1000 °C	1,300 [€/(kg CO/h)]	Waste water (~0.65 kg/kg CO)
	MeOH-synthesis	~0.13 [kg/kg MeOH]	-	0.6 - 0.9 [kg/kg MeOH]	9	0.15 [kWh/kg MeOH]	~-0.75 [kWh/kg MeOH] (240 - 270 °C)	~5,500 [€/(kg MeOH/h)]	Waste water (~0.14 kg/kg MeOH)
	Overall process	~0.2 [kg/kg MeOH]	1.0 - 1.5 [kg/kg MeOH]	-	6	0.15 [kWh/kg MeOH]	Heat Demand: 0.24 - 0.45 Waste heat: -0.75 [kWh/kg MeOH]	6,300 - 6,670 [€/(kg MeOH/h)]	Waste water (~0.73 kg/kg MeOH)

Table 11: Evaluation of the different methanol synthesis technologies.

	In accordance with the goal of the PtL-concept	Techno-logical readiness	Specific energy and reactant demand	Integration in the PtL system	By-/Waste products	Specific costs	Ø
Methanol from CO_2 & H_2	3	3	5	4	3	5	3.8
Methanol from CO & H_2	3	2	5	3	3	4	3.3

Narr Francke Attempto Verlag GmbH + Co. KG

Table 12: Evaluation of the different methanol to fuel technologies; *Criterion not evaluated, as not meaningful for this process step; †Data availability not sufficient for qualitative comparison.

	In accordance with the goal of the PtL-concept*	Techno-logical readiness	Specific energy and reactant demand†	Integration in the PtL system	By-/Waste products†	Spec. costs†	Ø
Methanol-to-Gasoline (MtG)		5		0			
Methanol-to-Jet (MtJ)		0		5			

Table 13: Process data for dimethyl ether (DME) synthesis [Investigated via in-house expert knowledge and literature]; References: [45; 62; 65-70].

		Reactant demand				TRL	Energy demand		Specific investment costs	Residues/ Waste products
		H_2	CO_2	CO	MeOH		electric	thermal		
DME from methanol	Methanol-synthesis	~0.2 [kg/kg MeOH]	1.4 - 1.5 [kg/kg MeOH]	-	-	6 - 8	0.11 - 0.17 [kWh/kg MeOH]	~-0.4 [kWh/kg MeOH] (210 - 300 °C)	~5,500 [€/(kg MeOH/h)]	Waste water (0.57 kg/kg MeOH) Exhaust gas, i.e. CO & CH_4 (0.91 kg/kg MeOH)
	DME-synthesis	-	-	-	1.4 - 1.7 [kg/kg DME]	9	-	(-0.03) - (-0.14) [kWh/kg DME]	-	Waste water (~0.4 kg/kg DME)
	Overall process	0.28 - 0.34 [kg/kg DME]	1.96 - 2.55 [kg/kg DME]	-	-	6 - 8	0.15 - 0.29 [kWh/kg DME]	(-0.6) - (-0.8) [kWh/kg DME]	-	Waste water (1.2 - 1.4 kg/kg DME) Exhaust gas (1.3 - 1.6 kg/kg DME)
DME from CO & H_2	RWGS	~0.07 [kg/kg CO]	1.6 - 1.7 [kg/kg CO]	-	-	6	-	0.4 - 0.5 [kWh/kg CO] with 700 - 1000 °C	1,300 [€/(kg CO/h)]	Waste water (~0.65 kg/kg CO)
	DME-synthesis	~0.17 [kg/kg DME]	-	~1.2 [kg/kg DME]	-	9	-	-1.24 [kWh/kg DME]	~7,900 [€/(kg DME/h)]	Waste water (~0.4 kg/kg DME) CO_2
	Overall process	~0.25 [kg/kg DME]	1.9 - 2.0 [kg/kg DME]	-	-	6	-	Need: 0.48 - 0.6 Waste: -1.24 [kWh/kg DME]	9,460 [€/(kg DME/h)]	Waste water (~1.2 kg/kg DME) CO_2
DME from CO_2 & H_2	Overall process	~0.25 kg/kg DME	~1.9 kg/kg DME	-	-	4-5	-	-0.74 kWh/kg DME	~7,900 [€/(kg DME/h)]	Waste water (~1.2 kg/kg DME)

Table 14: Evaluation of the different dimethyl ether (DME) synthesis technologies; *No data available

	In accordance with the goal of the PtL-concept	Techno-logical readiness	Specific energy and reactant demand	Integration in the PtL system	By-/Waste products	Specific costs	Ø
DME from methanol	3	3	3	3	2	*	2.8
DME from CO & H_2	3	2	3	3	3	2	2.7
DME from CO_2 & H_2	3	0	3	1	3	3	2.2

Co-catalyzed low temperature FT-synthesis was chosen. As refining steps, to obtain the desired fuel (gasoline, diesel and especially kerosene), a hydrocracker, a hydrogenation and an isomerization unit, as well as distillation units were integrated.

Fig. 2 shows the resulting flow sheet and the detailed coupling of the single technologies selected for the 10,000 t/a PtL plant. The 10,000 t/a fuels are divided into a kerosene fraction (C9 - C16; target product), a diesel fraction (C17 - C25), and a naphtha fraction (C6 - C8; usable for gasoline

Narr Francke Attempto Verlag GmbH + Co. KG

after further processing). For hydrogen production, the two electrolysis units were coupled in parallel. The produced H_2 and captured CO_2 are fed into the RWGS. The synthesis gas is then led into the FT reactor. The formed FT-crude (syncrude) is fed to a hot separator, where the waxes are separated from the remaining crude. The waxes are then hydrocracked and afterwards fed to a Middle distillate(M)-rectification unit. The remaining FT-crude is fed into a cold separator. The light products are fed back to the RWGS, and the heavier products are fed to the M-rectification. The head product of M-rectification runs to a Naphtha(N)-rectification, where the head product is fed back to the RWGS, the bottom product is the naphtha fraction. The bottom product of the M-rectification is fed to a hydrogenation unit, where the isomerization takes place in parallel, followed by a kerosene(K)-rectification. The head product is the kerosene fraction, and the bottom product is fed to a Diesel(D)-rectification. Here, the head product builds the diesel fraction. The bottom product is fed back to the hydrocracker.

4. Conclusion

The conceptual outline of a 10,000 t/a PtL plant is presented. The needed technology steps were identified, and the different technological options were evaluated. With regard to the technology selection, certain general assumptions were taken into consideration, such as the TRL, the robustness of the technologies, and their commercial availability. As result the initial equipment consists of an AEL and PEMEL for water electrolysis (H_2 production) and an amine scrubbing for CO_2 capture from biogenic sources (biogas plant, bioethanol plant).
Via a RWGS, the CO_2 and H_2 is converted to synthesis gas (CO, H_2), followed by a Co-catalyzed low temperature Fischer-Tropsch synthesis. The crude is then refined by hydrocracking, hydrogenation, isomerization, and distillation to achieve the three fuel fractions: kerosene, diesel, and naphtha. Furthermore, the coupling of these technologies was investigated and an integrated process flowsheet was developed.

5. Acknowledgment

This study was funded by the German Federal Ministry for Transport and Digital Infrastructure (BMVI) (03B40901).

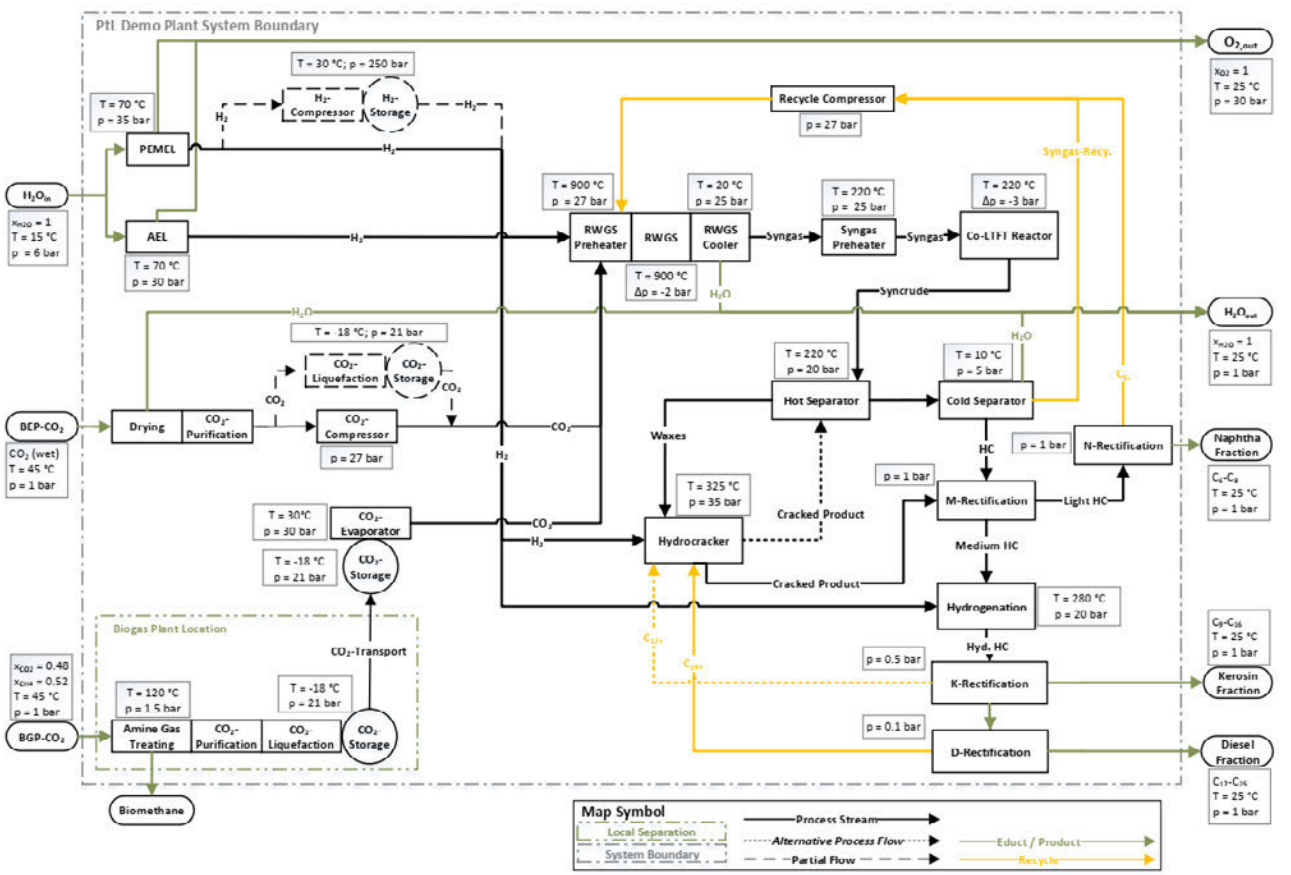

Fig. 2: Process scheme of a 10,000 t/a PtL plant; BGP: Biogas plant; BEP: Bioethanol plant; AEL: Alkaline electrolysis; PEMEL: Proton exchange membrane electrolysis, RWGS: Reverse water gas shift reaction, Syngas: Synthesis gas (CO, H_2); Co-LTFT: Cobalt catalyzed low temperature Fischer-Tropsch synthesis; Syncrude: Fischer-Tropsch (FT)-crude; M-Rectification: Middle-distillate rectification; HC: Hydrocarbons; Hyd.: hydrogenated; K-Rectification: Kerosene rectification; D-Rectification: Diesel rectification.

Narr Francke Attempto Verlag GmbH + Co. KG

References

[1] German Federal Environmental Agency, Indicator: Greenhouse gas emissions. Available online: https://www.umweltbundesamt.de/en/indicator-greenhouse-gas-emissions#at-a-glance (accessed on 31 May 2021).

[2] Klimaschutzprogramm 2030 der Bundesregierung zur Umsetzung des Klimaschutzplans 2050. Available online: https://www.bundesregierung.de/resource/blob/975226/1679914/e01d6bd855f09bf05cf7498e06d0a3ff/ 2019-10-09-klima-massnahmen-data.pdf?download=1 (accessed 31 May 2021).

[3] German Government, Entwurf eines ersten Gesetzes zur Änderung des Bundes-Klimaschutzgesetzes. Available online: https://www.bmu.de/fileadmin/Daten_BMU/Download_PDF/Glaeserne_Gesetze/19._Lp/ksg_aendg/Entwurf/ksg_aendg_bf.pdf (accessed on 31 May 2021).

[4] Agora Verkehrswende, Agora Energiewende and Frontier Economics (2018): The Future Cost of Electricity-Based Synthetic Fuels. Available online: https://static.agora-energiewende.de/fileadmin/Projekte/2017/SynKost_2050/Agora_SynKost_Study_EN_WEB.pdf (accessed on 31 May 2021).

[5] Global Alliance Powerfuels, Powerfuels Application Fields - Factsheets about powerfuels technologies and their areas of application. Availabe online: https://www.powerfuels.org/fileadmin/gap/Publikationen/Factsheets/Combined_Factsheets.pdf (accessed on 31 May 2021).

[6] Rao, A. G.; Bhat, A.: Hybrid Combustion System for Future Aero Engines. 2nd National Propulsion Conference NPC-2015, February 23-24, 2015, IIT Bombay, Powai, Mumbai, NPC2015-92.

[7] Federal ministry of education and research, P2X-How the Kopernikus project P2X converts renewable electricity into plastics and fuels, gases and heat. Available online: https://www.kopernikus-projekte.de/en/projects/p2x (accessed on 31 May 2021).

[8] Fraunhofer ISE, A Glimpse into Real-Time Methanol Synthesis: Dynamic Operation of a Miniplant at Fraunhofer ISE. Available online: https://www.ise.fraunhofer.de/en/press-media/press-releases/2020/a-glimpse-inot-real-time-methanol-synthesis-dynamic-operation-of-a-miniplant-at-fraunhofer-ise.html (accessed on 31 May 2021).

[9] C3-Mobility, Climate Neutral Fuels for the Traffic of the Future. Available online: http://www.c3-mobility.de/ (accessed on 31 May 2021).

[10] INERATEC, Industrial Power-to-Liquid Pioneer Plant 2022 in Germany. Available online: https://ineratec.de/en/power-to-liquid-pioneer-plant-2022/ (accessed on 31 May 2021).

[11] Haru Oni, Decarbonizing transportation. Available online: https://www.siemens-energy.com/global/en/offerings/renewable-energy/hydrogen-solutions/haru-oni.html (accessed on 31 May 2021).

[12] de Klerk, A.: Fischer-Tropsch Refining. 1st edn. Weinheim: Wiley-VCH, ISBN: 978-3-527-32605-1.

[13] Peng, X. D.: Analysis of the Thermal Efficiency Limit of the Steam Methane Reforming Process. Ind. Eng. Chem. Res., 51 (2012) 50, 16385 - 16392, doi: 10.1021/ie3002843.

[14] Buttler, A.; Spliethoff, H.: Current status of water electrolysis for energy storage, grid balancing and sector coupling via power-to-gas and power-to-liquids: A review. Renewable and Sustainable Energy Reviews, 82 (2018) 3, 2440 - 2454, doi.: 10.1016/j.rser.2017.09.003.

[15] Schneider, S.; Bajohr, S.; Graf, F.; Kolb, T.: Verfahrensübersicht zur Erzeugung von Wasserstoff durch Erdgas-Pyrolyse. Chem. Ing. Tech., 92 (2020) 8, 1023 - 1032, doi.: 10.1002/cite.202000021.

[16] Machhammer, O.; Bode, A.; Hormuth, W.: Ökonomisch/ökologische Betrachtung zur Herstellung von Wasserstoff in Großanlagen. Chem. Ing. Tech., 87 (2015) 4, 409 - 418, doi.: 10.1002/cite.201400151.

[17] Geres, R. et al.: Roadmap Chemie 2050. Auf dem Weg zu einer treibhausgasneutralen chemischen Industrie in Deutschland, 2019, ISBN: 978-3-89746-223-6.

[18] IEA, IEA G20 Hydrogen Report: Assumptions. Available online: https://iea.blob.core.windows.net/assets/29b027e5-fefc-47df-aed0-456b1bb38844/IEA-The-Future-of-Hydrogen-Assumptions-Annex_CORR.pdf (accessed on 31 May 2021).

[19] Timmerberg, S.; Kaltschmitt, M.; Finkbeiner, M.: Hydrogen and hydrogen-derived fuels through methane decomposition of natural gas - GHG emissions and costs. Energy Conversion and Management: X, 7 (2020), 100043, doi.: 10.1016/j.ecmx.2020.100043.

[20] Warren, K. E. H.: A techno-economic comparison of biogas upgrading technologies in Europe. Master Thesis (2012) at Jyväskylän yliopisto - University of Jyväskylä, Available online: https://citeseerx.ist.psu.edu/viewdoc/download?doi=10.1.1.456.1353&rep=rep1&type=pdf (accessed on 31 May 2021).

[21] ISET, Biogas upgrading to biomethane. European Biomethane Fuel Conference, Proceedings, February 21, 2008, Kassel, Germany.

[22] Persson, M.: Evaluation of Upgrading Techniques for Biogas.

[23] Ryckebosch, E.; Drouillon, M.: Techniques for Transformation of Biogas to Biomethane. Journal of Biomass and Bioenergy, 35 (2011) 5, 1633 - 1645, doi.: 10.1016/j.biombioe.2011.02.033.

[24] Hoyer, K. et al.: Biogas Upgrading - Technical Review, 2016, ISBN 978-91-7673-275-5.

Narr Francke Attempto Verlag GmbH + Co. KG

[25] Viebahn, P.; Horst, J.; Scholz, A.; Zelt, O.: Technologiebericht 4.4 Verfahren der CO2-Abtrennung aus Faulgasen und Umgebungsluft innerhalb des Forschungsprojekts TF_Energiewende. Available online: https://epub.wupperinst.org/frontdoor/deliver/index/docId/7062/file/7062_CO2-Abtrennung.pdf (accessed on 31 May 2021).

[26] Roode-Gutzmer, Q. I.; Kaiser, D.; Bertau, M.: Renewable Methanol Synthesis. ChemBioEng Reviews, 6 (2019) 6, 209 - 236, doi.: 10.1002/cben.201900012.

[27] Climeworks, Direct air capture – A technology to reverse climate change. Available online: http://www.climeworks.com/co2-removal/ (accessed on 31 May 2021).

[28] Climeworks 2020 - Product Sheet CO2 Capture Plant.

[29] Keith, D. W.; Holmes, G.; Angelo, D. St.; Heidel, K.: A process for capturing CO_2 from the atmosphere. Joule, 2 (2018) 8, 1573 - 1594, doi.: 10.1016/j.joule.2018.05.006.

[30] Fasihi, M.; Efimova, O.; Breyer, C.: Techno-economic assessment of CO_2 direct air capture plants. Journal of Cleaner Production, 224 (2019), 957 - 980, doi.: 10.1016/j.jclepro.2019.03.086.

[31] Sasol, Technology. Available online: https://www.sasol.com/innovation/gas-liquids/technology (accessed 31 May 2021).

[32] Shell, Pearl GTL. Available online: https://www.shell.com/about-us/major-projects/pearl-gtl.html. (accessed 31 May 2021).

[33] Umwelt Bundesamt, Power-to-Liquids - Potentials and Perspectives for the Future Supply of Renewable Aviation Fuel. Available online: https://www.umweltbundesamt.de/sites/default/files/medien/377/publikationen/161005_uba_hintergrund_ptl_barrierrefrei.pdf (accessed on 31 May 2021).

[34] Rezaei, E.; Dzuryk, S.: Techno-economic comparison of reverse water gas shift reaction to steam and dry methane reforming reactions for syngas production. Chemical Engineering Research and Design, 144 (2019), 354 - 369, doi.: 10.1016/j.cherd.2019.02.005.

[35] Wolf, A.; Jess, A.; Kern, C.: Syngas Production via Reverse Water-Gas Shift Reaction over a Ni-Al_2O_3 Catalyst: Catalyst Stability, Reaction Kinetics, and Modeling. Chemical Engineering Technology, 39 (2016) 6, 1040 - 1048, doi.: 10.1002/ceat.201500548.

[36] Dybkjaer, I.: Tubular reforming and autothermal reforming of natural gas - an overview of available processes. Fuel Processing Technology, 42 (1995) 2-3, 85 - 107, doi.: 10.1016/0378-3820(94)00099-F.

[37] Speight, J. G.: Handbook of Gasification Technology: Science, Processes and Applications, doi.: 10.1002/9781118773970.ch12.

[38] Chiesa, P.: Advanced technologies for syngas and hydrogen (H_2) production from fossil-fuel feedstocks in power plants. Advanced Power Plant Materials, Design and Technology, (2010), 383 - 411.

[39] Speight, J. G.: Gasification processes for syngas and hydrogen production. Gasification for Synthetic Fuel Production, (2015), 119 - 146.

[40] Summa, P.; Samojeden, B; Motak, M.: Dry and steam reforming of methane. Comparison and analysis of recently investigated catalytic materials. A short review. Polish Journal of Chemical Technology, 21 (2019) 2, 31 - 37, doi.: 10.2478/pjct-2019-0017.

[41] Kopernikus Projekte - Power2X, 1. Roadmap. Available online: https://dechema.de/dechema_media/Downloads/Positionspapiere/2018_Power_to_X.pdf (accessed on 31 May 2021).

[42] Kopernikus Projekte - Power2X, 2. Roadmap. Available online: https://dechema.de/dechema_media/Downloads/Positionspapiere/2019_DEC_P2X_Kopernikus_RZ_Webversion02-p-20005425.pdf (accessed on 31 May 2021).

[43] Kopernikus Projekte - Power2X, 2. Roadmap - Technischer Anhang. Available online: https://dechema.de/dechema_media/Downloads/Positionspapiere/2019_RM+2_0_technischer+Anhang_zusammengef%C3%BChrt-p-20005689.pdf (accessed on 31 May 2021).

[44] Snoeckx, R.; Bogaerts, A.: Plasma technology - a novel solution for CO_2 conversion?. Chem. Soc. Rev., 46 (2017), 5805 - 5863, doi.: 10.1039/C6CS00066E.

[45] Dieterich, V.; Buttler, A.; Hanel, A.; Spliethoff, H.; Fendt, S.: Power-to-liquid via synthesis of methanol, DME or Fischer–Tropsch-fuels: a review; Energy Environ. Sci., 13 (2020), 3207 - 3252, doi.: 10.1039/D0EE01187H.

[46] Schmidt, P.; Batteiger, V.; Roth, A.; Weindorf, W.; Raksha, T.: Power-to-Liquids as Renewable Fuel Option for Aviation: A Review, 90 (2018) 1-2, 127 - 140, doi.: 10.1002/cite.201700129.

[47] Mueller-Langer, F.: Analyse und Bewertung ausgewählter zukünftiger Biokraftstoffoptionen auf der Basis fester Biomasse. Dissertation, Technische Universität Hamburg-Harburg (2011).

[48] Leckel, L.: Hydrocracking of Iron-Catalyzed Fischer-Tropsch Waxes. Energy & Fuels, 19 (2005), 1795 - 1803, doi.: 10.1021/ef050085v.

[49] Farag, H. A.; Yousef, N. S.; Farouq, R.: Modeling and simulation of a hydrocracking unit. Journal of Engineering Science and Technology, 11 (2016) 6, 881 -898.

[50] Tao, L.; Milbrandt, A.; Zhang, Y.; Wang, W.-C.: Techno-economic and resource analysis of hydroprocessed renewable jet fuel. Biotechnology for Biofuels, 10 (2017), 10:261, doi.:10.1186/s13068-017-0945-3.

Narr Francke Attempto Verlag GmbH + Co. KG

[51] König, D. H.; Baucks, N.; Dietrich, R.-U., Wörner, A.: Simulation and evaluation of a process concept for the generation of synthetic fuel from CO_2 and H_2. Energy, 91 (2015), 833 - 841, doi.: 10.1016/j.energy.2015.08.099.

[52] Sun, C.: Direct syngas-to-fuel: integration of Fischer-Tropsch synthesis and hydrocracking in micro-structured reactors. Dissertation, KIT 2017, doi.: 10.5445/IR/1000078059.

[53] Bouchy, C.; Hastoy, G.; Guillon; E.; Martens, J. A.; Fischer-Tropsch Waxes Upgrading via Hydrocracking. and Selective Hydroisomerization. Oil & Gas Science and Technology, 64 (2009) 1, 91 - 112, doi.:10.2516/ogst/2008047.

[54] Yang, Q.; Qian, Y.; Zhou, H.; Yang, S.: Conceptual design and techno-economic evaluation of efficient oil shale refinery processes ingratiated with oil and gas products upgradation. Energy Conversion and Management, 126 (2016), 898 - 908, doi.: 10.1016/j.enconman.2016.08.022.

[55] Ahmed, A. M.; Jarullah, A. T.; Abed, F. M.; Mujtaba, I. M.: Modelling of an industrial naphtha isomerization reactor and development and assessment of a new isomerization process. Chemical Engineering Research and Design, 137 (2018), 33 - 46, doi.: 10.1016/j.cherd.2018.06.033.

[56] Faustine, C.: Environmental review of petroleum industry effluents analysis. Master Thesis (2008), KTH. Available online: https://www.diva-portal.org/smash/get/diva2:412122/fulltext01.pdf (accessed on 31 May 2021).

[57] NIST Chemistry Webbook. Available online: https://webbook.nist.gov/chemistry/ (accessed on 31 May 2021).

[58] Geleynse, S.; Brandt, K.; Garcia-Perez, M.; Wolcott, M.; Zhang, X.: The Alcohol-to-Jet Conversion Pathway for Drop-In Biofuels: Techno-Economic Evaluation. ChemSusChem, 11 (2018) 21, 3728 - 3741, doi.: 10.1002/cssc.201801690.

[59] Gogate, M. R.: Methanol-to-olefins process technology: current status and future prospects. Petroleum Science and Technology, 37 (2019) 5, 559 - 565, doi.: 10.1080/10916466.2018.1555589.

[60] Nieminen, H.; Laari, A.; Koiranen, T.: CO_2 Hydrogenation to Methanol by a Liquid-Phase Process with Alcoholic Solvents: A Techno- Economic Analysis. Processes, 7 (2019), 405 ff., doi:10.3390/pr7070405.

[61] Wright, M.: Techno-economic evaluations of biofuel technologies, Master Thesis (2008), Iowa State University, Available online: https://lib.dr.iastate.edu/cgi/viewcontent.cgi?article=16354&context=rtd (accessed on 31 May 2021).

[62] Michailos S.: Technoeconomic Assessment of Methanol Synthesis via CO_2 Hydrogenation, (2018).

[63] Schemme, S. et al.: H_2-based synthetic fuels: A techno-economic comparison of alcohol, ether and hydrocarbon production. International Journal of Hydrogen Energy, 45 (2020) 8, 5395 - 5414, doi.: 10.1016/j.ijhydene.2019.05.028.

[64] Pérez-Fortes, M., Schöneberger, J. C., Boulamanti, A., Tzimas E.: Methanol synthesis using captured CO2 as raw material: Techno-economic and environmental assessment. Applied Energy, 161 (2016), 718 - 732, doi.: 10.1016/j.apenergy.2015.07.067.

[65] CarbonNext: The next Generation of Carbon for the Process Industry - Deliverable 4.3: Economic and environmental impacts of most promising CCU pathways, Available online: http://carbonnext.eu/Deliverables/_/D4.3%20Economic%20and%20environmental%20impacts%20of%20most%20promising%20CCU%20pathways.pdf (accessed on 31 May 2021).

[66] Mendez, L. M.: Process design and control of dimethyl ether synthesis. Industriales, 2016, Available online: http://oa.upm.es/42670/1/TFG_LAURA_MARTIN_MENDEZ.pdf (accessed on 31 May 2021).

[67] Brynolf, S., Taljegard, M.; Grahn, M.; Hansson, J.: Electrofuels for the transport sector: A review of production costs. Renewable and Sustainable Energy Reviews, 81 (2018) 2, 1887 - 1905, doi.: /10.1016/j.rser.2017.05.288.

[68] Parbowo, H. S.; Ardy, A.; Susanto, H.: Techno-economic analysis of Dimethyl Ether production using Oil Palm Empty Fruit Bunches as feedstock - a case study for Riau. IOP Conf. Ser.: Mater. Sci. Eng. 543 (2019) 012060, doi.: 10.1088/1757-899X/543/1/012060.

[69] Clausen, L. R.; Elmegaard, B.; Houbak, N.: Technoeconomic analysis of a low CO_2 emission dimethyl ether (DME) plant based on gasification of torrefied biomass. Energy, 35 (2010) 12, 4831 - 4842, doi.: 10.1016/j.energy.2010.09.004.

[70] Bai, Z.; Ma, H.; Zhang, H.; Ying, W.; Fang, D.: Process simulation of dimethyl ether synthesis via methanol vapor phase dehydration. Polish Journal of Chemical Technology, 15 (2013) 2, 122 - 127, doi.: 10.2478/pjct-2013-0034.

Narr Francke Attempto Verlag GmbH + Co. KG

Scale-up of batch esterification of pyrolysis oils with higher alcohols from 250-ml-scale to 20-l-scale

Tim Schulzke
Fraunhofer UMSICHT, Institut für Umwelt-, Sicherheits- und Energietechnik, Oberhausen, Germany

Summary

Within the framework of the PyroMar collaborative project about the production of low-sulphur bio-based blendstocks for marine fuels, the esterification of condensates resulting from ablative fast pyrolysis of 2nd generation biomass with higher alcohols derived from lignocellulosic ethanol is investigated. To examine the scale-up of the chemical process three different experimental setups are used: a 3-neck-flask of 250 ml nominal volume, a 3-neck-flask of 2 l and a stirred tank reactor of 20 l. In all setups identical reaction mixtures (relative amounts of pyrolysis oil, butanol and solid acid catalyst) under the same conditions (external heating, operation under reflux, reaction end point indication) were converted and the product mixtures were analyzed. While the smallest setup needed only about 6 hours of operation to reach the end point, the two larger setups required 20 hours. The remaining water mass fraction in all experiments regardless of size and original water content was around 1 wt.-% and the acetic acid mass fraction could be reduced to half the value of the reaction mixture. Further scale-up to cubic metre scale for industrial production seems easily achievable.

1. Introduction

The marine sector contributes significantly to global greenhouse gas emissions by burning fossil based residual oil from refineries with low potential for electrification. In addition, these marine fuels traditionally contained high amounts of sulphur resulting in SO_x emissions. In recent years, the sulphur content in fuels is increasingly strictly regulated – starting in emission control areas and being extended to the high sea outside.
The existing Emission Control Areas (ECA) are the Baltic Sea, the English Channel, the North Sea and coastal areas of United States of America and Canada except for Alaska, Yukon, Northwest Territories, Nunavut and the north-eastern coast of Quebec. Enlargement of ECAs is in discussion for Mexican, Japanese, Norwegian and (southern parts of) Malaysian coast as well as the Mediterranean Sea. The fuel sulphur limit within ECAs is 0.1 wt.-% since 2015 and outside ECAs 0.5 wt.-% since 2020 for vessels without exhaust gas cleaning systems ("scrubbers") [1].
This leads to the idea to apply biomass-based fuels to reduce the emission of greenhouse gases by a renewable liquid energy carrier that is inherently low in sulphur. A promising candidate for that purpose is fast pyrolysis oil, a liquid that is obtained from condensation of vapours resulting from thermal degradation of solid biomass applying high heating rates at around 550 °C and short vapour residence times in the hot area [2]. The advantages of fast pyrolysis are the relatively simple process and the comparatively high liquid yield of up to even 70 wt.-%. Another important point is the possibility to process 2nd generation biomass with no food or fodder competition.
On the other hand there are some drawbacks: as the input material is composed of oxygen-containing natural polymers such as cellulose, hemicellulose (both hydrocarbons) and lignin, also the products from thermal degradation still include many oxygen-containing functional groups and water is formed, resulting in an overall low heating value [3]. Some of the oxygen-containing compounds are organic acids, aldehydes and ketones. While the acids lead to high Carbon Acid Numbers (CAN) and hence cause severe corrosion on standard material applied in pumps, boilers and engines, the aldehydes and ketones are very reactive, especially under acidic conditions, and result in products with increasing molecular weight even at room temperature over extended storage time, thus leading to increased viscosity. High water concentrations in the condensates, typical for herbaceous biomass like cereal straw, lead to spontaneous phase separation into an aqueous phase with high organic contamination and a very viscous, tarry phase, which still dissolves noticeable amount of water.
Due to the oxygen-containing functional groups in the organic molecules forming the liquid product it is quite polar and therefore not miscible with hydrocarbons. In particular in the beginning of an application of such pyrolysis oils as fuels in shipping, its availability would be scarce and restricted to a small number of harbours worldwide, why a separate tank system would be non-economical.

Narr Francke Attempto Verlag GmbH + Co. KG

One possible way to overcome these undesirable properties would be the chemical removal of the oxygen by hydrogenation. This would result in pure hydrocarbons, which are indistinguishable from petroleum-based ones and fully miscible on one hand and on the other hand water forms a second phase that can easily be separated. Such approach is investigated by several groups, e.g. by the BioMates consortium [4]. Unfortunately, this process requires a large amount of renewable hydrogen to remove the oxygen in form of water and quite sophisticated catalysts.
An alternative is to chemically mask the compounds that mainly provoke the undesired properties [5]. Luckily all three group of compounds – carboxylic acids, aldehydes and ketones – react with alcohols following the reaction schemes shown in Fig. 1 for acids and in Fig. 2 for aldehydes and ketones.

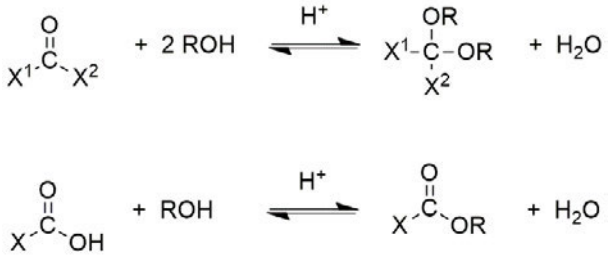

Figure 1: Reaction scheme of esterification

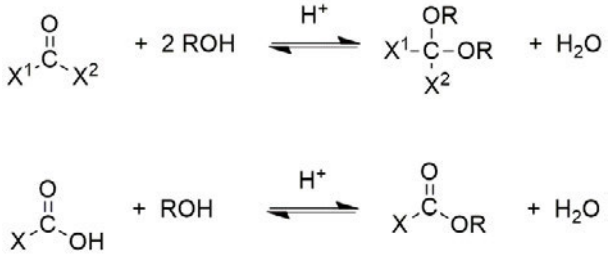

Figure 2: Reaction scheme of acetalization

The reactions are executed with an acidic catalyst under boiling conditions. The evolving vapour consists of an azeotrope made of water and the alcohol. To avoid the reaction mixture to deplete in alcohol, the vapour is condensed and returned to the reactor. Both reactions, esterification as well as acetalization, are equilibrium reactions. The formed reaction water together with the already present water in the pyrolysis oil prevent the reactions to fully proceed to the product side. To push the reaction towards the products, a very large overspill of alcohol would be necessary, which is expensive and could not be recovered after finishing the reaction, as distillation in presence of water would lead to significant rate of backwards reaction, thus cleaving the esters, acetals and ketals.
A better way to shift the equilibrium towards the products would be the continuous removal of water from the reaction mixture. This can be achieved by the application of alcohols with a longer carbon chain. Methanol, ethanol and propanols are all fully miscible with water, but beginning with butanols, higher alcohols exhibit a miscibility gap in the liquid phase and the azeotropic composition always fall into it. By that means the evaporating water can easily be separated from the higher alcohol in a Dean-Stark-Apparatus (Fig. 4 in the middle): the denser water is collected in the lower part of the burette and removed periodically while the lighter alcohol flows back to the reactor. Butanol typically is a product of petroleum refining, but it can be efficiently produced by catalytic condensation from ethanol as developed by Fraunhofer UMSICHT [6]. And if cellulosic ethanol is used for this catalytic condensation instead of starch- or sugar-based ethanol, the resulting butanol is as sustainable as the pyrolysis oil.
Putting all this together leads to the overall process approach, which is investigated within the framework of the PyroMar collaborative project, which started January 1st, 2020. The concept is given in Fig. 3.

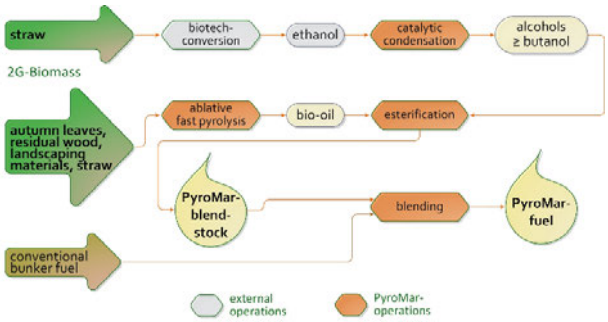

Figure 3: PyroMar concept for low sulphur marine fuels

The first line of action within the overall concept starts with cereal straw. After enzymatic decomposition it is fermented to ethanol, which serves as feedstock for the catalytic condensation at Fraunhofer UMSICHT to butanol. In the second line of action a wide variety of 2nd generation biomass like straw, autumn leaves, landscaping material, rice husk, decomposed and dried sewage sludge is converted to pyrolysis oils applying an ablative fast pyrolysis plant in laboratory scale with a capacity of about 5 kg/h biomass feed. The pyrolysis oil and the butanol are mixed and used as feedstock for the esterification and acetalization with a solid acid as catalyst. This catalyst is recovered by filtration after the reaction is completed. The project partner LKV (Chair of piston machines and combustion engines) at Rostock University than analyse the reaction products prior to do blend tests with conventional marine fuels. In the end engine tests are envisaged for a suitable blend. The project is round off by ecological and economic studies performed by ifeu (Institute for Energy and Environment Research) in Heidelberg.
In the following sections the process step of esterification and acetalization is further described with a strong focus on scale-up based on initial results.

Narr Francke Attempto Verlag GmbH + Co. KG

2. Experimental Setups

Fraunhofer UMSICHT started its work on pyrolysis oil upgrading by catalytic treatment with higher alcohols in the framework of a collaborative project named "Development of a combined process for the upgrading of pyrolysis oil with biogenic alcohols and hydrogen" together with Thuenen-Institute for Wood Research in Hamburg, funded by the German Federal Ministry for Food, Agriculture and Consumer Protection (grant nr. 22018811). The focus in this project lay on intensive catalyst screening and the identification of favourable process conditions. First results were presented during ECI's conference "Biorefinery I: Chemicals and Materials from Thermo-Chemical Biomass Conversion and Related Processes" in Crete 2015 [7]. Heterogeneous solid acid catalysts are easy to be removed after the reaction in contrast to homogeneous liquid acids like sulphuric acid or p-toluenesulfonic acid, which stay in the product mixture and need to be neutralized, e.g. with caustic soda, thus resulting in a salt residue not tolerable in engine application. From all the tested solid acids, Amberlyst70™, a polystyrene backbone with sulfonic acid functional groups, performed best with lowest water content and lowest TAN after reaction. As that catalyst was no longer available, it was decided to use a similar one from the same group Amberlyst36™ ever since.

All these experiments and the majority of the subsequent ones performed in the following years were conducted in a 250 ml 3-neck-flask immersed in a heated oil bath for temperature control shown in Fig. 4 (left photograph). For the engine tests of potential blend fuels at the partner LKV more than 100 l of PyroMar intermediates (esterified pyrolysis oils) are necessary to prepare the blend fuels. Such an amount cannot be supplied from laboratory setup with 250 ml flask and a typical batch amount of 160 ml liquid feedstock.

Figure 4: Small (250 ml, left) and medium scale (2 l, right) setup with Dean-Stark-Apparatus in the middle

Therefore one focus of the first two years in the PyroMar project is the scale-up of the esterification process to a batch reactor with reasonable size. As about 10 is a typical scale-up factor in chemical engineering, the next size of experimental setup is a 2 l 3-neck-flask (as 2.5 l flasks are not available), also immersed in a heated oil bath for temperature control, shown in Fig. 4 (right photograph). The Dean-Stark-Apparatus for water separation is the same as for the 250 ml setup (Fig. 4, middle). In this larger setup a half-moon impeller is used for stirring, hence the magnetic stir bar can be used to agitate the oil bath. The oil bath temperature is measured via PT100 temperature sensor and controlled by the heater below the oil bath. A small flow of nitrogen is passed through the reactors to inertize the atmosphere in the respective flask. A thermocouple is dunked in the reaction mixture to monitor the temperature progress over time.

From that size a real scale-up factor of 10 is achieved by using a 20 l stirred tank reactor with a heating jacket and two impellers stacked on a central shaft, shown in Fig. 5. The thermal oil flowing through the heating jacket is controlled by a thermostat and the reactor is inertized by a small flow of nitrogen as well. A PT100 temperature sensor is also installed to monitor the liquid's temperature over time. The condensate coming from the top cooler is caught in a Dean-Stark-Apparatus similar to that used in the smaller setups. Here, a capacitive level switch is installed to automatically detect the phase boundary between water and alcohol. Whenever this boundary rises to the switch position, it triggers a solenoid valve, which stays open for a fixed time. The flow is regulated by a needle valve, so that a fixed amount of about 21 ml of water is removed per opening period of the solenoid valve.

Figure 5: Large scale (20 l) setup

All experiments start with filling the reactors at room temperature with the respective amounts of pyrolysis oil, butanol and solid catalyst. Then the nitrogen flow is started as well as the flow of cooling water to the condenser and the oil bath or heating jacket is set to a temperature between 125 °C and 140 °C. The temperature of the reaction mixture rises fast until it reaches the boiling point at about 97 °C. Then the reflux starts and water evolves in the Dean-Stark-Apparatus from which it is removed

Narr Francke Attempto Verlag GmbH + Co. KG

periodically either manually for the smaller setups or automatically at large scale. With diminishing water fraction in the reaction mixture over time the temperature slowly increases. The reaction mixture is kept boiling until no more water evolves in the Dean-Stark-Apparatus. While for the smallest setup this is achieved within about 6 hours, the other setups need up to 20 hours. As the setups arte not designed for unattended operation, they have to be shut down over night. For that, the heating plate in the medium sized setup is switched

Table 1: Communalities and differences of experimental setups

	250 ml	2 l	20 l
Reactor	3-neck flask	3-neck flask	stirred tank
Stirrer	magnetic bar	half-moon impeller	2 impellers stacked on shaft
Heating system	oil bath (unstirred)	oil bath (stirred)	heating jacket
Catalyst Amberlyst™36	5 g	40 g	400 g
Batch volume	160 ml	1,280 ml	12,800 ml
Pyrolysis oil	80 ml / 100 ml / 120 ml	640 ml / 800 ml / 960 ml	6,400 ml / 8,000 ml / 9,600 ml
1-Butanol	80 ml / 60 ml / 40 ml	640 ml / 480 ml / 320 ml	6,400 ml / 4,800 ml / 3,200 ml
Oil/Alcohol-ratio	1:1 / 5:3 / 3:1	1:1 / 5:3 / 3:1	1:1 / 5:3 / 3:1
Water separation	DSA ≈ 20 ml, manually	DSA ≈ 20 ml, manually	DSA ≈ 50 ml, automatically

off and in the large scale setup the setpoint for the oil jacket is reduced to 50 °C. In the medium sized setup the stirrer is switched off as well, while in the large scale it stays on. The next day the heating system is set back to the original setpoint and the reflux starts after heating up exactly at the same boiling temperature as the experiment was interrupted the day before.
Table 1 lists the characteristics of the three experimental setups for direct comparison.

3. Results

Fig. 6 shows the temperature profile for exemplary experiments in small and medium scale while Fig. 7 depicts the temperature profile for the large scale setup. While in the smallest setup the boiling point of the reaction mixture is directly rising, the boiling temperature of in the medium sized setup stays longer around the boiling point of the water-butanol-azeotrope and rises slower. Although the batch volume increased by a factor of 8, the necessary reaction time increased by a factor of less than 4 only (both experiments were performed with the same pyrolysis oil and the same oil/alcohol-ratio). The further magnification of batch volume by a factor of 10 to the largest setup does not make the necessary reaction time for full water removal increase any further (this experiment had to be performed with another pyrolysis oil of similar composition with the same oil/alcohol-ratio).

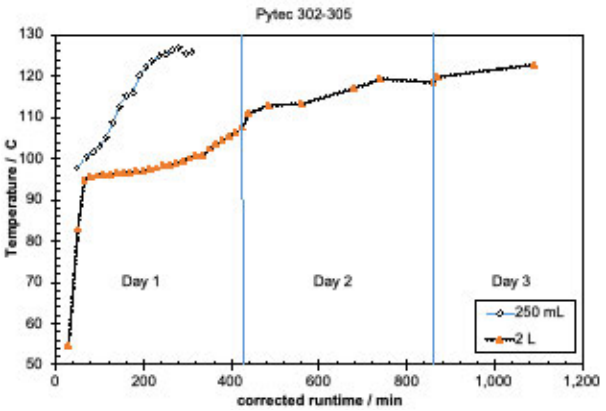

Figure 6: Reaction mixture temperature profile over time for small and medium scale setup

Fig. 7 additionally shows the profile of the removed water over reaction time. It can be seen clearly that at the beginning the slope is nearly linear and quite steep and after approximately 300 min it flattens more and more. At the end of the experimental run the time between the last two opening periods of the solenoid valve accounted for exactly 4 hours.

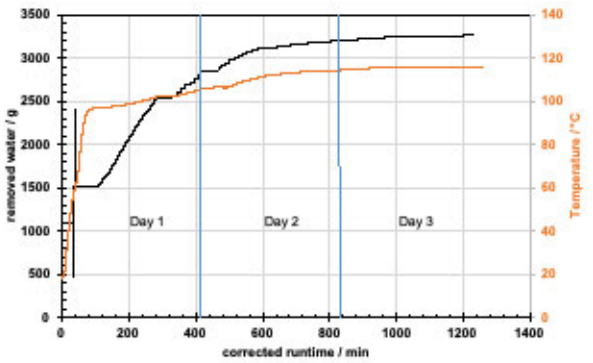

Figure 7: Reaction mixture temperature and separated water over time for large scale setup

Narr Francke Attempto Verlag GmbH + Co. KG

At the submission deadline for this contribution to the conference proceedings not all results from laboratory analyses were at hand. Therefore, in the following only preliminary results obtained for the small and medium scale experimental setups are presented.

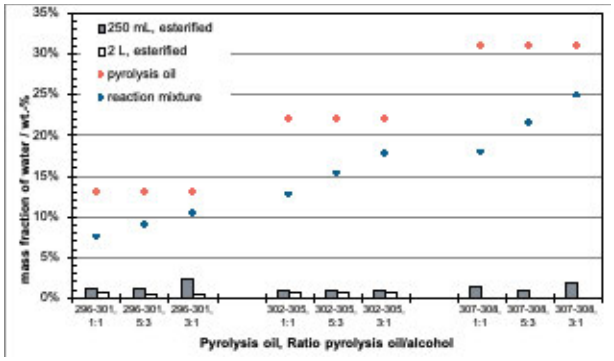

Figure 8: Water mass fraction for different experiments

Fig. 8 depicts the water mass fraction for several groups of experiments conducted with three different pyrolysis oils. All pyrolysis were based on a mixture of wheat and barley straw at equal share. For the experiment Pytec296-301 the pyrolysis temperature was set to 550 °C and the temperature of the first condenser and electrostatic precipitator to 75 °C. The experiment Pytec302-305 was done with a pyrolysis temperature of 500 °C and a condensation temperature of 70 °C. The last pyrolysis experiment Pytec307-308 was conducted at 450 °C and 70 °C, respectively. As a result of these differing operating conditions in pyrolysis and condensation, the water mass faction of the oils was 13 wt.-% for Pytec296-301, 22 wt.-% for Pytec302-305 and 31 wt.-% for Pytec307-308. After mixing with butanol, the water mass fraction of the reaction mixture is significantly lower due to physical dilution as can be seen clearly from Fig. 8. But regardless of original water mass fraction of the pyrolysis oil and mixing ratio with butanol, after the end of the esterification reaction the remaining water mass fraction is around 1 wt.-% for each experiment. The experiments in the medium sized setup are slightly below and the ones in the smallest equipment are consistently above that value. This could be a significant effect caused by different surface-to-volume ratio and subsequent different heat flux into the reaction mixture, but it could also be owing to the fact that with the very small total amounts of water in the small scale setup it is extremely difficult to decide, when there is no more water evolving in the Dean-Stark-Apparatus.

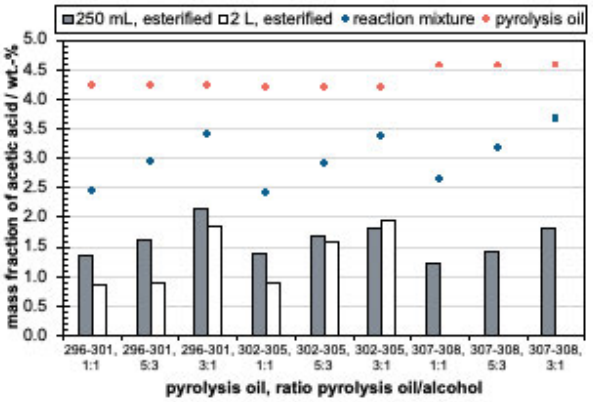

Figure 9: Acids mass fraction for different experiments

Another important quality indicator is the acetic acid mass fraction, which is presented in Fig. 9 for the same set of experiments. The acetic acid mass fraction is more or less not influenced by the pyrolysis and condensation conditions as the three pyrolysis oils exhibit very similar values of about 4.4 wt.-%. Again, the reaction mixture shows lower values due to physical dilution. After the reaction the remaining acetic acid mass fraction is approximately half of that of the reaction mixture. As for the water mass fraction the medium sized setup slightly performed better than the smallest equipment.

4. Conclusion

The preliminary results of the presented scale-up test campaign are quite promising. The remaining water mass fraction in all scales is around 1 wt.-% and the acetic acid concentration could be reduced to half the value of the reaction mixture. Further scale-up to cubic metre scale seems possible and the conversion might be performed within 20 hours, leaving 4 hours for filling, discharging and cleaning; so every day a batch can be treated to give an upgraded pyrolysis oil with only small amount of water and reduced concentration of acids.

5. Acknowledgement and disclaimer

The project behind this contribution to conference proceeding has received funding from the German federal Ministry of Economy and Energy BMWi under grant nr. 03EI5412 based on a decision by the German Bundestag. We thank BMWi for the funding and its funding agency PTJ for the supervision. Additionally, we thank Clariant, subsidiary Straubing for supplying us with the cellulose-based ethanol from agricultural residues. This publication reflects the author's view only. BMWi and PtJ are not responsible for any use that may be made of the information it contains.

Narr Francke Attempto Verlag GmbH + Co. KG

References

[1] International Maritime Organization: IMO 2020 – cutting sulphur oxide emissions. https://www.imo.org/en/MediaCentre/HotTopics/Pages/Sulphur-2020.aspx (accessed 29.05.2021)

[2] Conrad S., Blajin C., Schulzke T., Deerberg G. Comparison of fast pyrolysis bio-oils from straw and miscanthus. Environ Prog Sustainable Energy 39 (2019); e13287; doi: 10.1002/ep.13287

[3] Bridgwater AV. Review of fast pyrolysis of biomass and product upgrading. Biomass Bioenergy 38 (2012), 68-94; doi: 10.1016/j.biombioe.2011.01.048

[4] Schulzke T., Conrad S., Shumeiko B., Auersvald M., Kubicka D., Raymakers LFJM. Fuels from Reliable Bio-based Refinery Intermediates: BioMates. Waste Biomass Valor 11 (2020), 579–598; doi: 10.1007/s12649-019-00625-w

[5] Sundqvist T., Oasmaa A., Koskinen A. Upgrading Fast Pyrolysis Bio-Oil Quality by Esterification and Azeotropic Water Removal. Energy Fuels 29 (2015), 2527–2534; doi: 10.1021/acs.energyfuels.5b00238

[6] Breitkreuz K, Menne A, Kraft A. New process for sustainable fuels and chemicals from bio-based alcohols and acetone. Biofuels Bioprod Bioref 8 (2014), 504-15; doi: 10.1002/bbb.1484

[7] Schulzke T., Conrad S., Kaluza S., Van Loo T. Upgrading of fast pyrolysis condensates via esterification with higher alcohols. Biomass Bioenergy 103 (2017), 11-20; doi: 10.1016/j.biombioe.2017.05.010

Narr Francke Attempto Verlag GmbH + Co. KG

Novel purification routes for crude glycerol from biodiesel plants as a suitable feedstock for sustainable aviation fuel

Taha Attarbachi
University of Manchester, Manchester, UK
taha.attarbachi@postgrad.manchester.ac.uk

Martin Kingsley
Argent Energy Ltd., Ellesmere Port, UK
martin.kingsley@argentenergy.com

Dr. Vincenzo Spallina
University of Manchester, Manchester, UK
vincenzo.spallina@manchester.ac.uk

Summary

GLAMOUR (Glycerol to Aviation and Marine prOducts with sUstainable recycling) is a H2020 research project looking to demonstrate the conversion of bio-waste feedstock such as glycerol into jetfuel and marine diesel oil by combining syngas generation with inherent CO2 removal using gas solid reactions. A special emphasis is put on the integration into existing biodiesel manufacturing facilities. For a reliable working process, the feedstock must be pre-treated and all inorganic material must be removed in order to avoid poisoning of the catalyst. This manuscript concentrates on the most efficient removal of ashes in the crude glycerol of Argent Energy. Therefore, a simple splitting step was utilized in order to encourage a phase separation of the highly viscous, dark crude glycerol. The influence of water on this splitting step is presented. A reduction of the initial ash content by 50 wt.% could be achieved in preliminary experiments.

1. Introduction

Biofuels are pillars of a sustainable society and will play a significant relevant role in the coming decades and are superseding conventional fossil fuels increasingly. The EU set a target of 10 % for renewable energy use in transport for 2020 and increased this number to 14% for the year 2030 [1]. In particular, the aspect of increasing sustainability of biofuel production will play a more important role as the target increases. Advanced biofuels are considered the same product as first generation biofuels but utilizing waste-based, non-food feedstocks [2]. In the case of biodiesel this development has a significant impact due to the substitution of using waste-feedstocks such as tallow or used cooking oil instead of palm oil. However, in both cases a transesterification reaction is applied which yields by-product glycerol which is more impure when waste-based feedstocks are used. Hence, a big problem with an excess supply of highly impure glycerol arose during the last years which has been incinerated, used for cattle feed [3-4], biogas [5-6] generation or even disposed.

Glycerol, also known as Propane-1,2,3-triol, is a relevant product in our daily lives. It is a major component in the personal care and pharmaceutical industry due to its antimicrobial and antiviral properties, used as a sweetener in the food industry and is in its crude form subject to research for technical applications such as gasification for the production of hydrogen and others [7].
Early in the 20th century glycerol was produced primarily as a by-product of the saponification of fats and was used as a raw material for the production of nitroglycerine. During the 1st world war glycerol became a strategic resource and therefore the demand exceeded the supply leading to the first synthetic plants for the production of glycerol by microbial sugar fermentation. Furthermore, the replacement of natural soaps with synthetical washing detergents has led to an increase in glycerol demand which accelerated the shift towards competitive petrochemical (synthetic) production routes. German, I.G. Farben used the high-temperature chlorination of propene to allyl chlore process to produce glycerol [8]. About 25% of the global glycerol demand was met by the petrochemical synthesis from propylene before the introduction of biodiesel into the market

Narr Francke Attempto Verlag GmbH + Co. KG

in the early 2000s. The other 75% was obtained by the saponification of fats[9].
With the emergence of the biodiesel industry, the market changed significantly due to an excess supply of crude glycerol provided based on vegetable oils as well as waste feedstocks such as tallow, used cooking oil or even more impure feedstocks. During the transesterification reaction of triglycerides with methanol approximately 10 wt.% of glycerol is produced as a by-product. Hence, the biodiesel industry became the main supplier of glycerol for the world market leading to a lack of interdependence between supply and demand of glycerol.
Since most of the crude glycerol cannot be utilized due to major impurities, it is highly relevant to review conventional and most importantly recent and novel purification methods to prevent further excess supply of impure crude glycerol to the market.
This manuscript presents a simple method to reduce the amount of ashes significantly

2. Materials

2.1 Chemicals

The feedstocks used for the experiments are provided by Argent Energy Ltd. Depending on the location where the crude glycerol is drawn off at the plant, it has an almost black colour (Fig. 1a), is highly viscous or is yellowish and less viscous. In both cases, the crude glycerol contains about 35-75 wt.% glycerol. In table 1 the crude glycerol composition which was used in these experiments can be found.

Table 1: Crude glycerol composititon.

Glycerol [% w/w]	57.8%
Water [% w/w]	11.5%
Ash [% w/w]	12.7%
MONG [% w/w]	18.0%
pH [-]	5.7

85% Phosphoric acid from *Emsure* was used as an acidification agent while for the neutralization reaction 12.5 M potassium hydroxide from *Sigma Aldrich* was used. As a solvent 2-Propanol from *Sigma Aldrich* was used due to its high availability and high polarity. Activated carbon WP220-90 from *Pulsorb* was used for the finishing step and VWR 303 filter paper.

2.2 Analysis

The analysis of the probes were conducted according to the British standards. Glycerol content was analysed according to BS 5711-3-1979. Water content was measured according to BS 5711-8-1979. Ash content was measured according to BS 5711-6-1979.

3. Experimental

The first attempts to purify the glycerol were based on procedures in the literature, mainly based on Manosak et al. [10]derived from a waste used-oil utilizing biodiesel (methyl ester and Kongjao et al. [11]. These procedures did not work due to the highly viscous, dark organic content which was mixed with the glycerol, resulting in an emulsion. Acidification, neutralization and subsequent addition of alcohol did not show the expected results. Hence, in a first step the emulsion was stirred at 200-500 rpm for 30 min and poured into a separatory funnel to encourage phase splitting. This was also done with the addition of some water.

3.1 Addition of Water

To understand the effect of water, a serial experiment was set up. 100 g of crude glycerol was mixed with 200-5 g of water under stirring at 200-500 rpm for 30 min. The mixture was subsequently poured into a separatory funnel for overnight separation.

3.2 Acidification

After the phase separation, the mixture was acidified. During the acidification step, the pH was reduced to 2.5 at 200-500 rpm for 60 minutes at ambient temperature. After the acidification, the mixture was poured into a separatory funnel.

3.3 Neutralization

For the neutralization potassium hydroxide was used. The neutralization reaction was conducted at ambient temperature a stirring speed of 200-500 rpm and a time of 60 min. After the neutralization the mixture was poured into a separatory funnel to let the salts precipitate.

3.4 Solvent extraction

For the solvent extraction, a ratio of 2:1 (v/v) of 2-propanol was poured into the mixture and stirred for 20 min at 200-500 rpm. Due to the turbulence in the beaker, the mixture was again poured into a separatory funnel to encourage further precipitation of salts and overnight phase separation.

Narr Francke Attempto Verlag GmbH + Co. KG

3.5 Evaporation

The evaporation of the solvent was conducted at 85°C for 20 min at a stirring rate of 200-500 rpm. Prior to the evaporation, the mixture was separated by vacuum filtration to remove any precipitated salts.

3.6 Adsorption

In the last step, activated carbon (PULSORB WPS230-90) was used to remove any colour and residual organic contact with a smaller molecular size. Therefore, about 100g/L were added to a beaker with the evaporated solvent in it and stirred for two hours at 200-500 rpm.

3.7 Vacuum filtration

The blackish mixture was subsequently vacuum filtrated with 303 filtrate paper.

4. Results

At this stage only for the first splitting step quantitative results are available.

4.1 Splitting step

The first, simple splitting step had a significant effect on the crude glycerol (Fig. 1a). After a settling time of 24 h in a separatory funnel, the emulsion separated into two phases: a top organic layer which was entirely black and a bottom aqueous layer consisting most likely of glycerol, water and some short-chain organics which are soluble in the aqueous layer (Fig.1c). The layers were decanted with an average ratio of 80 wt.% aqueous and 20 wt.% organic layer.
The addition of water (Fig. 1b) led to reduced settling time, a brighter aqueous layer, less viscous aqueous and organic layer and a sharper interphase between both phases which improved the decanting. The more water added, the brighter the aqueous phase which can also be seen in figure 2.
The analysis of the water splitting step yielded the results in table 2. By reducing the amount of water, the amount of ashes are reduced as well.

Table 2

	STEP 1: Water splitting step		
Experimental run	mH20 [g]	mCrude glycerol [g]	Ash content [wt]
1.29	20.12	101.87	8.54
1.30	15.06	100.98	8.97
1.31	10.13	100.80	7.89
1.32	5.04	100.34	6.29

Similar results are achieved by using no water for the splitting step. The ash content could be reduced to 7.68 wt.% reducing it by approximately 40%.

After the solvent extraction, two phases were yielded (Fig. 1d). A top alcohol-glycerol phase and a bottom salt phase which was separated by vacuum filtration. After the addition of activated carbon, the mixture was vacuum filtrated again and a transparent mixture was yielded (Fig. 1e).

5. Conclusion and Outlook

The splitting step is a quick, simple and cheap way to separate crude glycerol in the first step and prepare it for subsequent steps. Adding some deionized water to this step will lead even to brighter colour of the aqueous phase and less viscosity, making the handling of the material easier. Furthermore, with the splitting a reduction of ash content by approximately 40% was reached.
In the future further experiments with deep refining technologies are expected to be conducted, namely ion-exchange chromatography, electrodialysis and adsorption with waste based materials.
Furthermore, additional efforts will be made to utilize the residual organic top layer in the future to avoid further waste and close the entire value chain.

[1] B. Flach, S. Lieberz, and S. Bolla, “GAIN Report - EU Biofuels Annual 2019,” *Glob. Agric. Inf. Netw.*, p. 52, 2019, [Online]. Available: https://apps.fas.usda.gov/newgainapi/api/report/downloadreportbyfilename?filename=Biofuels Annual_The Hague_EU-28_7-15-2019.pdf.

[2] M. M. K. Bhuiya, M. G. Rasul, M. M. K. Khan, N. Ashwath, and A. K. Azad, “Prospects of 2nd generation biodiesel as a sustainable fuel - Part: 1 selection of feedstocks, oil extraction techniques and conversion technologies,” *Renew. Sustain. Energy Rev.*, vol. 55, pp. 1109–1128, 2016, doi: 10.1016/j.rser.2015.04.163.

[3] V. R. Fávaro *et al.*, “Glicerina na alimentação de bovinos de corte: Consumo, digestibilidade, parâmetros ruminais e sanguíneos,” *Semin. Agrar.*, vol. 36, no. 3, pp. 1495–1505, 2015, doi: 10.5433/1679-0359.2015v36n3p1495.

[4] L. E *et al.*, “Crude Glycerol: By-Product of Biodiesel Industries As an Alternative Energy Source for Livestock Feeding,” *J. Exp. Biol. Agric. Sci.*, vol. 5, no. 6, pp. 755–766, 2017, doi: 10.18006/2017.5(6).755.766.

[5] J. Á. Siles López, M. de los Á. Martín Santos, A. F. Chica Pérez, and A. Martín Martín, “Anaerobic digestion of glycerol derived from biodiesel manufacturing,” *Bioresour. Technol.*, vol. 100, no. 23, pp. 5609–5615, 2009, doi: 10.1016/j.biortech.2009.06.017.

[6] Q. (Sophia) He, J. McNutt, and J. Yang, “Utilization of the residual glycerol from biodiesel production for renewable energy generation,” *Renew. Sustain. Energy Rev.*, vol. 71, no. January, pp. 63–76, 2017, doi: 10.1016/j.rser.2016.12.110.

Narr Francke Attempto Verlag GmbH + Co. KG

[7] H. W. Tan, A. R. A. Aziz, and M. K. Aroua, "Glycerol production and its applications as a raw material: A review," 2013, doi: 10.1016/j.rser.2013.06.035.
[8] T. Seidensticker and A. Behr, *Einführung in die Chemie nachwachsender Rohstoffe*, vol. 4, no. 1. 2016.
[9] R. Ciriminna, C. Della Pina, M. Rossi, and M. Pagliaro, "Special Feature Understanding the glycerol market," pp. 1432–1439, 2014, doi: 10.1002/ejlt.201400229.
[10] R. Manosak, S. Limpattayanate, and M. Hunsom, "Sequential-refining of crude glycerol derived from waste used-oil methyl ester plant via a combined process of chemical and adsorption," *Fuel Process. Technol.*, vol. 92, no. 1, pp. 92–99, 2011, doi: 10.1016/j.fuproc.2010.09.002.
[11] S. Kongjao and S. Damronglerd, "Purification of crude glycerol derived from waste used-oil methyl ester plant," vol. 27, no. 3, pp. 944–949, 2010, doi: 10.1007/s11814-010-0148-0.

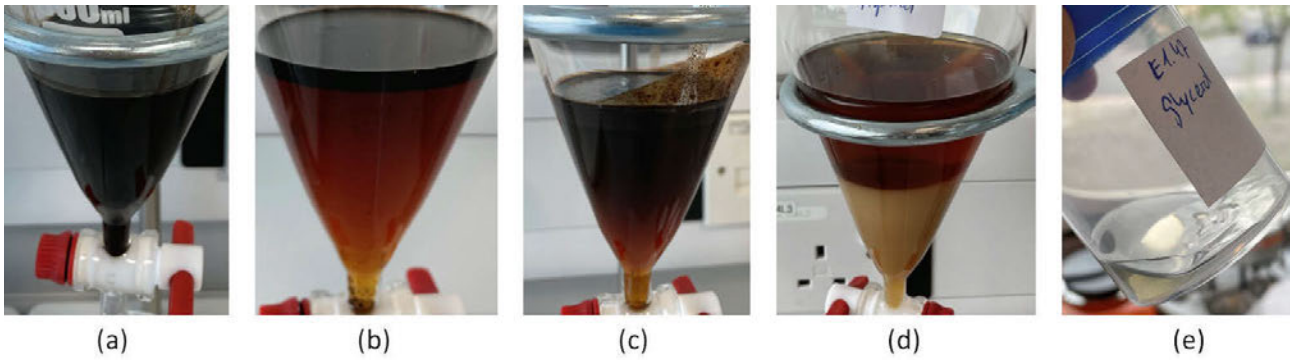

Figure 1: Different glycerol purification steps. (a) crude glycerol (b) glycerol after addition of 5g DI-water (c) glycerol after splitting step without water (d) glycerol after solvent addition and overnight separation (e) purified glycerol after adsorption

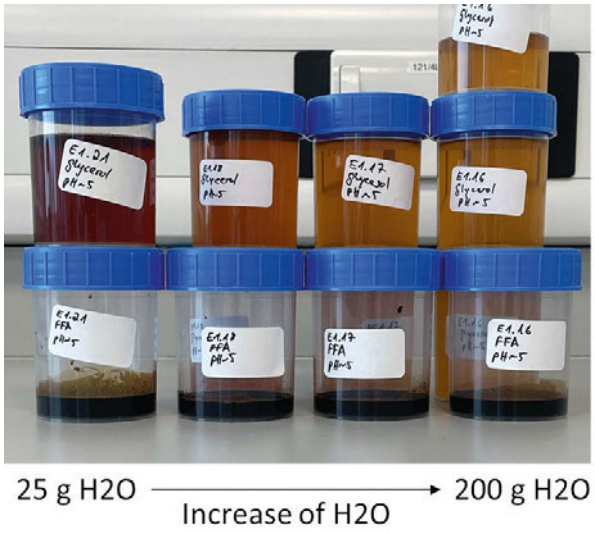

Figure 2: Water splitting step with increasing mass of water from left to right by constant crude glycerol mass.

Narr Francke Attempto Verlag GmbH + Co. KG

Recent developments in the field of oxymethylene ethers (OMEs) as diesel fuels

Ulrich Arnold
ulrich.arnold@kit.edu

Philipp Haltenort
Marius Drexler
Jörg Sauer
Karlsruhe Institute of Technology (KIT), Institute of Catalysis Research and Technology (IKFT), Hermann-von-Helmholtz-Platz 1, 76344 Eggenstein-Leopoldshafen, Germany

Summary

With respect to synthetic diesel fuels, so-called oxymethylene ethers (OMEs) are attracting considerable interest. This is mainly due to their diesel-like properties as well as a comparatively clean combustion with extremely low soot and NO_x emissions. From a chemical point of view, OMEs are short-chain acetals of the type $CH_3O(CH_2O)_nCH_3$, and especially derivatives with n = 3-5 are predestined for fuel applications. As can be seen from the molecular structure, synthesis of OMEs is based on methanol and thus, OMEs can be produced in sustainable manner from renewable resources if methanol is produced from renewables. Objective of the present study is a comprehensive description of the state of the art of OME fuels, regarding production, properties and evaluation. The work focusses on the synthesis of OMEs from dimethyl ether (DME), transacetalization reactions for the production of OMEs with variable end groups ($R^1O(CH_2O)_nR^2$), physico-chemical as well as fuel characteristics and evaluation of production processes.

1. Introduction

Regarding alternative diesel fuels, current research concentrates on so-called oxymethylene ethers (OMEs) [1]. From a chemical point of view, OMEs are oligomeric acetals with alternating carbon and oxygen atoms. Especially OMEs of the type $CH_3O(CH_2O)_nCH_3$ with n = 3-5 (OME_{3-5}) exhibit a diesel-like behavior [2,3]. Despite their favorable fuel characteristics, e.g. extremely low soot and NO_x emissions, availability on a larger scale is still limited and an improved production is envisaged [4].
According to the molecular structure, production of OMEs is based on methanol and methanol derivatives [5]. Within this work, innovative strategies for OME production are presented concentrating on the starting materials, catalysts and the resulting product spectra. All synthesis procedures lead to characteristic OME mixtures and strategies to influence the compositions are discussed. As an example, reactions of dimethyl ether (DME) with formaldehyde sources have been investigated and recent developments in this field are presented [6]. Another promising option is the synthesis of OMEs with different end groups, e.g. by transacetalization reactions of OMEs in the presence of acidic catalysts [7]. Thus, properties of OMEs can be tuned to a large extent and adapted to the respective requirements.
In addition to OME production, recent progress regarding analytics and physico-chemical as well as fuel characteristics are discussed. In this context, the current status regarding standardization is also addressed. From the perspective of users, practical criteria such as thermal, chemical and oxidation stability as well as compatibility of OMEs with materials and other fuel components are crucial and some aspects referring to this are considered. Furthermore, several studies on the evaluation of OME production are reviewed.

2. Synthesis of OMEs

Several synthesis strategies for OMEs have been described and usually, reactions of methanol or methanol derivatives with formaldehyde sources have been employed [1,4,5,8-12]. The classical pathway is based on the reaction of dimethoxymethane (DMM, Methylal, OME_1) with trioxane as the formaldehyde source [13]. The reaction offers a high yield of the desired OME_{3-5} fraction and low amounts of by-products are formed. However, the starting materials are costly and affect efficiency of the overall process chain. Therefore, current work con-

Narr Francke Attempto Verlag GmbH + Co. KG

centrates on alternative procedures such as direct OME synthesis from methanol and formaldehyde sources [14]. This pathway is advantageous but also challenging since water is released during acetalization reactions which is associated with the formation of byproducts. After reaction, water and the by-products have to be separated quantitatively from the product mixtures.
Regarding OME production on industrial scale, some plants are operating in China. Capacities around 40 kta^{-1} have been reported and OME synthesis from DMM and dewatered formaldehyde is the preferred technology [4].

2.1 Synthesis of OMEs from DME

An option for the anhydrous synthesis of OMEs is the reaction of DME, which can be considered as OME_0, with non-aqueous formaldehyde sources like trioxane (Figure 1) [6,15]. In own work, efficient catalysts for this reaction have been discovered and meanwhile, several studies on the reaction of DME with trioxane have been carried out. In early attempts, BEA zeolites have been employed as catalysts and exhibited remarkable activity in this reaction. Subsequently, a series of other zeolites has been tested and further promising catalysts, predominantly zeolites, have been identified.

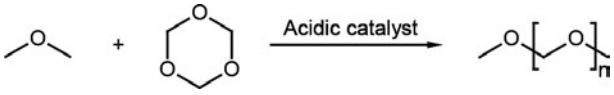

Figure 1: Synthesis of OMEs from DME and trioxane.

Compared to OME synthesis routes starting from DMM or methanol, the reaction is slow. This enables a kinetic control of product spectra, i.e. in the beginning of the reaction higher OMEs, especially OME_3, are dominating. These are degraded during the course of reaction and the product distribution is shifted towards short-chain OMEs. Such a behaviour is different from other synthesis procedures which usually proceed via chain growth, i.e. oligomerization reactions from short-chain OMEs to higher OMEs. The resulting mixtures contain mainly OME_{1-6} and concentrations of the OME components decrease with increasing chain length. Regarding by-products, methyl formate has been observed in many cases. However, the formation of methyl formate could be suppressed to a large extent by using improved catalysts.

2.2 Synthesis of (asymmetric) OMEs with higher end groups via transacetalization reactions

Very recently, modification of OMEs by transacetalization reactions has been described as a versatile strategy for the preparation of OMEs with variable end groups [7]. By this, asymmetric OMEs with different end groups are also accessible (Scheme 1). Regarding catalysts for this reaction, zeolites exhibited most promising performances.

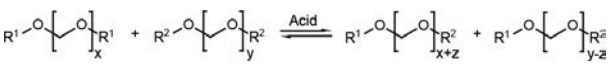

Scheme 1: Synthesis of asymmetric OMEs by acid-catalyzed transacetalization reactions.

Current work in this field concentrates on introducing ethyl, propyl, butyl and higher alkyl groups as well as functionalized groups, which enable further chemical modification. Properties of these new OMEs are determined and correlated with their molecular structures. Thus, structure-performance relationships can be determined, which support a rational fuel design according to the respective requirements.
Another useful application of transacetalization reactions is the conversion of short-chain OMEs (OME_1 and OME_2) or long-chain OMEs ($OME_{\geq 5}$) to OMEs with medium chain length. Thus, unwanted OMEs can be reacted to OMEs with appropriate chain length, which meet the respective requirements [16].

3. Analysis of OMEs

All synthesis procedures for oligomeric OMEs usually yield mixtures which contain predominantly OME_{1-6}. Since the properties of the individual OMEs vary widely, properties of different OME fractions largely depend on their compositions. Furthermore, impurities can remarkably influence properties and thus, reliable analysis techniques are necessary to separate and characterize the mixtures. Gas chromatography proved to be a powerful tool for the separation of complex mixtures [17,18] and spectrometric as well as spectroscopic methods such as mass spectrometry, FTIR or NMR spectroscopy have been adapted for a detailed characterization [19]. Formaldehyde contents in the reaction and product mixtures are an important aspect in OME synthesis and handling. Usually titration with sodium sulfite is employed but the method fails at low formaldehyde concentrations. Voltammetric determination has been reported to be a suitable method without cross-sensitivity with other components in the mixtures [20].

4. Properties and standardization of OMEs

Within the last years, several studies on OME properties appeared and supplemented previous work [19,21-23]. Various physico-chemical and fuel-related data are available now regarding single OMEs as well as mixtures containing different OMEs and different quantities of the components. In this context, the synthesis of high purity OME_2 was somewhat challenging since conventional procedures lead to OME_2 contaminated with the starting materials, especially trioxane. This problem could be solved by reacting trioxane with a large excess of OME_1 followed by thorough distillation [23]. OMEs with ethyl end groups instead of the ubiquitous methyl

Narr Francke Attempto Verlag GmbH + Co. KG

end groups have also been prepared and characterized in detail [19]. Altogether, properties of OMEs can be tuned to a large extent by tuning compositions or structures and based on comprehensive datasets generated within the last years an OME standard is elaborated currently [24].
Furthermore, the available datasets serve as a base for the development of models for the prediction of physico-chemical as well as fuel properties which supports a rational fuel design. Current activities range from the prediction of simple physico-chemical data like densities to the description of OME properties on a highly sophisticated theoretical level, e.g. by development of a force field for OMEs [25-27].
Regarding OME synthesis, data have been collected for modelling the reaction systems and to improve the procedures. This is particularly beneficial in the case of aqueous reaction mixtures which exhibit a complex phase behavior [28-31].

5. Stability and compatibility of OMEs

From the perspective of the user, criteria such as stability of OMEs and compatibility with materials, especially sealants, as well as other fuel components are crucial. Several studies on these topics have been published recently and a comprehensive overview is given in [32]. To illustrate current challenges, three examples are given in the following: (i) Regarding compatibility with other fuel components, interaction with lubricants is an important aspect, which has been addressed by several research groups, e.g. in a recent study on friction and wear [33]. (ii) In the case of oxygen-containing fuels like OMEs, oxidation stability needs to be investigated since oxygenates are known to be prone to further oxidation initiated by the formation of peroxides. This has been investigated in detail and the use of small quantities of antioxidants has been recommended [34]. (iii) If blending with other diesel fuels is envisaged, miscibility and interaction of the components needs to be addressed and compatibility with current standards must be ensured. In the case of OMEs, blending with conventional diesel fuel is possible up to an OME content of approximately 15%. Several attempts have been made to blend OMEs with HVO. In own work, OME/HVO blends could be prepared containing low amounts of OMEs (7 and 10%, respectively), but the cold behavior in terms of the CFPP value of such blends was affected [35]. A limited miscibility of OMEs and HVO was also reported by other groups and the preparation of such blends, e.g. by use of suitable additives, still remains a challenge [36-38].

6. Evaluation of OMEs

Regarding the evaluation of OMEs, several comprehensive studies appeared which compare OMEs to various other alternative fuels (Table 1, Ref.s [39-45]). However, analyses have been carried out on a highly generalized level and in many cases recent progress in the field of OME syntheses is not considered adequately.
A series of more specialized studies addressed the entire process chain from renewable raw materials to OMEs [46-49]. The process chain comprised production of synthesis gas by gasification of woody biomass, methanol and formaldehyde synthesis and finally OME synthesis via established technologies. The underlying thermodynamics have been analyzed and life-cycle as well as techno-economic assessments have been carried out. Production costs have been estimated for different biomass types. Production costs have also been assessed starting from methanol and considering the classical reaction of DMM with trioxane for OME production [50]. The costs largely depend on the methanol price and assuming a methanol price of 300 US$t^{-1} and a capacity of 1 Mio. ta^{-1} results in total production costs of about 615 US$t^{-1} for $OME_{3\text{-}5}$.
In many studies, OME synthesis from CO_2 and H_2 has been analyzed [43,51-53]. Such power-to-X concepts, with methanol as the key intermediate, are feasible but the multi-step processes are energy-intensive and largely depend on the availability of CO_2 and renewable energy. OME synthesis directly from CO_2 has also been reported [51,54]. However, yields are low and mainly OME_1 is formed in such highly integrated approaches.
Very recent studies focus on the role of hydrogen in the process chain [55]. This topic is crucial since hydrogen is needed for methanol synthesis. The required formaldehyde should be produced by a non-oxidative route, ideally by dehydrogenation of methanol, and thus, hydrogen could be recovered. Optimization of OME production by integration of process steps is also intensely investigated and considerable progress has been made in this field [56]. Currently, different OME synthesis procedures are compared taking also latest technical innovations into account [57]. Thus, identification of the most efficient pathway is envisaged.

Table 1: Selected studies on OME evaluation.

Study	Ref.
FVV-Kraftstoffstudie I: Zukünftige Kraftstoffe für Verbrennungsmotoren und Gasturbinen; FVV, Heft 1031 – 2013	[39]
FVV-Kraftstoffstudie III, Kurzfassung: Energiepfade für den Straßenverkehr der Zukunft; FVV, Ausgabe R586, 2018	[40]
FVV-Kraftstoffstudie III: Defossilisierung des Transportsektors; FVV, 09/2018	[41]

Narr Francke Attempto Verlag GmbH + Co. KG

2. Roadmap des Kopernikus-Projektes „Power-to-X“: Flexible Nutzung erneuerbarer Ressourcen (P2X), Optionen für ein nachhaltiges Energiesystem mit Power-to-X Technologien; DECHEMA, 31.08.2019, Frankfurt am Main, 1. Auflage, ISBN: 978-3-89746-218-2	[42]
Power-to-fuel as a key to sustainable transport systems – An analysis of diesel fuels produced from CO_2 and renewable electricity	[43]
Biogenous ethers: production and operation in a diesel engine	[44]
IEA Bioenergy Task 39, Commercialization of conventional and advanced liquid biofuels from biomass: Survey on Advanced Fuels for Advanced Engines; IEA Bioenergy Task 39, October 2018	[45]
Biomass-derived oxymethylene ethers as diesel additives: A thermodynamic analysis	[46]
An optimized process design for oxymethylene ether production from woody-biomass-derived syngas	[47]
A life cycle assessment of oxymethylene ether synthesis from biomass-derived syngas as a diesel additive	[48]
The development of the production cost of oxymethylene ethers as diesel additives from biomass	[49]
From methanol to the oxygenated diesel fuel poly(oxymethylene) dimethyl ether: An assessment of the production costs	[50]
Cleaner production of cleaner fuels: wind-to-wheel – environmental assessment of CO_2-based oxymethylene ether as a drop-in fuel	[51]
On the energetic efficiency of producing polyoxymethylene dimethyl ethers from CO_2 using electrical energy	[52]
Comparative well-to-wheel life cycle assessment of OME_{3-5} synfuel production via the power-to-liquid pathway	[53]
Power-to-OME - Processes for the Production of Oxymethylene Dimethyl Ether from Hydrogen and Carbon Dioxide	[54]
H_2-based synthetic fuels: A techno-economic comparison of alcohol, ether and hydrocarbon production	[55]
Optimal Integrated Facility for Oxymethylene Ethers Production from Methanol	[56]
Economic and life-cycle assessment of OME_{3-5} as transport fuel: a comparison of production pathways	[57]

7. Conclusions

In recent years, remarkable progress has been made in the field of OMEs regarding production, characterization and application. Promising synthesis procedures have been further developed, e.g. syntheses from methanol and DME employing different formaldehyde sources. Another option are chemical modifications, e.g. by transacetalization reactions which lead to new OMEs with tunable properties.

Various properties of OMEs have been determined and an OME standard is currently elaborated. Correlations between molecular structures of OMEs and their performances have been identified which are now implemented in models for the prediction of physico-chemical as well as fuel properties. This will support a rational fuel design according to the respective requirements as well as a targeted optimization.

Regarding compatibility of OMEs with materials and other fuel components, new and valuable insights have been gained. These will facilitate the handling of OMEs and also help to develop blending strategies.

Several studies on the evaluation of OME fuels are available now, e.g. life-cycle as well as techno-economic assessments. These indicate that sustainable production is possible in principle. One major challenge is certainly the availability of renewable starting materials as well as renewable energies. Ongoing work concentrates on these topics and a largely unexplored potential for further optimization is apparent.

Acknowledgement

Financial support from *Fachagentur Nachwachsende Rohstoffe/BMEL* (Joint research project: “Oxymethylene ethers (OME): Eco-friendly diesel additives from renewables”, funding code 22403814) is gratefully acknowledged. The authors also thank the *Bundesministerium für Bildung und Forschung* (BMBF) for funding within the Kopernikus Project “P2X: Flexible use of renewable resources – research, validation and implementation of “Power-to-X” concepts” (Research cluster FC-B3 “Oxymethylene ethers: Fuels and plastics based on CO_2 and hydrogen”, funding code 03FK2K0) and for funding within the NAMOSYN project (“Sustainable mobility with synthetic fuels”, funding code 03SF0566K0).

References

[1] B. Niethammer, S. Wodarz, M. Betz, P. Haltenort, D. Oestreich, K. Hackbarth, U. Arnold, T. Otto, J. Sauer, Alternative liquid fuels from renewable resources, *Chem. Ing. Tech.* 2018, *90(1-2)*, 99-112. DOI: 10.1002/cite.201700117

[2] M. Härtl, K. Gaukel, D. Pélerin, G. Wachtmeister, Oxymethylene Ether as Potentially CO_2-neutral Fuel for Clean Diesel Engines Part 1: Engine Testing, *MTZ worldwide* 2017, *78(2)*, 52-59. DOI: 10.1007/s38313-016-0163-6

Narr Francke Attempto Verlag GmbH + Co. KG

[3] E. Jacob, W. Maus, Oxymethylene Ether as Potentially Carbon-neutral Fuel for Clean Diesel Engines Part 2: Compliance with the Sustainability Requirement, *MTZ worldwide* 2017, *78(3)*, 52-57. DOI: 10.1007/s38313-017-0002-4

[4] K. Hackbarth, P. Haltenort, U. Arnold, J. Sauer, Recent Progress in the Production, Application and Evaluation of Oxymethylene Ethers, *Chem. Ing. Tech.* 2018, *90(10)*, 1520-1528. DOI: 10.1002/cite.201800068

[5] C.J. Baranowski, A.M. Bahmanpour, O. Kröcher, Catalytic synthesis of polyoxymethylene dimethyl ethers (OME): A review, *Appl. Catal., B* 2017, *217*, 407-420. DOI: 10.1016/j.apcatb.2017.06.007

[6] P. Haltenort, K. Hackbarth, D. Oestreich, L. Lautenschütz, U. Arnold, J. Sauer, Heterogeneously catalyzed synthesis of oxymethylene dimethyl ethers (OME) from dimethyl ether and trioxane, *Catal. Commun*. 2018, *109*, 80-84. DOI: 10.1016/j.catcom.2018.02.013

[7] P. Haltenort, L. Lautenschütz, U. Arnold, J. Sauer, (Trans)Acetalization Reactions for the Synthesis of Oligomeric Oxymethylene Dialkyl Ethers Catalyzed by Zeolite BEA25, *Top. Catal.* 2019, *62(5-6)*, 551-559. DOI: 10.1007/s11244-019-01188-9

[8] M. Shi, Y. Wang, J. Wang, F. Dai, Y. Yu, H. Zhang, Q. Li, A review on processes for synthesis of polyoxymethylene dimethyl ethers, *Tianranqi Huagong* 2015, *40(4)*, 91-96.

[9] T. Bhatelia, W. J. Lee, C. Samanta, J. Patel, A. Bordoloi, Processes for the production of oxymethylene ethers: promising synthetic diesel additives, *Asia-Pac. J. Chem. Eng.* 2017, *12*, 827-837. DOI: 10.1002/apj.2119

[10] Y. Yang, J. Zhang, C. Zhang, R. Li, Research progress in polyoxymethylene dimethyl ethers, *Shiyou Huagong, Petrochemical Technology* 2018, *47(11)*, 1268-1275. DOI: 10.3969/j.issn.1000-8144.2018.11.017

[11] H. Liu, Z. Wang, Y. Li, Y. Zheng, T. He, J. Wang, Recent progress in the application in compression ignition engines and the synthesis technologies of polyoxymethylene dimethyl ethers, *Applied Energy* 2019, *233-234*, 599-611. DOI: 10.1016/j.apenergy.2018.10.064

[12] R. Sun, I. Delidovich, R. Palkovits, Dimethoxymethane as a Cleaner Synthetic Fuel: Synthetic Methods, Catalysts, and Reaction Mechanism, *ACS Catalysis* 2019, *9(2)*, 1298-1318. DOI: 10.1021/acscatal.8b04441

[13] L. Lautenschütz, D. Oestreich, P. Haltenort, U. Arnold, E. Dinjus, J. Sauer, Efficient synthesis of oxymethylene dimethyl ethers (OME) from dimethoxymethane and trioxane over zeolites, *Fuel Process. Technol.* 2017, *165*, 27-33. DOI: 10.1016/j.fuproc.2017.05.005

[14] N. Schmitz, J. Burger, H. Hasse, Reaction Kinetics of the Formation of Poly(oxymethylene) Dimethyl Ethers from Formaldehyde and Methanol in Aqueous Solutions, *Ind. Eng. Chem. Res.* 2015, *54(50)*, 12553-12560. DOI: 10.1021/acs.iecr.5b04046

[15] C.F. Breitkreuz, N. Schmitz, E. Stroefer, J. Burger, H. Hasse, Design of a Production Process for Poly(oxymethylene) Dimethyl Ethers from Dimethyl Ether and Trioxane, *Chem. Ing. Tech.* 2018, *90(10)*, 1489-1496. DOI:10.1002/cite.201800038

[16] Y. Zheng, F. Liu, L. Guo, T. Wang, J. Wang, Molecular size reforming of undersized and oversized polyoxymethylene dimethyl ethers, *RSC Advances* 2016, *6(81)*, 77116-77125. DOI: 10.1039/C6RA08255F

[17] Y.-Y. Zheng, Q. Tang, J.-F. Wang, T.-F. Wang, Determination of the correction factor of polyoxymethylene dimethyl ethers in gas chromatography without standard samples, *Gao Xiao Hua Xue Gong Cheng Xue Bao/Journal of Chemical Engineering of Chinese Universities* 2015, *29(3)*, 505-509. DOI:10.3969/j.issn.1003-9015.2015.04.23.02

[18] G. Zhu, F. Zhao, D. Wang, C. Xia, Extended effective carbon number concept in the quantitative analysis of multi-ethers using predicted response factors, *Journal of Chromatography A* 2017, *1513*, 194-200. DOI: 10.1016/j.chroma.2017.07.036

[19] L. Lautenschütz, D. Oestreich, P. Seidenspinner, U. Arnold, E. Dinjus, J. Sauer, Physico-chemical properties and fuel characteristics of oxymethylene dialkyl ethers, *Fuel* 2016, *173*, 129-137. DOI: 10.1016/j.fuel.2016.01.060

[20] I. Bogatykh, T. Osterland, H. Stein, T. Wilharm, Voltammetric determination of formaldehyde at low concentrations in the synthetic fuel oxymethylene dimethyl ether, *Energy Fuels* 2019, *33(11)*, 11078-11081. DOI: 10.1021/acs.energyfuels.9b02481

[21] R.H. Boyd, Some physical properties of polyoxymethylene dimethyl ethers, *J. Polym. Sci.* 1961, *50(153)*, 133-141.

[22] M. KANG, H. SONG, F. JIN, J. CHEN, Synthesis and physicochemical characterization of polyoxymethylene dimethyl ethers, *J. Fuel Chem. Technol.* 2017, *45(7)*, 837-845. DOI: 10.1016/S1872-5813(17)30040-3

[23] D. Deutsch, D. Oestreich, L. Lautenschütz, P. Haltenort, U. Arnold, J. Sauer, High Purity Oligomeric Oxymethylene Ethers as Diesel Fuels, *Chem. Ing. Tech.* 2017, *89(4)*, 486-489. DOI: 10.1002/cite.201600158

[24] T. Wilharm, H. Stein, I. Bogatykh, Fahrplan zu einer OME-Spezifikation (Roadmap to an OME specification), J. Liebl et al. (Ed.), Internationaler Motorenkongress 2020, Proceedings, Springer, Wiesbaden, 2020. DOI: 10.1007/978-3-658-30500-0_13

Narr Francke Attempto Verlag GmbH + Co. KG

[25] D. Wang, F. Zhao, G. Zhu, Z. Li, C. Xia, High-cetane additives for diesel based on polyoxymethylene dimethyl ethers: Density behavior and prediction, *Journal of Molecular Liquids* 2017, *234*, 403-407. DOI: 10.1016/j.molliq.2017.03.105

[26] A. Kulkarni, E.J. García, A. Damone, M. Schappals, S. Stephan, M. Kohns, H. Hasse, A Force Field for Poly(oxymethylene) Dimethyl Ethers (OMEn), *Journal of Chemical Theory and Computation* 2020, *16(4)*, 2517-2528. DOI: 10.1021/acs.jctc.9b01106

[27] D.L. Bartholet, M.A. Arellano-Treviño, F.L. Chan, S. Lucas, J. Zhu, P.C. St. John, T.L. Alleman, C.S. McEnally, L.D. Pfefferle, D.A. Ruddy, B. Windom, T.D. Foust, K.F. Reardon, Property predictions demonstrate that structural diversity can improve the performance of polyoxymethylene ethers as potential bio-based diesel fuels, *Fuel* 2021, *295*, 120509. DOI: 10.1016/j.fuel.2021.120509

[28] Z. Zhuang, J. Zhang, X. Liu, D. Liu, Liquid–liquid equilibria for ternary systems polyoxymethylene dimethyl ethers + para-xylene + water, *J. Chem. Thermodynamics* 2016, *101*, 190-198. DOI: 10.1016/j.jct.2016.05.016

[29] N. Schmitz, A. Friebel, E. von Harbou, J. Burger, H. Hasse, Liquid-liquid equilibrium in binary and ternary mixtures containing formaldehyde, water, methanol, methylal, and poly(oxymethylene) dimethyl ethers, *Fluid Phase Equilibria* 2016, *425*, 127-135. DOI: 10.1016/j.fluid.2016.05.017

[30] X. Li, J. Cao, M.A. Nawaz, Y. Hu, D. Liu, Experimental and Correlated Liquid–Liquid Equilibrium Data for Ternary Systems (Water + Poly(oxymethylene) Dimethyl Ethers + Toluene) at T = 293.15 and 303.15 K and p = 101.3 kPa, *J. Chem. Eng. Data* 2019, *64(12)*, 5548-5557. DOI: 10.1021/acs.jced.9b00653

[31] S. Schemme, S. Meschede, M. Köller, R.C. Samsun, R. Peters, D. Stolten, Property Data Estimation for Hemiformals, Methylene Glycols and Polyoxymethylene Dimethyl Ethers and Process Optimization in Formaldehyde Synthesis, *Energies* 2020, *13(13)*, 3401-3429. DOI: 10.3390/en13133401

[32] J. Schröder, K. Görsch, Storage Stability and Material Compatibility of Poly(oxymethylene) Dimethyl Ether Diesel Fuel, *Energy Fuels* 2020, *34(1)*, 450-459. DOI: 10.1021/acs.energyfuels.9b03101

[33] A.L. Nagy, J. Knaup, I. Zsoldos, A friction and wear study of laboratory aged engine oil in the presence of diesel fuel and oxymethylene ether, *Tribol. Mater. Surf. Interfaces* 2019, *13(1)*, 20-30. DOI: 10.1080/17515831.2018.1558026

[34] I. Bogatykh, T. Osterland, H. Stein, T. Wilharm, Investigation of the Oxidative Degradation of the Synthetic Fuel Oxymethylene Dimethyl Ether, *Energy Fuels* 2020, *34(3)*, 3357-3366. DOI: 10.1021/acs.energyfuels.9b04464

[35] D. Oestreich, L. Lautenschütz, U. Arnold, J. Sauer, Production of oxymethylene dimethyl ether (OME)-hydrocarbon fuel blends in a one-step synthesis/extraction procedure, *Fuel* 2018, *214*, 39-44. DOI: 10.1016/j.fuel.2017.10.116

[36] M. Unglert, D. Bockey, C. Bofinger, B. Buchholz, G. Fisch, R. Luther, M. Müller, K. Schaper, J. Schmitt, O. Schröder, U. Schümann, H. Tschöke, E. Remmele, R. Wicht, M. Winkler, J. Krahl, UFOP-Fachkommission Biokraftstoffe und Nachwachsende Rohstoffe, Handlungsfelder und Forschungsbedarf bei Biokraftstoffen, 1. Aufl., Göttingen, Cuvillier, 2019. ISBN 978-3-7369-7088-5, eISBN 978-3-7369-6088-6

[37] S. Proschke, M. Unglert, Charakterisierung der Mischbarkeit gealterter Kraftstoffe, https://www.tac-coburg.de/images/BKS_2019_Charakterisierung_der_Mischbarkeit_gealterter_Kraftstoffe.pdf

[38] A. Omari, B. Heuser, S. Pischinger, C. Rüdinger, Potential of long-chain oxymethylene ether and oxymethylene ether-diesel blends for ultra-low emission engines, *Applied Energy* 2019, *239*, 1242-1249. DOI: 10.1016/j.apenergy.2019.02.035

[39] https://www.fvv-net.de/fileadmin/user_upload/medien/materialien/FVV-Kraftstoffstudie_LBST_2013-10-30.pdf

[40] https://www.fvv-net.de/fileadmin/user_upload/medien/materialien/FVV_Kraftstoffe_Studie_Defossilisierung_R586_final_v.3_2019-06-14_DE.pdf

[41] https://www.fvv-net.de/fileadmin/user_upload/medien/materialien/FVV_Kraftstoffe_Studie_Energiepfade_final_v.3_2018-10-01_DE.pdf

[42] https://dechema.de/dechema_media/Downloads/Positionspapiere/2019_DEC_P2X_Kopernikus_RZ_Webversion02-p-20005425.pdf

[43] S. Schemme, R.C. Samsun, R. Peters, D. Stolten, Power-to-fuel as a key to sustainable transport systems – An analysis of diesel fuels produced from CO_2 and renewable electricity, *Fuel* 2017, *205*, 198-221. DOI: 10.1016/j.fuel.2017.05.061

[44] A. Damyanov, P. Hofmann, B. Geringer, N. Schwaiger, T. Pichler, M. Siebenhofer, Biogenous ethers: production and operation in a diesel engine, *Automotive and Engine Technology* 2018, *3*, 69-82. DOI: 10.1007/s41104-018-0028-x

[45] http://task39.sites.olt.ubc.ca/files/2018/10/Survey-on-Advanced-Fuels-for-Advanced-Engines-IEA_Bioenergy_T39_AFAE_DBFZ.pdf

[46] X. Zhang, A. Kumar, U. Arnold, J. Sauer, Biomass-derived oxymethylene ethers as diesel additives: A thermodynamic analysis, *Energy Procedia* 2014, *61*, 1921-1924. DOI: 10.1016/j.egypro.2014.12.242

Narr Francke Attempto Verlag GmbH + Co. KG

[47] X. Zhang, A.O. Oyedun, A. Kumar, D. Oestreich, U. Arnold, J. Sauer, An optimized process design for oxymethylene ether production from woody-biomass-derived syngas, *Biomass Bioenergy* 2016, *90*, 7-14. DOI: 10.1016/j.biombioe.2016.03.032

[48] N. Mahbub, A.O. Oyedun, A. Kumar, D. Oestreich, U. Arnold, J. Sauer, A life cycle assessment of oxymethylene ether synthesis from biomass-derived syngas as a diesel additive, *J. Cleaner Prod.* 2017, *165*, 1249-1262. DOI: 10.1016/j.jclepro.2017.07.178

[49] A.O. Oyedun, A. Kumar, D. Oestreich, U. Arnold, J. Sauer, The development of the production cost of oxymethylene ethers as diesel additives from biomass, *Biofuels, Bioprod. Biorefin.* 2018, *12(4)*, 694-710. DOI: 10.1002/bbb.1887

[50] N. Schmitz, J. Burger, E. Ströfer, H. Hasse, From methanol to the oxygenated diesel fuel poly(oxymethylene) dimethyl ether: An assessment of the production costs, *Fuel* 2016, *185*, 67-72. DOI:10.1016/j.fuel.2016.07.085

[51] S. Deutz, D. Bongartz, B. Heuser, A. Kätelhön, L. Schulze Langenhorst, A. Omari, M. Walters, J. Klankermayer, W. Leitner, A. Mitsos, S. Pischinger, A. Bardow, Cleaner production of cleaner fuels: wind-to-wheel – environmental assessment of CO_2-based oxymethylene ether as a drop-in fuel, *Energy Environ. Sci.* 2018, *11*, 331-343. DOI: 10.1039/c7ee01657c

[52] M. Held, Y. Tönges, D. Pélerin, M. Härtl, G. Wachtmeister, J. Burger, On the energetic efficiency of producing polyoxymethylene dimethyl ethers from CO_2 using electrical energy, *Energy Environ. Sci.* 2019, *12*, 1019-1034. DOI: 10.1039/C8EE02849D

[53] C. Hank, L. Lazar, F. Mantei, M. Ouda, R.J. White, T. Smolinka, A. Schaadt, C. Heblinga, H.-M. Henning, Comparative well-to-wheel life cycle assessment of OME_{3-5} synfuel production *via* the power-to-liquid pathway, *Sustainable Energy Fuels* 2019, *3*, 3219-3233. DOI: 10.1039/C9SE00658C

[54] D. Bongartz, J. Burre, A. Mitsos, Power-to-OME - Processes for the Production of Oxymethylene Dimethyl Ether from Hydrogen and Carbon Dioxide, *Chem Ing. Tech.* 2018, *90(9)*, 1155. DOI: 10.1002/cite.201855050

[55] S. Schemme, J.L. Breuer, M. Köller, S. Meschede, F. Walman, R.C. Samsun, R. Peters, D. Stolten, H_2-based synthetic fuels: A techno-economic comparison of alcohol, ether and hydrocarbon production, *International Journal of Hydrogen Energy* 2020, *45(8)*, 5395-5414. DOI: 10.1016/j.ijhydene.2019.05.028

[56] M. Martín, J. Redondo, I.E. Grossmann, Optimal Integrated Facility for Oxymethylene Ethers Production from Methanol, *ACS Sustainable Chem. Eng.* 2020, *8(16)*, 6496-6504. DOI: 10.1021/acssuschemeng.0c01127

[57] D.F. Rodríguez-Vallejo, A. Valente, G. Guillén-Gosálbez, B. Chachuat, Economic and life-cycle assessment of OME_{3-5} as transport fuel: a comparison of production pathways, *Sustainable Energy Fuels* 2021, *5(9)*, 2504-2516. DOI: 10.1039/D1SE00335F

Narr Francke Attempto Verlag GmbH + Co. KG

Production of sustainable fuels by heterogeneously catalyzed oligomerization of C_2-C_4 olefins

Constantin Fuchs
Karlsruhe Institute of Technology, Institute of Catalysis Research and Technology, Eggenstein-Leopoldshafen, Germany
Constantin.Fuchs@kit.edu

Matthias Betz
Karlsruhe Institute of Technology, Institute of Catalysis Research and Technology, Eggenstein-Leopoldshafen, Germany

Dr. Ulrich Arnold
Karlsruhe Institute of Technology, Institute of Catalysis Research and Technology, Eggenstein-Leopoldshafen, Germany

Prof. Dr.-Ing. Jörg Sauer
Karlsruhe Institute of Technology, Institute of Catalysis Research and Technology, Eggenstein-Leopoldshafen, Germany

Summary

Particle formation during engine combustion is favoured in the presence of aromatics. However they offer high octane ratings. Aromatic-free fuels consequently produce lower particulate emissions than currently used fuels made from crude oil. Such synthetic fuels may be produced by heterogeneously catalyzed oligomerization of olefins like ethene, propene and butenes. The oligomerization of higher olefins has so far been less in the focus of fuel synthesis, but is promising with respect to the degree of branching and the octane rating.
In this paper the possibilities of producing fuels by oligomerization of C_2-C_4 olefins will be shown. Sources of sustainable olefins like the methanol-to-olefins process are presented, followed by the state of the art regarding the oligomerization. Furthermore, the set-up of a lab-scale plant is introduced and recent results concerning the co-oligomerizations of propene and 1-butene are presented. It is visible that mixtures of these two components as feeds effect their conversions and the resulting product spectra due to varying reactivities.

1. Introduction

The main source of airborne contaminates in the cities are products from the combustion of organic substances. The combustion of fossil fuels will lead to increase the CO_2 content of the air. Additionally, side products like soot, SO_2, NOx etc. worsen the quality of air especially in large cities.
Fuels currently used in combustion engines are mainly based on fossil raw materials, relatively easy to handle and are characterized by their high energy density [1]. For spark-ignition engines, currently aromatics are indispensable. They offer the advantage of high octane ratings [2], but are considered to be precursors of particle formation [3]. In aviation, kerosene also consists of high proportions of aromatics up to $x_{Aromatics}$ = 26,5 vol.% [4].
During combustion, aromatics-free may consequently reduce the particulate emissions compared to currently used fossil fuels. With regard to air pollution control, aromatics-free fuels based on sustainable sources represent a low-emission option for the continued use of internal combustion engines in urban areas [5, 6].
In addition, renewable fuels offer the possibility in all respects to operate vehicles with low emissions and also to be used in the existing fleets. A further advantage of such synthetic fuels is the possibility of adjusting specific physico-chemical fuel properties through targeted synthesis of individual components. However, to balance the octane rating in aromatics-free paraffinic fuels,

Narr Francke Attempto Verlag GmbH + Co. KG

the degree of branching of the paraffin molecules must be increased.

Nowadays, the production of high quality, aromatic-free gasoline is still proving difficult. The heterogeneously catalyzed oligomerization of propene, as well as butenes in addition to ethene has so far been less investigated regarding the synthesis of fuels, but considering the molecule's degree of branching and thus as well the octane rating, it is promising. There are already industrial-scale processes that convert these olefins into fuels, but these were invented several decades ago and have not been pursued and further developed since then for economic reasons [7–9]. Furthermore the octane rating of the produced gasoline is not sufficient for today's standards [7, 10].

The focus of own work is on the investigation of the heterogeneously catalyzed oligomerization of alkenes with carbon chain lengths between C_2 and C_4. The aim is to produce high-octane gasoline fuels that meet the EN 228 standard from sustainable olefins. Yields of sideproducts like kerosene and diesel are to minimize.

Subsequently, the current states of the art related to the production of sustainable olefins, followed by heterogeneous oligomerization are shown and completed by lab-scale experiments of the latter process.

2. State of the art

2.1 Sources of sustainable olefins

Starting from sustainable methanol, olefins can be produced via the methanol-to-olefins (MtO) process. This conversion takes place according to the following simplified equation:

$$n\ CH_3OH \rightarrow [CH_2]_n + n\ H_2O \qquad (1)$$

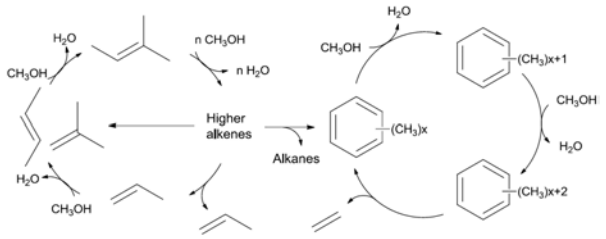

Figure 1: Double cycle reaction mechanism in the case of MtO catalysts [25]

From DME, via the DtO process, this is also viable [11]. At lower pressures (p = 1 - 30 bar) and higher temperatures (T = 450 - 600 °C) compared to the methanol-to-gasoline (MtG) process [12, 13], the synthesis of shorter hydrocarbons is favoured [14, 15]. Both methanol-based processes were developed in the 1980s [15, 16]. In addition to Mobil, UOP and Norsk Hydro (now Ineos) brought the process to market readiness in the 1990s, using H-SAPO-34 as a catalyst in a low-pressure fluidised bed reactor. This concept enables efficient temperature control and continuous catalyst regeneration [17].

ZSM-5 zeolites and SAPO zeotypes are commercially used for the MtO process. Both catalysts have Brønsted acid sites in structured micropores. The pore system of the aluminosilicate ZSM-5 is three-dimensional and has an average pore diameter of d_{Pore} = 5,5 Å. H-SAPO-34 is a silica aluminophosphate with a cage structure and pore sizes of only d_{Pore} = 3,8 Å. The small pore diameters favour the formation of small molecules and prevent the diffusion and formation of larger molecules. This explains the high selectivity to linear, light olefins. Aromatics and higher branched hydrocarbons are too large to diffuse out of the pore structure [18–20]. However, the smaller the pores of the catalysts, the faster this leads to their blockage and thus deactivation due to the deposition of coke.

For the MtO reactions, catalysts with moderate acid strength and density of the acid centres are required. A high acid strength has a beneficial effect on the activity of the catalyst, but it is also deactivated faster due to the likewise increased formation of coke [21–23].

The formation of the olefins takes place through the formation of alkyl residues on aromatics and their subsequent spin-off. The aromatics are trapped in the catalyst structure, cannot diffuse out due to their size and serve as a co-catalyst. Side chains are formed on the aromatics through the addition of methanol. The separation of these leads to the formation of ethene. Propene and butenes are formed by subsequent methylation of ethene [24]. This double-cycle mechanism was consolidated by Björgen et al. [25] and is shown in Figure 1.More information on the synthesis of olefins from methanol and the catalysts that can be used for this purpose, as well as other influencing parameters, can be found in the review articles [15, 16]. Process flow diagrams of various other MtO processes are also shown.

Alternatively, the dehydration of fermentative alcohols offers the possibility of producing their corresponding olefins on a regenerative basis. This is further explained below using iso-butanol as an example. The conversion of iso-butanol to iso-butene takes place by means of acid dehydration via an elimination mechanism, as shown in Figure 2 [26].

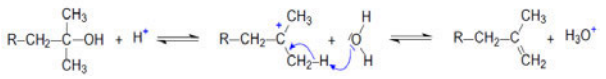

Figure 2: Elimination reaction of iso-butanol to iso-butene [26].

By protonation of the OH group and formation of a carbenium ion, water splits off and iso-butene is formed. The reaction preferably takes place at p < 7 bar via γ-Al_2O_3 catalysts [27]**.** SAPO, H-ZSM-5 or heteropolyacid catalysts can also be used. [28]. With alcohols such

Narr Francke Attempto Verlag GmbH + Co. KG

as n-butanol, the elimination takes place at different positions, resulting in butene mixtures. With isobutanol, however, iso-butene is always formed due to symmetry. To overcome the activation energy of the reaction, temperatures of T = 250 - 350 °C are advan-tageous [26, 29, 30].
Direct conversion of ethanol to butenes is also possible. On a zinc-zirconium oxide catalyst at temperatures of T = 450 °C and p = 1 bar, selectivities S and yields Y of above 80% are achieved with complete conversion X of ethanol to iso-butene. The reaction requires water as a co-feed so that it proceeds via intermediates such as acetaldehyde and acetone to iso-butene. The ZnO in the catalyst reduces the acidity of the Lewis and Brønsted acid sites of the ZrO_2 and thus increases the basicity. This suppresses undesirable side reactions such as the dehydration of ethanol and the polymerisation of acetone. The dehydration of ethanol to acetaldehyde and its conversion to acetone via aldol condensations and dehydrations is promoted by the basic centres. The Brønsted sites are responsible for the final acid-catalysed conversion of acetone to iso-butene [31].
Furthermore, with Ag-ZrO_2/SiO_2 catalysts, the direct conversion of ethanol to a butene-rich (1-, 2-butenes and butadiene) olefin mixture is possible at conversions of X = 99% and a selectivity of S = 88%. By adjusting the co-feed to hydrogen, the ratio of butenes to butadiene can be regulated [32].
A direct fermentation of olefins from biomass is also possible. Global Bioenergies, for example, has developed a process for the fermentative production of isobutene and is currently operating a first pilot plant in Leuna. The conversion takes place in stirred tank reactors at p = 4 bar and T = 32 °C using gene-modified E. coli bacteria, which produce iso-butene directly from sugars [33, 34]. The bacteria are currently specialised in the conversion of glucose. However, the straw hydrolysate is largely composed of glucose and xylose, and also contains inhibiting substances from the biomass. The adaptation of the bacteria to these conditions still needs further research, but the conversion of xylose to iso-butene is already possible. Lignin, on the other hand, cannot be converted [35].

2.2 Oligomerization

The produced olefins are then fed to the oligomerization process. There, the lower olefins are converted into higher olefins, only low contents of aromatics will be generated. As an example, this is shown below in a general formula for ethene, propene and butene.

$$a\ C_2H_4 + b\ C_3H_6 + c\ C_4H_8 \rightarrow w\ C_5H_{10} + x\ C_6H_{12} + y\ C_7H_{14} + z\ C_8H_{16}\ldots \quad (2)$$

For the conversion, acid sites especially Brønsted sites are important to achieve a first protonation to form carbenium-ions [36]. The subsequent chain growth is the result from this initial step. Exemplary, Table 1 summarizes three oligomerization processes, which are industrially realised at scale and briefly described below.

In the 1980s, the Mobil Olefins to Gasoline and Distillate (MOGD) process was developed by Mobil Oil Corp. (now ExxonMobil). In this process, olefins from the methanol-to-olefins process are converted to gasoline, kerosene and diesel on an acidic ZSM-5 catalyst (d_{Pore} = 5.5 Å) in several reactors connected in series. In the MOGD process, four fixed-bed reactors are operated simultaneously, one of which is regenerated due to coke formation while the other reactors are in operation (Figure 3). The process takes place at T = 150 - 200 °C and p = 7 - 12 bar [7]. By adjusting the process conditions, the ratio of gasoline to distillate can be varied between 0.2 and 100.

Table 1: Overview of the MOGD, Polynaphtha and Catpoly processes with regard to reaction conditions and reaction control.

	MOGD (Exxon-Mobil) [7]	Polynaphtha (Axens IFP) [8]	Catpoly (UOP) [9]
Catalyst	Zeolite ZSM-5	Silica-Alumina	Solid phosphoric acid
***T* [°C]**	150 - 200	150 - 200	180 - 200
***p* [bar]**	7 - 12	30 - 50	30 - 40
***LHSV* [m³/h /m³ Catalyst]**	1 - 2	0,3 - 0,5	0,5 - 1
Conversion to fuels [%]	> 90	95 - 98	90 - 95
Reactor type	Adiabatic fixed bed reactor	Fixed bed reactor	Hordes reactor

Table 2: Properties of fuels from MOGD process [7].

	Gasoline	Kerosene	Diesel
Relative density* [-]	0,73	0,78	0,78
Research octane number [-]	92		
Motor octane number [-]	79		
Cetane number [-]			52
Composition			
Paraffins[wt.%]	4	95	
Olefins [wt.%]	94	1	
Aromatics [wt.%]	2	4	

*related to the density of water at T = 4 °C

Narr Francke Attempto Verlag GmbH + Co. KG

The advantage of this synthesis is the higher product quality of the gasoline compared to a methanol-to-gasoline process, since, for example, it does not or only contain minor quantities below 5 wt.% any particle-promoting aromatics. Also durol is not present, a quadruple-methylated C_{10}-aromatic with a high melting point ($T_{melting,Durol}$ = 78 - 81 °C) [37, 38].
To remove the heat of the exothermic reaction, intercoolers are used after the reactors. Table 2 shows fuel-relevant key properties as well as the composition according to substance groups of the gasoline, kerosene and diesel fractions. Kerosene and diesel were previously hydrotreated with hydrogen.
The polynaphtha process developed by the Institute Français du Pétrol (now Axens IFP) uses C_3-C_5 olefins as reactants. These are converted to oligomeric gasoline and gas oil on a silica-alumina catalyst in the same temperature range, but at significantly higher pressures (p = 30 - 50 bar) than in the case of the MOGD process. In order to obtain higher yields of longer oligomers in the form of gas oil, parts of the LPG fraction, as well as the oligomeric gasoline, is recycled and oligomerized again. Accumulating deposits on the catalysts can be burnt off by adding an air/steam mixture and thus, the catalysts can be regenerated [8].
Honeywell UOP's Catpoly process was already developed in the 1930s. It uses solid phosphoric acid (SPA) as a catalyst and is run with comparable operating windows to the Polynaphta process. However, the conversion of the C_3 and C_4 olefins takes place in a horde reactor and not in several fixed-bed reactors connected in series. [9]. Light olefins are recycled for further oligomerization to higher oligomers.
In addition to the processes of fuel synthesis from olefins, processes based on alcohols have been developed. These also use the principle of oligomerization and offer the advantage of sustainable production of the educts by fermentative processes based on sugar-containing biomass. Sustainable alcohols are dehydrated to olefins, which than undergo oligomerization primary to molecules in the kerosene range. These "Alcohol to Jet" processes (short AtJ) are continuously developed and optimized for example by Lanzatech/PNNL and Gevo [39].

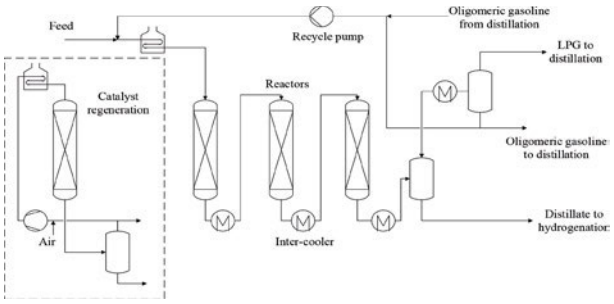

Figure 3: Flow scheme of the MOGD process [7].

3. Experimental

3.1 Lab-scale plant

Experiments for the oligomerization of C_2-C_4 olefins are performed in a laboratory plant with a maximum production volume of 2.5 l/week. Ethene is supplied in gaseous form, propene and butenes are pumped into the reactor as liquids. Argon is also available as an inert gas. The fixed-bed reactor has an inner diameter of d_i = 16 mm and is divided into 3 zones. The inlet and outlet bed only consist of silicon carbide of particle size d = 250 - 500 µm. Both areas are separated by the reaction zone, in which SiC is also present, but mixed with catalysts. In general, tests at up to T = 350 °C and p = 70 bar are possible. Liquid products are subsequently condensed out, collected and after the experiments analysed offline with a gas chromatograph (Agilent 6890 with DB-1 column). Gas is sent to an online gas chromatograph (HP 5890 with RT-Alumina BOND/Na_2SO_4 column) and analysed there.

3.2 Catalysts and catalyst support materials

Silica alumina support materials impregnated with transition metals like nickel are used as catalysts for the oligomerization. This combination has already proven to be very effective regarding ethene oligomerization [40, 41]. Furthermore it enables high olefin conversions at mild reaction conditions (T = 80 – 200 °C, $p_{Olefins}$ = 10 – 50 bar, $WHSV$ = 2 – 10 h^{-1}).
Boehmite SIRALOX® with varying Al_2O_3 / SiO_2 ratios and thus also different strengths and numbers of Lewis and Brønsted acid sites are used as catalyst support. Table 3 shows exemplary some properties of SIRALOX® 20.

Table 3: Properties of SIRALOX® 20 catalyst support [42].

	SIRALOX® 20
Al_2O_3 / SiO_2 [%]	80 / 20
BET [m²/g]	420
Pore volume [ml/g]	0,8

The support material is doped with nickel up to a certain amount using the incipient wetness impregnation method, described below. First, the catalyst support is calcined at T = 550 °C for t = 8 h^{-1}. Afterwards a nickel salt is dissolved in water and applied according to the desired mass fraction of nickel. Finally, the impregnated catalyst support is dried and calcined again and then brought to the same particle size as the SiC.
For the first experiments in the plant, m = 5 g of the SIRALOX® 20 loaded with 2 wt.% Ni are used each time. The reactor is heated to T = 120 °C and pressur-

Narr Francke Attempto Verlag GmbH + Co. KG

ized to p_{total} = 20 bar. Always argon is used as inert gas with a molar fraction of x_{Ar} = 20 mol.% to control the thermal output of the exothermal reaction and maintain a constant bed temperature. The oligomerization of the pure olefins 1-butene and propene is performed with a catalyst loading of *WHSV* = 2 h^{-1} Due to instabilities in the feed-dosing, evoked by too low mass flows for the pumping units, the co-oligomerization of butene and propene is held with doubled *WHSV* of 4 h^{-1} to prevent fluctuation in the feeding system.

4. Results and discussion

4.1 1-Butene oligomerization

The first experiments were performed with 1-butene. Figure 4 shows the conversion *X*, the mass fractions of the produced liquids corresponding to their individual carbon lengths are presented in Figure 5.

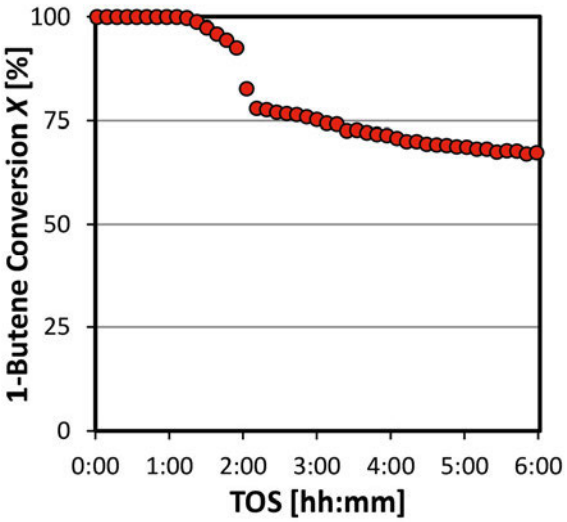

Figure 4: 1-Butene conversion over time-on-stream (TOS) during oligomerization (T = 120 °C, p_{C4H8} = 16 bar, WHSV = 2 h^{-1}).

Due to educt accumulation in the reactor during the initial period, no 1-butenes or isomers of it, formed by the thermal equilibrium, leave the reactor. Therefore, the calculation of butene conversion, which is coupled to the inlet and outlet streams, provides a complete conversion of *X* = 100% at the start of the experiment (Figure 4). After around *t* = 2 h, the reaction begins to enter a steady state, where the conversion is stabilizing on an almost constant level (*X* ~ 70%). After *t* = 6 h the experiment is finished, the olefin feeding is turned off, followed by a flushing phase under Argon flow to rinse out remaining products from the reactor.
The mass composition (Figure 5) shows a high selectivity in the liquid of around *S* = 60% to C_8, the dimer of butenes. The rest of the converted butenes primarily form trimers or tetramers, represented by C_{12} and C_{13+}. In total, 118 different liquid components are generated with high selectivities about *S* > 85% to hydrocarbons in the gasoline and kerosene range.

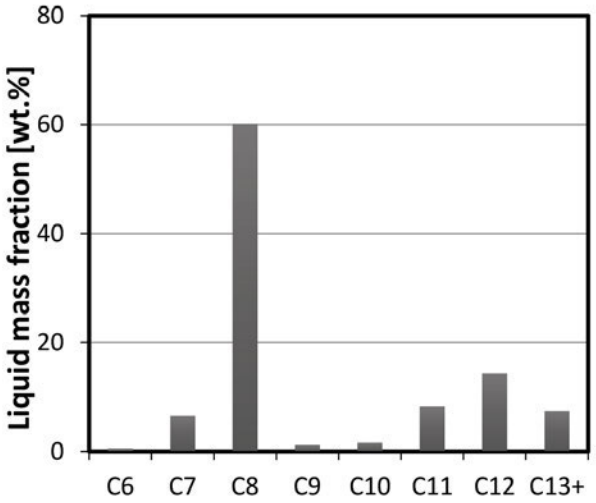

Figure 5: Liquid mass fractions of the 1-butene oligomerization (T = 120 °C, p_{C4H8} = 16 bar, WHSV = 2 h^{-1}).

4.2 Propene oligomerization

Afterwards, the propene oligomerization was held under the same reaction conditions as before. In Figure 6 the propene conversion is portrayed, Figure 7 illustrates the liquid mass fractions. In the gaseous phase, only propene is detected.

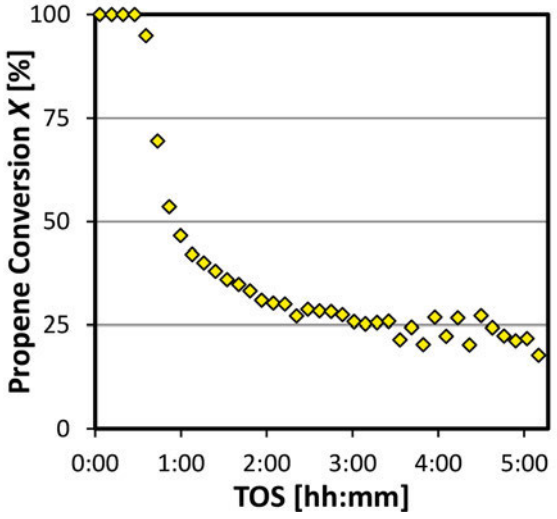

Figure 6: Conversion of propene during oligomerization (T = 120 °C, p_{C3H6} = 16 bar, WHSV = 2 h^{-1}).

Narr Francke Attempto Verlag GmbH + Co. KG

Immediately visible is the significantly lower conversion of propene (X ~ 20%) in comparison to butene. Due to its molecular structure, propene is not as reactive as butene. Futhermore there are no isomers of propene like the 2-butenes or iso-buten in the case of butene. Those isomers may easier form higher, more reactive carbenium-ions. As conclusion, propene needs higher amounts of Brønsted acid sites, whereas butene oligomerization also takes place on surfaces with lower density and acidity of acid sites.

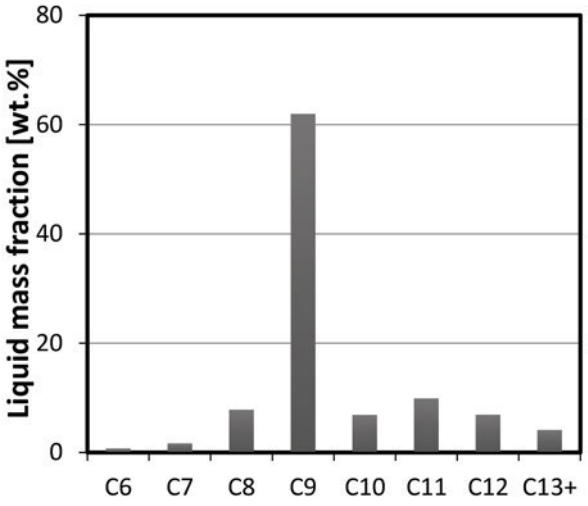

Figure 7: Liquid mass fractions of the propene oligomerization (T = 120 °C, p_{C3H6} = 16 bar, WHSV = 2 h^{-1}).

In Figure 7 is shown, that dimerisation to C_6 almost does not take place, respectively is only an intermediate to higher olefins like the preferably formed trimer C_9. The formation of hydrocarbons which are no integer multiples of propene is related to metathesis reactions. In contrast to the butene oligomerization, with 208 liquid components, the propene coupling leads to almost twice as many different molecules. In the analyzed product range, due to its smaller carbon chain lenght higher degrees of oligomerization of propene are conceivable than of butene. For example to produce a C_{12} olefin, 3 butene but 4 propene molecules are needed, The resulting increased coordination possibilities for oligomers of the same carbon chain length may lead to a higher quantity of different isomers.

4.3 Co-oligomerization of propene and 1-butene

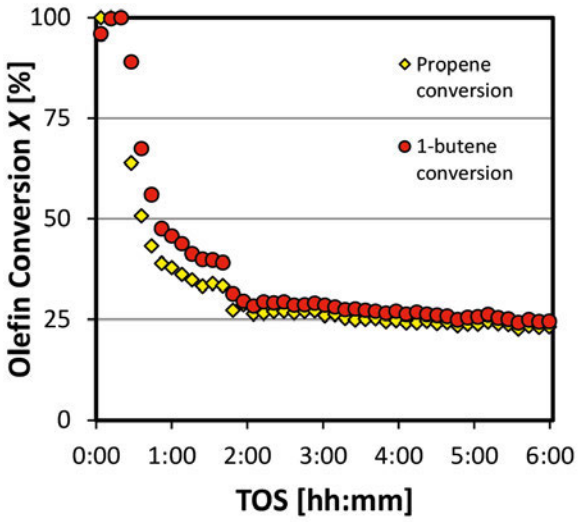

Figure 8: Olefin conversion during the co-oligomerization of 1-butene (T = 120 °C, pC3H6 = 8 bar, pC4H8 = 8 bar, WHSV = 4 h-1).

The Figures 8 and 9 illustrate the results of the co-oligomerization of propene and butene. The conversion of C_3H_6 is shown as yellow rhombs, C_4H_8 is marked with red circles. Both conversions drop down after the start quite significant and settle at around X = 25 – 30 mol.%. For propene this behaviour is already shown in the section before, but for butene the conversion is significantly lower than in the sole butene oligomerization.

Due to the co-oligomerization of molecules with different carbon chain lenght and more possibilities for their coupling, a wider product range arises. This is also reflected in the once more increased quantity of 248 liquid components.

The products of di-, tri- and tetramerization reactions of propene and butenes (mainly C_6, C_8, C_9 and C_{12}) amount in total to 42,5 wt.%. Compounds of chain lenghts formed by both educts, propene and butene, like C_7, C_{10} or C_{11}, amount to more than 50 wt.%. Concluded from this, oligomerization reactions of various olefins as feed are at least as, if not slightly, preferential to reactions of one sole sort of olefins.

Narr Francke Attempto Verlag GmbH + Co. KG

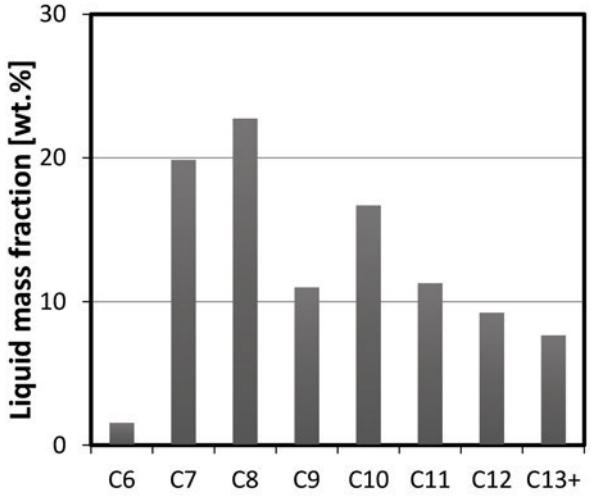

Figure 9: Liquid mass fractions of the co-oligomerization of propene and 1-butene (T = 120 °C, p_{C3H6} = 8 bar, p_{C4H8} = 8 bar, WHSV = 4 h^{-1}).

Noteworthy, propene dimerization to C_6 as product is still not as present as butene dimerization. Apart from this, the trimer C_9 is formed with about 10 wt.%. Furthermore the C_{10}-fraction has, with almost 17 wt.%, a ten times higher mass fraction due to co-oligomerization of propene and butene. Consequently, C_6 has to be an intermediate which then undergoes higher oligmerization processes. Even the synthesis of C_7 oligomers by coupling of one butene and one propene molecule is more favoured compared to the formation of C_6. Thus, butenes promote the reaction of propene, but on the other hand, in presence of propene the conversion of butene is significantly reduced by more than 60%. This effect has to be investigated in future experiments and compared with results from feed-compositions provided by MtO processes.

5. Summary and Outlook

The heterogeneously catalyzed oligomerization represents great potential for renewable fuels with emission-reduced properties. A broad spectra of fuels (gasoline, kerosene or diesel) may be synthesized with high selectivities. In comparison to the Fischer-Tropsch process with low selectivities [43], this is benficial and favoured for industrial application. Employing a lab-scale plant, first results showed high gasoline selectivities. Even kerosene is producable with high selectivity. In general, the catalyst shows high activity and can be adapted to the production of desired fuel ranges.

Recent results show, that compared with butenes, propene requires a higher density of acid sites as the carbenium-ion formed is not as reactive as the one formed by butenes.

In addition, the effects of the feed composition in respect to liquid product fractions were shown. A higher quantity of components can be observed during propene oligomerization. Attributed to higher degrees of oligomerization and increased coordination possibilities, a broader spectra of olefins and a higher quantity of different isomers is formed. For co-oligomerization with both molecules the same effect was shown since oligomers with chain lengths originated by coupling of propene and butenes are also formed.

Next to the detemination of the degrees of branching in the liquid products, the effect of reduced butene conversion during co-oligomerization has to be investigated in future experiments.

6. Acknowledgement

The authors gratefully acknowledge the financial support from the *Ministerium für Verkehr Baden Württemberg* as well as the *Strategiedialog Automobilwirtschaft BW* within the framework of the project “reFuels – rethinking fuels”.

References

[1] Bertau M, Kraft M, Plass L, Wernicke H-J (2019) Methanol – der Kraftstoff, der uns morgen antreibt. In: Maus W (Hrsg) Zukünftige Kraftstoffe, Bd 4. Springer Berlin Heidelberg, Berlin, Heidelberg, S 480–531

[2] American Petroleum Institute (1958) Knocking Characteristics of Pure Hydrocarbons. ASTM International

[3] Eckert P, Rakowski S (2019) Schadstoffbildung. In: Merker GP, Teichmann R (Hrsg) Grundlagen Verbrennungsmotoren, Bd 42. Springer Fachmedien Wiesbaden GmbH, Wiesbaden, S 943–977

[4] D02 Committee Specification for Aviation Turbine Fuels. ASTM International, West Conshohocken, PA. doi:10.1520/D1655-16A

[5] Europäische Union (2007) Verordnung (EG) Nr. 715/2007 des Europäischen Parlaments und des Rates vom 20. Juni 2007 über die Typgenehmigung von Kraftfahrzeugen hinsichtlich der Emissionen von leichten Personenkraftwagen und Nutzfahrzeugen (Euro 5 und Euro 6) und über den Zugang zu Reparatur-und Wartungsinformationen für Fahrzeuge

[6] Europäische Union (2017) Verordnung (EU) 2017/1151 der Kommission vom 1. Juni 2017 zur Ergänzung der Verordnung (EG) Nr. 715/2007 des Europäischen Parlaments und des Rates über die Typgenehmigung von Kraftfahrzeugen hinsichtlich der Emissionen von leichten Personenkraftwagen und Nutzfahrzeugen (Euro 5 und Euro 6)

Narr Francke Attempto Verlag GmbH + Co. KG

und über den Zugang zu Fahrzeugreparatur- und -wartungs-informationen, zur Änderung der Richtlinie 2007/46/EG des Europäischen Parlaments und des Rates, der Verordnung (EG) Nr. 692/2008 der Kommission sowie der Verordnung (EU) Nr. 1230/2012 der Kommission und zur Aufhebung der Verordnung (EG) Nr. 692/2008 der Kommission

[7] Tabak SA, Krambeck FJ (1985) Shaping process makes fuels Hydrocarbon Process (United States), Bd 64.9, S 72–74

[8] Leprince P, Balvet BB (Hrsg) (2001) Conversion processes. Petroleum Refining V.3, Institute Français du Pétrole. Éditions Technip, Paris

[9] York D, Scheckler J, Tajbl D (1997) UOP catalytic Condensation Process For Transportation Fuels. In: Robert A. Meyers (Hrsg) Handbook of Petroleum Refining Processes. McGraw-Hill, Kap. 1-3

[10] DIN Deutsches Intitut für Normung e. V. Krafstoffe - Unverbleite Ottokraftstoffe - Anforderungen und Prüfverfahren Deutsch Fassung EN 228:2012+A1:2017

[11] Magomedova M, Galanova E, Davidov I, Afokin M, Maximov A (2019) Dimethyl Ether to Olefins over Modified ZSM-5 Based Catalysts Stabilized by Hydrothermal Treatment. Catalysts 9(5):485. doi:10.3390/catal9050485

[12] Hindman M (2017) ExxonMobil - methanol to gasoline (MTG). Syngas Technology Conference

[13] Hindman M, Harand M, Rajagopalan S (2017) Integrated Methanol Separation And Methanol-To-Gasoline Conversion Process. ExxonMobil Research and Engineering Company (WO 2018/187039)

[14] Chen JQ, Bozzano A, Glover B, Fuglerud T, Kvisle S (2005) Recent advancements in ethylene and propylene production using the UOP/Hydro MTO process. Catalysis Today 106(1-4):103–107. doi:10.1016/j.cattod.2005.07.178

[15] Xu S, Zhi Y, Han J, Zhang W, Wu X, Sun T, Wei Y, Liu Z (2017) Advances in Catalysis for Methanol-to-Olefins Conversion Advances in Catalysis, Bd 61. Elsevier, S 37–122

[16] Boltz M, Losch P, Louis B (2013) A General Overview on the Methanol to Olefins Reaction: Recent Catalyst Developments. Advanced Chemistry Letters 1(3):247–256. doi:10.1166/acl.2013.1032

[17] Olsbye U, Svelle S, Bjørgen M, Beato P, Janssens TVW, Joensen F, Bordiga S, Lillerud KP (2012) Conversion of methanol to hydrocarbons: how zeolite cavity and pore size controls product selectivity. Angew Chem Int Ed Engl 51(24):5810–5831. doi:10.1002/anie.201103657

[18] de Chen, Moljord K, Fuglerud T, Holmen A (1999) The effect of crystal size of SAPO-34 on the selectivity and deactivation of the MTO reaction. Microporous and Mesoporous Materials 29(1-2):191–203. doi:10.1016/S1387-1811(98)00331-X

[19] Park JW, Lee JY, Kim KS, Hong SB, Seo G (2008) Effects of cage shape and size of 8-membered ring molecular sieves on their deactivation in methanol-to-olefin (MTO) reactions. Applied Catalysis **A:** General 339(1):36–44. doi:10.1016/j.apcata.2008.01.005

[20] Hereijgers BP, Bleken F, Nilsen MH, Svelle S, Lillerud K-P, Bjørgen M, Weckhuysen BM, Olsbye U (2009) Product shape selectivity dominates the Methanol-to-Olefins (MTO) reaction over H-SAPO-34 catalysts. Journal of Catalysis 264(1):77–87. doi:10.1016/j.jcat.2009.03.009

[21] Schulz H (2010) "Coking" of zeolites during methanol conversion: Basic reactions of the MTO-, MTP- and MTG processes. Catalysis Today 154(3-4):183–194. doi:10.1016/j.cattod.2010.05.012

[22] Wilson S, Barger P (1999) The characteristics of SAPO-34 which influence the conversion of methanol to light olefins. Microporous and Mesoporous Materials 29(1-2):117–126. doi:10.1016/S1387-1811(98)00325-4

[23] Chen D, Moljord K, Holmen A (2012) A methanol to olefins review: Diffusion, coke formation and deactivation on SAPO type catalysts. Microporous and Mesoporous Materials 164:239–250. doi:10.1016/j.micromeso.2012.06.046

[24] Svelle S, Joensen F, Nerlov J, Olsbye U, Lillerud K-P, Kolboe S, Bjørgen M (2006) Conversion of methanol into hydrocarbons over zeolite H-ZSM-5: ethene formation is mechanistically separated from the formation of higher alkenes. J Am Chem Soc 128(46):14770–14771. doi:10.1021/ja065810a

[25] Bjørgen M, Joensen F, Lillerud K-P, Olsbye U, Svelle S (2009) The mechanisms of ethene and propene formation from methanol over high silica H-ZSM-5 and H-beta. Catalysis Today 142(1-2):90–97. doi:10.1016/j.cattod.2009.01.015

[26] Latscha HP, Kazmaier U, Klein HA (2016) Die Eliminierungs-Reaktionen (E1, E2). In: Latscha HP, Kazmaier U, Klein H (Hrsg) Organische Chemie. Springer Berlin Heidelberg, Berlin, Heidelberg, S 143–151

[27] Latscha HP, Kazmaier U, Klein HA (2016) Ungesättigte Kohlenwasserstoffe (Alkene, Alkine). In: Latscha HP, Kazmaier U, Klein H (Hrsg) Organische Chemie. Springer Berlin Heidelberg, Berlin, Heidelberg, S 63–75

[28] Wang WC, Tao L, Markham J, Zhang Y, Tan E, Batan L, Warner E, Biddy M (2016) Review of Biojet Fuel Conversion Technologies

[29] Gunst D, Alexopoulos K, van der Borght K, John M, Galvita V, Reyniers M-F, Verberckmoes A (2017) Study of butanol conversion to butenes over H-ZSM-5: Effect of chemical structure on activity, selectivity and reaction pathways. Applied

Narr Francke Attempto Verlag GmbH + Co. KG

Catalysis A: General 539:1–12. doi:10.1016/j.apcata.2017.03.036

[30] Zhang D, Barri SA, Chadwick D (2011) n-Butanol to iso-butene in one-step over zeolite catalysts. Applied Catalysis A: General 403(1-2):1–11. doi:10.1016/j.apcata.2011.05.037

[31] Sun J, Zhu K, Gao F, Wang C, Liu J, Peden CHF, Wang Y (2011) Direct conversion of bio-ethanol to isobutene on nanosized Zn(x)Zr(y)O(z) mixed oxides with balanced acid-base sites. J Am Chem Soc 133(29):11096–11099. doi:10.1021/ja204235v

[32] Dagle VL, Winkelman AD, Jaegers NR, Saavedra-Lopez J, Hu J, Engelhard MH, Habas SE, Akhade SA, Kovarik L, Glezakou V-A, Rousseau R, Wang Y, Dagle RA (2020) Single-Step Conversion of Ethanol to n -Butene over Ag-ZrO 2 /SiO 2 Catalysts. ACS Catal. 10(18):10602–10613. doi:10.1021/acscatal.0c02235

[33] Tretbar M, Witzel T, Hauffe A, Junghans U, Bulc A, Pufky-Heinrich D (2018) Feasibility Study on the Etherification of Fermentative-Produced Isobutylene to Fully Renewable Ethyl Tert-Butyl Ether (ETBE). Catalysts 8(11):514. doi:10.3390/catal8110514

[34] Bockrath R (2014) Improved Fermentation Method (WO 2014/086780 A3)

[35] Thibaut D, Paques F, Global Bioenergies (2017) Report on extensive assessment of GBE's original IBN strain on a series of 2G substrates (growth, sugar consumption…)

[36] O'Connor CT (2008) Oligomerization. In: Ertl G (Hrsg) Handbook of heterogeneous catalysis, 2. Aufl. Wiley-VCH, Weinheim, Chichester

[37] Trippe F (2013) Techno-ökonomische Bewertung alternativer Verfahrenskonfigurationen zur Herstellung von Biomass-to-Liquid (BtL) Kraftstoffen und Chemikalien. Zugl.: Karlsruhe, KIT, Diss., 2013. Produktion und Energie, Bd 3. Technische Informationsbibliothek u. Universitätsbibliothek; KIT Scientific Publishing, Hannover, Karlsruhe

[38] Kvisle S, Fuglerud T, Kolboe S, Olsbye U, Lillerud KP, Vora BV (2008) Methanol-to-Hydrocarbons. In: Ertl G (Hrsg) Handbook of heterogeneous catalysis, 2. Aufl, Bd 4. Wiley-VCH, Weinheim, Chichester, S 1894

[39] Kaltschmitt M, Neuling U (2018) Biokerosene. Springer Berlin Heidelberg, Berlin, Heidelberg

[40] Heveling J, Nicolaides CP, Scurrell MS (1998) Catalysts and conditions for the highly efficient, selective and stable heterogeneous oligomerisation of ethylene. Applied Catalysis A: General 173(1): 1–9. doi:10.1016/S0926-860X(98)00147-1

[41] Finiels A, Fajula F, Hulea V (2014) Nickel-based solid catalysts for ethylene oligomerization – a review. Catal. Sci. Technol. 4(8):2412–2426. doi:10.1039/C4CY00305E

[42] Doped Aluminas. Silica-Aluminas Mixed Metal Oxides Hydrotalcites. http://www.sasolgermany.de/fileadmin/doc/alumina/0271.SAS-BR-Inorganics_Siral_Siralox_WEB.pdf. Zugegriffen: 26. Mai 2021

[43] Dry ME (2008) The Fischer-Tropsch (FT) Synthesis Processes. In: Ertl G (Hrsg) Handbook of heterogeneous catalysis, 2. Aufl. Wiley-VCH, Weinheim, Chichester

Narr Francke Attempto Verlag GmbH + Co. KG

Improve by Ind 4.0 the Heterogeneous Catalysts for CO_2 Hydrogenation to Liquid Fuels

Dr. rer. nat. Paul Olaru
AGIR-SETEC Head Lab.
IMNR-INCDMNR Bucharest, Romania

Summery

The process for methanol synthesis using captured CO2 was shown by a system engineering analysis based on planetary boundaries. Reverse water-gas shift reaction (RWGS: CO2 + H2 → CO + H2O) is mostly determined by the heterolytic splitting of H2 on the oxygen vacancies acting as catalytic center Its thermocatalytic production (CO2 + 3H2 → CH3OH + H2O) from captured CO2 and renewable H2 or CO2-rich feeds obtained via technology gasification is an attractive approach to effectively combat global warming. Today, the large-scale commercial production of methanol is mainly from syngas (a CO and H2 mixture), which are generated by fossil resources (mainly coal and natural gas) via processes including the gasification of coal as well as the steam reforming of natural gas. Small amounts of CO2 (about 2–8%) are typically added to the CO/H2 stream to balance the H/C ratio to the desired stoichiometry and to accelerate the reaction rate. Methanol formation: (1) CO + 2H2 = CH3OH, ΔH298K = − 90.6 kJ mol¯1; (2) CO2 + 3H2 = CH3OH + H2O, ΔH298K = − 49.5 kJ mol¯1; Reverse water-gas-shift reaction (RWGS): (3) CO2 + H2 = CO + H2O, ΔH298K = − 41.2 kJ mol¯1.

1. Introduction

Industry 4.0 - from talk to practice. Digital trust and data analyses are the foundation of Ind 4.0 Data fuels Industry 4.0 and successful data analytics is the prerequisite for successful implementation of digital enterprise applications. It's time to move from a phase of discovery and understanding what data is available and what it is worth to one of insights and action. *'First movers'* are already making the shift and using data analytics to help drive decision-making. As digital ecosystems expand, so does the importance of establishing strong levels of digital trust, backed up by transparency and non-repudiation that provides proof of the integrity and origin of one's own and third party data. More than half of respondents expect (fig.1) their Industry 4.0 investments to yield a return within two years or less, given investment of around 5% p.a. of annualrevenue.

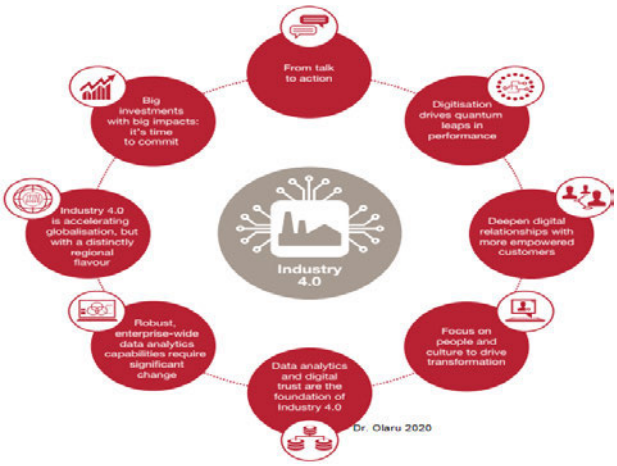

Fig. 1

2. Process

In comparing the commercial production of methanol via syngas (see eq. (1)), methanol formation from CO_2 hydrogenation requires an extra amount of hydrogen since extra H_2 is necessary to remove one oxygen atom from CO_2 through water formation as a by-product (see eq. (2)). Moreover, the thermodynamics for methanol production from CO_2 are not as favorable as that from CO, thus the one-pass methanol yield of the CO_2-based process is lower than that of the syngas-based process.

Narr Francke Attempto Verlag GmbH + Co. KG

The equilibrium yield of methanol from CO at 200ºC is greater than 80%, while that from CO_2 at 200ºC is less than 40%. In addition, several side reactions (e.g. the formation ethers, ketones, higher alcohols or hydrocarbons). Methanol synthesis from CO_2 and H_2 is an exothermal reaction with a decrease in reaction molecule number, according to ***Le Chatelier's principle***, the optimization of the reaction conditions such as high pressure and low temperature thermodynamically favors CO_2 conversion to methanol. However, taking the chemically inert nature of CO_2 and the reaction rate into consideration, a reaction temperature higher than 242°C that favors the CO_2 activation and methanol formation is usually adopted. In addition, under methanol synthesis conditions, the RWGS reaction becomes highly facile in thermodynamics.

2.1 Hydrogenation CO_2 to Methanol

Recently, significant progress has been made indeveloping more efficient catalysts for CO2 hydrogenation to CH3OH, including metal-supported catalysts,bimetallic systems, and reducible metal oxides. During CO2 hydrogenation, the formation of the undesired CO through RWGS is a competitive reaction to methanol synthesis. However, the low temperature and/or high space velocity usually result in low single pass CO2 conversion. Thus, it remains a great challenge to simultaneously obtain high CO2 conversion and high methanol selectivity. Industrial methanol production from CO2-containing syngas uses the well-known Cu-ZnO-Al2O3 catalysts. Currently, CH3OH synthesis from catalytic CO2 hydrogenation has been implemented at the pilot-plant level. In Europe, *power-to-liquid* (PTL) fuels obtained from surplus renewable electricity via water electrolysis-derived H2 and CO2 have received much attention, and a number of PTL-related studies were recently reported. Liquid hydrocarbon (C5+) fuels including gasoline (C5-11), jet fuel (C8-16), and diesel (C10-20) play an instrumental role in the global energy supply chain and are wildly used as transportation fuels around the world. Besides, alcohols such as methanol, ethanol, and other higher alcohols (C2+OH) are clean and multipurpose fuels.In both academic researchand industrial practices, (fig.2), great progress has been made in the synthesis of C1 molecules such as methanol (CH3OH) from CO2 hydrogenation. Currently, the largest plant, Carbon Recycling International (CRI)'s CO2-to-renewable-methanol plant in Iceland, is capable of producing 4000 t/year of methanol by converting about 5500 t/year of CO2.However, direct reduction of CO2 to C2+ products is still a grand challenge due to the lack of efficient catalysts with high stability, as the activity of C-C coupling is low and the formation of byproduct water can easily deactivatethevarious catalysts for CO2 conversion. Syngas (CO/H2) and CH3OH are the most important C1 platform molecules, and their conversions to value-added products via the Fischer-Tropsch synthesis (FTS) and methanol to hydrocarbons (MTH) processes, respectively, were extensively applied in industry.Therefore, combining the *reverse water-gas shift (RWGS)* with FTS and combining high-temperature methanol synthesis with MTH over bifunctional/multifunctional catalysts are two efficient strategies for direct CO2 hydrogenation to C2+ hydrocarbons including liquid hydrocarbons. Moreover, the synthesis of C2+ alcohols is even more
challenging than C2+ hydrocarbons either in CO2 or CO hydrogenation, which requires more precise control of the C-C coupling.

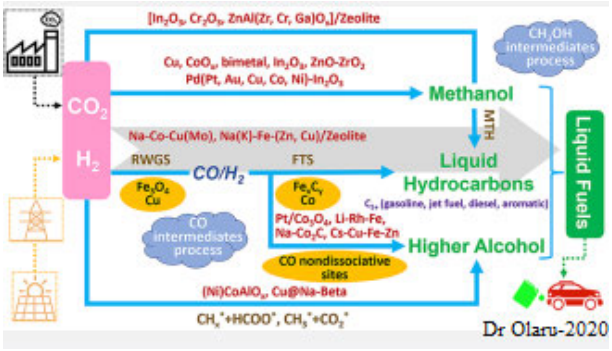

Fig. 2

The supported copper materials have attracted much attention and have been extensively investigated for CO2 hydrogenation to CH3OH. The methanol synthesis reaction is known to show strong support effects. Using a suitable support material can enhance CH3OH selectivity, attributed to structural, electronic, and chemical promotional effects. For example, CH3OH selectivity is usually high (>70%) at 200-260 °C when ZrO2 is used as the support.[30,32]. Recently, several works have clarified the origin of the promotional effect of the ZrO2 support that is unknown before. Larmier et al. confirmed that the Cu/ZrO2 interface can promote the conversion of the formate intermediates to methanol by combined experimental and computational investigations.[30]. Tada et al. found that the interfacial sites on Cu/a-ZrO2 (a-: amorphous) are favored for methanol production compared to those on tetragonal and monoclinic ZrO2 supported Cu.[33]. Additionally, the oxygen vacancies on tetragonal ZrO2 were proposed to play a crucial role in enhancing the activity of methanol formation by stabilizing the Cu+ active sites adjacent to them.[32]. Lam et al. suggested that the surface Lewis acid Zr(IV) sites with Cu particles in the vicinity are responsible for improving CH3OH activity and selectivity on the Cu/ZrO2-based catalysts.[31]. Apart from conventional metal oxides, researchers recently also explored other supports such as TiO2 nanotubes [34] and Mg-Al layered double hydroxide (LDH) [35] to promote methanol formation. To simultaneously improve the intrinsic activity and catalyst stability, researchers directly used Cu-Zn-based LDH as the precursor to synthesize an efficient methanol synthesis catalyst with a confined structure, in which the ac-

Narr Francke Attempto Verlag GmbH + Co. KG

tive metallic Cu phase is highly dispersed and partially embedded in the remaining oxide matrix.[36,29] Li et al. prepared ultrathin Cu-Zn-Ga LDH nanosheets by the aqueous miscible organic solvent treatment method and further increased Cu surface areas and dispersion of the resulting Cu-based catalysts (fig. 1A).[37].The CH3OH *space time yield* (STY) is 0.59 g_{MeOH} g_{cat}^{-1} $h^{-1}$with selectivity of ~49% at CO2 conversion of ~20%. On the other hand, scientists also tried to use silica and metal-organic frameworks to confine small Cu nanoparticles and developed highly efficient Cu-based catalysts for CO2 hydrogenation.[40-44].Example, Liu et al. synthesized three-dimensional porous Cu@ZrO2 framework catalysts using the Cu@UiO-66 precursor, which displays CH3OH STY of 0.796 g_{MeOH} g_{cat}^{-1} h^{-1} and a long-term stability for 105 h with a selectivity of 78.8% and conversion of 13.1% at 258°C, 4.5 MPa, 21 600 mL g^{-1} h^{-1} and H2/CO2 = 3 [43].Recently, several groups have developed novel cobalt (Co)- based catalytic systems that display a promising performance for methanol synthesis from CO2 hydrogenation.[45-48]. Co catalysts are widely used and extensively studied for FTS and can easily catalyze the CO2 methanation reaction.[2,17,46,49-52]. The high performance for CH3OH synthesis over Co-based catalysts was attributed to the formation of a new active phase, rather than the conventional metallic Co phase. Our works [7],were conducted to predict theeffect of operating conditions on syngas conversionand temperature profiles of the cobalt-based FTSreaction in the FT reactor. The kinetic modelproposed in the present study was shown to beeffective for application to a commercial softwarepackage (Multiphysics). Li et al. Reported MnOx nanoparticles supported on a mesoporous Co3O4 for methanol production at low pressure (0.1-0.6 MPa). [45].They showed the importance of the CoO phase and revealed the strong interaction between MnOx nanoparticles and Co@CoO core-shell grains, which enhances the performance of CO2 hydrogenation to CH3OH. Lian et al. ascribed the increased CH3OH selectivity to the oxygen defects on the surface of Co@Co3O4 core-shell active species supported on the nitrogen-doped carbon material, which is derived from zeolitic imidazolate framework precursors.[47].Wang et al. Also inferred that the cobalt oxide phase on silica supported Co catalyst with Co-O-SiOn linkages via Co phyllosilicates could suppress the CO and CH4 formation and promote methanol production (fig.3B) [48]. This novel Co catalyst shows CH3OH STY of 0.096 g_{MeOH} g_{cat}^{-1} h^{-1} (3.0 mmol g_{cat}^{-1} h^{-1}) with a selectivity of 70.5% at 8.6% conversion at 320 °C. Because the H2 splitting ability of cobalt oxide is lower than the metallic Co phase, the activities of these Co-based methanol synthesis catalysts are to be further enhanced. Moreover, the mechanism of this new active site inhibiting the CO2 methanation and RWGS reactions needs to be further clarified. Various bimetallic materials including: Pd-Cu,[3,5], Pd- Ga,[6,17], Pd-In,[6,8], Pd-Zn,[9], Ni-Ga,[2.6], In-Rh,[17], In-Cu,[8,9], In-Co,[7], In Ni,[11,12] and Ni-Cu [15-17], have also been examined for methanol production from CO2 hydrogenation. Among these catalysts, some non-noble metal-based bimetallics were designed for efficient CO2 hydrogenation to CH3OH at low pressure. In recent years, reducible oxides have received considerable attention due to their excellent performance with high CH3OH selectivity in a wide range of temperatures (210-310 °C). Nearly 100% selectivity can be attained over cubic In2O3 nanomaterial and In2O3 supported on monoclinic ZrO2 at CO2 conversions of less 5.5% under 300 °C, 5.0 MPa, 20 000 mL g^{-1} h^{-1} and H2/CO2 = 4,[4]. Researchers have clearly demonstrated the structure sensitivity of the In2O3 catalyst in terms of both the phase and the exposed facet by combined computational and experimental studies.[7,8], Danget al. reported a successful work of computer-aided rational design of more efficient In2O3 catalysts for CO2 hydrogenation to CH3OH.[8].

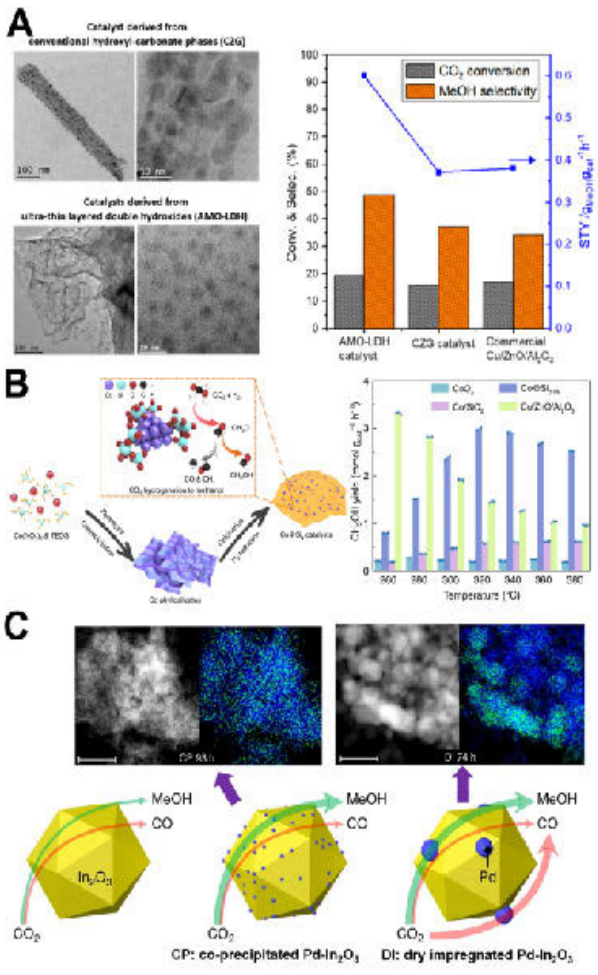

Fig. 3: **(A)** TEM images of Cu-Zn-Ga catalysts derived from conventional hydroxyl-carbonate phases and ultrathin LDH (left) as well as their performance (right). [37]. Reaction conditions: 270 °C, 4.5 MPa, 18 000 mL g^{-1} h^{-1}, and H2/CO2 = 3. **(B)** Synthesis and catalysis strategies (left) as well as CO2 hydrogenation performance (right) of Co@Six catalysts.[48]. Reaction con-

Narr Francke Attempto Verlag GmbH + Co. KG

ditions: 260-380 °C, 2.0 MPa, 6000 mL g^{-1} h^{-1} and H2/CO2 = 3. **(C)** HAADF-STEM images and corresponding EDX maps (top) of indium (blue) and palladium (green) for the spent coprecipitated (CP, left) and dry impregnated (DI, right) Pd-In2O3 catalysts with 0.75 wt % Pd as well as illustration for the distinct role of Pd in equilibrated S1 and S2 catalysts with pure In2O3 as a reference.[24].The thickness of the arrows qualitatively suggests the methanol and CO formation rates. Reprinted with permission from refs [37,48] Copyright 2020 American Chemical Society

The In2O3/ZrO2 catalyst system, the ZrO2 support remarkably boosted the activity of the In2O3 catalyst and prevented its sintering.[24.29]. It was suggested that synergic effects between In2O3 and ZrO2 carriers favorably tuned CH3OH selectivity by changing thereaction pathway.[8], Frei et al. also investigated the electronic, geometric, and interfacial phenomena related to the peculiar promotional effects of the monoclinic ZrO2 carrier on In2O3.[31] Less-pronounced lattice mismatching between In2O3 and ZrO2 favors the formation of more surface oxygen vacancies on In2O3, which is beneficial for methanol synthesis. The lower H2 splitting ability of In2O3 compared with metal catalyst, palladium (Pd) was introduced to enhance H2 activation and facilitate oxygen vacancy formation and thereby substantially promote the activity of In2O3.[12,13], CO2 conversion over In2O3 supported highly dispersed Pd nanocatalyst reached above 20% with CH3OH selectivity of ~70%and STY up to 0.89 g_{MeOH} g_{cat}^{-1} h^{-1},[13] which is about 2-5 times higher than pure In2O3 under similar reaction conditions. Moreover, the incorporation of Pd atoms in the In2O3 matrix forming low-nuclearity Pd clusters can simultaneously increase the activity, selectivity and long-term stability (fig.3C),[14]. Different from dry impregnated Pd-In2O3, this nanostructure can effectively avoid Pd clustering and minimize In2O3 sintering; thus, CH3OH STY dropped slightly from 1.01 to 0.96 g_{MeOH} g_{cat}^{-1} h^{-1} after time-on-stream of 500 h at 280 °C, 5.0 MPa, 48 000 mL g^{-1} h^{-1}, and H2/CO2 = 4. The addition of Pt, Au, Cu, Co, or Ni can also benefit the generation of active hydrogen species.[19,25-29].

3. Ind 4.0 –possible new solutions

Palladium atoms replacing indium atoms in the active In3O5 ensemble attract additional palladium atoms deposited onto the surface forming low-nuclearity clusters, which foster H2 activation and remain unaltered, enabling record productivities for 500 h.

In2O3, recently discovered for CO2 hydrogenation tomethanol [17,18]. Indeed, although this reducible oxide is very selective and durable, especially when supported on ZrO2, owing to the presence of frustrated Lewis pairs [19,20], and single ensembles [21,22], its H2-splitting ability is limited [23] Palladium was shown to generate bulk intermetallic compounds with indium [24,25], which were superior to In2O3 in liquid-phase CO2 hydrogenation [26], but were exclusively active for the competitive *reverse water–gas shift* (RWGS) reaction when applied in the gas phase as nanoparticles supported on silica [27]. A synthetic method devised to deposit palladium nanoparticles on In2O3 minimizing alloy formation [28], led to a system displaying enhanced methanol formation, which was ascribed to the higher availability of activated hydrogen, fostering the desired hydrogenation reaction and vacancy formation on the oxide surface. These contrasting findings highlight that the true relevant speciation and action mechanism of palladium are poorly understood. More importantly, to maximize the promoting effect and thus process-leveladvantages, the H2-splitting ability of palladium should be exploited while minimizing its high efficacy for the RWGS reaction as a stand-alone metallic phase [29,31] As single palladium atoms supported on carbon nitride are active in alkyne semihydrogenation and photocatalytic CO2 reduction [32-34], and possess distinct electronic properties compared to agglomeratedpalladium, calculations indicate that the (R)WGS reaction on Pd(111) requires at least three palladium atoms [35] , and the selectivity of platinum on MoS2 in CO2 hydrogenation was dictated by the cluster mono-/binuclearity [36], we conceived atomic dispersion as a strategy to curtail detrimental effects while preserving beneficial attributes. This approach would simultaneously grant improved metal utilization and robustness, if palladium atoms are well anchored to the In2O3 structure. Aiming at deriving synthesis–structure–performance relations, we emphasized experimental methods as well as theoretical means, which comprise a prominent tool to uncover the impact of structure on activity and selectivity [37-39] but have rarely been applied to link preparation to structure

3.1 Solution of the palladium application

The samples ***co-precipitated catalyst (CP)***=S1 and *dry impregnation (DI)=S2* were studied through a battery of characterization techniques to elucidate the palladium speciation. X-ray diffraction (XRD)confirmed the bixbyite (i.e., a defective fluorite-type) structure of In2O3 in both systems (Fig. 4), the lowest-energy surface of which presents a protruding In3O5(O) substructure, which generates the active site in acetylene and CO2 hydrogenation after removal of the (O) atom [21], and an adjacent sunken region. The average particle size of In2O3 was calculated at 9 nmfor the fresh materials and increased to 15 and 25 nm for used S1and S2 catalysts, respectively. Moderate sintering was also observed earlier for unpromoted In2O3 [17,22]. A weak reflection at 39.5° 2θ specific to Pd0 was detected only for the used S2 material. High angle annular dark-field scanning transmissionelectron microscopy (H-STEM) images and indium and palladium maps acquired by energy-disper-

Narr Francke Attempto Verlag GmbH + Co. KG

sive X-ray spectroscopy (EDX) indicate that palladium is extremely well dispersed in the fresh samples (fig.4)). The S1 material used in the reaction for 93 h appeared virtually unaltered. In contrast, In2O3 particles increased their size to ca. 30 nm and palladium nanoparticles formed using the S2 catalyst for 74 h (fig.4) the latter having an average size of 2.8 nm based on high resolution transmission electron microscopy (HRTEM, (figs.4).

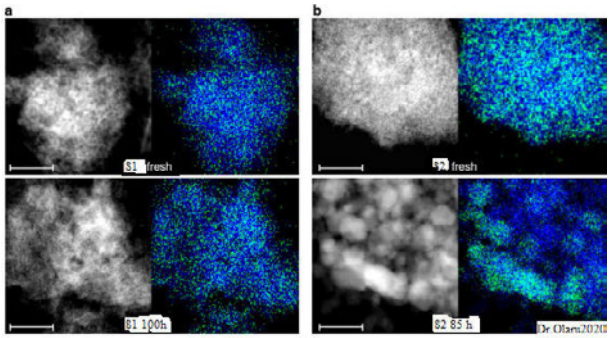

Fig. 4: Microscopy analysis of palladium-promoted In2O3 catalysts. H-STEM images and corresponding EDX maps of indium (blue) and palladium (green) for the catalysts produced by **a**-S1 and **b**-S2 with 0.75 wt.% Pd in fresh form and after the tests depicted in Fig. 4b. The scale bar in all panels is 50 nm

4. Experimental nuclearity correlation.

Intrigued by the selectivity-nuclearity correlation uncovered by the theoretical studies for S1 catalysts, we conducted a complementary experiment to link palladium agglomeration and its impact on methanol selectivity. When the S2 catalyst was tested keeping the CO2 conversion at 2–3%, the methanol selectivity remained at ca. 83% for 6 h, followed by a linear decline owing to a progressively greater impact of the RWGS reaction till a value of 58% after 9 h on stream. Characterization of the specimen retrieved at the end of the test confirmed severe sintering of palladium and In2O3 (particle sizes of 12 and 28 nm, respectively). A sample generated by a repeated experiment ending before the onset of the selectivity change still showed an extremely high-palladium dispersion based on STEM-EDX, as expected. This supports that agglomerates of only few Pd atoms are required to start favoring the RWGS reaction and highlights the importance of controlling the promoter nanostructure upon synthesis and preserving it upon .reaction. (figs.5). Figure 5 presents the most significant S1 and S2 catalysts' models and their features, highlighting the remarkable matching of information derived from experiments and from theory. Gibbs energy profiles for methanol and CO formation from CO2 were calculated based on the elementary steps found optimal for In2O3. The activation of the S1 catalyst starts with H2 dissociation onto two O atoms located nearby the lattice palladium species, followed by transfer of one H atom to form water, which desorbs creating a vacancy. It was introduced as a novel technique to elucidate vacancy formation and short-range crystallinity in (palladium-promoted) In2O3 catalysts, and theoretical modeling provided sound understanding of the structure and functioning of the active sites in the two systems. In the S1 catalyst, embedding one Pd atom in the In2O3 matrix enables a controlled growth of extra-lattice atoms, leading to the stabilization of low-nuclearity palladium clusters. The number of vacancies does not increase but their electronic properties are strongly modified, permitting improved H2 dissociation. The small size of the palladium cluster is crucial to curtail the RWGS reaction on palladium sites, which is relevant already for clusters of 3 extra-lattice promoter atoms. In the S2 catalyst, palladium steadily agglomerates with time on stream forming particles. These aid methanol production by supplying activated hydrogen that fosters the formation of surface vacancies on In2O3 and the hydrogenation of the CO2 therein adsorbed. Still, they consume a significant part of the H2 split by converting CO2 into CO on their own surface (fig. 6).

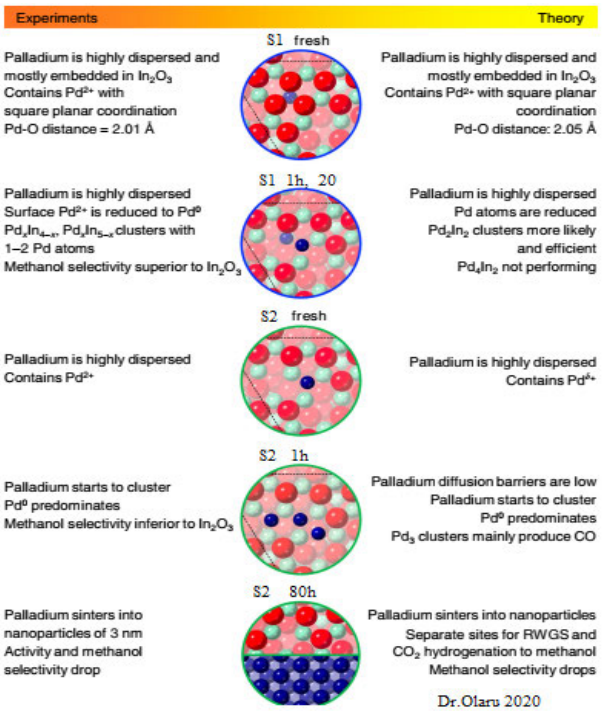

Fig. 5: Experimental and theoretical description of palladium sites. Most relevant surface models representing the S1 and S2 catalyst in fresh, activated, and used forms and their main features derived from experiments and theory.

Narr Francke Attempto Verlag GmbH + Co. KG

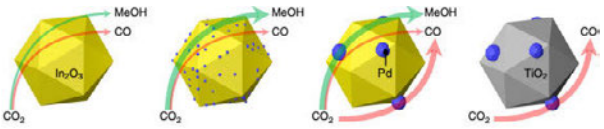

Fig. 6: Schematic representation of the distinct role of palladium in equilibrated S1 and S2 systems with In2O3 and Pd-TiO2 as references. The thickness of the arrows qualitatively indicates the products formation rates. Reaction conditions: P = 5 MPa, H2:CO2 = 4, and WHSV = 48,000 $cm3_{STP}$ h^{-1} g_{cat}^{-1}

5. Results and Discussion

Our fixed bed reactor model for FTS using a cobalt catalyst was developed. This kinetic model has twoseries of multi-tubular FT reactors over a cobalt catalyst, and the Multiphysics was applied to simulate and predict the profiles of syngas conversion, feed concentration, oil selectivity, and temperature in the reactor under a variety of conditions including: feed temperature, syngas space velocity, and coolant temperature. Results show overall CO conversion of 50% and controlled temperature applied in operatingtemperatures of 215 °C to 235 °C in the first step ofthe multi tubular reactor. Moreover, the effect of coolant temperature was evaluated to determine optimum operating conditions to achieve more conversion and higher heat flux to keep the FT tubes near isothermal conditions. Non-isothermal reactor was investigated in this study for different feed temperature to get higher selectivity of jet fuel (this sentence does not make sense. Further simulation shows higher productivity and selectivity to control the catalytic Fischer-Tropsch (FT) packed bed rector near isothermal conditions, which started at a temperature of 235 °C. One of these problems is that this type of kinetic model cannot estimate the exact amount of heat released by exothermic reactions through the FT reactor. It is well known that the heat released from producing one mole of decane is different from the heat released by producing ten moles of methane. 154 kJ and 207 kJ of heat are released per CO moleconsumed in each case. The syngas molar ratio of H2/CO=4 was fed through the top of the first stage with a temperature of 235 °C, was kept at the operating conditions of 300 *psig*, and was finally passed through the packed bed. The FT product from the first stage (unconverted syngas) was removed from the end of the reactor tube and fed to the top of the second stage of the reactor. The synthesis temperature was maintained by circulation of pressurized water in the shell. To control the inside temperature of the reactor according to theexothermic reactions therein, saturated water wasused to adjust the profile temperature inside the reactor to prevent coking of the catalysts. Water was heated to create saturated liquid water and was then pumped into the reactor. The average particle size of In2O3 increased by only 2 nm compared with S2-92 h (14 and 18 nm, respectively). Owing to the addition of TiO2 as a diluent in this test, which could not be separated from the used catalyst, changes in porous properties and vacancy density could not be investigated. The methanol STY was 0.92 g_{MeOH} h^{-1} g_{cat}^{-1}, which is, to our knowledge, the highest sustained productivity reported for CO2-based methanol synthesis over a heterogeneous catalyst. Specifically, our catalyst reaches a 16%-higher methanol STY than the best performer reported and at a cca. 62% shorter residence time. The latter enables a reduction in reactor size by 62%, which is a strong gain for a prospective industrial process. Moreover, S1 is a synthesis method that has been successfully implemented for catalyst manufacture at the large scale for numerous applications, whereas the polymer-assisted route used for the benchmark appears of limited industrial amenability. Controlled growth of extra-lattice atoms, leading to the stabilization of low-nuclearity palladium clusters. The number of vacancies does not increase but their electronic properties are strongly modified, permitting improved H2 dissociation. The small size of the palladium cluster is crucial to curtail the RWGS reaction on palladium sites, which is relevant already for clusters of 3 extra-lattice promoter atoms. In the S2 catalyst, palladium steadily agglomerates with time on stream forming particles. These aid methanol production by supplying activated hydrogen that fosters the formation of surface vacancies on In2O3 and the hydrogenation of the CO2 therein adsorbed. Still, they consume a significant part of the H2 split by converting CO2 into CO on their own surface (Fig. 6). These contrasting palladium speciations also explain the profoundly diverse time-on-stream behaviors of the two catalysts. Palladium embedded into indium oxide attracts the scarce palladium in pockets, avoiding its clustering, and facilitates water desorption minimizing In2O3 sintering, whereas palladium deposited onto In2O3 easily agglomerates and leads to catalyst sintering by spilling too much activated H2 to the oxide, causing over-reduction, and by excessively retaining water, provoking crystals coalescence. Hence, anchoring of palladium clusters to the In2O3 lattice is an unprecedented approach to effectively enhance activity and selectivity, and more importantly, to maintain the promotional effect in the long term, an aspect fully disregarded in previous studies on palladium-promoted In2O3 systems. In addition, low-nuclearity palladium clusters grant the possibility to operate the catalyst at reduced temperature, with hydrogen-lean feeds, and in the presence of greater amounts of water, altogether implying strong economic and ecologic benefits at a process level. So, propose our strategy to engineer promotion at the atomic scale marks a step ahead toward green methanol production and holds great general potential for tailoring new or existing promoted systems in current and emerging applications of heterogeneous catalysis. Most companies believe they will see a return on investment (ROI) within two years or less (fig. 7) for their Industry 4.0 projects. Just over a third of companies anticipate a longer timescale of three to five years, for Industry 4.0 investments to pay for themselves.

Narr Francke Attempto Verlag GmbH + Co. KG

Figure 7 **Most companies expect Industry 4.0 investments to pay back within two years**

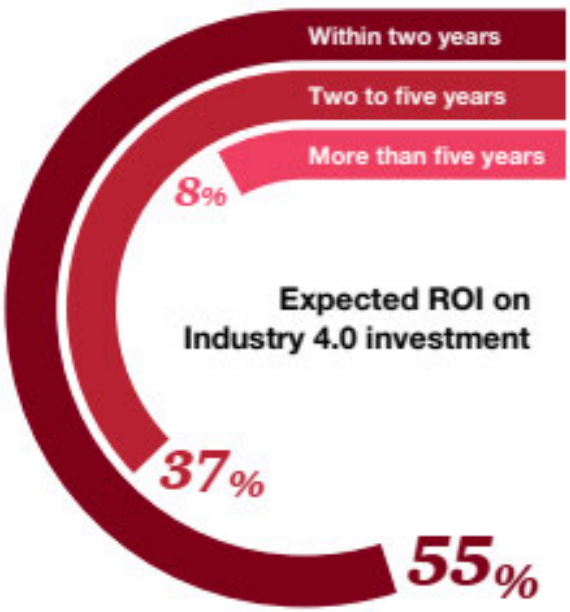

References

[1] Rui, N.; Zhang, F.; Sun, K.; Liu, Z.; Xu, W.; Stavitski, E.; Senanayake, S. D.; Rodriguez, J. A.; Liu, C.-J. Hydrogenation of CO2 to Methanol on a Auδ+-In2O3-x Catalyst. ACS Catal. 2020,

[2] Li, M. M.; Zou, H.; Zheng, J.; Wu, T. S.; Chan, T. S.; Soo, Y. L.; Wu, X. P.; Gong, X. Q.; Chen, T.; Roy, K.; Held, G.; Tsang, S. C. E. Methanol Synthesis at a Wide Range of H2/CO2 Ratios over a Rh-In Bimetallic Catalyst. Angew. Chem.,

[3] Guil-Lopez, R.; Mota, N.; Llorente, J.; Millan, E.; Pawelec, B.; Fierro, J. L. G.; Navarro, R. M. Methanol Synthesis from CO2: A Review of the Latest Developments in Heterogeneous Catalysis. Materials 2019, 12 (23), 3902.

[4] Din, I. U.; Shaharun, M. S.; Alotaibi, M. A.; Alharthi, A. I.; Naeem, A. Recent developments on heterogeneous catalytic CO2 reduction to methanol. J. CO2 Util. 2019, 34, 20-33.

[5] S. Mitchell, T.F. Segawa, R. Hauert, C. Drouilly, D. Curulla Ferr´e, J. P´erez-Ramírez, Indium oxide as a superior catalyst for methanol synthesis by CO2 hydrogenation, Angew. Chem. Int. Ed. 55 (2016)6261–6265.

[6] B. Qin, Y. Yang, H. Wang, J. Cai, Y. Han, S. Li, P. Gao, Y. Sun, Rationally designed indium oxide catalysts for CO2 hydrogenation to methanol with high activity and selectivity, Sci. Adv. 6 (2020),

[7] Olaru, P.et el. New Carbon Capture, Converted in Electricity (CCCE) technology by (UCnF) Reinforced Shape Memory Polymers-(SMPs) Nanostrip Multilayers, International Colloquium Fuels –TAE 27 to 29 June 2017 in Stuttgart / Ostfidern, Germany

[8] Behr, A. Methanol: the basic chemical and energy feedstock of the future. Angew. Chem. Int. Ed. 53, 12674–12674 (2014).

[9] Álvarez, A. et al. Challenges in the greener production of formates/formic acid, methanol, and DME by heterogeneously catalyzed CO2 hydrogenation processes. Chem. Rev. 117, 9804–9838 (2017).

[10]. Wang, J. et al. A highly selective and stable ZnO-ZrO2 solid solution catalyst for CO2 hydrogenation to methanol. Sci. Adv. 3, e1701290 (2017).

[11 Vogt, C. et al. Unravelling structure sensitivity in CO2 hydrogenation over nickel. Nat. Catal. 1, 127–134 (2018).

[12] Wang, L. et al. Incorporating nitrogen atoms into cobalt nanosheets as a strategy to boost catalytic activity toward CO2 hydrogenation. Nat. Energy 2,869–876 (2017).

[13] Behrens, M. Promoting the synthesis of methanol: understanding the requirements for an industrial catalyst for the conversion of CO2. Angew. Chem. Int. Ed. 55, 14906–14908 (2016).

[14] Xu, J. et al. Methanol synthesis from CO2 and H2 over Pd/ZnO/Al2O3: catalyst structure dependence of methanol selectivity. Appl. Catal. A 514, 51–59 (2016).

[15] Yang, H. B. et al. Atomically dispersed Ni(I) as the active site for electrochemical CO2 reduction. Nat. Energy 3, 140–147 (2018).

[16] Loiland, J. A., Wulfers, M. J., Marinkovic, N. S. & Lobo, R. F. Fe/γ-Al2O3 and Fe-K/γ-Al2O3 as reverse water-gas shift catalysts. Catal. Sci. Technol. 6,5267–5279 (2016).

[17] Martin, O. et al. Indium oxide as a superior catalyst for methanol synthesis by CO2 hydrogenation. Angew. Chem. Int. Ed. 55, 6261–6265 (2016).

[18] Gao, P. et al. Direct conversion of CO2 into liquid fuels with high selectivity over a bifunctional catalyst. Nat. Chem. 9, 1019–1024 (2017).

[19] Zhang, S. et al. Solid frustrated-Lewis-pair catalysts constructed by regulations on surface defects of porous nanorods of CeO2. Nat. Commun. 8, 15266(2017).

[20] Ghuman, K. K. et al. Photoexcited surface frustrated Lewis pairs for heterogeneous photocatalytic CO2 reduction. J. Am. Chem. Soc. 138, 1206–1214 (2016).

[21] Albani, D. et al. Semihydrogenation of acetylene on indium oxide: proposed single-ensemble catalysis. Angew. Chem. Int. Ed. 56, 10755–10760 (2017).

Narr Francke Attempto Verlag GmbH + Co. KG

[22] Frei, M. S. et al. Mechanism and microkinetics of methanol synthesis via CO2 hydrogenation on indium oxide. J. Catal. 361, 313–321 (2018).
[23] Ye, J., Liu, C.-j, Mei, D. & Ge, Q. Methanol synthesis from CO2 hydrogenation over a Pd4/In2O3 model catalyst: a combined DFT and kinetic study. J. Catal. 317, 44–53 (2014).
[24] Lorenz, H. et al. Pd–In2O3 interaction due to reduction in hydrogen: consequences for methanol steam reforming. Appl. Catal. A 374, 180–188 (2010).
[25] Rameshan, C. et al. Impregnated and co-precipitated Pd–Ga2O3, Pd–In2O3 and Pd–Ga2O3–In2O3 catalysts: influence of the microstructure on the CO2 selectivity in methanol steam reforming. Catal. Lett. 148, 3062–3071 (2018).
[26] García-Trenco, A. et al. PdIn intermetallic nanoparticles for the hydrogenation of CO2 to methanol. Appl. Catal. B 220, 9–18 (2018).
[27] Ye, J., Ge, Q. & Liu, C.-J. Effect of PdIn bimetallic particle formation on CO2reduction over the PdIn/SiO2 catalyst. Chem. Eng. Sci. 135, 193–201 (2015).
[28] Rui, N. et al. CO2 hydrogenation to methanol over Pd/In2O3: effects of Pd and oxygen vacancy. Appl. Catal. B 218, 488–497 (2017).
[29] Arena, F. et al. Solid-state interactions, adsorption sites and functionality of Cu-ZnO/ZrO2 catalysts in the CO2 hydrogenation to CH3OH. Appl. Catal. A 350, 16–23 (2008).
[30] Erdöhelyi, A., Pásztor, M. & Solymosi, F. Catalytic hydrogenation of CO2 over supported palladium. J. Catal. 98, 166–177 (1986).
[31] Pettigrew, D. J., Trimm, D. L. & Cant, N. W. The effects of rare earth oxides on the reverse water-gas shift reaction on palladium/alumina. Catal. Lett. 28,313–319 (1994).
[32] Vilé, G. et al. A stable single-site palladium catalyst for hydrogenations. Angew. Chem. Int. Ed. 54, 11265–11269 (2015).
[33] Mitchell, S., Vorobyeva, E. & Pérez-Ramírez, J. The multifaceted reactivity of single-atom heterogeneous catalysts. Angew. Chem. Int. Ed. 130, 15538–15552 (2018).
[34] Gao, G., Jiao, Y., Waclawik, E. R. & Du, A. Single atom (Pd/Pt) supported on graphitic carbon nitride as an efficient photocatalyst for visible-light reduction of carbon dioxide. J. Am. Chem. Soc. 138, 6292–6297 (2016).
[35] Li, Q., García-Muelas, R. & López, N. Microkinetics of alcohol reforming for H2 production from a fair density functional theory database. Nat. Commun. 9, 526 (2018).
[36] Li, H. et al. Synergetic interaction between neighbouring platinum monomers in CO2 hydrogenation. Nat. Nanotechnol. 13, 411–417 (2018).
[37] Nørskov, J. K., Bligaard, T., Rossmeisl, J. & Christensen, C. H. Towards the computational design of solid catalysts. Nat. Chem. 1, 37–46 (2009).
[38] Medford, A. J. et al. From the Sabatier principle to a predictive theory of transition-metal heterogeneous catalysis. J. Catal. 328, 36–42 (2015).
[39] Jimenez-Izal, E. & Alexandrova, A. N. Computational design of clusters for catalysis. Annu. Rev. Phys. Chem. 69, 377–400 (2018).
[40] Tauster, S. Strong metal-support interactions. Acc. Chem. Res. 20, 389–394 (1987).
[41] Abbet, S. et al. Identification of defect sites on MgO(100) thin films by decoration with Pd atoms and studying CO adsorption properties. J. Am. Chem. Soc. 123, 6172–6178 (2001).
[42] Bergeret, G. & Gallezot, P. in Handbook of Heterogeneous Catalysis Vol. 2. (eds Ertl, G., Knözinger, H., Schüth, F. & Weitkamp, J.) 738–765 (Wiley-VCH, Weinheim, 2008).
[43] Capdevila-Cortada, M. & López, N. Entropic contributions enhance polarity compensation for CeO2(100) surfaces. Nat. Mater. 16, 328–334 (2017).
[44] Snider, J. L. et al. Revealing the synergy between oxide and alloy phases on the performance of bimetallic In–Pd catalysts for CO2 hydrogenation tomethanol. ACS Catal. 9, 3399–3412 (2019).
[45]. Garcıa-Muelas, R., Li, Q. & López, N. Density functional theory comparison of methanol decomposition and reverse reactions on metal surfaces. ACS Catal. 5, 1027–1036 (2015).
[46] Chorkendorff, I. & Niemantsverdriet, J. W. in Concepts of Modern Catalysis and Kinetics Vol. 1 (eds Chorkendorff, I. & Niemantsverdriet) 79–128 (WileyVCH, Weinheim, 2003)
[47] Kresse, G. & Furthmüller, J. Efficiency of ab-initio total energy calculations for metals and semiconductors using a plane-wave basis set. Comput. Mater. Sci. 6, 15–50 (1996).
[48] Kresse, G. & Hafner, J. Ab initio molecular dynamics for liquid metals. Phys.Rev. B47, 558–561 (1993).
[49] Perdew, J. P., Burke, K. & Ernzerhof, M. Generalized gradient approximation made simple, Phys. Rev. Lett. 77, 3865–3868 (1996).
[50] Blöchl, P. E. Projector augmented-wave method, Phys. Rev. B50, 17953–17979 (1994).
[51] Frisch, M. J. et al. Gaussian 09, Revision A.02. (Gaussian, Inc., Wallingford CT,2016).
[52] Köhler, L. & Kresse, G. Density functional study of CO on Rh(111). Phys. Rev.B 70, 165405 (2004)

Narr Francke Attempto Verlag GmbH + Co. KG

Production of renewable biomethane using bioresources and hydrogen

Kati Görsch
DBFZ Deutsches Biomasseforschungszentrum gemeinnützige GmbH, Leipzig, Germany
kati.goersch@dbfz.de

Maria Braune
DBFZ Deutsches Biomasseforschungszentrum gemeinnützige GmbH, Leipzig, Germany

Philipp Knötig
DBFZ Deutsches Biomasseforschungszentrum gemeinnützige GmbH, Leipzig, Germany

Summary

The Pilot-SBG project (SBG = synthetic biogas) is a research and demonstration project for the production of biomethane, which is to be used as a climate-friendly and renewable fuel in the transport sector. Therefore, the DBFZ is planing and implementing the construction and operation of a pilot plant on a technical scale. In the pilot plant previously unused biogenic residues, by-products, and wastes are to be converted to biomethane. The plant concept combines anaerobic digestion with innovative pre- and post-treatment processes such as hydrothermal processes, digestate processing, and catalytic methanation. The main objectives are to increase the biomethane yield using the carbon dioxide from the biogas process and externally supplied hydrogen as well as to enhance the product portfolio of the whole plant by separating valuable by-products. The project is completed by accompanying investigations, including feedstock potential analysis, assessments as well as a comprehensive feasibility study for a plant on a commercial scale.
This paper addresses the overall research and demonstration project, plant specifications, and challenges.

1. Introduction

In 2018, the Greenhouse gas (GHG) emissions in the transport sector in Germany were higher than in 1990 (164 versus 162 Mio. t carbon dioxide (CO_2) equivalent [1]). The target set by the former climate protection law required a reduction of 52 to 55 Mio. t CO_2 equivalents and climate neutrality until 2050. In the new climate protection law an additional reduction of 10 Mio. t CO_2 equivalents until 2030. Climate neutrality is to be achieved in 2045.
Concerning different scenarios [2-5], these targets for the contribution of the transport sector are very ambitious and will not be achieved by substituting fossil fuels solely. In summary, the transport sector is faced with enormous challenges in enabling sustainable and climate-friendly mobility. In addition to reducing final energy consumption by avoiding and shifting traffic and increasing the efficiency of drives used in the modes of transport, the use of renewable energy sources is of great importance.
Biomethane may be a climate-friendly solution as an advanced fuel for the transport sector, especially. The requirement for advanced biomethane is that the raw materials have to comply with RED II [6], annex IX Part A, for the production of biogas/biomethane from raw materials that often can only be processed with advanced technologies.

2. Research and demonstration project Pilot-SBG

In the Pilot-SBG project previously unused biogenic residues, by-products, and wastes, that are listed in the RED II, are to be converted to biomethane used as compressed natural gas (CNG). The DBFZ is therefore planing and implementing the construction and operation of a pilot plant on a technical scale, in which technologies established at the DBFZ will be used in one process chain.
The activities concerning the pilot plant (preliminary tests, commissioning, operation) are flanked by accompanying investigations and assessments as well as a comprehensive feasibility studies for a commercial-scale plant.

2.1 Plant concept

For such a complex pilot plant, extensive planning was necessary. A central process of the pilot plant is the anae-

Narr Francke Attempto Verlag GmbH + Co. KG

robic digestion to biogas. To improve the digestibility, the organic waste and residues are first pretreated depending on their composition, e.g. shredded, mixed, and hydrothermal processed (HTP) (see figure 1). Biogas consists primarily of methane and carbon dioxide (CO_2). With the aim to increase the overall methane yield, the biogenic CO_2 is converted to methane This is done via catalytic methanation of the biogas with externally supplied hydrogen (H_2) (in a conventional process, CO_2 is separated from biogas and fed to the methanation reactor - this separation does not take place here). After the catalytic methanation step, the product gas is expected to contain only traces of CO_2 and H_2. The aim is to separate residual CO_2 with a downstream sodium hydroxide scrubber to get almost pure methane with a hydrogen content within the legal requirements for use as a fuel in the transport sector. After anaerobic digestion, the digestate is further treated in different processes depending on the feedstock and desired product. The solid/liquid separation is realised with a screw press separator, a decanter centrifuge resp. a chamber filter press. Liquid phase filtrations are done with ultrafiltration and reverse osmosis modules. For solid product generation hydrothermal carbonization and thermal drying steps may be applied. The liquid phase is used to recycle process water into upstream process steps for adjusting the dry matter (dm) content and separating valuable by-products. These products expand the plant's product portfolio may include HTC char from waste-based feedstocks, solid and liquid fertilisers, as well as digestate that can be returned to the field.

The concept will also consider the extent to which a demand side management can be applied to the corresponding processes. Therefore, data for a plant in a commercial scale will be generated on a pilot scale basis.

The pilot plant is followed by a tank facility so that the produced methane can be used as CNG in a company-own vehicle.

A scheme of the process chain respectively a three-dimensional model of the plant can be found in fig. 1 respectively fig. 2.

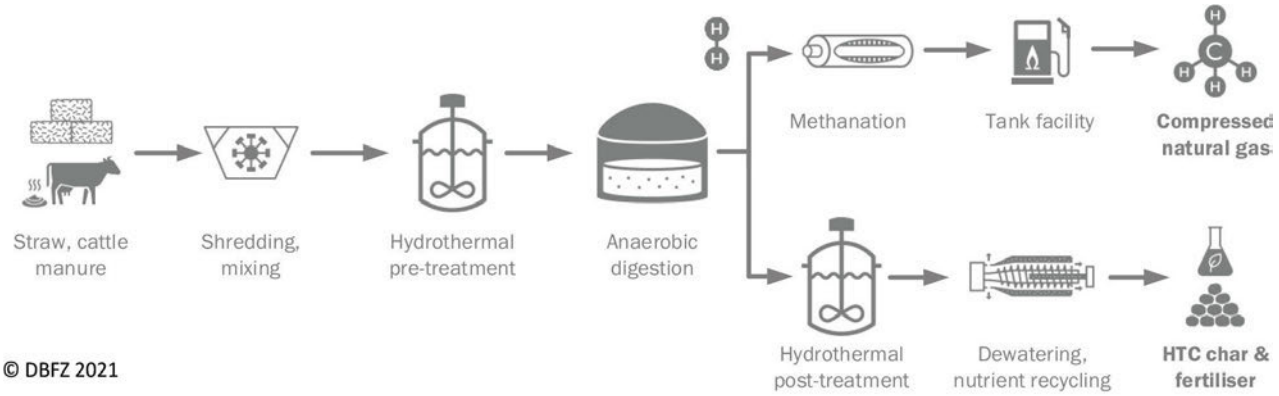

Fig.1: Process steps of the Pilot-SBG plant, exemplary for the rural scenario.

2.2 Operating scenarios of the pilot plant

Biogenic residues and waste materials are used in the pilot plant, for which two scenarios were defined. One is a rural scenario with straw and cattle manure as feedstocks, and the other is an urban scenario with organic waste and green cuttings as raw materials.

The scale of the pilot plant was selected with the background of being able to present the complex process chain, to demonstrate the feasibility of the implementation in principle and to apply scalable equipment as well as industrial standard equipment.

As an example, the approximate mass balance for the rural scenario is given here: 7.3 t a^{-1} of cattle manure with 8% dry matter ($\%_{dm}$) are fermented with 2.0 t a^{-1} of cereal straw with 85%$_{dm}$. With the addition of 0.1 t a^{-1} (under standard conditions) hydrogen, 0.6 t a^{-1} (under standard conditions) methane is obtained. About 1.7 t a^{-1} of solid fertiliser and minerals with 65%$_{dm}$ and 3.2 t a^{-1} liquid fertiliser with 4%$_{dm}$ can be separated as by-products.

2.3 Scale-Up and technical challenges

Feedstock. The scope of the anaerobic digestion is an optimised biogas yield. By using optimal aligned feedstocks as mixtures the anaerobic digestion process is expected to be stabilised. Lignocellulosic feedstocks such as straw and green cuttings are challenging materials for this conversion step. Therefore, the influence of hydrothermal pre-treatment of the lignocellulosic substrates on the anaerobic digestion is investigated. From a technical point of view, the hydrothermal pre-treatment of straw could also lead to a prevention of floating layers, which has to be verified in practice.

Straw is a very challenging feedstock. It has a very low bulk density when loosened, which leads to difficulties in efficient processing. Other challenges include the high viscosity of the straw-manure feedstock mixture and the habit of straws to wrap around agitators, which may lead to poor agitatability or the tendency of this mixture to block the outlet of the reactor. Therefore, it was neces-

Narr Francke Attempto Verlag GmbH + Co. KG

sary to adapt especially the design and configuration of the HTP reactor. The developed HTP reactor has a volume of 750 l, which is unique in the German research community. It is filled via a screw conveyor and emptied via a bottom outlet. An acceptable heating rate is realised via direct steam insertion and heat transfer through the reactor shell using a thermostate operating with heat transfer oil. This measures considerably shorten the duration of the complete hydrothermal process (from filling to emptying). Sufficient mixing of this difficult feedstock is realised via an adjustment of the agitator design. The new design ensures that the complex reactor content is permanently lifted, so that compaction on the reactor bottom and walls is avoided. High viscosities are tackled with a very high agitator torque. In addition, the rotational direction of the agitator can be reversed. In that case the agitator works as a conveyer which supports the full depletion of the reactor.

Another point for ensuring routine operation is the availability of feedstocks in the required quantity. The DBFZ is not a bulk buyer, so sometimes it is not even worth setting up a contract, but continuous production depends on regular deliveries of the feedstocks.

Plant dimensions and scale-up. The pilot plant will be built on a technical scale. Due to the relatively low throughput, it was necessary to make compromises in some parts, e.g. with regard to

- upscaling strategies from laboratory to pilot scale: Which degree of effort is reasonable?
- technical options available on the market: What is possible in this scale?
- the degree of automation required for parts of such a complex plant: What is necessary with regard to plant safety and ensuring weekend operation?

For example, in a commercial scale it would not be efficient to shred straw to such a degree as in the laboratory scale. This will always be a decision between optimisation of digestibility and therefore increase of the biogas yield on the one hand and time and costs for shredding on the other hand.But at pilot scale and even more on a laboratory scale, shredding and representative sampling of the feedstock material is much more important. Since anaerobic digestion also depends, among other things, on the available surface area of the feedstock materials, the use of larger straw particles at pilot scale (compared to laboratory scale) may have an impact on microbial conversion. That needs to be observed in the routine operation of the pilot plant.

For ensuring routine operation it is necessary to feed the system also on weekends from automated supply tanks. Furthermore, storage facilities must be created and it must be ensured that the feedstocks do not degrade during storage (in the refridgeration unit and in the supply tank) or change in such a way that the organic components, which are necessary for the anaerobic process, have already degraded by the time they are used. This anaerobic degradation during storage had to be included in safety considerations – therefore all storage vessels are equipped with safety valves and the storage unit is monitored with gas quality sensors.

After the plant has been commissioned and completion of the test phase, it is to go into continuous operation. The entire process chain is to be represented over planned campaigns, each with a duration of about six months. For smooth continuous operation, plant parameters should not be altered frequently. This requires preliminary tests for the individual modules.

One example is the composition of the biogas from the anaerobic digestion step, which depends on the used feedstock. In the case of methanation, this has an impact on the upstream biogas purification, the selection of the catalyst, the operating points, the stability of the whole synthesis process, and the conversion rates. Therefore, suitable biogas plants had to be found, possible gas sampling points identified, and gas sampling carried out. After these analyses, it was technically possible to mix a model biogas with the most important corresponding trace gases (hydrogen sulphide, siloxanes) for further experiments concerning the methanation step.

For the investigation of separation processes, digestate is needed in an appropriate quantity and quality, which is based on similar feedstocks as those to be used in the scenarios. Unfortunately, digestate is a very complex mixture containing e.g. extracellular polymeric substances and a wide mixture of organic substances which is not easy to reproduce. For solid-liquid separation, for example, effective flocculants and flocculation aids need to be identified and the challenges of that are not to be underestimated.

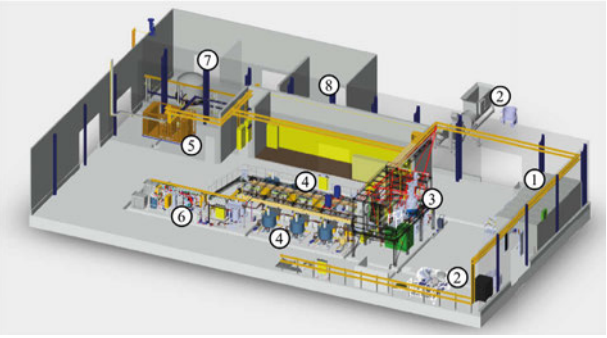

Fig. 2: Three-dimensional model of the pilot plant with (1) possibilities for storage and cooling, (2) equipment for shredding and mixing, (3) hydrothermal treatment, (4) anaerobic digestion in two reactor lines (continuous stirred tank reactor line and plug flow reactor line), (5) biogas purification and methanation, (6) process water recycling and separation of valuable by-products, (7) biomethane storage tanks, and (8) a CNG tank facility (not visible).

Narr Francke Attempto Verlag GmbH + Co. KG

Coupling of technologies. In the pilot plant, the interfaces between individual process steps must also be coordinated with regard to the composition of the substances, so that the required quality is ensured for the subsequent process step. Therefore, gases are monitored and measures for the separation of disturbing components are inplemented: Adding oxygen to the biogas after the anaerobic digestion to separate hydrogen sulphide as well as water removal are both measures with the aim to protect the downstream methanation process. It is also important to coordinate the material flow quantities from the individual modules. Therefore, buffer vessels are planned at some interfaces.
In addition, coupling this number of processes each with specific safety needs demands a superior safety concept. Now small malfunctions in one process can have an impact throughout the entire pilot plant. A comprehensive hazard and operability analysis (HAZOP) had to be performed in order to adress and counteract safety issues. As a result, a combination of technological measures (gas detection, air ventilation, flair system etc.) and organisational measures (personal protection equipment, standard operating procedures etc.) were incorporated in the engineering documentation.
Quality management of the product also plays a major role since it will be used to safely fuel a CNG vehicle of the DBFZ car pool. One parameter in the present fuel standard is the hydrogen content with a maximum of 2% (based on the volume). Therefore, technological adaptions had to be made after methanation, e.g. water separation or hydrogen detection, which ensure to generate a product that can be refuelled. In the case of inadequate product mixtures, these gas flow is lead to the flair system for safe combustion.
Last but not least, it was necessary to construct a new building, due to the fact, that there was no suitable available fulfilling the requirements. The new facility is adapted to the safety requirements, the scale of the pilot plant and the used materials flows. It has an own wastewater system, so that process water can be treated and recycled if required.

3. Accompanying investigations

3.1 Feedstock potentials

The suitable raw materials were identified in a feedstock potential analysis and evaluated with their available quantities. The theoretical biomass potential of digestible biomasses in Germany amounted to 145.2 Mio. tonnes of dry matter (t_{dm}) in 2015. Of this, an amount of 38.5 Mio. t_{dm} has already been used as technical potential - of which, in turn, almost the entire quantitiy can be optimised in its use. The amount of 22.9 Mio. t_{dm} of digestible biomass was still mobilisable in Germany in 2015. [7]
The ranking of biomasses in terms of their mobilisability potential results in the largest quantities for cereal straw, cattle manure and green waste. The quantities of these three biomasses account for nearly 19 Mio. t_{dm} (average value, annual fluctuations possible due to climatic conditions), i.e. 80% of the considered digestible biomasses that can be mobilised [8]. All data can be accessed via the DBFZ resource database, a publicly available online tool for biomass monitoring [9].
The mentioned biomass quantities result in an energy quantity of 97 to 279 petajoules (PJ) of biomethane from mobilisable biogenic digestible residues. This amount of energy can be converted into the so-called substitution potential, which describes the proportion of energy currently supplied by fossil fuels that can be replaced by the product biomethane. Based on the energy demand of 2015, this amount of energy corresponds to a total substitution potential of 4% to 11% in the transport sector. The impact for individual transportation options that are difficult to electrify is, e.g., 13% to 40% for CNG and LNG trucks, respectively, and more than 87% for the bunkering of seagoing vessels. [8].

3.2 Assessments and feasibility study

The entire project is accompanied by comprehensive assessments (technical, economic, and ecological) with the focus on a possible commercial scale.Therefore, a potential plant dimension had to be defined first. For this purpose, a SWOT analysis was carried out for three different possible plant dimensions. From the compilation and evaluation of the SWOT analysis, the consideration of a plant size/dimension of 1,300 $m^3\ h^{-1}$ (under standard conditions) methane in biogas (before the methanation step) appeared to be reasonable. After catalytic methanation, a biomethane output of almost 2,400 $m^3\ h^{-1}$ (under standard conditions) can be achieved.
A feasibility study for the construction of a commercial plant is carried out in order to consider location issues, market conditions, and stakeholder interests.
With regard to the questions concerning the stakeholders, it is important to determine which conditions must be fulfilled, so that they are open to participate, especially the raw material suppliers must be willing to provide the substrates for a commercial plant concept. Conducting interviews in selected regions which are particularly important in terms of raw material availability is intended to identify factors that may be conducive or inhibiting with regard to implementation. Based on the analysis of the raw material availability and the visualisation of the spatial distribution, priority districts/regions will be identified using a geographic information system. Interviews are conducted to trace current raw material utilisation routes, among other things, in order to identify, where the Pilot-SBG concept can provide an advantage compared to the existing route.

Narr Francke Attempto Verlag GmbH + Co. KG

4. Concluding remarks

The Pilot-SBG project is aligned with current political and legal requirements and strategies. By using available biogenic residues and waste materials and recycling nutrients as well as minerals, the link to a circular economy is established. The German National Hydrogen Strategy is addressed by integrating green hydrogen to increase the methane yield through methanation of the CO_2 contained in biogas. In the planned pilot plant hydrogen will be provided via gas cylinders for reasons of economic efficiency. But in a later commercial scale a so called SynBioPTX approach is adopted with hydrogen provided by renewable sources. During economic assessment this is one of the considered aspects. Furthermore, the objectives of the Climate Protection Plan are targeted, when biomethane is provided as a climate-friendly renewable fuel for non-electrifiable transport sectors.

5. Acknowledgement

The research and demonstration project Pilot-SBG (https://www.dbfz.de/en/projects/pilot-sbg/) is financed by the German Federal Ministry of Transport and Digital Infrastructure within the framework of the Mobility and Fuels Strategy.

References

[1] Klimaschutzbericht 2019. BMU (ed). Date: 18.08.2020. https://www.bmu.de/fileadmin/Daten_BMU/Download_PDF/Klimaschutz/klimaschutzbericht_2019_kabinettsfassung_bf.pdf.

[2] Öko-Institut e. V., Fraunhofer Institut für System- und Innovationsforschung (eds.), 2015. Klimaschutzszenario 2050. Studie im Auftrag des BMU. https://www.oeko.de/oekodoc/2451/2015-608-de.pdf.

[3] T. Bründlinger, J. E. König, O. Frank, D. Gründig, C. Jugel, P. Kraft, O. Krieger, S. Mischinger, P. Prein, H. Seidl, S. Siegemund, C. Stolte, M. Teichmann, J. Willke, M. Wolke. Deutsche Energie-Agentur GmbH (ed.). dena-Leitstudie 2018. Integrierte Energiewende - Impulse für die Gestaltung des Energiesystems bis 2050. https://www.dena.de/fileadmin/dena/Dokumente/Pdf/9261_dena-Leitstudie_Integrierte_Energiewende_lang.pdf.

[4] P. Gerbert, P. Herhold, J. Burchardt, S. Schönberger, F. Rechenmacher, A. Kirchner, A. Kemmler, M., Wünsch. BDI (ed.). Klimapfade für Deutschland 2018. https://bdi.eu/publikation/news/klimapfade-fuer-deutschland/.

[5] Verkehr in Zahlen 2019/2020. https://www.bmvi.de/SharedDocs/DE/Publikationen/G/verkehr-in-zahlen-2019-pdf.pdf?__blob=publicationFile.

[6] Richtlinie (EU) 2018/2001 des Europäischen Parlaments und des Rates vom 11. Dezember 2018 zur Förderung der Nutzung von Energie aus erneuerbaren Quellen.

[7] A. Brosowski, T. Krause, U. Mantau, B. Mahro, A. Noke, F. Richter, T. Raussen, R. Bischof, T. Hering, C. Blanke, P. Müller, D. Thrän, D.: How to measure the impact of biogenic residues, wastes and by-products. Biomass and Bioenergy, 127 (2019) dx.doi.org/10.1016/j.biombioe.2019.105275.

[8] A. Brosowski, T. Krause, U. Mantau, B. Mahro, A. Noke, F. Richter, T. Raussen, R. Bischof, T. Hering, C. Blanke, P. Müller, D. Thrän. Schlussbericht "Arbeitsgruppe Biomassereststoffmonitoring", 5.06.2019. https://www.fnr-server.de/ftp/pdf/berichte/22019215.pdf.

[9] https://webapp.dbfz.de/ (always available)

Narr Francke Attempto Verlag GmbH + Co. KG

Fuels Quality Research

Narr Francke Attempto Verlag GmbH + Co. KG

Plasma cross-linked vegetable oil as fuels additives: effect of vegetable oil nature, viscosity and Functionalization.

Dr. Rémi Absil
Green Frix, Blandain, Belgium

Frédéric Danneaux
Green Frix, Blandain, Belgium

Summary

Plasma reactors enable Green Frix to cross-link oils and substances to generate bio-based oils and additives for the industry with a large improvement of their oxidative stability, lubricity, friction modification, rheology behavior, ... The process developed and patented by Green Frix offers a large panel of non-Newtonian products with various viscosities and rheologies (, shear-thinning, thixotropy, adaptive relaxation time,…) and can offer tailor-made solution. Previous studies on the effects of vegetable oil methyl esters on diesel fuel lubricity have shown an increase in lubricity associated with the addition of these esters.[1] In this study, we examine the effect of various additives based on cross-linked vegetable oils. The effect of their nature, viscosity and functionalization are investigated. Additive levels of 0–0.1% of specific polymerized vegetable oils were added to diesel fuel and the resulting lubricity was measured using the High Frequency Reciprocating Rig method.

1. Introduction

Automotive Fuels are complex formulation of chemicals where compositions highly impact the lubricity of the diesel Fuels. In the 90s', the concern of keeping the environment green, regulations change to lower the value of sulfur content in diesel up to maximum 500 ppm. More recently, several countries are going further and limit the concentration of sulfur to a maximum of 50 ppm. As so, different processes have been applied to get rid off the sulfur. Unfortunately, during the process, several other components involved in the lubricity get also removed. Therefore, low sulfur diesel required higher concentrations of additives or blending with other substances to achieve sufficient lubricity.[2] Biofuels gain increasing interest over the years. Underlying, there is a large trend to develop and promote sustainable, non-toxic and biodegradable additives.

Plant-based oils such as canola, linseed, soy, sunflower and palm are common sources of sustainable feedstocks. These oils present several advantages such as biodegradability, lubricity, high flash point and good solvency (ability to dissolve additives and disperse contaminants). However, their poor oxidative and thermal stabilities, low viscosities are drawback limiting their application. Large number of papers have been published on vegetable oils and vegetable oil derivatives as additives or based fuels to substitute petroleum-based products by fixing their above-mentioned downsides. It is known that poor oxidation stability and poor lubricity affecting bio-based products are challenges that need to be settled. Several studies demonstrates that the used of well know fatty acid methyl ester (FAME) increased diesel fuel lubricity at concentration lower than 1%.[3],[4] Moreover, fatty acid composition, presence of functional group, molecular weight of the FAME are factor impacting the lubricity of the respective diesel.[5],[6] Hydroxyl functionalized FAME based on castor oil present more lubricity compared to their respective counterpart without any hydroxyl function.[7] Later, investigation confirmed that the structure of fatty acid presents a high importance. Indeed, it was showed that the lubricity respectively increased with the unsaturation of the FAME. Moreover, the paper suggests that vegetable oil based FAME mixtures consistently perform better as lubricity additives than their respective single fatty acid counterpart making the fatty acid distribution an important key factor fort the efficiency of the lubricity additives.[1] Plasma techniques applied to oils is a century old story. With its fundamental research program, Green Frix investigated the link between plasma energy and non-newtonian behaviors. Plasma energy will impact the cross-linking resulting in different level of shear-thinning. With low sulfur fuels, increasing admission pressure, risk of failure increases. Envision a fuel containing of a non-newtonian component will contribute to absorb the increase of load related to this evolution. The process enables to create low molecular weight vegetable oil (oligomers).

Narr Francke Attempto Verlag GmbH + Co. KG

The cross-linking process can be carried on; hence products will move from oligomers to polymers to achieve viscosity up to 6000mm²/s at 40°C. Herein, we describe for the first time the use of plasma technologies to promote vegetable oligomers and polymers. In the following section we will detail the effect of the plasma treatment on the properties of the additives used for the fuel lubricity. The new polymers additives will be examined by several techniques including surface tension measurements, thermo-gravimetric analysis to study their physicochemicals properties. Finally, we will discuss the rheological properties of the plasma polymerized oils. Several oils will be tested in diesel fuels as additives. Effect of molecular weight, oil nature and functional group on lubricity of the diesel fuel will be highlighted by HFRR test following ISO 12156.

2. Materiel and method

2.1 Materials

Base oils were purchased at Aveno NV (Nieuwelandenweg 32 /1 2030 Antwerp Belgium. Oils present a yellow color and a specific gravity of 0.92-0.93 at 15°C. ColFadol products used in this study were prepared using the Green Frix plasma process reported in the patent.[8] Un-additivated Diesel fuel was received from Total (Belgium, Antwerpen) and used as received.

2.2 Viscosity measurement

Viscosity measurement were realized using a Lauda viscosimeter according to ASTM D 445-06 Method.

2.3 SEC

Size exclusion chromatography (SEC/GPC) was performed in $CHCl_3$ at 23°C using either a Polymer Laboratories liquid chromatograph equipped with Rheodin manual injection (loop volume = 200 µl, solution conc. = 1 mg/ml), a Pl-DRI refractive index detector and two PLgel columns.

2.4 FTIR analysis

The FTIR spectra were recorded on a Bruker IFS 66v/S spectrometer in Attenuated Total Reflectance (ATR) mode with 4 cm^{-1} resolution. The background and sample spectra were obtained in the 500-4000 cm-1 wave-number range.

2.5 Surface tension measurement

Surface tension measurements were realized at room temperature with a Krüss tensiometer K10ST Krüss using De Nouy Ring method.

2.6 TGA analysis

The measurements were performed on a TA instrument Q 500 Thermogravimatric analyser. A ramp of temperature of 10°C/per minutes was applied.

2.7 Rheological behavior

The measurements were performed on an Anton Paar MCR302 rheometer equipped with a plate/plate shear module. The gap used is one millimeter. Shear thinning ISO 2884-1were used as guideline fort the measurements.

2.8 Lubricity determination

Lubricity determinations were performed at 60 °C (controlled to 1 °C), according to the standard method ISO 12156 with an HFRR lubricity tester from PCS Instruments.

3. Results

3.1 Synthesis of polymer

Synthesis of the whole polymer of vegetable oil in this study have been synthesized by plasma cross-linking. Polymerisation take place in the plasma reactor has described earlier in the patent. The oil present several interesting properties like controlled viscosity, non-newtonien behavior (shear thinning, thixotropy,…) and controlled relaxation time depending on the parameters used in the plasma. Proof of polymerisation can be attested by size exclusion chromatography as depicted in Figure 1.

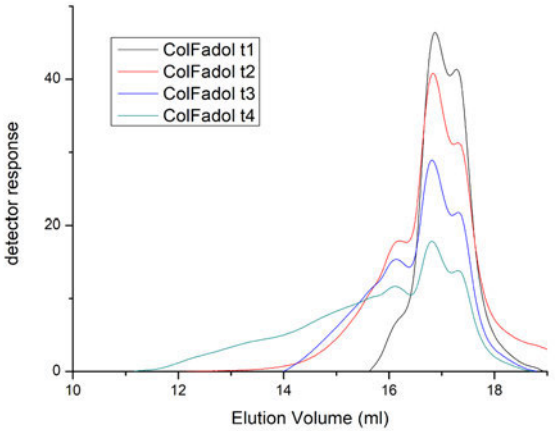

Figure 1: Evolution of the molecular weight distribution of polymerized oil with time of treatment.

As depicted in Figure 1, for a fixed level of Plasma energy, the highest the time of treatment, the highest the molecular weight will become and therefore it will be accompanied by an increase of viscosity. The plasma technologies allow good control over the broad viscosity and provide several

Narr Francke Attempto Verlag GmbH + Co. KG

advantages. First, the process is metal-free, non-oxidative and provide a decreased of the iodine value of the oil offering better oxidation stability compared to pure vegetable oil. The decrease of iodine value is confirmed by FTIR. It can be noticed in Figure 2 the decrease of the signals corresponding to alkene stretch and alkene bend respectively around 3100 cm-1 and 720 cm^{-1} in FTIR. Secondly, it does provide high molecular weight vegetable with viscosity index > 200 up to 380 for the highest viscosity. Viscosity data can be found in the Table 1 below. Finally, plasma polymerisation technologies can offer non-newtonian biobased polymer depending on the viscosity and plasma parameters used. Moreover, functionalisation of the oil is possible as depicted in the Table 1. ColFadol 700-P is a phosphate organic functionalized oil and SunFadol 800 OH is a hydroxyl functionalized oil. All these results indicates that vegetable oils can be functionalized, and polymers of vegetable oil has been obtained by plasma polymerization. Good control of molecular weight and viscosity can be achieved depending on the plasma parameters and time of reaction.

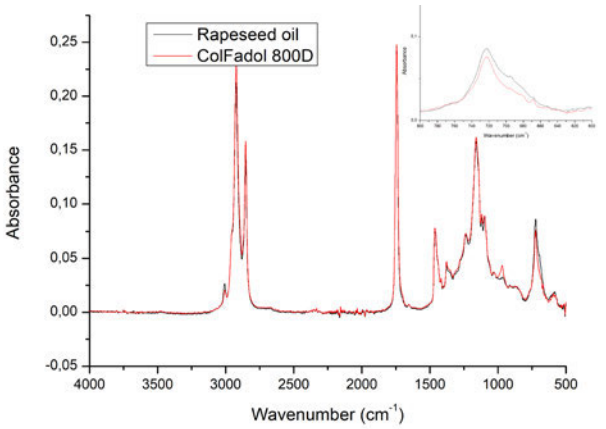

Figure 2: FTIR comparison of pure vegetable oil and ColFadol 800D

Table 1: viscosity measurements of additives diluted in diesel for the HFRR test.

Product	V40 (mm²/s)	V100 (mm²/s)	VI
ColFadol 68 S	73.35	14.40	206.0
ColFadol 700-P	705.91	116.30	266.2
SunFadol 800 OH	772.87	114.02	249.3
ColFadol 800 D	792.43	125.74	264.5
ColFadol 3000 D	3162.36	478.75	334.2

3.2 TGA analysis

TGA analysis demonstrate good thermal stability of the polymerized oil over the process from the low molecular weight oil to high molecular weight oil. The thermal stability of the product is > to 300°C as attested by Figure 3. Moreover, there is very limited amount of remaining solid at the end of the analysis suggesting that the biobased additives will not form ash after its used in the fuels.

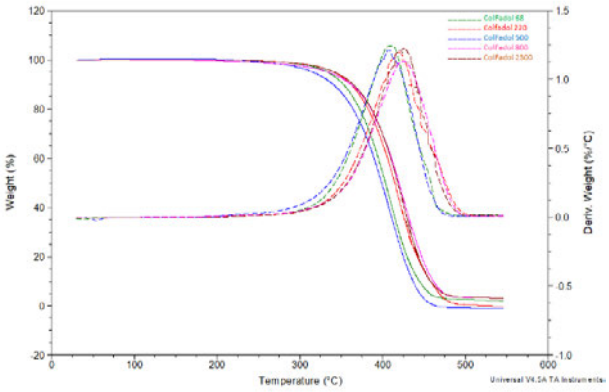

Figure 3: TGA analysis of low to high polymerized vegetable oil.

3.3 Surface tension characterization

Atomization of fuels is considered as the initial process in combustion. It has been studied for more than 40 years. [9],[10],[11] These studies showed the importance of surface tension on fuels properties. Surface tension of additives for fuels is suggested to highly important role within the final fuels properties as surface tension impact drastically the atomization phenomena in the combustion of the fuels. Larges number of papers has been published on modification of vegetable oil with various chemistries to provide higher lubricity by introducing polar group like epoxide[12] or by varying the oil nature,…[13,14,15,16,1] Therefore, as surface tension is a critical factor for fuels properties, we studied the effect of the plasma treatment on the surface tension as molecular weight change occurs, the effect of the oil nature (unsaturation) and presence of functional group (hydroxyl) on the final surface tension. The surface tension of each compound was measured at 25°C and value are depicted in Figure 4.

Narr Francke Attempto Verlag GmbH + Co. KG

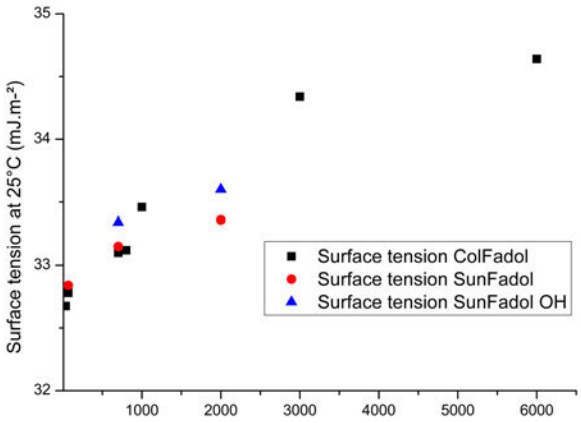

Figure 4: Evolution of surface tension with oil nature and viscosity of the thickened oil.

On Figure 4, several behaviours can be noticed for the plasma polymerized oils. First, the viscosity increased is accompanied with an increased-on surface tension. This increased of surface tension with viscosity (or molecular weight) has been already noticed for polymer.[17,18,19] Based on this data, we can say that the molecular weight dependence of plasma polymerized oils can be explained according to literature. It has been showed that surface tension for medium to high molecular weight polymer is proportional to Mn^{-1}. The dependence is attributed to the fact that polymer can be seen as two different kind of building blocks: the repetitive units which represent the majority of the mass of the polymer and the end group. Since end group concentration is low for high molecular weight polymer, it is expected that bulk properties like surface tension followed the dependence of Mn^{-1}.[20,21] Interestingly, surface tension of plasma polymerized oils showed the same trend as cited in literature. Moreover, the presence of functional group (hydroxyl) increases surface tension of the oil for similar viscosity *i.e.* molecular weight. Interestingly, OH functionalized Plasma polymerized oils present higher surface tension compared to their unfunctionalized polymer (same range of Mw). As surface tension is a bulk property and largely dominated following literature by the cohesive energy density[22], it does make sense that increases the content of hydrogen-bond increases this cohesive energy density and therefore the surface tension. Overall, the magnitude of the surface tension changes is small compared to their unpolymerized oil. The small surface tension increase is likely to cause little if any change in the atomization characteristics of a fuel.

3.4 Rheological characterization

It is known that polymers can modify viscosity and rheological behavior of fluids.[23] Typical example are the multigrade oils where viscosity temperature improvement has been made during the past years. Currently most polymers used in such application are petrobased polymers. [24,25] In this section, we are interested to demonstrate the possibility of using Biobased polymerized oils as VI improver but also rheological modifier. In this section, we will study the effect of the addition of polymerized vegetable oil on the improvement of viscosity for several oil. VI comparison and viscosity evolution will be compared to demonstrate the positive effect of the addition of the plasma biobased additive. In regards of fuel economy, there is a large trend to decrease the motor oil viscosity for both passage car motor oil (PCMO) and heavy-duty diesel engine oil (HDDEO). It is believed that additives will play an important role for the development of new and better fluid with fuel economy characteristic.[26]

In this section, we look first at the effect of the addition of several plasma polymerized oil as additives on final viscosity and how it improves the viscosity. Results are showed in Figure 5. It can be noticed that the addition of 5 to 10% of the additives can lead up to a viscosity increase of 51 % compared to the reference oil. Interestingly, the use of 5 % of high viscosity plasma polymerized oils lead to similar viscosity at 100°C but present different viscosity temperature behavior as depicted in Figure 6. This data demonstrated the effect of the polymer as effective VI improver.

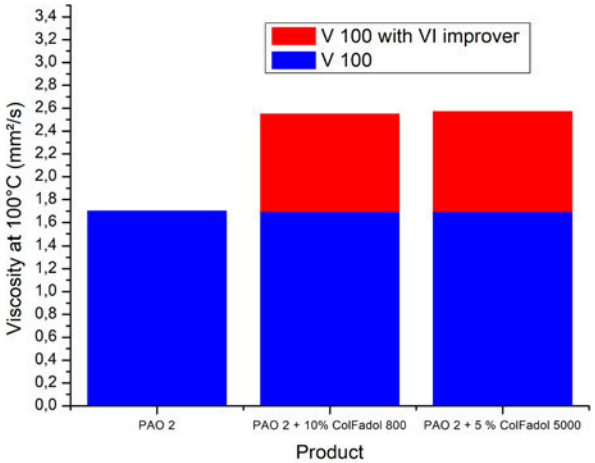

Figure 5: viscosity improvement of a PAO 2 fluid with addition of two different plasma polymerized oil.

Narr Francke Attempto Verlag GmbH + Co. KG

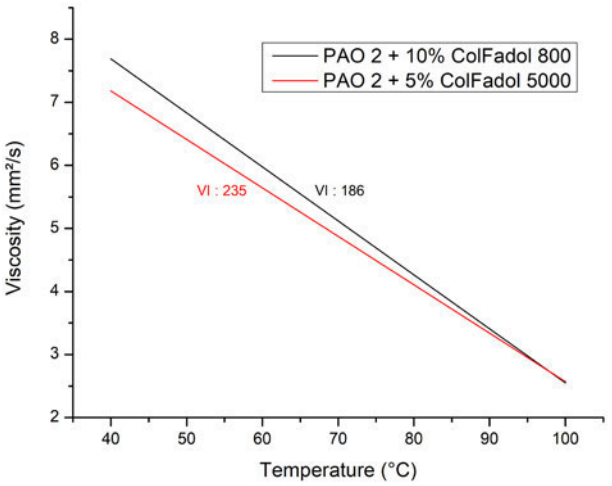

Figure 6: VI evolution with addition of ColFadol polymer in PAO.

In the next paragraph, we will investigate the shear thinning behavior of the plasma polymerized oil. Formulators favored multigrade oil for specific reason. As mentioned, they present better temperature response but also multigrade oil present lower viscosity compared to monograde oil under high shear rates encountered in most engine components. This can be explained by the shear thinning of the lubricants where the polymer align in the shear field. This fact also explains why multigrade lubricants produce lower fuel consumption than monograde lubricants.[27] In this section, several plasma polymerized oils has been studied to investigate their shear-thinning behavior. Oil viscosity, oil nature and plasma mode has been investigated. Results are respectively depicted in Figure 8 and *Figure 9*. The shear thinning has been studied by applying low and high shear over time. Temporary viscosity loss is recordded by following the evolution of viscosity over time taking into account the shear applied. In figure 7, it can be noticed that the higher the viscosity *i.e.* the higher the molecular weight, the higher is the shear thinning for a fixed shear. This observation is consistant with litterature. Moreover, polymerized oils based on sunflower oil present higher shear thinning compared to rapeseed oils as depicted in Figure 8.

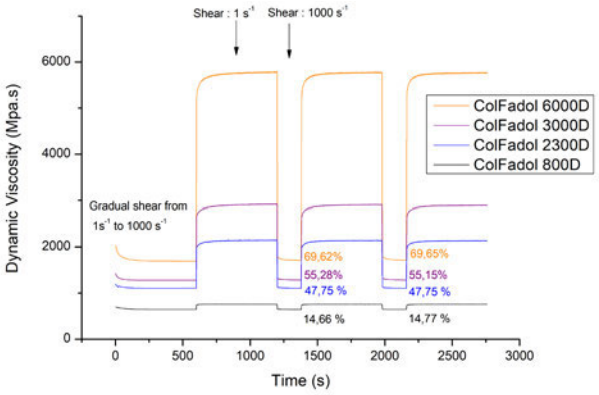

Figure 7: shear thinning behavior evolution with viscosity of the plasma polymerized oil oils additives

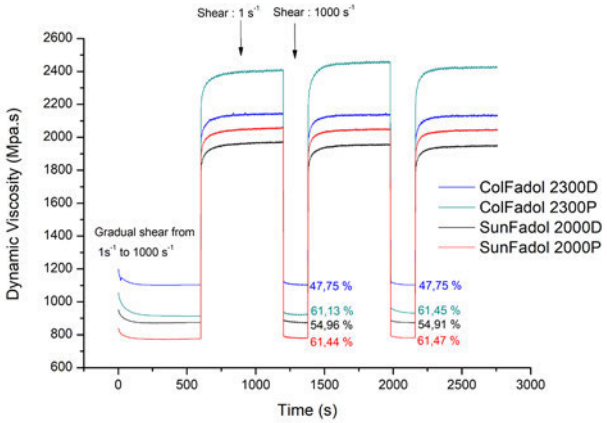

Figure 8: shear thinning behavior evolution with the oil nature within the plasma polymerized oil additives

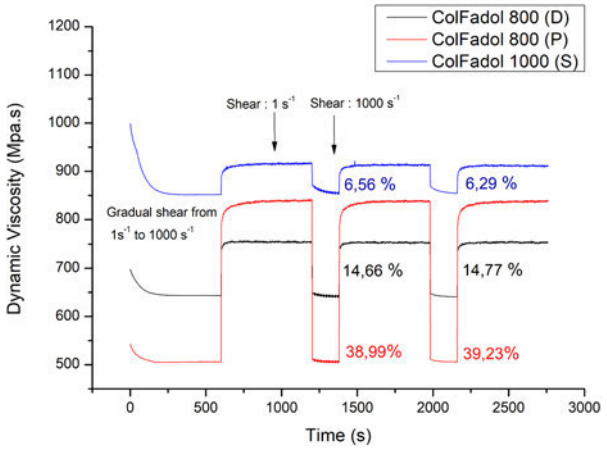

Figure 9: shear thinning behavior evolution with the plasma parameters within the plasma polymerized oil additives

It has been showed that the oils nature (*i.e.* fatty acid distribution) impact the respective shear thinning behavior of the finals polymers produced by plasma. Finally, we investigated the plasma effect on the shear thinning be-

Narr Francke Attempto Verlag GmbH + Co. KG

havior. As depicted in *Figure 9*, shear thinning behavior can be tailored for a target viscosity from around 5-6 % to up to 39 % of shear thinning for a viscosity ranging from 750 to 900 Mpa.s. The plasma technologies offer new possibilities of the technique to promote new types of rheological modifiers with tailor made possibilities depending on the application and used of the final product. The capability to choose the appropriate shear-thinning level, relaxation time, … open new ways to address issues related to the increasing load in application like higher pressure in injectors, increased torque in shafts, axles, bearings, … because it enables the fluid (or grease) to absorb part of the load without being compressed (heated up).

3.5 HFRR Test: diesel lubricity

Due to the polar nature of the plasma polymerized oil oil, investigation of their lubricity properties as diesel additives is investigated. In this section several oil and their effect on lubricity will be discussed depending on their nature, concentration, and viscosity. The oils characteristics used in this section are detailed in Table 1. Lubricity was assessed using Iso 12156. Lubricity, as determined per HFRR test, can be evaluated using the lubricity specification in the petrodiesel standard EN 590. The reference diesel used here (ULSD) showed poor lubricity in the neat form (Table 2) with scar value around 580 µm.

Table 2: results obtained by HFRR with petrobased diesel as reference fluid

Additives added	Additive concentration (ppm)	Wear scar (um)
Reference	0	580
ColFadol 68 S	1000	530
ColFadol 700-P	1000	400
SunFadol 800 OH	1000	430
ColFadol 800 D	1000	400
ColFadol 800 D	500	540
ColFadol 800 D	250	560
ColFadol 3000 D	1000	420

All sample additives with 1000 ppm showed good lubricity except for the low molecular weight additives (ColFadol 68 S). Addition of Colfadol 800D and ColFadol 700-P showed the best results in term of lubricity even though the difference is little compared with other samples. The additives reduced the wear scar value up to 31 %. The results are in accordance with the previous articles as polar ester groups in vegetable oils enable to adhere to metal surfaces and, therefore, possess good boundary lubrication properties. Addition of concentration below 1000 ppm led to a decrease of lubricity. Interestingly, the functionalization of the oils does not seem change drastically the wear scar. This observation is surprising as it has been referred that castor oil FAME showed better lubricity compared to their counterparts FAME.[28] Two explanations are emphasized. The functionalization content is to low leading to insufficient functional group in contact with the surface or the functionalized of the side chain of the polymer does not play a role and adsorption of the surface is mainly done by the ester group present in the triglycerides. Viscosity range of the additives play an important role as to low does not offer good lubricity and to high does not improve more the wear scar as depicted by the results of ColFadol 68 (S) and ColFadol 3000 (D).

4. Conclusions

- Polymerization of vegetable oil can be achieved by plasma treatment leading to molecules of high viscosity, high molecular weight and high viscosity index.
- Polymer produced are liquid polymers making them more easily manipulable.
- Plasma polymerized oil can be used as viscosity improver and rheological modifiers increased viscosity at 100°C up to 51 %.
- TGA analysis demonstrates that low residue offering potential ashless additives for fuel.
- Plasma polymerized oil at low additive level significantly improved the lubricity of ULSD. Addition of 1000 ppm decreased the wear scar of 31 %. The additives concentrations are 10 times lower compared to additivation with FAME (1%)

Our future work will be dedicated to improve the lubricity by increasing the polar functionality within the additive and optimized the molecular weight range for optimum effect for the fuel lubricity.

Reference

[1] Geller Daniel P. and Goodrum John W, Effects of specific fatty acid methyl esters on diesel fuel lubricity. Fuel, 83 (2004), 2351–2356

[2] Zengshe Liu *et al*., Improvement of Diesel Lubricity by Chemically Modified Tung-Oil-Based Fatty Acid Esters as Additives. Energy Fuels, 33 (2019), 5110- 5115

[3] G. Anastopoulos E. Louis *et al.*, Influence of aceto acetic esters and di-carboxylic acid esters on diesel fuel lubricity. Tribol Int, 34 (2001), 749-755

[4] Titipong I, Dalai AK, Desai P., Evaluating esters derived from mustard oil as potential diesel additives. J Am oil Chem Soc, 88 (2011), 391–402

[5] Dias JM, Alvin FMCM, Almeida MF., Comparison of the performance of different homogeneous alkali catalysts during transesterification of waste and virgin oils and evaluation of biodiesel quality. Fuels, 87 (2008), 3572–3578

Narr Francke Attempto Verlag GmbH + Co. KG

[6] Balamurugan K, Kanagasabapathy N, Mayilsamy K. Studies on soyabean oil-based lubricant for diesel engines. J Sci Ind Res, 69 (2010), 794–797
[7] D.C. Drown, K. Harper, E. Frame, Screening vegetable oil alcohol esters as fuel lubricity enhancers. J Am oil Chem Soc, 78 (2001), 579-584
[8] Godfroid T. *et al.*, U.S. Patent 20190203153
[9] Msipa, C. K. M.; Goering, C. E.; Karcher, T. D. Vegetable Oil Atomization in a Diesel Engine. Trans. ASAE, 26 (1983), 1669-1672
[10] Allen, C. A. W.; Watts, K. C. Comparative Analysis of the Atomization Characteristics of Fifteen Biodiesel Fuel Types. Trans. ASAE, 43 (2000), 207-211
[11] Zhang P. *et al.*, Spray, atomization and combustion characteristics of oxygenated fuels in a constant volume bomb: A review. J. Traffic Transp. En (Engl, Ed.), 7 (2020), 282-297
[12] Kenneth M. Doll, Bryan R. Moser, and Sevim Z. Erhan, Surface Tension Studies of Alkyl Esters and Epoxidized Alkyl Esters Relevant to Oleochemically Based Fuel Additives. Energy & Fuels, 21 (2007), 2007-3047
[13] Brajendra K. Sharma, Kenneth M. Doll, Sevim Z. Erhan, Ester hydroxy derivatives of methyl oleate: Tribological, oxidation and low temperature properties, Bioresource Technology, 99 (2008), 7333–7340
[14] Kenesey E, Ecker A. Oxygen bond to improve the lubricity of fuel. Tribologic Schmierungstechnik, 50 (2003), 21–26
[15] Titipong I, Dalai AK, Desai P., Evaluating esters derived from mustard oil as potential diesel additives. J Am oil Chem Soc, 88 (2011), 391–402
[16] Drown DC, Harper K, Frame E. Screening vegetable oil alcohol esters as fuel lubricity enhancers. J Am Oil Chem Soc,78 (2001), 579–584
[17] Edwards H., Surface Tensions of Liquid Polyisobutylenes, Journal of Applied Polymer Science, 12 (1968), 2213-2224
[18] Legrand D.G. and Gaines G.L., The Molecular Weight Dependence of Polymer Surface Tension, Journal of Colloid and Interface Science, 31 (1969), 162-167
[19] Thompson R.B, MacDonald J.R., Chen P, Origin of change in molecular-weight dependence for polymer surface tension, Physical Review (2008), 78, 030801
[20] Sauer, B. B., and DiPaolo, N.V., Surface tension and dynamic wetting on polymers using the Wihelmy method: Applications to high molecular weights and elevated temperatures, J. Colloid Interface Sci. (1991), 144**,** 527-537.
[21] Jalbert, C., Koberstein, J. T., Yilgor, I., Gallagher, P., and Krukonis, V., Molecular weight dependence and end-group effects on the surface tension of poly(dimethylsiloxane), Macromolecules (1993), 26**,** 3069-3074
[22] G. T. Dee and B. B Sauer, The surface tension of polymer liquids, Advances in Physics, 47(1998), 161–205
[23] Selby, T.W. The Non-Newtonian Characteristics of Lubricating Oils. ASLE Transactions, 1 (1958), 68-81
[24] Covitch, M.J. Olefin Copolymer Viscosity Modifiers. Lubricant Additives, CRC Press, Boca Raton (2009), 283- 314
[25] Kinker, B.G. Polymethacrylate Viscosity Modifiers and Pour Point Depressants. Lubricant Additives, CRC Press, Boca Raton (2009), 315-337
[26] Canter, Neil, Fuel economy: The role of friction modifiers and VI improvers, Tribology & Lubrication Technology, Park Ridge, 69 (2013), 14-27
[27] De Carvalho M.J. *et al.* Lubricant viscosity and viscosity improver additive effects on diesel fuel economy, Tribology International, 43 (2010) 2298–2302
[28] Drown DC, Harper K, Frame E. Screening vegetable oil alcohol esters as fuel lubricity enhancers. J Am Oil Chem Soc, 78 (2001),579–584

Narr Francke Attempto Verlag GmbH + Co. KG

Influence of variable oxygen concentration on the accelerated ageing of liquid fuels

Chandra Kanth Kosuru
Tec4Fuels GmbH, Aachen, Germany

Simon Eiden
Tec4Fuels GmbH, Aachen, Germany

Klaus Lucka
Tec4Fuels GmbH, Aachen, Germany

Summary

Temperature has always been the vital parameter in case of fuel ageing. In the accelerated ageing method, liquid fuels are subjected to higher temperatures with compressed gas as the atmosphere, to induce stress and accelerate the thermal or thermo-oxidative process leading to a fast-ageing process. In this method, the heating rate, cooling rate and the oxygen concentration (in the gas phase) have always been constant with variable temperature and ageing time; depending on the fuel quality. In the current topic, a middle distillate fuel will be subjected to accelerated ageing with variable oxygen concentration in the gas phase and keeping the temperature and ageing time constant. The impact of variable oxygen concentration on the auto-oxidation will be discussed with the help of some initial observations. Furthermore, the impact of this oxygen variations on the physio-chemical properties of the fuel and therefore the fuel stability itself will also be discussed.

1. Introduction

Ageing of liquid fuel has always been of prime importance in estimating their quality over extended periods of time. The degradation of liquid hydrocarbons due to oxidation with the oxygen, from atmosphere or from the interacted gas medium, is called as ageing. In general, these ageing reactions take places over the course of months to years depending on the fuel quality and the surrounding atmospheric or ambient conditions. The common oxidation reactions are very well described by Biernat [1] with radical chain reactions. The critical part of this oxidation lies on the initiation step where the separation of the allyl radical starts [1, 2]. This required the longer time depending on different factors, where the following steps are in general very fast and self-accelerating chain reactions [1, 3]. So, the initiation step of the reaction is considered as the time taking step, also known as induction time, required to start the ageing and this in turn represented as the stability time for estimating the quality of the fuel over longer periods of time [2].
Accelerated ageing methods have helped in this regard, to analyze the ageing behavior of fuel over longer periods in short amount of time [2, 4]. The principal idea behind these methods is to induce stress on the fuel and force the oxidation reactions [1, 2, 5]. For this the medium is provided with abundant oxygen and heated to higher temperatures to provide the required activation energy for the reaction to start. After the initiation step the reaction flow is self-sustaining and fast chain reactions [2, 4]. Thus, the fuel can be aged in a short amount of time, which in turn takes months, to analyze the long-term behavior. The application of such methods for the novel fuels such as E-fuels could help in estimating their long-term behavior in the existing infrastructure and also implement necessary changes. They can be on the fuel side, by adding Additives or from the infrastructure side such as sealing materials, etc [1, 3].
Current paper discusses one of the typical accelerated ageing methods and its applications. This paper covers the unknown territories of the method such as

1. The impact of variable heating and cooling rates on the ageing method and ageing phenomenon
2. The impact of variable oxygen content available for the ageing of liquid fuels.

The idea behind the current investigation is to understand the detailed impact of different parameters on the fuel ageing and also implying towards the criticalities of the method itself.

Narr Francke Attempto Verlag GmbH + Co. KG

2. Test setup

Current section explains the test setup that is developed at Tec4Fuels. Figure 1 shows the P&ID diagram of the test setup.

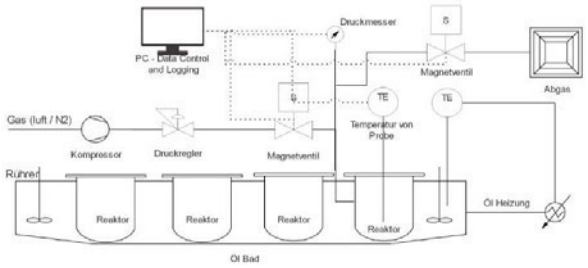

Figure 1: P&ID of the accelerated ageing test setup

The test setup consists of an oil bath, in which the reactors can be placed for heating. The bath can accommodate 8 reactors simultaneously. The bath is equipped with a heating coil heater which is used to heat up the bath to the required temperature. The Stirrers at each end of the bath and the heating coil pump in the middle of the bath helps to maintain the bath temperature through out test period. The fuel sample will be placed in a clean reactor and placed in the bath. The reactor is a 1.5 litre steel vessel to which a thermocouple, pressure sensor and a magnetic valve are attached. The pressure inside the reactor is limited to 10 bar due to the sensitivity of the pressure sensor. The reactors are compatible with Diesel, Gasoline and similar type of fuels and further cooling fluids were also tested. These reactors are filled with the required amount of fuel, 500 ml to 1 litre and then filled with required gas medium (Air, Nitrogen or Oxygen). The reactors can be placed inside the bath and the test times are flexible depending upon the requirement or fluid quality. The temperature settings are also flexible from 60 °C to 150 °C, depending on the fluid type. As the bath can accommodate 8 reactors, the fluids that can be used are flexible from 8 different type of fluids to same fluid for reproducibility tests. After the experiment, the reactors are removed from the bath, cooled down and de-pressurised before opening the cap and collecting the sample. As the temperature conditions, reactor volumes are the same, the experiments are highly reproducible. The pressure curve determines the stability of the fluid sample. The consumption of oxygen by the fluid for the oxidation reaction is reciprocated by a pressure drop due to the reduction of oxygen partial pressure. Thus, the time required for the pressure drop to occur indicate the stability of the fluid sample also known as the Induction time. The comparison between the induction times of different fluid samples indicates the comparison of their stability. The fluid samples are also analysed before and after the ageing experiment, in order to determine their degradation over time. Figure 2 indicate a sample pressure curve from the ageing of standard heating oil.

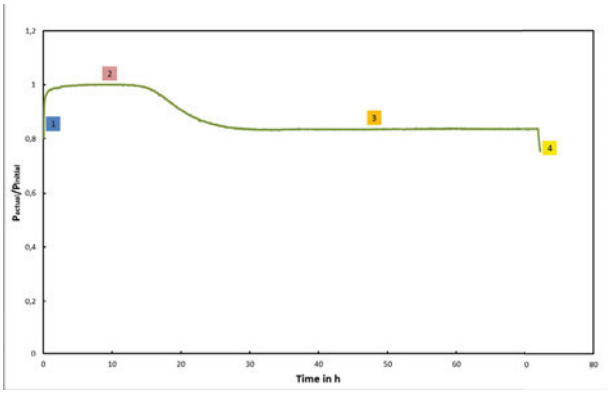

Figure 2: Sample pressure curve of a typical BigOxy test. The pressure drop is observed between phases 2 and 3.

3. Test Matrix

In the current investigation, a standard heating oil was used according to DIN 51603-1. The current test matrix consists of two different types of experiments a) with variable heat up rates and b) varying the oxygen concentration available for the ageing method. In the first case, the heating rate can be varied by placing the reactor in the bath at different times. In this case, one reactor was placed before the heat up of the oil bath and heated up together, while the second method is to place the reactor after the bath has arrive the required temperature. The former method is called as ramp heating while the second method is known as fast heating. The pressure and temperature of both the reactors were kept constant at 5 bar and 105 °C.

Second type of experiments involves varying the oxygen concentration. This was achieved by changing the gas pressure inside the reactor. The gaseous atmosphere in the current experiments was air. With varying the air pressure inside the reactor, the partial pressure of oxygen is also varied. Thus, different reactors are filled with different pressure from 1.2 bar, 2 bar, 3 bar and 5 bar. The temperature of the fuel is kemp content in both the test methods at 105 °C. this temperature was determined to be the idle temperature setting for Diesel like fuels by Koch, in his investigations.

4. Analysis

Figure 3 indicates the pressure curves of the variable heating rate experiment. The experiment was repeated several times to observe the repeatability of the test. From the pressure curves it is evident that the change of heating rate has no impact on the induction time. This was also proved by comparing the analytical data of the fuel sample. This means that the fuel quality was the same in the heat up cases after the ageing for 72 hours. If the curves are observed closely the ramp heating suggests that it has observed the heat almost 30 minutes longer than

Narr Francke Attempto Verlag GmbH + Co. KG

the fast-heating case. But it has no impact on the overall stability or the ageing of the fuel. This phenomenon can be explained by supporting the argument by Koch in his ageing method investigations. "The temperature has a big impact on the ageing of the fuels. Also, until a certain temperature limit, the ageing is, in general, slow due to the lack of required activation energy and the rate might increase rapidly after certain temperature limit". Since in the ramp heating case, the fuel has observed lower temperature for almost 15 minutes and only a few minutes of higher temperature relative to fast heating, the impact on the ageing is negligible. Thus, the heating rate in general can be neglected in the ageing method unless the heating rate is too slow and takes much longer time to reach the maximum temperature point. So, fast heating method is generally recommended to keep the method highly repeatable and avoid any additional impacts.

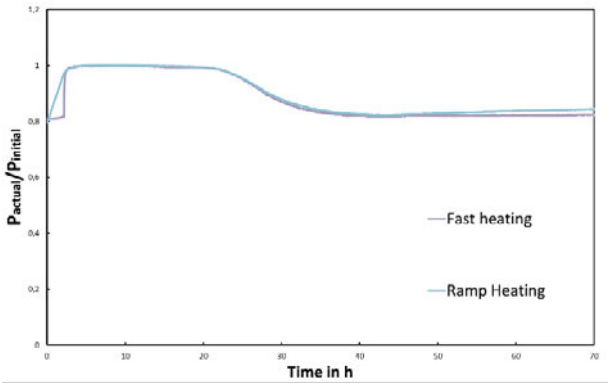

Figure 3: Pressure curves with different heat up rates

Figure 4 shows the pressure curves at different initial gas pressure in the atmosphere. The first indication is that the induction times have been the same in all the cases. This can be explained by implying that the activation energy required in all the cases is similar irrespective of the oxygen concentration. So, the initiation step has started at the same point in all the four cases. But a close observation has shown that the pressure drop is different in different cases.

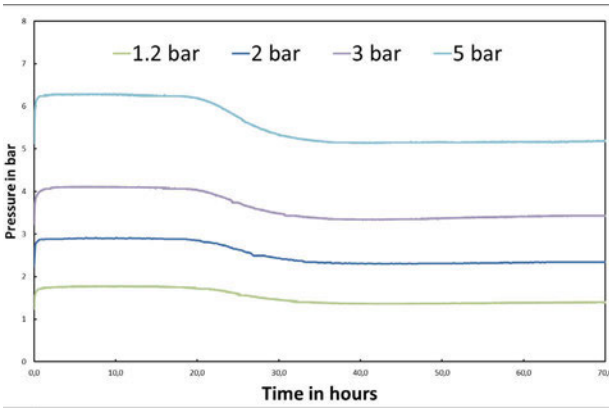

Figure 4: Pressure curves with variable oxygen concentration

In case of 1.2 bar pressure reactor the pressure drop is 20 % imply that all the oxygen from the reactor gas volume is absorbed, while in case of 5 bar the absorption is limited. In terms of quantity that has been absorbed, in 5 bar pressurised reactor, more oxygen is consumed compared to the 1.2 bar reactor. In the following table the absorbed oxygen quantities were mentioned. Thus, the variable oxygen consumption has shown a direct correlation with the acid content and water content of the fuel sample after ageing. The higher the amount of oxygen consumed the higher the water and acid contents. Thus, implies that by controlling oxygen content in the gas phase the ageing method can be controlled. Implying that the atmosphere where the fuel is stored in the real time is also very important along with the temperatures it is exposed to.

Table 1: Comparison of Acid content and water content with the rate of oxygen consumption (% of oxygen consumed from the available gas phase)

		Acid content in mgKOH/g	Water content mg/kg	% of O2 consumed
MD1	Fresh	0,006	95,65	
MD1	1,2Bar	0,245	133,2	100%
MD1	2 Bar	0,266	110,3	95%
MD1	3 Bar	0,446	142,9	88%
MD1	5 Bar	0,796	166,8	54%

5. Conclusion and outlook

In the current paper two variable that impact the ageing methodology are briefly discussed. The heating rate has low to no impact on the complete ageing method until the heating rate is not too slow. Also, the oxygen concentration available for the ageing method has a direct impact on the fuel quality after the ageing method. These analyses show a respectable argument on the above-mentioned statements, but a further investigation is still due considering different additional variable that may impact the degradation process. For example, the presence of different oxygen concentration in the gas phase but with similar gas pressure inside the reactor. This could lead to different diffusion rates and can lead to more oxygen consumption and different ageing products. These cases are still under investigation. Similarly, the variable cooling method, and the impact of thermal ageing alone after the pressure drop are also few important variables that must be investigated.

Narr Francke Attempto Verlag GmbH + Co. KG

References

[1] Biernat K (Ed.). *Storage Stability of Fuels*. InTech (2015).

[2] Chandra Kanth Kosuru, Natalia Eurich, Simon Eiden (Ed.). *Development of a Test method for Accelerated ageing of Gasoline fuels* (2019).

[3] Owczuk M, Kołodziejczyk K. Liquid Fuel Ageing Processes in Long-term Storage Conditions. In: Biernat K (Ed.). *Storage Stability of Fuels*. InTech (2015).

[4] Koch W, Eiden S, Feldhoff S, Diarra D. *Entwicklung Einer Neuen Prüfmethode Zur Bewertung Der Stabilität Von Heizölen Mit Biogenen Anteilen: Winfried Koch, Simon Eiden, Sebastian Feldhoff, David Diarra*. Deutsche Wissenschaftliche Gesellschaft für Erdöl, Hamburg (2017).

[5] Black S, Ferrell JR. Accelerated aging of fast pyrolysis bio-oil: a new method based on carbonyl titration. *RSC Adv.* 10(17), 10046–10054 (2020).

Narr Francke Attempto Verlag GmbH + Co. KG

Improving Hydrogenated Vegetable Oils Green Credentials and Value to Producers and End Users

Dhanesh Goberdhan and Robin Hunt
Infineum, UK Ltd

Summary

Hydrogenated vegetable oils (HVOs) are a sustainable alternative to diesel fuel. They are described as both fossil-free and Fatty Acid Methyl Ester (FAME) free fuels. HVOs are paraffinic renewable diesel fuels produced from sustainable raw materials. In addition to their green credits, they have superior cetane and oxidation stability properties over conventional diesel and FAME. These advantages with their green credentials have resulted in a growing market share as both a biofuel and biofuel component.
HVOs are produced by isomerisation processes of a range of different vegetable oil sources, such as rapeseed, palm and soya oil, or even waste and residual fat fractions.
In this paper we demonstrate how the appropriate use of cold flow additive technology can further enhance the opportunities for HVO by:

– Increasing the flexibility of production sources. That is the range of raw materials, and processing to produce HVOs.
– Reducing the production costs (and energy used) by reducing the required level of isomerisation to meet low temperature requirements.
– Increasing flexibility for end users, by increasing the range of different types and sources of HVOs that meet specification requirements.

This provides producers and users of HVOs with additional opportunities to optimise the value of their operations.

1. Introduction:

There has been increasing interest in the production of chemicals and fuels from biomass, from renewable sources, driven by the desire to decarbonise the transport sector due to global concerns towards greenhouse gas emission. This is supported by Governmental and European Union policy. For example, in the Renewable Energy Directive, RED [1] and RED II [2] directives on the promotion of the use of energy from renewable sources.
Hydrogenated Vegetable Oil (HVO) is a fast-growing next second-generation fuel with production plants being built globally. HVO is created through the hydrogen treatment of a renewable oil, which can be from a vegetable source. For example, Rapeseed, Soya and Palm Oil. Despite it being referred to as a "hydrogenated vegetable oil" it can also be produced from common non-vegetable sources, e.g., Tallow or used kitchen oil [3] It is referred to as a next generation biofuel as it is believed to be an advancement on first generation biofuels based on Fatty Acid Methyl Esters (FAME) [4].

The advantage of HVOs over FAME is that first-generation biofuels are derived from crops that potentially compete with food production. In addition, HVOs have better cetane number than fossil fuel derived diesel and better oxidative stability properties than FAME [5].

2. Chemistry of HVOs

HVOs can be produced by one or more step catalytic hydrotreating of different triglycerides containing vegetable oils. This causes the complicated hydrocarbons to be broken down into simpler straight chain alkanes. with typical production of a mixture of n-alkanes, namely $C_{15}H_{32}$, $C_{16}H_{34}$, $C_{17}H_{36}$ and $C_{18}H_{38}$ [6]. A further step is then carried out to isomerise the fuel and convert more of the straight chain alkanes into branched iso-alkanes. This is called isomerisation. The relative ratio of the n-alkanes will depend on the source of the vegetable oils.

Narr Francke Attempto Verlag GmbH + Co. KG

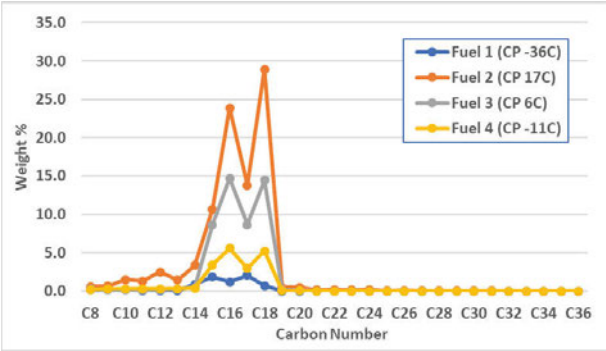

Fig.1: Gas chromatogram (GC) of 4 HVO fuels with differing Cloud Points (CP) showing the n-alkane distribution. Fuel characteristics are shown in Appendix 1.

Figure 1 shows the n-alkane distribution of how the n-alkane distribution varies for four different HVO samples. The Cloud Point (CP) of the fuel is determined by the level of isomerisation of the samples. The CP is the temperature where the precipitating wax can be visibly observed [10]. From the n-alkane analysis in Figure 1, the lower levels of isomerisation, Fuel 2 and Fuel 3, correspond to higher level of C16/C18 n-alkanes. Whereas high levels of isomerisation, Fuel 1 and Fuel 4, have lower levels C16/C18 n-alkanes.

3. Cold flow issues

Diesel fuel derived from fossil fuels also contain n-alkanes. At low temperatures the n-alkanes precipitates as thin rhombohedral plates (Figure 2a). These crystals can block fuel filters designed to protect diesel injectors and pumps. This would result in fuel starvation to the engine, leading to a loss of power and/or stalling, and even potential failure of the engine to start. [7]

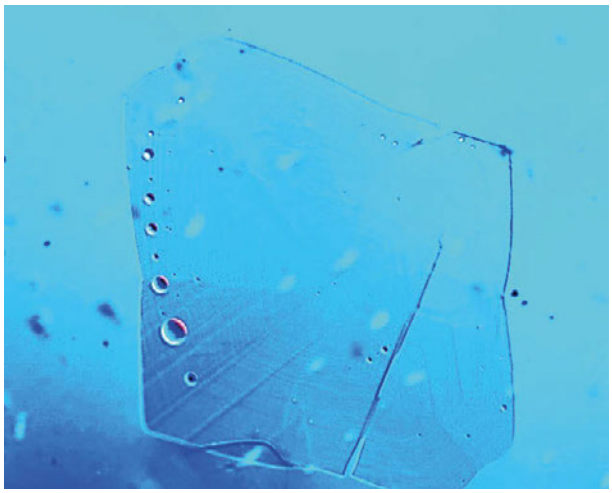

Fig 2a: Photomicrograph of wax crystal precipitated from untreated diesel fuel.

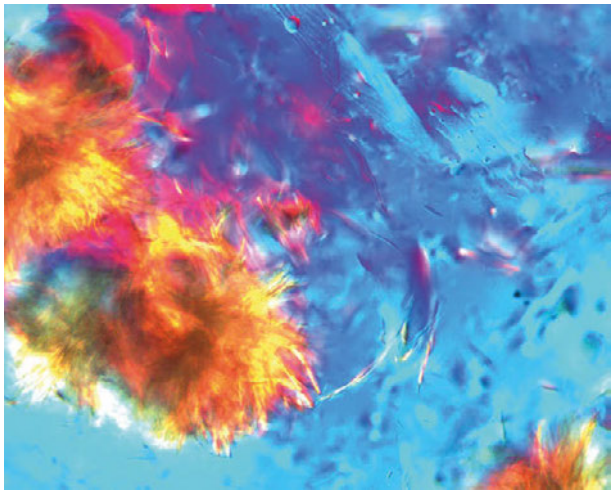

Fig 2b: Photomicrograph of wax crystal precipitated from untreated HVO.

In contrast, the wax that precipitates from HVO, Figure 2b, shows uncontrolled crystal growth. In the case of this HVO, the wax precipitates too rapidly to allow the formation of the flat planar crystal arising from the slower wax crystal growth seen in Figure 2a.

4. Low temperature Properties of HVOs

The low temperature properties of hydrocarbon fuels such as diesel, FAME and HVOs can be undesirable if wax precipitates at too high a temperature. This is governed by the distribution of the long-chain n-alkanes within the fuel. The high molecular weight n-alkanes become supersaturated during cooling, which results in their precipitation. These straight chain alkanes form the waxes that will crystallise out of solution and cause the filter blocking issues. [8]
HVO can be produced from a variety of different feedstocks. HVOs from different sources will have different distributions of n-alkanes. The most prominent change is that the finished HVO will have different ratios of C16 and C18 carbon chains.

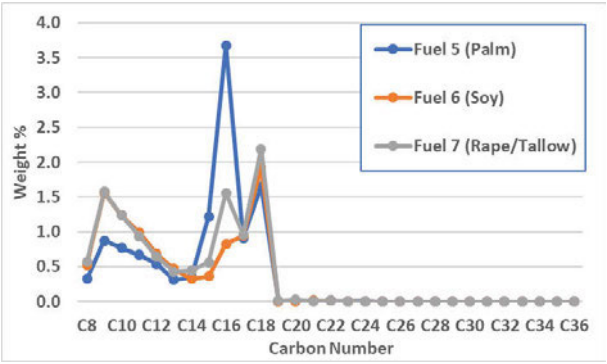

Fig. 3: GC trace showing the n-alkane distribution of HVOs produced from different sources.

Narr Francke Attempto Verlag GmbH + Co. KG

The different base oils produce a different ratio of C16 and C18 n-alkanes depending on the distribution of fatty acids in the original oil. However, this seems to have little effect on the base fuel characteristics, CP and CFPP (See Appendix 1). The CP seemingly dominated by the total level of the n-alkane rather than the distribution of n-alkanes (Figure 4).

5. Potential solutions low temperature issues

5.1 Isomerisation

In the production of HVOs the isomerisation step has a significant effect on the low temperature properties of the HVO [9]. The isomerisation step converts the long n-alkanes into more branched structures which have better solubility and would precipitate as wax at lower temperatures.

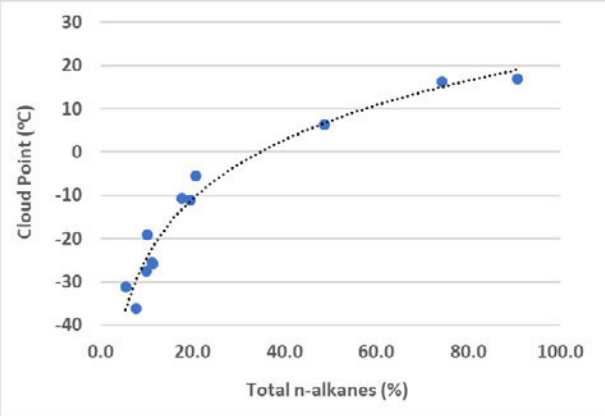

Fig 4: Graph showing a variety of HVO samples, comparing the base cloud with the total n-alkanes, derived from GC analysis.

The CP of the HVO decreases with increasing levels of isomerisation of the total n-alkane content, increasing levels of isomerisation lowers the base cold flow properties of the finished HVO. From the data in Figure 3 and 4, the level of isomerisation is more significant than the source of the HVO. Whilst isomerisation can reduce low temperature issues by reducing the amount of n-alkane wax, it is an energy intensive process and alternative solutions may offer more value to refiners.

5.2 Dilution BX/ Co-processing

Use of HVOs as a blend component is also an alternative route to improve the sustainability credits fossil diesel. HVO can be combined with diesel and acts as a bio component. This can be done in two ways. One, by blending with the distillate diesel, allowing close control over the level of HVO being added. Two, by co-processing. Co-processing involves the addition of the renewable oil to the diesel stream in the refinery prior to the standard hydrotreating required to reduce sulphur fuel levels. The blend of the renewable oil and gas oil components are then hydrotreated together, resulting in a similar product to a fossil diesel blended with an HVO. This results in less control over the HVO created, but removes some blending and hydrogenation complexity.
The high variation of characteristics from blending HVO into diesel can results in a fuel with a range of low temperature properties. The differences in the finished fuel will be due to both the variation in the HVO, from the level of isomerisation and the variation in the source oils, as well as due to the variation in the fossil diesel characteristics. The differences in the final fuel characteristics will influence the low temperature properties for the finished blend.

5.3 Use of additive technology to achieve low temperature targets in HVOs and HVO blends

Cold flow additives can be used to treat both pure HVOs and blends of HVOs in fossil fuel.

5.3.1 Cold flow additives for pure HVO:

As we have seen, the cold flow attributes of an HVO sample depend heavily on the level of isomerisation applied. An alternative methodology to achieving the required low temperature performance targets is to use cold flow additives. This would enable the use of a less isomerised HVO in the blend. Cold flow additives can have a significant effect, allowing refiners to achieve an improvement to CFPP performance of more than 5°C when the correct additive is used. In a pure HVO, because the fuel is highly paraffinic the fuels will be difficult to treat due to the high level of wax precipitation. However, additive treatability improves with higher levels of isomerisation (see Figure 5).

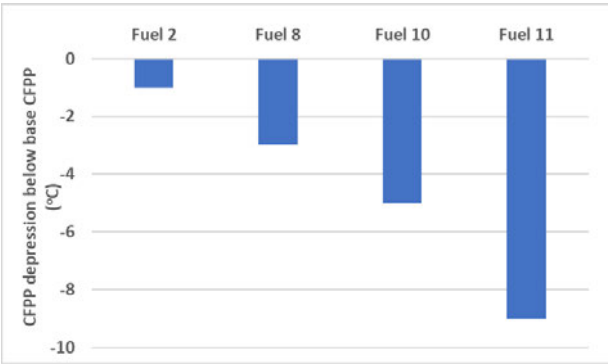

Fig 5: Bar chart representing depression of CFPP when treated with 5000 ppm of cold flow additive for HVOs of different CP. Fuel 2 CP is 17 °C; Fuel 8 CP is-6°C; Fuel 10 CP is -19 °C and Fuel 11 CP is -31 °C

Even though the source of the raw material has little effect on base characteristics it can have an impact on how the

Narr Francke Attempto Verlag GmbH + Co. KG

fuel responds to additives. This can result in differing additives needs for HVOs produced with different base oils. This adds an extra layer of complexity to additive formulation (see Figure 6).

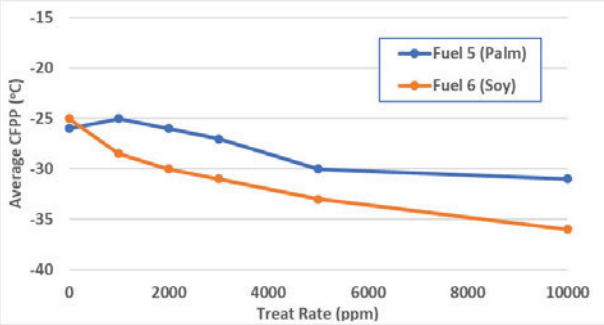

Fig.6: CFPP treat curve for an additive technology in two HVOs with similar CPs but different vegetable oil sources

Figure 6 shows how the same additive technology gives different levels of additive response in HVOs with similar CP and untreated CFPPs. Fuel 6 which shows a greater level of response than Fuel 5. 2000 ppm of additive is required to get a 5 degree improvement in CFPP in Fuel 6. However, Fuel 5 requires 10,000 ppm of the same cold flow additive. In this case, the source of the base oil can have a significant impact on additive response of the finished HVO.

5.3.2 Cold flow additives for BX/Blended/co-processed HVO

Additive selection is highly dependent on the overall n-alkane content of the finished fuel. This can act as a limiting factor when deciding how much and which kind of HVO can be added into a blend. When the original diesel already has a high n-alkane content, this can limit the level of HVO quantity and quality that can be added.

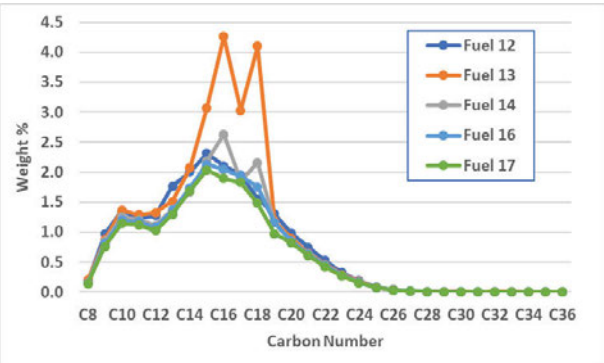

Fig 7: Graph showing the GC n-alkane plots of different HVOs blended into a gasoil sample, Fuel 12, at 10%. Details of Fuel blends is shown in Appendix 1.

Figure 7, shows that the addition of different HVOs with different CPs, blended at 10% into diesel impact the n-alkane distribution. The different HVOs have a range of CPs due to different levels of isomerisation. As seen in Section 5.1, the greater the level of isomerisation, the lower the CP and the lower the level of n-alkanes. Thus, the n-alkane distribution of the fuel blends is most perturbed by the addition of the higher CP HVOs. That is, Fuel 13, which is a blend of HVO with a CP 17 °C and Fuel 14, with a HVO with a CP of -6 °C, show the greatest difference compared to those fuels with lower CPs. That is, Fuel 16 with a HVO with CP of -19 °C and Fuel 17 with a HVO of -31 °C.

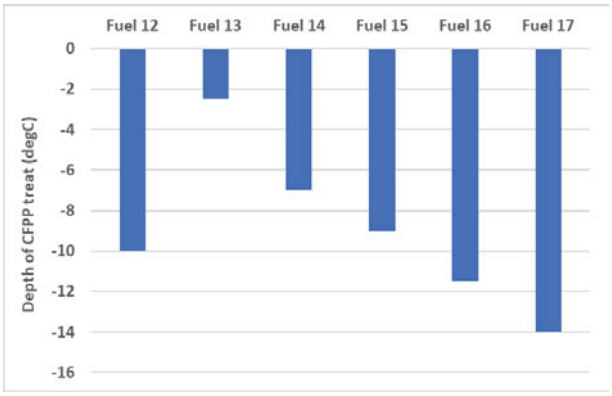

Fig 8: Bar chart of CFPP decrease from base CFPP, for a variety of different HVO/diesel blends, treated with cold flow at 500 ppm. The fuel characteristics are shown in Appendix 1.

As seen in Figure 8, increasing the levels of HVO isomerisation can improve CFPP response within a blend, but CFPP of low level isomerised HVO can still be improved by specialist additives.
The correct additive selection is crucial for optimum low temperature performance. Different additive technologies providing optimum performance depending on the different levels of n-alkane in the final fuel blend. With high levels of isomerised HVOs performing in a similar fashion to a standard diesel. As the level of isomerisation, and hence n-alkane levels from the HVO increase, more advanced chemistries are needed to achieve an adequate level of performance.

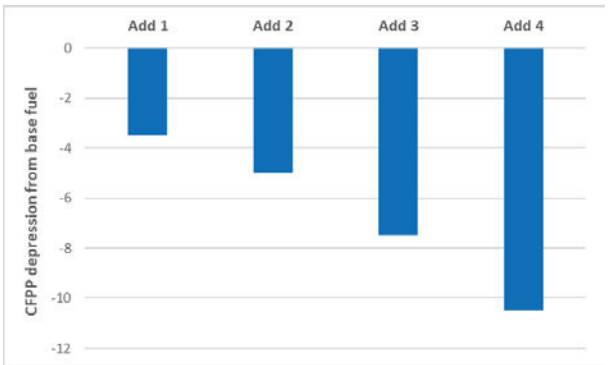

Fig 9: Chart showing the CFPP decrease from base CFPP, for a variety of different additives at the same treat rate.

Narr Francke Attempto Verlag GmbH + Co. KG

Figure 9 shows the sensitivity of the fuel blend to different cold flow additive technologies. Additive 4 gives the greatest CFPP depression. Dependant on the HVO characteristics the choice of cold flow additive selection is crucial

6. Discussion

A key property in the utilisation of HVOs is their low temperature properties. As HVOs are produced by isomerisation, you can choose to use a high level of isomerisation to be generate a HVO with the required low temperature properties by isomerising the waxes in the HVO to give the required low temperature properties. However, HVO manufacturing units may only be set up to produce one level of isomerisation, and thus this solution could lack flexibility when supplying markets with a range of different low temperature requirements. This can result in an over specified product for a particular market.

An alternative methodology to overcoming the low temperature issue and also an alternative way of deploying HVOs would be to use the HVO as a blend component. That is, to produce a BX fuel by blending with an appropriate middle distillate and at an appropriate level of HVO to produce a fuel of the required low temperature properties. However, the properties of distillate fuels and their low temperature properties can be highly varied themselves. So that it is not always possible to both predict and obtain the desired cold flow properties by simply blending the two together. This is also even more of a potential issue when producing a co-processed HVO, where there is potentially even more issues in being able to tailor the production to specific cold flow properties consistently. The use of cold flow additives allows the use of HVOs which have lower levels of isomerisation to be used more flexibly in different markets. This has the additional benefit of reducing the isomerisation costs. In addition, it can more flexibly deal with HVOs produced from a variety of different sources.

7. Conclusion

Hydrogenated vegetable oils (HVOs) are a sustainable alternative to diesel fuel. They are paraffinic renewable diesel fuels produced from sustainable raw materials. Their green credentials have resulted in a growing market share as both a biofuel and biofuel component.

A key property in the utilisation of HVOs is their low temperature properties. These low temperature properties are governed by the balance of iso and n-alkanes that are present in the HVO. These levels are governed by the level of isomerisation in production and also the source of the material used to produce the HVO. Different methodologies are available to improve low temperature properties of HVOs and HVO containing distillate fuels.

This paper identifies how the appropriate use of cold flow additive technology can further enhance the opportunities and value of using HVOs by

1. Increasing the flexibility of production sources. That is the range of raw materials, and processing to produce HVOs.
2. Reducing the production costs (and be greener by using less energy) by reducing the required level of isomerisation and still meet low temperature requirements.
3. Increasing flexibility for end users, by increasing the range of different types and sources of HVOs that meet specification requirements.

This provides producers and users of HVOs with additional opportunities to optimise the value of their operations.

References

[1] “An overview of biofuel policies across the world” Energy Policy,38 (11) 2010, 6977-698

[2] EU Science Hub, “Reference Regulatory Framework” https://ec.europa.eu/jrc/en/jec/reference-regulatory-framework

[3] Cremonez, P. A., Teleken, J.G., and Thompson Weiser Meier, T.W., “Potential of green diesel to complement the Brazilian energy production”, Energy Fuels 35(1) 2021, 176–186

[4] https://www.icis.com/explore/resources/news/2019/11/28/10449207/insight-rise-of-hvo-to-be-the-downfall-of-traditional-biodiesel-in-europe.

[5] Neste Oil, “Hydrogenated vegetable oil (HVO)-premium renewable biofuel for diesel engines”, February 2004

[6] Liu Y., Sotelo R., Boyás, Murata K., Minowa T., and Sakanishi K., “Hydrotreatment of vegetable oils to produce bio-hydrogenated diesel and liquefied petroleum gas fuel over catalysts containing sulfided Ni–Mo and solid acids” Energy Fuels, 25(10) (2011), 4675-4685

[7] Brown G.I., Lehmann E.W. and K. Lewtas., “Evolution of Diesel Fuel Cold Flow – The Next Frontier” SAE Technical Paper 890031

[8] Tang X., Corzo D.M.C., Lai X., Roberts K.J., Dowding P. and More I., “Solubility and crystallisability of the ternary system: Hexadecane and octadecane representative in fuel solvents” Fuel 226 (15) Aug 2018, 665-664

[9] Aatola H., Larmi M., Sarjovaara T and Mikkonen S., “Hydrotreated Vegetable Oil (HVO) as a Renewable Diesel Fuel: Trade-off between NOx, Particulate Emission, and Fuel Consumption of a Heavy Duty” Engine SAE Technical Paper 2008-01-2500

[10] Holder, G.A. and Winkler, J., “Wax crystallisation from diesel fuels. Part 1. Cloud and pour pheno-

Narr Francke Attempto Verlag GmbH + Co. KG

mena exhibited by solutions of binary n-paraffin mixtures", Journal of the institute of petroleum, 51(499) 1965, 228-252

Definitions, acronyms and abbreviations

BX Fossil fuel with X% biofuel component
CFPP Cold filter Plugging Point test
CP Cloud Point
FAME Fatty acid methyl ester
GC Gas Chromatogram
HVO Hydrogenated Vegetable Oil

Appendix 1
HVO and fuel blend characteristics
1a HVO characteristics

Refinery ID	Fuel 1	Fuel 2	Fuel 3	Fuel 4	Fuel 5	Fuel 6	Fuel 7	Fuel 8	Fuel 9	Fuel 10	Fuel 11
Fuel type	HVO	HVO	HVO	HVO	Palm Base HVO	Soy Base HVO	Rape / Tallow Base HVO	HVO	HVO	HVO	HVO
Density Kg/m3		782	780	780	775	770	768	776	782	780	780
Cloud Point °C	-36	17	6	-11	-26	-28	-26	-6	-11	-19	-31
CFPP °C	-41	14	0	-13	-26	-25	-24	-9	-12	-22	-34
Cetane Index (CI)		94	95	92	88	85	84	91	96	94	94
N_Alkanes											
C8	0.169	0.620	0.264	0.197	0.323	0.530	0.571	0.211	0.154	0.378	0.115
C9	0.182	0.680	0.178	0.300	0.877	1.557	1.579	0.360	0.250	0.482	0.185
C10	0.149	1.531	0.147	0.327	0.772	1.240	1.244	0.348	0.294	0.411	0.196
C11	0.115	1.325	0.144	0.309	0.672	0.990	0.940	0.333	0.251	0.296	0.156
C12	0.103	2.497	0.204	0.292	0.543	0.684	0.645	0.344	0.225	0.214	0.142
C13	0.075	1.472	0.294	0.307	0.309	0.474	0.430	0.190	0.342	0.254	0.168
C14	0.887	3.401	0.491	0.380	0.346	0.320	0.445	0.261	0.528	0.462	0.175
C15	1.867	10.680	8.683	3.408	1.222	0.362	0.562	1.375	1.879	0.945	0.632
C16	1.191	23.868	14.737	5.583	3.682	0.823	1.556	7.457	3.160	1.626	1.023
C17	2.087	13.820	8.646	2.977	0.915	0.946	0.961	1.630	4.035	2.323	1.341
C18	0.716	28.903	14.474	5.250	1.656	1.928	2.192	7.909	6.225	2.493	1.186
C19	0.015	0.510	0.163	0.075	0.008	0.007	0.012	0.019	0.066	0.009	0.034
C20	0.026	0.518	0.124	0.073	0.013	0.010	0.024	0.068	0.053	0.023	0.032
C21	0.029	0.132	0.001	0.023	0.012	0.010	0.009	0.002	0.011	0.019	0.013
C22	0.033	0.185	0.025	0.021	0.014	0.013	0.011	0.021	0.013	0.043	0.008
C23	0.029	0.147	0.019	0.010	0.009	0.008	0.008	0.013	0.011	0.045	0.004
C24	0.020	0.179	0.021	0.008	0.004	0.003	0.004	0.022	0.017	0.049	0.002
C25	0.009	0.056	0.007	0.003	0.002	0.001	0.004	0.030	0.012	0.075	0.002
C26	0.005	0.087	0.010	0.003	0.001	0.000	0.000	0.025	0.009	0.019	0.002
C27	0.001	0.028	0.002	0.001	0.001	0.000	0.000	0.017	0.005	0.010	0.001
C28	0.001	0.033	0.001	0.000	0.001	0.000	0.000	0.007	0.002	0.001	0.001
C29	0.006	0.034	0.002	0.000	0.001	0.000	0.000	0.002	0.001	0.001	0.000
C30	0.001	0.044	0.001	0.001	0.000	0.000	0.000	0.003	0.002	0.000	0.000
C31	0.002	0.047	0.003		0.000	0.000	0.000	0.003	0.001	0.002	0.000
C32	0.002	0.004	0.000		0.000	0.000	0.000	0.000	0.003	0.003	0.000
C33	0.000	0.002	0.002		0.000	0.000	0.000	0.003	0.000	0.001	0.000
C34		0.001			0.001	0.000	0.000	0.001	0.003	0.001	0.001
C35		0.003			0.000	0.000	0.000	0.000	0.000	0.001	0.000
C36					0.000	0.000	0.000	0.000	0.000	0.004	0.000
Total n-alkanes	7.7	90.8	48.6	19.5	11.4	9.9	11.2	20.7	17.6	10.2	5.4

Narr Francke Attempto Verlag GmbH + Co. KG

1b Fuel blend characteristics

Refinery ID	Fuel 12	Fuel 13	Fuel 14	Fuel 15	Fuel 16	Fuel 17
Fuel type	EN590 Diesel Fuel	90% Fuel 12 + 10% Fuel 2	90% Fuel 12 + 10% Fuel 8	90% Fuel 12 + 10% Fuel 9	90% Fuel 12 + 10% Fuel 10	90% Fuel 12 + 10% Fuel 11
Density Kg/m3	824					
Cloud Point °C	-6	-5	-7	-7	-6	-7
CFPP °C	-7	-11	-9	-10	-9	-7
Sulphur %	0.0008					
Cetane Index (CI)	58					
N_Alkanes						
C8	0.172	0.199	0.157	0.068	0.151	0.142
C9	0.967	0.875	0.845	0.811	0.807	0.762
C10	1.351	1.366	1.253	1.214	1.199	1.144
C11	1.240	1.291	1.202	1.177	1.168	1.120
C12	1.277	1.323	1.111	1.083	1.073	1.025
C13	1.767	1.511	1.380	1.382	1.361	1.301
C14	2.001	2.068	1.669	1.776	1.743	1.685
C15	2.313	3.073	2.188	2.237	2.128	2.039
C16	2.104	4.264	2.628	2.220	2.046	1.898
C17	1.956	3.031	1.857	2.122	1.935	1.831
C18	1.550	4.099	2.158	1.986	1.754	1.479
C19	1.305	1.180	1.153	1.164	1.156	0.975
C20	0.981	0.895	0.856	0.855	0.849	0.823
C21	0.747	0.645	0.634	0.629	0.633	0.612
C22	0.527	0.467	0.451	0.438	0.442	0.419
C23	0.324	0.290	0.279	0.274	0.278	0.266
C24	0.189	0.180	0.170	0.163	0.164	0.157
C25	0.088	0.076	0.078	0.077	0.076	0.071
C26	0.041	0.043	0.039	0.037	0.036	0.034
C27	0.016	0.014	0.021	0.016	0.015	0.014
C28	0.007	0.007	0.009	0.008	0.008	0.006
C29	0.003	0.007	0.004	0.003	0.003	0.003
C30	0.001	0.007	0.002	0.002	0.001	0.000
C31	0.001	0.001	0.001	0.001	0.000	0.001
C32		0.004	0.000	0.000	0.001	0.000
C33		0.004	0.000	0.000	0.000	0.000
C34		0.002	0.000	0.000	0.000	0.001
C35		0.000	0.001	0.001	0.000	0.000
C36		0.000	0.001	0.001	0.002	0.000
Total n-alkanes	20.9	26.9	20.1	19.7	19.0	17.8

Narr Francke Attempto Verlag GmbH + Co. KG

Enhancement of engine lifetime with premium fuel

Marcella Frauscher
AC2T research GmbH, Wiener Neustadt, Austria

Adam Agocs
AC2T research GmbH, Wiener Neustadt, Austria

Thomas Wopelka
AC2T research GmbH, Wiener Neustadt, Austria

Andjelka Ristic
AC2T research GmbH, Wiener Neustadt, Austria

Florian Holub
OMV Downstream GmbH, Vienna, Austria

Wolfgang Payer
OMV Downstream GmbH, Vienna, Austria

Summary

In order to evaluate the impact of premium fuels containing elevated levels of friction modifier (FM) additives regarding wear, engine test bench investigations were performed with a conventional fuel and with a premium fuel containing FM. All tests utilised an artificially aged engine oil that simulated the condition of a reference used oil after 25,000 km of operation. Thus, a large-scale artificial ageing of 180 L engine oil was carried out with oil condition monitoring by means of conventional parameters and high-resolution mass spectrometry. Oil analysis confirmed a comparable condition of the artificially aged oil with the reference used oil. Additionally, SRV® tribometer experiments with the artificially aged oil proved a significantly higher coefficient of friction compared to the fresh oil but similar tribological performance compared to the reference used oil. During the engine bench tests, wear was monitored via wear particle concentration in the oil by means of optical emission spectroscopy as well as by radio isotope concentration method with activated piston rings. Both analytical methods found a significantly lower wear in the engine bench test operated with premium fuel with FM compared to tests with conventional fuel. Moreover, subsequent used oil analysis from bench test oil samples by mass spectrometry showed a transfer of the FM from the fuel into the engine oil. In particular, an increase in FM with proceeding engine operation time was observed. Hence, the usage of premium fuels may lead to enhanced engine lifetime.

1. Introduction

In times of high claims towards sustainability the possibility to enhance lifetime of combustion engines by boosting aged engine oil via high-quality fuels with elevated levels of additives such as FM is a topic of high interest in the automotive and fuel sector. Within this study, a comprehensive approach was chosen comprising the artificial generation of an engine oil commercially available but in a well-defined condition comparable to an oil towards its end of lifetime, engine test rig runs with basic and premium fuels, and high-resolution wear measurement as well as mass spectrometry. The results revealed a significant impact of the fuel quality on the engine oil as well as on the occurring wear in the engine.

2. Materials and methods

A reference used oil after 25,000 km of operation was characterised by conventional parameters such as oxidation or viscosity, and high-resolution MS to identify the residual FM content. According to this condition a large-scale artificially oil alteration similar as described in [1] using elevated temperature, synthetic air and shear stress was conducted. This resulted in 180 L aged oil with the same characteristics as the reference used oil, and almost fully degraded FM.

Narr Francke Attempto Verlag GmbH + Co. KG

The similarity was not only shown by analytical results, but also with SRV® tribometer experiments. Experiments were carried out with following parameters:100Cr6 polished plate 100Cr6 standard ball, 50 N, 1 mm and 30 Hz. Aliquots of the fresh, the artificially aged and the reference used oil were tested.
As top compression rings in the engine test rig, standard X90CrMoV18 rings were used for the engine bench test. For the wear measurement with the radio-isotope concentration (RIC) method the piston rings were activated in a cyclotron facility, which means that a known amount of radioactive tracer isotopes was produced within a surface layer of the piston rings with a few micrometres thickness. As tracer isotope Co57 was used. The RIC method mainly consists of a gamma radiation detector, which detects the emitted gamma activity of the tracer isotopes. The amount of wear can be derived with two methods: 1) by measuring the activities of each piston ring before and after the bench test. The difference of the measured activities can be converted to a wear volume or wear height, and 2) by measuring the activity of the lubricant which transports the wear particles containing the tracer isotopes to the radiation detector in a closed lubricant circuit [2]. The latter method can be used as continuous wear measurement during a test run, which was not done in this study.
Engine test rig experiments with artificially aged oil without noteworthy residual FM content were performed with commercially available basic and premium fuel, whereas the premium fuel contained an additive package including a higher dose of FM. At the beginning, during the experiment and at the end of the test rig runs (120 h in total) oil sample aliquots were taken to monitor the FM content via MS.
Additionally, the activated piston rings were measured by RIC and wear was determined after the test runs. For the determination of the piston ring wear the piston ring activities were measured before and after the engine bench test in a well-defined position. These measurements were repeated thirty times for statistical reasons to reduce the uncertainties. The wear volume or average wear height were calculated from the differences of the activities before and after the engine bench test.

3. Results

3.1 Artificial oil ageing in large scale

In accordance to the reference used oil (25,000 km) the artificially aged oil was produced with an oxidation of 18 A/cm, fully consumed anti-wear additive and partially consumed antioxidants within 55 hours in a large-scale alteration device (see figure 1).

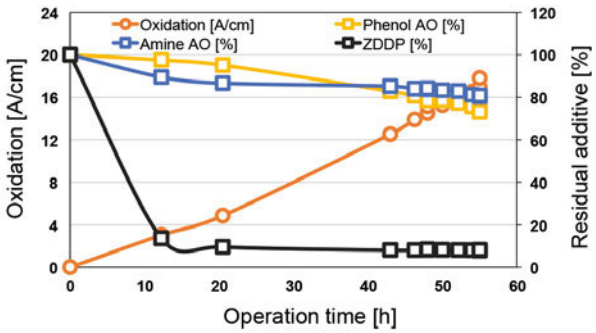

Figure 1: An increasing oxidation while partially to fully depletion of additives was detected during large scale artificial ageing.

A viscosity index decrease, which indicates the decomposition of the oil by the applied shear stress during the entire time, and an oxidation increase was monitored during the entire ageing process. The FM depletion was determined in the end sample by MS. It was confirmed that in the desired end condition of the aged oil, the anti-wear additive as well as the FM were fully depleted (see figure 1).
To show the similarity in performance with the reference used oil from the field SRV® tribometer experiments were performed. Both, the artificially aged oil as well as the reference used oil showed similar results regarding coefficient of friction and friction curve, while the fresh oil was performing significantly better.

3.2 Piston ring wear with RIC

Table 1 shows the results of the RIC wear measurements of the piston rings for test runs carried out with basic fuel without FM and premium fuel containing FM. The wear volume is the total wear volume worn off throughout the whole test and the wear height is meant to be the average wear height over the whole running surface calculated by dividing the wear volume by this surface area. The results are given as relative values comparing the premium with the basic fuel.

Table 1: piston ring wear volume and average wear height for engine bench tests without (basic fuel) and with (premium fuel) friction modifier (FM) relative to each other

Test specification	Piston ring wear volume	Piston ring wear height
Basic fuel	100 %	100 %
Premium fuel	23,69 %	23,77 %

The results show a significant reduction in wear volume for the premium fuel compared to the basic fuel by more than a factor of 4.

Narr Francke Attempto Verlag GmbH + Co. KG

3.3 Characterisation of used engine oil with MS

During both engine test rig experiments, with basic and premium fuel, engine oil aliquots were taken, and elemental analysis and MS measurement were conducted. The elemental analysis revealed a faster and slightly higher increase of iron in the oil with increasing running time for the test with basic fuel not containing any friction modifier. The MS explains this observation by revealing significant differences in the engine oil samples. While for both engine oil series only a slight decrease of antiwear additives and phenolic antioxidants was found there was a significant change regarding the FM content and the aminic antioxidants. The samples from the experiment with basic fuel did not only show no FM increase, but also a higher degree of aminic antioxidant depletion, further increasing with longer operation time. For the engine test rig performed with premium fuel a considerable amount of FM was detected in the oil samples. This content was increasing over the operation time, and at the same time degradation products were built up. Compared with the content in the premium fuel itself, a remarkably higher amount of FM was found in the engine oil after 120 h of operation time than in the pure premium fuel. This indicates a transfer from the fuel to the engine oil, and an accumulation of the FM over time as depicted in figure 2.

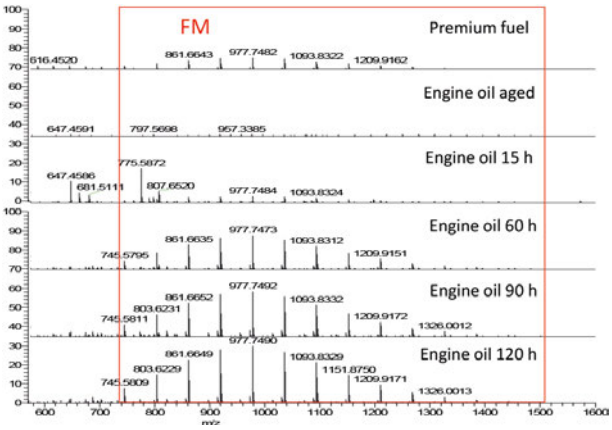

Figure 2: Mass spectra of the premium fuel containing FM, engine oil samples after large-scale ageing with fully depleted FM, and samples after an operation time from 15 – 120 h.

4. Summary and conclusion

By using the large-scale ageing device with selected and pre-defined conditions, the generation of a test oil similar to a reference used oil regarding the desired oil parameters was enabled. The degradation of the FM was detected by high-resolution MS in both oils, the reference used oil as well as the artificially aged oil and their similar performance was confirmed by SRV® tests. Engine test rig experiments with activated piston rings were performed using a basic fuel without FM and a premium fuel including a FM additive package. RIC measurements of the piston rings revealed a considerably higher wear when using the basic fuel compared to test runs with premium fuel. MS measurements of engine oil samples were able to explain this effect, as an accumulation of FM additive in the oil when using premium fuels was observed. A transfer from fuels containing FM additives in certain amount takes place, and an improvement in wear behaviour is achieved. This effect was additionally observed with piston rings already showing wear from previous test runs. Hence, an enhanced lifetime by wear reduction when a premium fuel is used regularly can be concluded.

5. Acknowledgements

The work presented was funded by the Austrian COMET program (Project InTribology, Nr. 872176) and carried out at the “Excellence Centre of Tribology” (AC2T research GmbH).

Referenssces

[1] Besser C., Agocs A., Ronai B., Ristic A., Repka M., Jankes E., McAleese C., Dörr N.: Generation of engine oils with defined degree of degradation by means of a large scale artificial alteration method, Tribol. Int., Vol 132, p 39-49, Elsevier B.V., ISSN 0301-679X, DOI 10.1016/j.triboint.2018.12.003, 2018

[2] Jech, M. (2012): Wear Measurement at Nanoscopic Scale by means of Radioactive Isotopes. Vienna University of Technology.

Narr Francke Attempto Verlag GmbH + Co. KG

No-Harm Testing: Adaptation of HiL-testing to different types of liquid fuels and fuel component types

Chandra Kanth Kosuru
Tec4Fuels GmbH, Herzogenrath, Germany

Simon Eiden
Tec4Fuels GmbH, Herzogenrath, Germany

Hajo Hoffmann
Tec4Fuels GmbH, Herzogenrath, Germany

Klaus Lucka
Tec4Fuels GmbH, Herzogenrath, Germany

Summary

Tec4Fuels has developed hardware in the loop test benches which are being used for testing the fuel-material interaction for diesel and all diesel quality alternative fuels. They consist of passenger car fuel components such as in-tank pump, fuel filter, high pressure pump, rail and injector connected in a closed loop. These test benches have been capable of reproducing IDID (internal diesel injector deposits) with the diesel quality fuels. Currently, the scope of hardware in the loop testing is being extended to gasoline and gasoline quality alternative fuels. In addition to passenger car fuel components, the test benches are now capable to handle the heavy-duty equipment, marine engine components etc. Tec4Fuels has been part of several EU Horizon 2020 projects such as REDIFUEL, IDEALFUEL, and BMWi projects like C3-Mobility in the aspect of fuel-material interactions. In this regard, the current topic discusses the adaptation of hardware in the loop test benches to different alternative fuels and fuel components. This paper also includes the initial observations on the fuel component interactions, especially injector deposit formation.

1. Background

Compatibility testing is an important aspect with regards to the introduction of novel fuels, their blends and additional additive packages. To introduce a new product into the market, its impact on the current and future infrastructure has to be analysed and necessary changes have to be made. The motor tests such as DW10 or XUD9 are effective for such testing but also expensive, very high fuel is required, and high infrastructure is demanded [1, 2]. In this aspect, a cost-efficient method with less fuel requirements and time saving, less infrastructure demanded methods would be a premium choice as an initial step before motor tests [3]. TEC4FUELS has developed such a non-engine hardware in the loop (HiL) test method This HiL method can test the compatibility of the FIE (Fuel injection equipment) components with as less as 30 litres of fuel and in just 100 h of effective runtime [3].
This methodology has already been introduced into different EU-Projects where new synthetic fuels are being developed and their compatibility tests are of prime importance [1, 4]. Current paper explains the principle of the method briefly and how it's being adapted to different project requirements, along with some initial observations from the testing.

2. Hardware in the loop Test Method

The principle involved in the current HiL test method is to have as close testing conditions as possible to the Engine test but in a simplified manner [2]. This was achieved by avoiding the combustion step of the engine tests. Due to the absence of combustion, the method allows us to collect back the fuel into the tank and reuse. This way a relatively smaller fuel volume can be used to test the compatibility of the FIE. Also, due to the absence of combustion the injector control required for the test method is much simpler, very less infrastructure requirements and highly versatile with the test conditions. This method also gives the advantage of incorporating variety of FIE components with a simple change in few test bench components. Figure 1 shows the P&ID diagram of the HIL test bench for diesel and diesel like fuels.

Narr Francke Attempto Verlag GmbH + Co. KG

In this test bench all the FIE components from in-tank pump, filter, high pressure pump, rail to injector is connected in series. The fuel is then injected into the reactor, where the fuel is allowed to condense and flow back to the fuel tank through a heat exchanger. To simulate the impact of combustion on the injector, the injector nozzle is heated to a required set temperature. Furthermore, the vibrations and exhaust gases involved due to combustion are missing. But lack of combustion has given more flexibility of the test conditions.

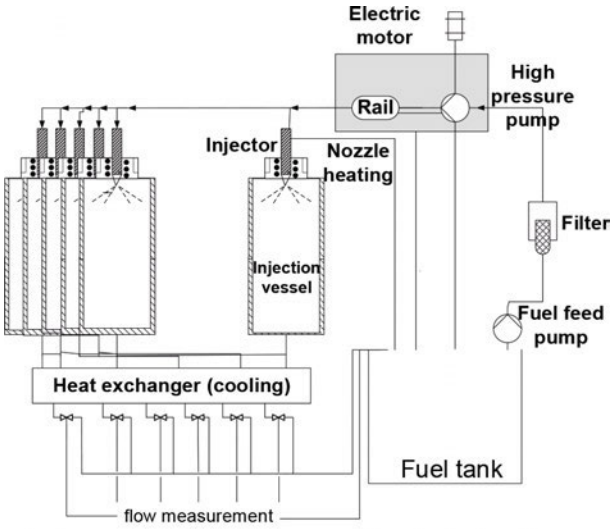

Figure 1: P&ID diagram of a Diesel HiL system

The test conditions are free to select including test runtimes from a continuous run to a cyclic test run. The fuel volume can be as low as 30 litres with the test run times reduced to just 100 hours of effective runtime. The test cycle is free to choose according to the requirement. The ON-OFF phases can induce more stress on the component and the fuel to estimate their long-term behaviour. The off-Phases are also important, to allow the fuel to cool down to as low as ambient conditions allowing the ageing products to settle down on the component surfaces. The infrastructure requirements for the testbench are rather simple which can avoid the commissioning challenges, the switching between different types of injectors can be achieved by a simple switch of the heating block, which fixes the injector to the reactor. Furthermore, this allows to investigate each component of the FIE system individually and continuously monitor their performance. Also considering the challenges of requiring 1000 litres of fuel for an engine test, this can be optimised by using as low as 30 litres for the entire test. This could be especially beneficial in the case of testing Novel fuels, where the production of 1000 litres for the engine test is a big challenge. Similarly for a short test of the impact of additive the fuel requirements can be significantly reduced. Furthermore, due to the use of same fuel in loop, this allows the fuel to degrade over time, and also gives an idea on how the fuel would behave in the long term and its impact of on the FIE system. Similar to the above-mentioned diesel test system, the sample principle is being used for a Gasoline HiL system and further, the principle is being adapted to different fluid testing systems such as shipping industry, E-mobility (cooling fluid testing), etc.

3. Initial observations

In one of the current EU Projects, named as REDIFUEL (Robust and Efficient processes and technologies for drop in renewable FUELs for road transport) a diesel like synthetic fuel is being developed using the syngas through a Fischer Tropsch synthesis. This fuel consists of a mixture of paraffinic components and a mixture of higher chain alcohol. The presence of alcohol mixture helps to reduce the emissions and also achieve an almost sootless combustions. The fuel shows a high potential of Drop In capability and is much similar to EN590 properties. In this project the developed REDIFUEL (RF) is being tested as pure component but also as a blend component with diesel B0 and B7. For testing the compatibility of this fuel an Euro4 FIE system has been used to estimate the Drop In capability in the current infrastructure. The test parameters are selected according to a nominal load condition. They are 1300 bar rail pressure, with an injector nozzle temperature varying from 230 °C and 280 °C, with injector control at 17 Hz frequency and 800 µs energizing time. The test has been run in cycle with 16 hours of on phase and 8 hours of break (in intervals of 4 h on and 1 hour break) to induce higher stress conditions for the fuel and the FIE.
The pure and blend component (blend with B0) of the REDIFUEL has shown high compatibility with all the fuel components. The functionality of all the FIE components is intact, and no abnormalities have been detected. The mass flow rate through the inject or has also been constant throughout the test method. The alcohols are in general hygroscopic and lead to a rise in water content of the fuel, but the has not shown any impact on the component and all the components have shown full functionality after the experiment time. In a follow up test with the blend of B7 with the Redifuel, the injector has failed after 90 hours of testing. The initial blockage (no flow through the injector) was observed at almost 90 hours and after 100 hours the injector solenoid was failed due to the lack of flow. The test has been repeated twice to confirm the issue and the behaviour was reproduced the same way in both the cases. To solve the issue two types of DCA (deposit control additive) have been introduce into the blend in two different experiments. These additivities have solved the issue of injector blocking and lead to a smooth running of the injector after 100 hours of HiL testing. Also, the flow rate in this case was observed to the constant. In comparison between different blends, it has been determined that the inclusion of 7 % FAME had an impact in the failure.

Narr Francke Attempto Verlag GmbH + Co. KG

Figure 2: Dis-assembly of a Euro 4 injector.

Figure 2 shows the dis-assembly of the faulty injector after the HiL test. The injector has been opened and check for deposits and the possible cause for the blockage. It has been observed that the Brass ring (Magnified on the right side) has been stuck, which should freely rotate to allow the fuel flow through the injector. This has led to the injector failure. The failure has been similar in repeated tests as well. Further information from the experts have indicate that this is a typical type of IDID (internal diesel injector deposits) that can occur in a long-term real-time operation. This implies that the HiL method can successfully reproduce the IDID and also been able to find a solution in the development phase of the fuel.
In a different project, C3-Mobility, similar HiL test bench has been developed but for a Gasoline like fuel testing. In this project, Pure 2-Butanol and MtG are tested for their compatibility with the FIE of a gasoline engine. The test parameters were set at 250 bar rail pressure and injector parameters to 33 Hz frequency and 4 ms energizing time. These conditions are considered a as high load engine operation. The nozzle temperature is set to 150 °C as proposed according to a typical gasoline engine parameter. The tests were performed for 500 h of runtime in a cycle of On-Off phases. After the testing of different blends, it has been observed that Pure components if MtG, 2-Butanol and EU6 have shown no deposit formation. But the 50 % blend of 2-Butanol with the EU6 has shown deposit formation on the injector as shown in the figure 3.

Figure 3: Comparison of injector nozzle between different experimentsKos

Furthermore, the HiL testing is being adapted to a different fluid testing system. This method is also being developed for testing the Bio-HFO, a biofuel which is being developed for the marine applications in the project named as IDEALFUEL. Also, the HiL method is free to adapt from a domestic heating system to a E-mobility system. In the E-Mobility, the cooling fluids are subjected to higher stress to cool the engine components. This provides the scope of testing different cooling fluids for their durability, safety, operability and finally compatibility with different E-mobility systems.

4. Conclusion and Outlook

The current study has shown how the test benches are capable of reproducing IDID, and also their flexibility of testing multiple components. This test method shows a good potential of being an initial screening method for novel fuels and additives before being implemented in complex or expensive motor tests. All the novel fuels are expected to be Drop-in capable, so that the transformation from production to market is smooth enough. In this regard, these non-engine test benches could be key in implementing into research. Currently, the method is being adapted to Marine and E-mobility sector and must further investigated its detailed potential of serving as a standard test procedure for the Novel engine components before being introduced into the market.

References

[1] C. Kosuru, H. Hoffmann, K. Lucka. OME: Fit-for-purpose-testing of alternative fuels on the specific topic of the evaluation of OME's drop-in compatibility, 103 (2019).
[2] Hoffmann H. A contribution to the investigation of internal Diesel injector deposits ([1. Auflage]). Shaker Verlag, Aachen (2018).
[3] Hoffmann H, Sebastian Deist, Koch W, Lucka K. Development of a Non-Engine Fuel Injector Deposit Fuel Test: Results.
[4] C. Kosuru, S. Eiden, H. Hoffmann, K. Lucka. Compatibility Studies of Alternative Fuels on Fuel System Components and Materials.

Narr Francke Attempto Verlag GmbH + Co. KG

Application of Renewable Fuels

Narr Francke Attempto Verlag GmbH + Co. KG

Laminar burning velocities of ethanol and butanol isomers

Sebastian Feldhoff
OWI Science for Fuels gGmbH

Summary

The laminar burning velocity is an important parameter governing the properties of combustion. It can for ex-ample be used to validate reaction mechanisms. However, the laminar burning velocity is not easily measured. The heat flux method is one of the methods to measure the laminar burning velocity. The heat flux burner consists of a thin, brass burner plate with a hexagonal pattern of holes. The burner plate is heated in such way that the premixed mixture flowing though the burner plate is heated. Now the heat gained by the unburnt mixture compensates the heat loss of the flame. The advantage is that mixture velocities higher and lower than the laminar burning velocity can be stabilized on this burner. In contrast to other methods, it is possible to determine the laminar burning velocity at a state of a nearly adiabatic stretchless flame by means of interpolation. The heat flux experimental setup at OWI has been further improved to provide more accurate measurement data of the laminar burning velocity. Recently, a new test series has been started investigating burning velocities of different alcohols, such as ethanol and butanol with air. Recent investigations focus on butanol isomers. Burning velocities have been measured in a wide fuel-air ratio from 0.6 to 1.6 and compared to numerical calculations, which have been performed with Cantera. The study provides an overview of the laminar burning velocity depending on fuel composition and presents the data in comparison to numerical data.

1. Introduction

The adiabatic laminar burning velocity (LBV) is an important parameter governing the properties of combustion. It can for example be used to validate reaction mechanisms and is often needed in designing of different industrial and domestic burners. This is the reason that research has focused on the adiabatic burning velocity of several types of fuel-oxidizer mixtures. However, the adiabatic burning velocity is not easily measured. There are several experimental methods to measure laminar burning velocity: the Bunsen flame method, the spherically expanding flame method, the stagnation flame method, and the flat flame burner method, including the Heat Flux method. A detailed overview of different methods can be found in [1] and [2].
The heat flux burner consists of a thin, brass burner plate with a hexagonal pattern of holes. The burner plate is heated in such way that the premixed mixture flowing though the burner plate is heated. Now the heat gained by the unburnt mixture compensates the heat loss of the flame. The advantage is that mixture velocities higher and lower than the adiabatic burning velocity can be stabilized on this burner. In contrast to other methods, it is possible to determine the laminar burning velocity at a state of a nearly adiabatic stretchless flame by means of interpolation, rather than extrapolation. This has as advantage that the uncertainties due to extrapolation are circumvented.

In this study the Heat Flux method has been applied to measure laminar burning velocities of ethanol as well as butanol isomers with air at atmospheric pressure.

2. Heat Flux Method

The main parts of the Heat Flux burner are shown in Figure 1. One of the main burner elements is a 2 mm thick brass burner plate with an effective diameter of approximately 30 mm and a uniform perforation. A conditioned heating jacket operates at a constant temperature, which is set to keep a temperature difference between unburnt gas and the heating jacket between $\Delta T = 60$ K and $\Delta T = 75$ K. A plenum chamber is surrounded by a cooling jacket, which maintains the temperature of the plenum chamber at a temperature equal to that of the unburnt gas mixture. To measure a radial temperature profile in the burner plate, fifteen thermocouples are attached to the burner plate.

Narr Francke Attempto Verlag GmbH + Co. KG

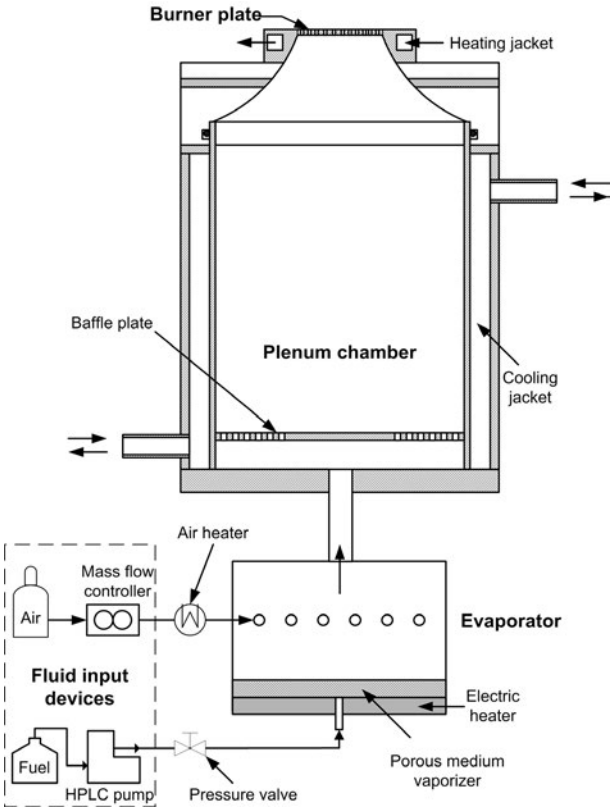

Figure 1: Schematic view of the Heat Flux burner

To stabilize an adiabatic flame on top of the burner plate the net heat flux should be equal to zero. For gas velocities U_G lower than the laminar burning velocity S_L the net heat flux is positive and the burner plate has a higher temperature than the heating circuit. This results in a radial heat flux from the burner plate center to the edge and the burner plate center achieves the highest temperature. The net heat flux is negative, when the gas velocity is higher than the LBV. In this case the temperature at the center of the burner plate is the lowest measured temperature, due to the reverse direction of the radial heat flux. For a flat temperature profile, the net heat flux is zero, which means that all the heat transferred from the flame to the burner plate is transferred then to the unburnt gas mixture. This situation corresponds to adiabatic flame conditions and the corresponding gas velocity U_G equals to the laminar burning velocity S_L.

2.1 Temperature profile along the burner plate

The temperature profile over the burner plate is used to determine if there is a net heat gain or heat loss by the mixture. In the adiabatic state, the heat loss is equal to the heat gain by the burner plate. Assuming that the conductivity of the burner plate is not temperature (and thus r) dependent, solving the energy equation leads to the following equation for the temperature distribution along the burner plate:

$$\bar{T}_p(r) = T_{center} - \frac{q}{4\lambda h} r^2$$

In this equation, T_p is the temperature as a function of the radius r. q is the net heat flux from the unburnt gas mixture to the plate, λ the conduction coefficient of the burner plate, and h is the height of the burner plate. The temperature along the burner plate is described by a parabola, with the symmetry axis at the center of the burner plate [3].
For gas velocities U_G lower than the laminar burning velocity S_L the net heat flux q is positive and the burner plate has a higher temperature than the heating circuit. This results in a radial heat flux from the burner plate center to the edge and the burner plate center achieves the highest temperature (Figure 2 mid). The net heat flux is negative, when the gas velocity is higher than the laminar burning velocity. In this case the temperature at the center of the burner plate is the lowest measured temperature, due to the reverse direction of the radial heat flux (Figure 2 top).

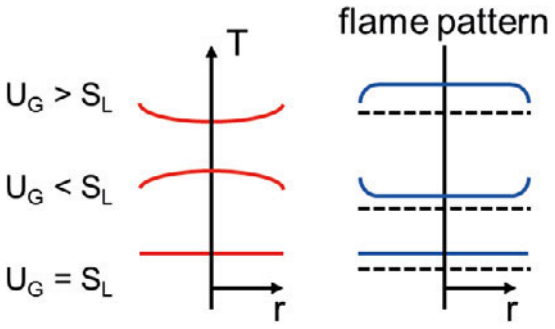

Figure 2: Temperature profile and flame pattern over the burner plate at various U_G (schematic)

For a flat temperature profile, the net heat flux q is zero, which means that all the heat transferred from the flame to the burner plate is transferred then to the unburnt gas mixture. This situation corresponds to adiabatic flame conditions and the corresponding gas velocity U_G equals to the laminar burning velocity S_L. Additionally, in the adiabatic case the temperature of the burner plate should be equal to the heating jacket temperature [4].

3. Numerical simulation

The numerical simulation of the laminar burning velocity is performed using the Cantera software. The basis of the software is the calculation of the flame by solving the chemical and kinetic equations of combustion. Due to the nearly adiabatic and one-dimensional combustion on the Heat Flux burner, the flame can be considered independent of the heat losses to the burner plate and can therefore be simulated as a free flame. This also allows the comparison between the experimental and calculated

Narr Francke Attempto Verlag GmbH + Co. KG

values. Furthermore, the calculations are used to estimate the experimental parameters, especially the gas velocity ranges, and to calculate the adiabatic burning rate. The flame has been modeled as a freely-propagating, premixed flame (1-D) with air as the oxidizer at atmospheric pressures and an unburnt gas temperature of 338 K.
All calculations of the laminar burning velocity are carried out with two existing detailed chemical kinetic mechanisms a) cloudflame [5] and b) CRECK [6] to which the experimental data is compared with for validation.

4. Results and discussion

To evaluate the performance of the Heat Flux method including the recently made improvements on reliability, several sets of experiments have been carried out. In the first place, the laminar burning velocity of ethanol was determined as it serves as a well-known reference to evaluate the accuracy of the experimental setup. The results show a good agreement with the obtained numeric data in the range of ϕ = 0.6 - 1.6 (equivalence ratio). Both mechanisms show very similar results. In the range of ϕ = 1.0 - 1.4 the experimentally obtained data differ slightly from numerical results, however, the overall expectations were met (Figure 3). The maximum LBV for ethanol is about 51.6 cm s^{-1} at ϕ = 1.1 (experimental).

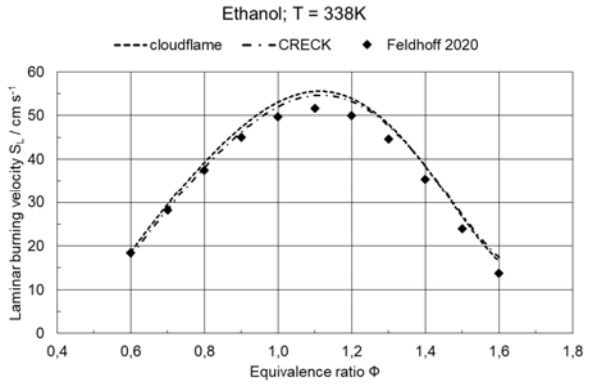

Figure 3: Laminar burning velocity of ethanol-air-mixtures: experimental and numerical data

The following experiments were related to butanol isomers (1-Butanol and 2-Butanol) at the same thermodynamical conditions. It was found, that burning velocities of both butanol isomers were lower compared to ethanol (Figure 4). The maximum LBV for 1-butanol is ca. 47.8 cm s^{-1} and for 2-butanol ca. 46.1 cm s^{-1} at ϕ = 1.1 (experimentals). This is due to the chemical bounds inside the molecules and was shown in literature before [7]. The difference is low at equivalence ratios < 1.0 and increases towards higher equivalence ratios. This behaviour can also be found in the results of the numerical simulations for both 1-butanol and 2-butanol (Figures 5 and 6). However, the obtained experimental data is in line with the numerical data.

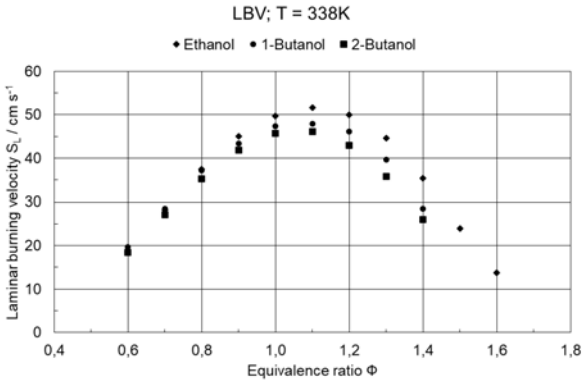

Figure 4: Laminar burning velocity of ethanol and butanol air-mixtures: experimental data

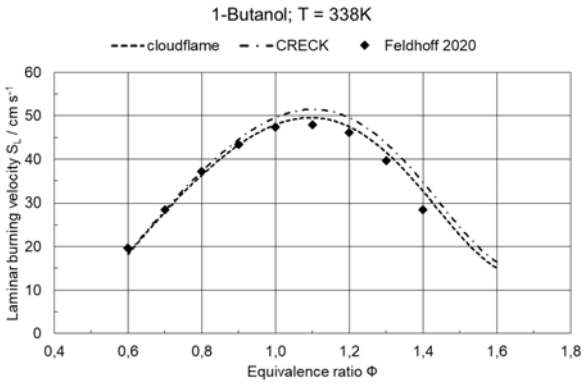

Figure 5: Laminar burning velocity of 1-butnaol-air-mixtures: experimental data and numerical data

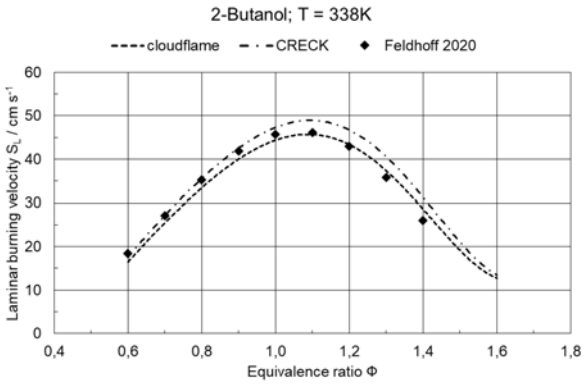

Figure 6: Laminar burning velocity of 2-butnaol-air-mixtures: experimental data and numerical data

5. Conclusion

The focus within this study was the determination of the adiabatic laminar burning velocity of ethanol and butanol isomers with the Heat Flux method. It was found that the adiabatic laminar burning velocity is highly depen-

Narr Francke Attempto Verlag GmbH + Co. KG

dent on fuel composition and is less for butanol isomers compared to ethanol. Furthermore, the difference in S_L of 1-butanol vs. 2-butanol shows that the molecules' geometrical structure is affecting the burning velocity, which has been shown by other researchers. In general, the experimental data is in good agreement with all the results of the numerical simulations.

References

[1] Egolfopoulos, F.N.; Hansen, N.; Ju, Y.; Kohse-Höinghaus, K.; Law, C.K.; Qi, F.: "Advances and challenges in laminar flame experiments and implications for combustion chemistry", Prog. Energy Combust. Sci. 43 (2014) 36–67. doi:10.1016/j.pecs.2014.04.004.

[2] Nilsson, E.J.K.; Konnov, A.A.: "Flame Studies of Oxygenates", in: F. Battin-Leclerc (Ed.), Clean. Combust. Green Energy Technol., London, 2013: pages 231–280. doi:10.1007/978-1-4471-5307-8_10.

[3] Bosschaart, K.J.: "Analysis of the Heat Flux Method for Measuring Burning Velocities", PhD. Thesis, Eindhoven University of Technology.

[4] De Goey, L.P.H.; van Maaren, A.; Quax, R.M.: "Stabilization of adiabatic premixed laminar flames on a flat flame burner", Combustion Science Technology, Volume 92, pages 201–207.

[5] S. Mani Sarathy, Patrick Oßwald, Nils Hansen, Katharina Kohse-Höinghaus. Alcohol combustion chemistry, Progress in Energy and Combustion Science, 2014, pages 0360-1285. https://doi.org/10.1016/j.pecs.2014.04.003

[6] Pelucchi, M., Cavallotti, C., Ranzi, E., Frassoldati, A., Faravelli, T., Relative Reactivity of Oxygenated Fuels: Alcohols, Aldehydes, Ketones, and Methyl Esters, Energy & Fuels, 30(10), pages 8665-8679 (2016), DOI: 10.1021/acs.energyfuels.6b01171

[7] Xiaolei Gu, Zuohua Huang, Si Wu, Qianqian Li, Laminar burning velocities and flame instabilities of butanol isomers–air mixtures, Combustion and Flame, Volume 157, Issue 12, 2010, pages 2318-2325, ISSN 0010-2180, DOI: 10.1016/j.combustflame.2010.07.003

Narr Francke Attempto Verlag GmbH + Co. KG

Application of Wood Gas in Internal Combustion Engines – Efficiency and Emissions

Dipl.-Ing. Jure Galović*, Assoc. Prof. Dr. Peter Hofmann
Institute of Powertrains and Automotive Technology, TU Wien, Vienna, Austria

Dipl.-Ing. Tom Popov, Dipl.-Ing. Dr. techn. Stefan Müller
Institute of Chemical, Environmental and Bioscience Engineering, TU Wien, Vienna, Austria

Dipl.-Ing. Dr. techn. Christof Weinländer
GLOCK Ecoenergy
Bengerstraße 1, 9112 Griffen, Austria

Dominik Frieling, M.Sc.
GLOCK Technology
Gaston-GLOCK-Park 1, 9170 Ferlach, Austria
*Corresponding author - e-mail address: jure.galovic@ifa.tuwien.ac.at (J. Galović)

Summary

A significant contribution to reach the goals of Paris' climate agreement and to become greenhouse-gas-free by 2050 can be provided by utilizing alternative fuels in internal combustion engines. More precisely, the conversion of CO_2 neutral wood gas from air gasification in stationary internal combustion engines enables sustainable power generation. However, due to its variable composition, especially H_2 and H_2O content, as well as low heating value, the engine operation with wood gas is challenging. As a part of the research projects, the wood gas production process and its utilization in the internal combustion engine of a wood gas Combined Heat and Power plant (P_{el}<100kW_{el}) have been analyzed. In addition, the engine operation with various wood gas compositions has been investigated on the adaptive engine test bench with a gas mixer at TU Wien. Based on these investigations, a joint experimental approach to optimize the wood gasification process and the engine operation is defined. Regardless of the adverse properties of wood gas for engine operation, high efficiency and low emissions can be realized with selective optimization measures of the engine and combustion process.

1. Introduction

Power generation from renewable energy sources is becoming increasingly important to reduce greenhouse gas (GHG) emissions and their adverse impact on climate change. To achieve the ambitious EU energy and climate goals, which envisage decarbonization by 2050 [1], the transformation of energy systems from centralized to decentralized structures coupled with smart grids shall be strived. In addition to volatile renewable sources such as wind and photovoltaic, the wood gas Combined Heat and Power plants (wgCHP) have a crucial role in power generation and grid stability during the volatile energy demand. For instance, the main advantage of wgCHPs is decentralized power and heat generation by utilizing regenerative and sustainable biomass such as wood chips as feedstock. As shown in Fig. 1, the wood captures CO_2 from the atmosphere for its growth. During its utilization as the feedstock within the wgCHP, CO_2 is returned to the atmosphere. Therefore, wood can be considered a CO_2 neutral energy source [2] since no additional CO_2 from fossil fuels is released.

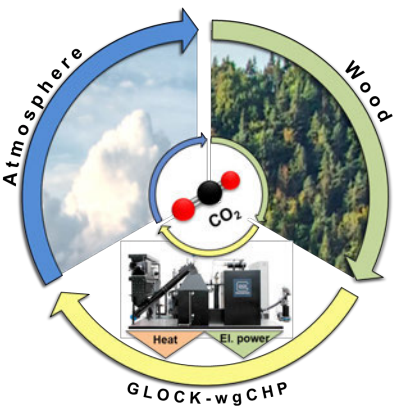

Figure 1: CO_2 recycling by the use of wgCHP

Narr Francke Attempto Verlag GmbH + Co. KG

The GLOCK-Group has also specialized in the production of innovative, highly efficient, and environmentally friendly wood gas CHPs, which offer the possibility to produce self-sufficient and CO_2-neutral heat and electricity from the renewable raw material wood. With the decentralized and constantly available energy supply of its wgCHP, the GLOCK-Group wants to actively shape the current and future energy supply to achieve climate protection, pioneer in the decentralized energy supply, and preserve resources for the future generation.

GLOCK-wgCHP systems are based on the autothermal gasification of wood chips or wood pellets and internal combustion engine (ICE), which utilizes the gasification product wood gas. In particular, the developed wgCHP systems have power ranges from 10-50kW_{el} and 35-110kW_{th} and can cover power demand for homes or small hotels. However, constant development is necessary to increase the efficiency and thus the viability of the plant. Though the most challenging aspect is to ensure high system efficiency and long-term durability under various operating conditions that affect the gasification process and engine operation.

The product of biomass gasification is a gas mixture that consists of combustible gases carbon monoxide (CO), hydrogen (H_2), methane (CH_4) as well as high molecular hydrocarbon compounds (C_xH_y). It also contains specific incombustible gases, carbon dioxide (CO_2), water vapor (H_2O) and, when air is used as a gasification agent, high amounts of nitrogen (N_2). These gases reduce the calorific value of the mixture. Moreover, tars and dust in product gas are seen as impurities. The product gas composition is depending on the design of the gasifier, the gasification agent as well as the type and quality of the biomass feedstock. Fixed bed gasifiers with air as gasification agent lead to product gases with low heating values and high amounts of nitrogen (N_2). Mixtures of air and steam as gasification agent could lead to higher amounts of hydrogen (H_2) in product gas [3]. By using only steam as a gasification agent in allothermal gasification, a hydrogen rich (H_2-rich) and nitrogen free (N_2-free) product gas can be obtained. This concept is used in the dual fluidized bed steam gasifier for the gasification of a wide range of different feedstocks [4] and has been successfully demonstrated in a pilot CHP in Güssing, Austria, for over 100.000 operating hours until 2016 [5]. The concept of "heat pipe reformer" reported in [6] also supplies a gas mixture with a high fraction of H_2 and a low fraction of inert gases. An overview of different gasifier technologies as well as a ranking of gasifiers for CHP applications according to key performance indicators is given in [7].

Several investigations of engine operation and the combustion process with different gas compositions have been reported in [8], [9], and [10]. Among the gas constitutes, H_2 favors a fast combustion process within the engine and ensures flame propagation, especially when high fractions of inert gases are present [11]. Due to its high laminar flame velocity, combustion of highly diluted mixtures in extreme lean operation with high efficiency and low emissions is possible [10].

The wgCHP development aims to attain high efficiency with low pollutant emissions and minor influence on air quality by applying optimal operational strategy combined with modern engine technology. In the framework of the present work, the investigation of the GLOCK-wgCHP plant and operation of the wood gas engine is presented. In the first part, the operating principle of GLOCK-wgCHP is described. In the second part, the methodology for wood gas analysis and investigation of the wgCHP operation is presented. In addition, the developed engine test bench, as well as methodology for laboratory investigations of the combustion process, are described. With these methods, the wgCHP operation was analyzed and the developed test engine could be verified for further investigations. In particular, it was investigated to what extent the combustible mixture can be diluted for lean operation. Thereby, several wood gas mixtures that could be supplied from different gasification processes were utilized by the test engine, and the engine efficiency and exhaust gas emissions were analyzed. Further, the results obtained from conducted measurements of operating wgCHP and during investigations on the engine test bench at the Institute of Powertrains and Automotive Technology (IFA) at TU Wien are discussed. Finally, an outlook for an optimal operating strategy with high engine efficiency and low exhaust gas emissions as well as an approach for further development are given.

2. GLOCK-wgCHP and Wood Gas Engine

2.1 Configuration of GLOCK-wgCHP

The configuration of GLOCK-wgCHP is schematically presented in Fig. 2. Throughout the process, the wood chips are fed to the gasifier, where they undergo the gasification process. The produced wood gas is extracted from the gasifier and then passed to a hot dry gas filter where char and dust are separated. Before entering the engine, the wood gas is cooled down in a heat exchanger, filtered through an additional safety wet filter, and mixed in a venturi nozzle with air. Thereby, the airflow is controlled using a throttle valve. The applied wood gas engine is based on the geometry of an industrial diesel engine, which has been modified for spark ignition (SI) operational mode. The compression ratio (ε) has been reduced due to different fuel characteristics compared to diesel. A big displacement volume of the engine ensures feasible power output during operation with wood gas. Since the engine is naturally aspirated, the intake manifold pressure is below the atmospheric pressure because the suction of the wood gas is driven by the engine. The engine drives the generator at constant engine speed, which converts the mechanical energy into the electrical energy. Prior to releasing the engine exhaust gas in the at-

Narr Francke Attempto Verlag GmbH + Co. KG

mosphere, it is cooled down in an exhaust gas cooler. The exhaust gas and wood gas heat exchangers, as well as the engine coolant circuit, are connected to the heating grid.

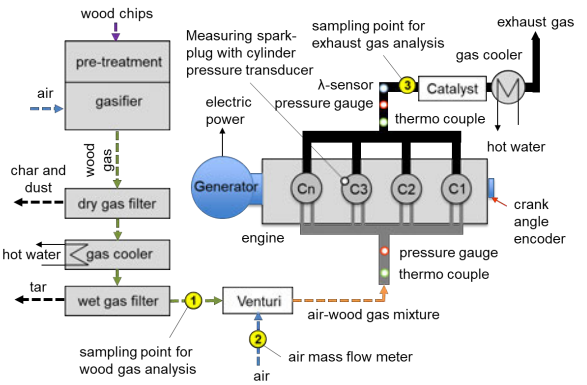

Figure 2: Schematic view of GLOCK-wgCHP

2.2 Wood Gasification and Wood Gas Properties

For GLOCK-wgCHP, fixed bed downdraft gasifiers are used. Downdraft means that wood chips and gas are moving in the same downwards direction inside the gasifier. This type of gasifier consists of four different reaction zones, as shown in Fig. 3. Wood chips are fed on the top. Without the presence of oxygen, the wood chips are heated up, and at the first stage, water is being vaporized and the chips are being dried. At higher temperatures, the pyrolysis takes place where the volatiles of the wood are going into the gas phase. In the combustion or oxidation zone, the gasification agent air is being introduced and the wood chips are partially burned under the presence of oxygen. In the reduction zone, the main gasification reactions as stated in [12] and [13] take place:

	$\Delta H_{R,850\,°C}$	
$C + H_2O \rightarrow CO + H_2$	+135,7 kJ/mol	(1)
$C + CO_2 \rightarrow 2CO$	+169,4 kJ/mol	(2)
$C + 2H_2 \rightarrow CH_4$	-89,8 kJ/mol	(3)
$CO + H_2O \leftrightarrow CO_2 + H_2$	-33,6 kJ/mol	(4)
$CH_4 + H_2O \leftrightarrow CO + 3H_2$	+226,8 kJ/mol	(5)
$CH_4 + CO_2 \leftrightarrow 2CO + 2H_2$	+260,4 kJ/mol	(6)

As reactions in the reduction zone are mostly endothermic, heat is required for them to take place. This heat is being generated in the oxidation zone, defining the autothermal gasification character of this type of gasifier. After the reduction zone, wood gas and solid particles char and ash leave the gasifier.

The advantage of downdraft gasifiers is the potentially low tar content in the wood gas. Tars are mainly released during pyrolysis and, while passing the oxidation zone, are being thermally cracked. Making this kind of gasifier suitable for combined heat and power generation with gas engines without the need for extensive gas cleaning steps [13]. Though, the downdraft gasifiers require specific feedstock properties such as a defined particular size to maintain a specific pressure drop throughout the bed and moisture contents of less than 20-25%. High pressure drops or moisture contents can negatively affect the temperatures in the different zones and the gasification process, leading to potentially higher tar contents [13], [14].

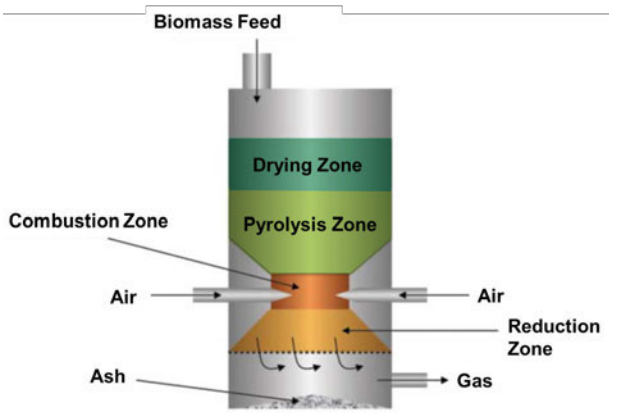

Figure 3: Reaction zones in downdraft gasifier [15]

3. Methodology

In the framework of the present work, the investigations were conducted on the operating GLOCK-wgCHP and the developed engine test bench at IFA-TU Wien.

3.1 Wood Gas Analysis and Operation of GLOCK-wgCHPs

The focus of measurements conducted on the wgCHP was placed on the analysis of wood gas composition and wood gas utilization in engine. For investigations, the wgCHP is equipped with measurement instruments for gas analysis, air mass flow measurement, pressure gauges, thermocouples, engine indicating instruments, λ-sensor, and data acquisition systems. A measuring spark plug with integrated cylinder pressure sensor type 6113C Kistler is used to indicate cylinder pressure. Fig. 4 shows the GLOCK-wgCHP with measurement instruments.

Narr Francke Attempto Verlag GmbH + Co. KG

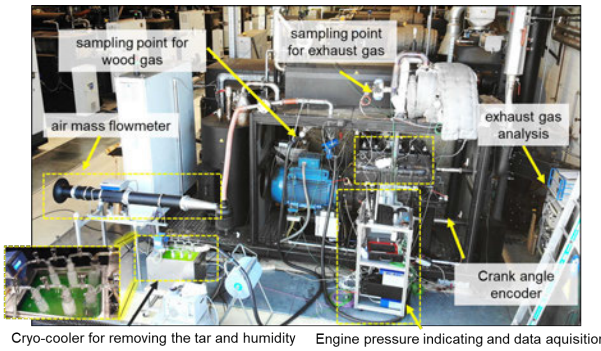

Figure 4: GLOCK-wgCHP with the measurement instruments

For the analysis of the wood gas composition, online and offline measurements were conducted at sampling point 1 in Fig. 2. Fig. 5 shows the gas cleaning setup for the online and offline measurements. For the online measurements, the wood gas was filtered with washing bottles filled with toluol and placed in a cryo-cooler at – 8°C in order to remove tar and water from the wood gas. After filtration the components H_2, CO, CO_2 and CH_4 have been measured continuously with a Rosemount NGA 2000 analyser. C_2H_4, C_2H_6, C_3H_8 and N_2 have been measured with a gas chromatograph (GC). Every 20 minutes the GC pulled a gas sample for the analysis leading to a discontinued recording of the higher carbon hydrogens and nitrogen. Offline measurements were conducted for tar and water content in accordance to DIN CEN/TS 15439 [16]. The principle for the tar and water removal from the wood gas is the same as for the online measurements. The only difference is the precise recording of the taken gas volume during the offline measurement in order to have a reference for the amount of tar and water in the wood gas stream. The taken offline samples were than analyzed at the TU Wien Test Laboratory for Combustion Systems by means of gravimetric and gas chromatographic/mass spectrometric (GC/MS) analyses.

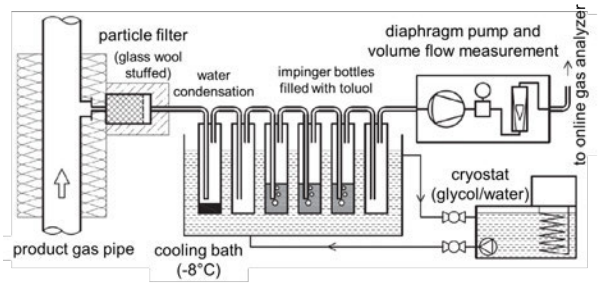

Figure 5: Gas cleaning setup for online and offline measurements. Modified from [17]

Further, air mass flow ($\dot{m}_{Air}$) for the engine operation was measured at the intake of air supply pipe (sampling point 2, see Fig. 2) by the flowmeter, based on the ultrasonic transit-time differential technique. To measure the oxygen proportion in the exhaust gas, the λ-sensor was applied in the exhaust gas pipe. Due to the composition of wood gas, a calibration factor determined on the engine test bench was used to calculate the actual relative air fuel ratio (λ). The mass flow of wood gas ($\dot{m}_{Fuel}$) is calculated according to equation (*7*) [18]:

$$\lambda = \frac{\dot{m}_{Air}}{A_{min} \cdot \dot{m}_{Fuel}} \quad (7)$$

The air required for complete combustion of wood gas, i.e., the stoichiometric air/fuel ration (A_{min}), is determined by solving the elementary combustion reactions for each combustible component as stated in [19]:

$$CO + 0{,}5O_2 = CO_2 \quad (8)$$
$$H_2 + 0{,}5O_2 = H_2O \quad (9)$$
$$CH_4 + 2O_2 = CO_2 + H_2O \quad (10)$$
$$C_2H_4 + 3O_2 = 2CO_2 + 2H_2O \quad (11)$$
$$C_2H_6 + 3{,}5O_2 = 2CO_2 + 3H_2O \quad (12)$$
$$C_3H_8 + 5O_2 = 3CO_2 + 4H_2O \quad (13)$$

The composition of raw exhaust gas was measured continuously, whereby the volumetric concentration of CO, CO_2, O_2, and NO were logged. The exhaust gas was collected on the sampling point 3 (see Fig. 2) for the analysis.

The wgCHP engine was operated lightly leaner than stoichiometric, at the highest possible load and constant engine speed during the conducted measurements. Thereby, the spark advance variations on the maximum load at constant engine speed have been performed. The gas analysis was conducted for 30 minutes. During the gas analysis, the engine cylinder pressure was indicated in 200 consecutive cycles for several times. Thereby the measurements occurred in the middle engine cylinder. The operating parameters of the gasification process have not been changed in the framework of this investigation.

3.2 Setup of Engine Test Bench with Gas Mixer

The test bench architecture and methodology is adopted from [20] and modified for the investigation of the wgCHP engine and operation with mixed wood gas. The in-line gas engine has been modified to operate as a single-cylinder engine, as presented in Fig. 6.

Narr Francke Attempto Verlag GmbH + Co. KG

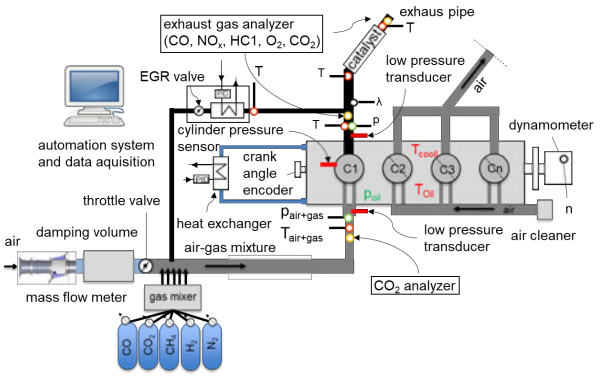

Figure 6: Schematic view of the adapted single-cylinder engine equipped with measurement instruments at the engine test bench

The high demand of the gas components makes single-cylinder operation reasonable since the investigation focuses on combustion process development. Only cylinder one is fired; the other three are deactivated by separated intake and exhaust manifolds. The fired one is equipped with a cooled piezoresistive pressure transducer (quartz) for cylinder pressure measurement. The intake and exhaust pipes of the fired cylinder are equipped with thermocouples, pressure gauges, and piezoelectric pressure transducers. The mixed wood gas is injected into the intake pipe, whereby the air mass flow and the intake pressure are controlled by an air throttle valve. Further, air mass flow ($\dot{m}_{Air}$) for the engine operation is measured at the intake of air supply pipe. For gas analysis, sampling points in intake and exhaust pipes are adapted. The composition of raw exhaust gas is measured continuously based on the infra-red principle (CO and CO_2), paramagnetic principle (O_2), as well as by flame ionization detector (CH_4) and chemiluminescence analyzer for nitric oxide (NO) and nitrogen dioxide (NO_2). NO and NO_2 are usually grouped together as nitrogen oxides (NO_X) [21]. Additionally, a pipe that connects the exhaust and intake manifold for exhaust gas recycled (EGR) was designed. The EGR mass flow is controlled by an electrically adjustable EGR valve. To obtain it, the CO_2 volumetric fraction is also measured in the intake pipe based on the infra-red principle. The test bench automation system comprises the engine control (by wgCHP engine control unit) and data acquisition. Engine indicating occurs by AVL Indicom.

Due to the long warm-up phase, as well as the high volatile gas composition, utilizing a gasifier for the engine test bench is not suitable. Instead, a gas mixer for the supply of wood gas composition has been developed for laboratory experiments. As schematically presented in Fig. 7, the gas mixer consists of controlling software and hardware components. The calculation and control of the mixing process are based on the required wood gas composition and mass flow. The hardware involves mass flow sensors, solenoid valve coils, and gas analyzer. The gas mixing process occurs in the engine intake manifold, whereby each individual component of the gas mixture can be injected with a defined mass flow. The single gas components are supplied from the gas pressure cylinders (combustible gases and part of inert gases) and recycled from exhaust gas (water vapor and part of other inert gas components). Thereby, the mass flow of EGR ($\dot{m}_{EGR}$) is determined from the measured CO_2 concentration in the fresh charge. With the information of exhaust gas composition, the mass flow of each component supplied from EGR can be calculated.

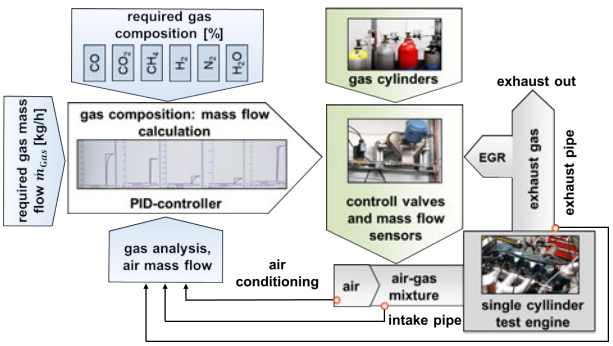

Figure 7: Schematic view of developed gas mixer for gas supply of test engine

For simplification of the mixed wood gas composition, volume fractions of higher HC compounds are substituted by an additional volume fraction of CH_4 equivalent to the initial lower heating value (LHV). At the test engine, λ is determined from the measured mass flow of each wood gas constitute ($\dot{m}_{Fuel}$) and air ($\dot{m}_{Air}$) supplied to the engine according to equation *(7)*. Thereby A_{min} is calculated by solving the elementary combustion reactions for each combustible component. In addition, λ is also calculated from the measured exhaust gas and wood gas composition according to [22] and [23] to check the conformity of determined values.

The same operating points analyzed on the operating wgCHP engine are measured again on the engine test bench. The results are compared to validate the experimental approach and check the accordance between the wgCHP engine and the test engine. The measurements occurred at the defined constant load (intake manifold pressure), engine speed, gas composition, λ and temperature of the fresh charge corresponding to the conditions during wgCHP operation.

In order to investigate the effects of wood gas composition on efficiency and exhaust gas emissions, the test engine is fuelled with different mixtures. These mixtures represent the possible wood gas composition that different concepts of biomass gasification could supply. Thereby, the H_2 mole fraction in investigated mixtures is increased, and the fractions of other components are reduced, respectively. The measurements of engine operation are carried out at several operating points, all defined with a constant load (intake manifold pressure) and engine speed, which correspond to wgCHP operation.

Narr Francke Attempto Verlag GmbH + Co. KG

Thereby, the parameter λ is varied. The engine spark timing for measured operating points is adjusted to give the maximum indicated mean effective pressure (imep) for a given engine operating parameters.

4. Results

4.1 Wood Gas Analysis

Fig. 8 depicts measured wood gas composition during the online gas analysis at the wgCHP. N_2 is not shown in the Fig.8. One can see that the volume fraction of the wood gas constitutes significantly fluctuates with time. The observed fluctuations seems to be characteristic for fixed bed gasifiers and have also been reported in [24].

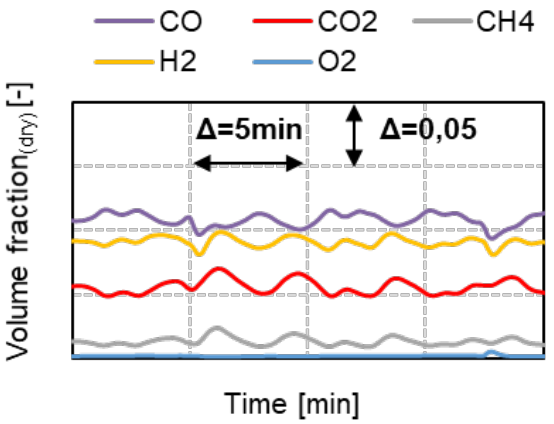

Figure 8: Fluctuations of wood gas composition (dry) during online gas analysis

The average wood gas composition is presented in Fig. 9. The highest volume fraction of the combustible components in wood gas has CO, followed by H_2 and CH_4. The C_2H_4, C_2H_6, C_3H_8 have low volume fractions. The analyzed wood gas contains a high amount of inert gases CO_2, N_2, and H_2O (the latest is not shown in Fig. 9). Besides, the wood gas contains tar compounds, S-compounds, N-compounds, Cl-compounds, and dust. Although they have adverse effects on the engine operation and exhaust gas after-treatment system, as reported in [25], they do not significantly influence the combustion process due to low content. Therefore, they are neglected for investigations on the engine test bench.

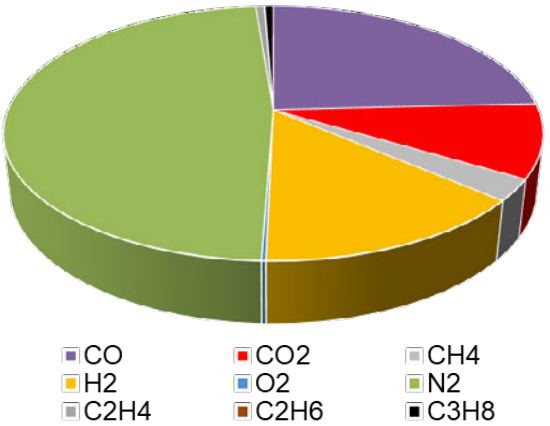

Figure 9: Wood gas composition (dry) at the wgCHP

Respective to the volume fractions of combustible components, CO and H_2 have the highest contribution to the LHV of wood gas. Although the hydrocarbons are present with a low amount, their contribution to the LHV of wood gas is significant (see Fig. 10). In addition, the stoichiometric air-fuel ratio is low due to the high content of inert gases in wood gas composition. Therefore, a high mass flow of wood gas compared to the mass flow of air is needed for the engine operation.

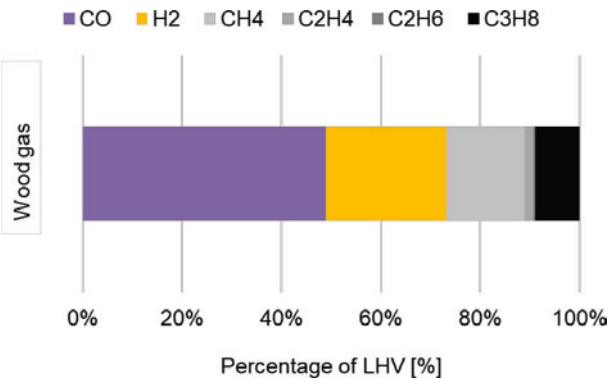

Figure 10: Contribution of wood gas constitutes to the LHV

The results obtained during the online gas analysis show that the gas composition fluctuated over the time of measurements. Due to the observed fluctuations of gas composition, an engine test bench with precisely adjustable operating conditions and gas composition offers a viable solution for investigating combustion and engine development. The results gathered during the measurements of the operating wgCHP present a data basis for validation of the developed test engine.

4.2 Comparison of wgCHP Engine and Test Engine Operation

The results of the measurements of the wgCHP engine and the single-cylinder test engine are compared to va-

Narr Francke Attempto Verlag GmbH + Co. KG

lidate the operation of the developed single-cylinder test engine and gas mixer. The measurements on the engine test bench occurred at the same operating conditions as on the wgCHP engine – constant load (intake manifold pressure), engine speed, fresh charge composition, as well as the pressure level and temperature of the fresh charge. Thereby, the spark advance variations were performed. The focus of comparison is placed on the combustion process and exhaust gas emissions.

Combustion Process

Fig. 11 shows the indicated mean effective pressure (imep), as well as the coefficient of variance (COV_{imep}), measured at the engine test bench and on the operating wgCHP engine. It can be seen that the observed data are in good agreement over the investigated operating points. The shaded area presents the spark timing, which gives the maximum imep in the absence of irregular combustion phenomena. Since only indicated values are observed, the spark timing that gives maximum imep is considered as optimal in the framework of this study. According to [21], this timing also gives the minimum specific fuel consumption. As spark was advanced from optimal settings, imep slightly decreased; as the spark was retarded from optimal settings, the imep decreased. Considering the combustion stability, the COV_{imep} increased exponentially, as the spark was retarded from initially advanced timing.

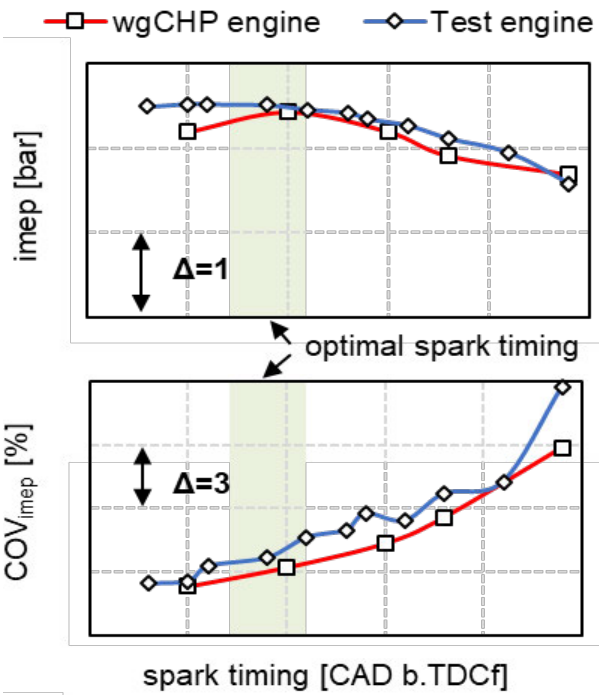

Figure 11: Combustion process of wood gas engines – indicated mean effective pressure (imep, on the top), coefficient of variance (COV_{imep}, on the bottom)

Fig. 12 shows the combustion duration (MFB 5-90%), ignition delay, and center of combustion (MFB50%) measured at the engine test bench and on the operating wgCHP engine. The combustion duration linearly increased as the spark was retarded from initially advanced spark time. The center of combustion was linearly shifted toward the optimum and then further toward the TDC, as the spark was advanced from initially retarded settings. The ignition delay remained constant over the variations of spark advance since the composition of fresh charge was not changed during the conducted measurements.

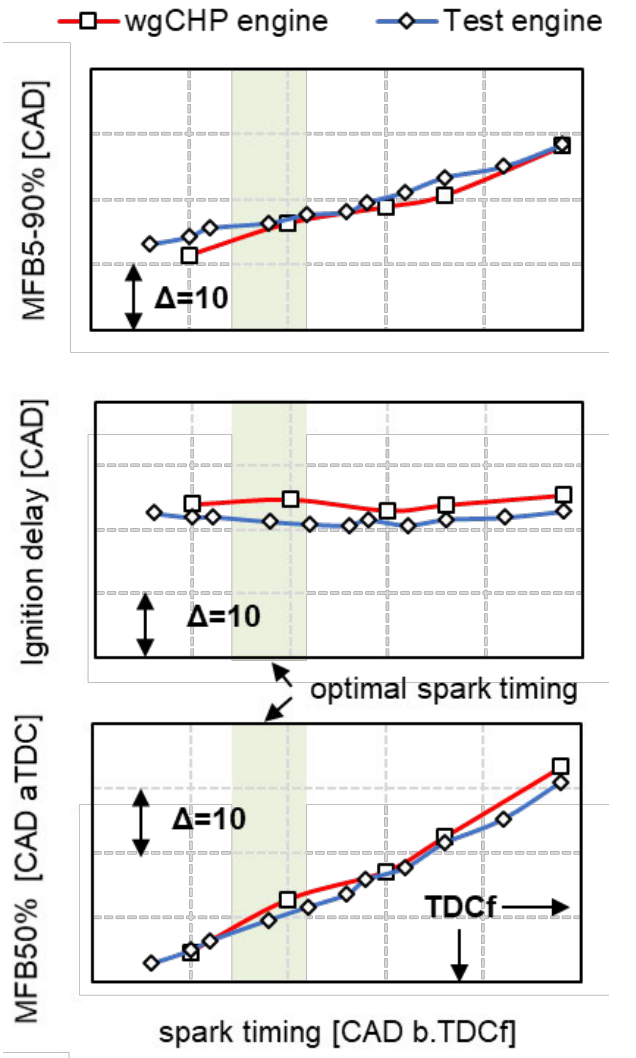

Figure 12: Combustion process of wood gas engines – combustion duration (MFB5-90%, on the top), ignition delay (middle) and combustion center (on the bottom)

Narr Francke Attempto Verlag GmbH + Co. KG

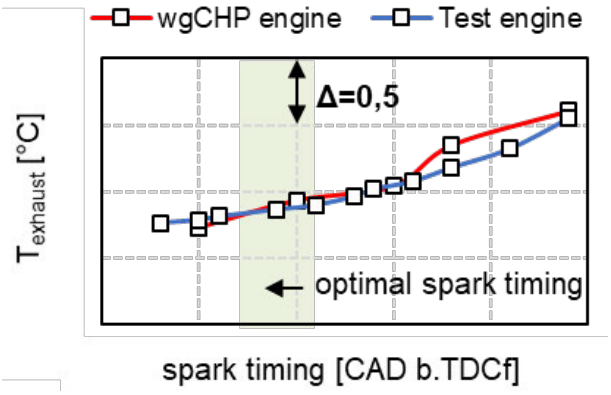

Figure 13: Combustion process of wood gas engines – exhaust gas temperature ($T_{exhaust}$)

Fig. 13 shows the exhaust gas temperature ($T_{exhaust}$) measured at the engine test bench and the operating wgCHP engine. As the spark was retarded from initially advanced settings, the exhaust temperature increased. That results in reduced engine efficiency and heat loss to the combustion chamber [21].

Emissions

Fig. 14 shows the raw exhaust gas emissions of CO and NO measured at the engine test bench and the operating wgCHP engine. Due to the limitations of measurement instruments, the exhaust emissions of the wgCHP engine could not be measured over all operating points. However, it can be seen that the CO and NO linearly increased as the spark was advanced from initially retarded settings. The increase in CO is less intensive than in NO over investigated operating points for both engines. Retarding of the spark from the initially advanced settings reduces the peak cylinder pressure and temperature, and thereby hinders the NO formation. This approach could sometimes be used for NO_X emission control [21]. Further, high cylinder pressures during advanced spark are favorable for filling the crevice volumes with an unburned mixture that does not participate in the combustion process and contributes to a slight increase of the CO emissions.

Discussion

The same trends observed in both engines proved the accordance of single-cylinder engine operation on the test bench with wgCHP engine operation. Minor discrepancies in results could be attributed to fluctuations of wood gas composition supplied by the gasifier (see Fig. 8). For example, an alteration of gas composition during logging of 200 consecutive engine cycles could significantly affect cylinder pressure measurements and combustion analysis results. In addition, the exhaust gas emissions could be affected in the same way. On the engine test bench, the operating conditions were held constant during the conducted measurements. Furthermore, the observed long combustion duration and ignition delay indicated that the combustion process occurred moderately and negatively affected the engine efficiency.

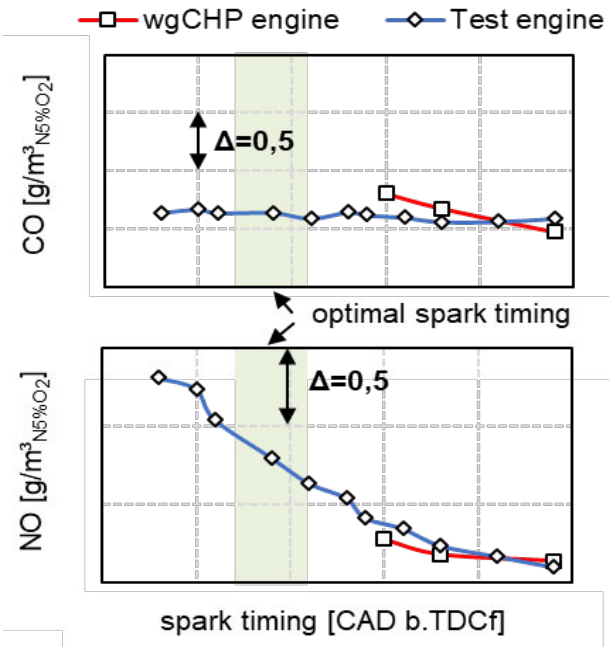

Figure 14: Raw exhaust gas emissions of wood gas engines – carbon monoxide (CO, on the top) and nitric oxide (NO, on the bottom)

4.3 Effects of H_2 in Wood Gas Composition on Engine Efficiency and Emissions

The engine operation with different wood gas mixtures was investigated on the engine test bench. For this purpose, the percentage of H_2 in gas mixtures was increased, whereby the percentage of other components was reduced respectively. These mixtures represent the possible wood gas composition supplied from different gasification concepts. Thereby, the effects of H_2O content were not investigated in the scope of this research work. The composition and properties of wood gas mixtures are listed in Table 1.

Table 1: Composition and properties of wood gas mixtures for investigation on the engine test bench

	Mixture 1	Mixture 2	Mixture 3
CO [$\%_{vol.dry}$]	24	21	18
CO_2 [$\%_{vol.dry}$]	9	8	7
CH_4 [$\%_{vol.dry}$]	5	5	4
H_2 [$\%_{vol.dry}$]	14	25	35
N_2 [$\%_{vol.dry}$]	48	41	36
LHV [kJ/kg]	5,7	7	8,6
A_{min} [kg/kg]	1,6	2	2,4

Fig. 15 shows that the combustion occurs faster and ignition delay is reduced as the H_2 percentage in mixture was higher over measured operating points. Correspondingly, the spark timing was also set closer to the TDC during

Narr Francke Attempto Verlag GmbH + Co. KG

engine operation with hydrogen rich mixtures in order to get the maximum imep for a given engine operating parameters. Thereby, the COV_{imep} during engine operation with hydrogen rich mixtures increases less intensive with increasing λ, indicating higher combustion stability. This trend is significant at very lean engine operation (see Fig. 16).

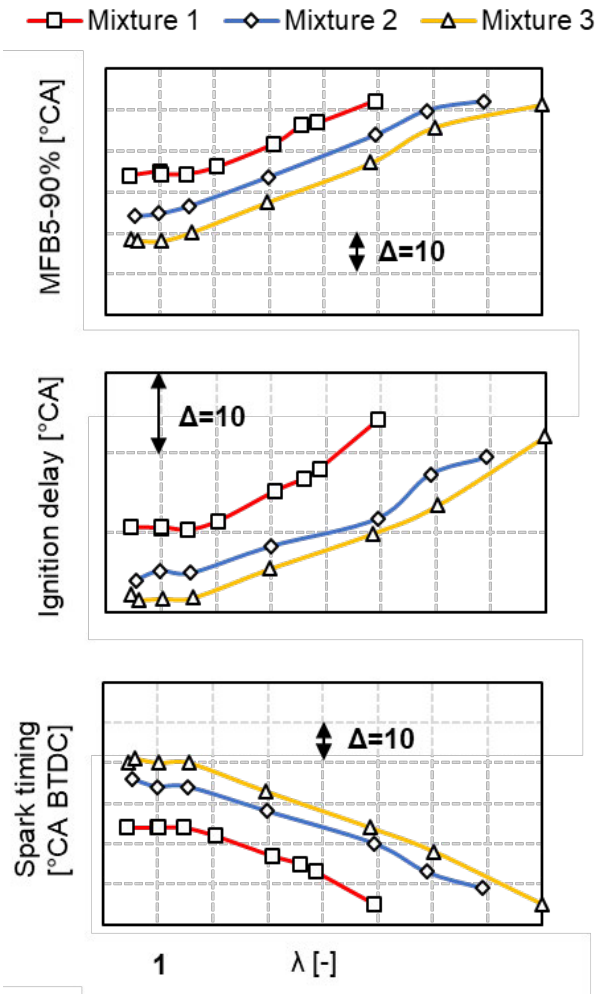

Figure 15: Effects of H_2 in wood gas on lean operation – combustion duration (MFB5-90%, on the top), ignition delay (middle) and spark timing (on the bottom)

The achieved indicated engine efficiency (η_i) increased significantly as the H_2 percentage in the wood gas mixtures was higher, especially in the lean operating points (see Fig. 16). As a result of H_2 enrichment, the lean operation could be extended to over 30%. Irregular combustion and self-ignition have not been observed during the investigation.

The observed trends of CO and NO_X are presented in Fig. 17. On the one hand, the CO emissions increased less intensive as the λ increased by engine operation with H_2 rich wood gas mixtures. On the other hand, the NO_X was higher at the engine operation with H_2 rich mixtures. However, the NO_X decreased intensively as the λ increased, and therefore, due to the extended lean operation, low NO_X emissions at the operating points with high efficiency can be achieved.

Discussion

The lean engine operation can be extended for 30% with H_2 rich wood gas mixtures. Due to the high laminar flame velocity of H_2, stabile combustion of mixtures with higher dilution is possible. In addition, the combustion occurs faster as the percentage of H_2 in mixtures is higher over the measured point in the lean operation. As a result, higher η_i can be achieved. Moreover, reduced share of the unburned fuel (CO, C_xH_y and H_2 from wood gas) over the measured operating points in lean operation indicate the increase of combustion efficiency as the H_2 percentage in gas mixtures is increased. Further, higher NOx emissions were observed at engine operation with H_2 rich gas mixtures over the measured points. As the H_2 favors the combustion process, higher combustion temperatures could be reached. Since NO_X formation is mainly driven by the peak temperature, the NO_X emissions increased as its percentage in wood gas mixtures was higher. However, the NO_X decreased, as engine was operated leaner. Thus, the lean operation can be considered as the approach for reducing NO_X emissions.

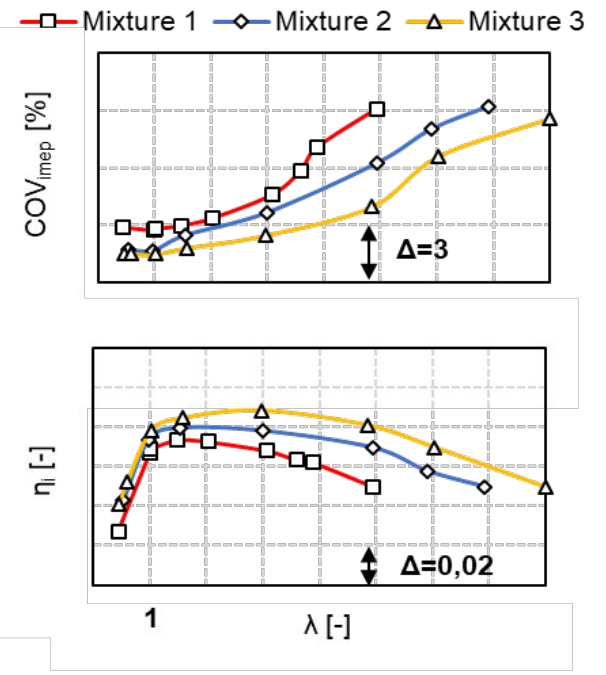

Figure 16: Effects of H_2 in wood gas on lean operation – coefficient of variance (COV_{imep}), and indicated efficiency (η_i)

Narr Francke Attempto Verlag GmbH + Co. KG

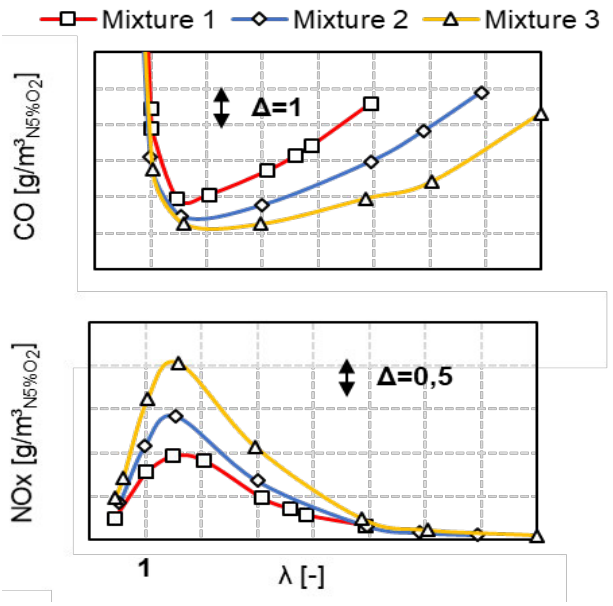

Figure 17: Effects of H_2 in wood gas on lean operation – exhaust gas emissions

5. Summary and Outlook

Summary

This paper presents the methodology for investigating the GLOCK wgCHP and the wood gas engine on an engine test bench at IFA-TU Wien. In addition, engine operation with different wood gas mixtures was investigated. The operating wgCHP plant has been equipped with measurement instruments for investigations of engine operation and gas analysis. In addition, a wgCHP engine on the engine test bench has been modified to operate as a single-cylinder engine and equipped with measuring instruments as well. For the supply of the test engine with mixed wood gas, a gas mixer has been developed. The gas mixer enables the supply of different wood gas mixtures with high accuracy.

The conducted gas analysis on the operating wgCHP shows that wood gas composition fluctuates over time due to complex processes within the gasifier. The produced wood gas contains a high amount of inert gases N_2 and CO_2. The highest volume fraction of the combustible components has CO, followed by H_2 and C_xH_y. The results obtained during the investigations of operating wgCHP present a data basis for investigations on the test engine. Due to the observed fluctuations in gas compositions, an engine test bench with precisely adjustable operating conditions and gas composition offers a viable solution for investigating the combustion process and engine development.

By comparing the wgCHP engine and test engine operation, the same trends in imep, COVimep, combustion duration, ignition delay, exhaust temperature, and CO and NO emissions are observed in both engines. These results prove the accordance of the wgCHP engine and single-cylinder engine operation on the test bench. Minor discrepancies observed between several measurements could be attributed to the fluctuations of wood gas composition on the operating wgCHP. The observed combustion duration and ignition delay indicate that the combustion process occurs moderately and negatively affects engine efficiency.

In order to investigate the effects of different wood gas compositions on the engine operation, experiments have been conducted on the engine test bench. For this purpose, the percentage of H_2 in the investigated wood gas mixtures was increased, and the percentage of other components was decreased respectively. Over the investigated lean engine operating points, higher efficiency was achieved by utilizing hydrogen rich wood gas mixtures. Due to the high laminar flame velocity of H_2, faster and stabile combustion of mixtures with higher dilution was possible. Moreover, reduced share of the unburned fuel (CO, C_xH_y and H_2 from wood gas) over the measured operating points in lean operation indicate the increase of combustion efficiency as the H_2 percentage in gas mixtures has been increased. Higher NO_X emissions over the measured points were achieved at engine operation with hydrogen rich gas mixtures due to higher combustion temperatures. As the dilution of the combustible mixture was higher (high λ), NO_X emissions significantly decreased.

The results in this paper demonstrate the potential for improvement of the combustion process within the wood gas engines. Furthermore, the accordance of the developed test engine with the wgCHP engine has been proved. With the presented methodology and developed hardware, different engine operating strategies and modern engine technology can be investigated further.

Outlook

The activities within the project go beyond the investigations presented in this paper. A joint experimental approach to optimize the engine operation for wood gas can be defined based on conducted measurements. An optimal engine design, coupled with modern technology, would ensure the lowest possible exhaust emissions and high durability with maximized electrical efficiency under given conditions. In particular, optimizing the combustion chamber for high charge motion could reduce combustion duration and improve combustion stability even at lean operation.

A possible approach to increasing the power output and overcoming the adverse effects of lean operation would be applying a turbocharger. In that way, the efficiency could benefit even more from exhaust heat recovery and extreme lean operation. However, more effort is needed to overcome the adverse effects of tars and other condensables in wood gas composition. Besides the measures, such as cleaning of wood gas, maintaining the gasification parameters, or utilizing

Narr Francke Attempto Verlag GmbH + Co. KG

higher quality wood, a modification of mixture formation could contribute to avoiding tar condensation within the system.
Further, an adaptive combustion control would ensure optimal engine operation despite permanent fluctuations of wood gas composition. In that way, possible irregular combustion and knock would be avoided.

6. Nomenclature

A_{min} = stoichiometric air/fuel ration
COV_{imep} = coefficient of variation (COV) in indicated mean effective pressure
EU = European Union
FFG = Die Österreichische Forschungsförderungsgesellschaft (eng. The Austrian Research Promotion Agency)
EGR = exhaust gas recycled
GHG = greenhouse gas
GC = gas chromatograph
HC = hydrocarbon
IFA = Institut für Fahrzeugantriebe und Automobiltechnik (eng. Institute of Powertrains and Automotive Technology)
imep = indicated mean effective pressure
LHV = lower heating value
$\dot{m}_{Air}$ = air mass flow
$\dot{m}_{EGR}$ = mass flow of EGR
$\dot{m}_{Fuel}$ = fuel mass flow
MS = mass spectrometer
MFB5-90% = combustion duration
MFB50% = center of combustion
P_{el} = electric power
SI = spark ignition
TDC = top dead center
$T_{exhaust}$ = temperature of exhaust gas
ΔH_R = reaction enthalpy
ε = compression ratio
λ = relative air fuel ratio
η_i = indicated engine efficiency

7. Acknowledgment

The achievements presented in this paper were obtained in the framework of the research projects “holzgasBHKW+” (Grant Nos. 871725, eCall 22011585) commissioned by the Austrian Research Promotion Agency (FFG) and the GLOCK ResearchLab, founded by GLOCK Privatstiftung. The authors would like to thank the Austrian Research Promotion Agency and GLOCK Privatstiftung for founding these projects. The authors acknowledge also all partners involved in the projects at GLOCK Technology, GLOCK Oekoenergie, GLOCK Energie, Institute of Chemical, Environmental and Bioscience Engineering, and Institute of Powertrain and Automotive Technology at TU Wien.

References

[1] European Commission: Communication from the Commission to the European Parliament, the European Council, the Council, the European Economic and Social Committee and the Committee of the Regions, The European Green Deal; COM 640 final, 2019; [Online], Available: https://eur-lex.europa.eu/legal-content/EN/TXT/?uri=COM%3A2019%3A640%3AFIN. Accessed on 23.06.2021.

[2] Tyrchniewicz, A.; Meyer, M.: Offsetting CO2 Emissions - Tree Planting on the Prairies. International Institute for Sustainable Development. Jan. 22. 2002. [Online], Available: https://www.iisd.org/publications/offsetting-co2-emmisions-tree-planting-prairies, Accessed: 23.06.2021.

[3] Sharma, S.; Sheth, P. N.: Air–steam biomass gasification: Experiments, modeling and simulation. Energy Conversion and Management, vol. 110; 2016, pp. 307–318. https://doi.org/10.1016/j.enconman.2015.12.030.

[4] Benedikt, F.; Schmid, J.C.; Fuchs, J.; Mauerhofer, A. M.; Müller, S.; Hofbauer, H.: Fuel flexible gasification with an advanced 100 kW dual fluidized bed steam gasification pilot plant. Energy, vol. 164; 2018, pp. 329–343. https://doi.org/10.1016/j.energy.2018.08.146.

[5] Bolhàr-Nordenkampf, M.; Rauch, R.; Bosch, K.; Aichernig, C.; Hofbauer, H.: Biomass CHP Plant Güssing – Using Gasification for Power Generation. In Proc. of the 2nd Regional Conference on Energy Technology Towards a Clean Environment, 12-14 February 2003, Phuket, Thailand; 2003.; pp. 566-572; [Online], Available: https://www.researchgate.net/publication/270160090_Biomass_CHP_Plant_Gussing_-_Using_Gasification_for_Power_Generation

[6] Herdin, G.; Zankl, M.: Die Nutzung von Synthesegas im Gasmotor – thermodynamische Analyse. In Proc. of the 13. Tagung Der Arbeitsprozess des Verbrennungsmotors, 22.-23. September 2011, Graz, Austria.; 2011; pp. 568–582.

[7] Thomson, R.; Kwong, P.; Ahmad, E.; Nigam, K. D. P.: Clean syngas from small commercial biomass gasifiers; a review of gasifier development, recent advances and performance evaluation, International Journal of Hydrogen Energy, vol. 45; 2020. pp. 21087–21111. https://doi.org/10.1016/j.ijhydene.2020.05.160.

[8] Herdin, R.; Herdin, A.; Grewe, F.; Knepper, S.: Ready t(w)o Gas – The Hydrogen Engine with Variable Natural Gas Blending Gas Blending by 2G. OAVK (Hrsg.); 42nd Internationales Wiener Motorensymposium, 29–30 April 2021, Vienna, ISBN: 978-3-9504969-0-1

[9] Hernandez, J.J.; Lapuerta, M.; Serrano, C.; Melgar, A.: Estimation of the Laminar Flame Speed of Pro-

Narr Francke Attempto Verlag GmbH + Co. KG

ducer Gas from Biomass Gasification. Energy and Fuels, vol. 19, 2005. pp. 2172–2178. https://doi.org/10.1021/ef058002y.

[10] Ulfvik, J.; Achilles, M.; Tuner, M.; Johansson, B.; Ahrenfeldt, J.; Schauer, F. X.; Henriksen, U.: SI Gas Engine: Evaluation of Engine Performance, Efficiency and Emissions Comparing Producer Gas and Natural Gas. SAE paper 2011-01-0916, 2011.; https://doi.org/10.4271/2011-01-0916.

[11] Schneßl, E.; Kogler. G.; Wimmer, A.: Großgasmotorenkonzepte für Gase mit extrem niedrigem Heizwert. WTZ (Hrsgb.); In Proc. of the 6th Dessau Gas Engine Conference, 26. - 27. March 2009. Dessau-Roßlau, Germany; pp. 271-293.

[12] Lv, P.; Yuan, Z.; Ma, L.; Wu, C.; Chen, Y.; Zhu, J.: Hydrogen-rich gas production from biomass air and oxygen/steam gasification in a downdraft gasifier. Renewable Energy, vol. 32, 2007. pp. 2173–2185. https://doi.org/10.1016/j.renene.2006.11.010.

[13] Kaltschmitt, M.; Hartmann, H.; Hofbauer, H.: Energie aus Biomasse. Berlin, Heidelberg: Springer Berlin/Heidelberg, ISBN: 9783662474372, 2016.

[14] Martínez, J.D.; Mahkamov, K.; Andrade, R. V.; Silva Lora, E. E.: Syngas production in downdraft biomass gasifiers and its application using internal combustion engines. Renewable Energy, vol. 38, 2012. pp. 1–9. https://doi.org/10.1016/j.renene.2011.07.035.

[15] Sadaka, S.: Gasification, Producer Gas and Syngas. US Dept. Agriculture, and Country Gov. Cooperation, University of Arkansas, FSA1051. [Online], Available: https://www.uaex.uada.edu/publications/PDF/FSA-1051.pdf, Accessed on 23.06.2021.

[16] Biomass gasification - Tar and particles in product gases - Sampling and analysis. European Committee for Standardization, DIN Deutsches Institut für Normung, Beuth Verlag, Berlin, 2006.

[17] Diem, S.: Messbericht über die Messungen am BHKW GGV2.7 in Griffen der Fa. GLOCK Technology GmbH. TU Wien Prüflabor für Feuerungsanlagen, PL-20029-P, 2020.

[18] Pischinger, R.; Klell, M.; Sams, T.: Thermodynamik der Verbrennungskraftmaschine. 3. Aufl.; Wien: Springer Verlag, ISBN: 978 3211992760, 2009.

[19] Lackner, M.; Palotá, Á.B.; Winter, F.: Combustion. Weinheim: Wiley-Vch, ISBN: 978 3527333516, 2013.

[20] Damyanov, A. A.: Combustion Process Development and Diesel Engine Suitability Investigations for Oxygenated Alternative Fuels. Ph.D. dissertation, Institute for Powertrains and Automotive Technology, TU Wien, 2019.

[21] Heywood, J.B.: Internal Combustion Engine Fundamentals. 2nd ed.; New York: McGraw-Hill Education, ISBN: 9781260116106, 2018.

[22] Brettschneider, J.: Berechnung des Luftverhältnisses λ von Luft-Kraftstoff-Gemischen und des Einflusses von Meßfehlern auf λ. Robert Bosch GmbH, Bosch Technische Berichte 6, Germany, 1979. pp. 177–186.

[23] Brettschneider, J.: Erweiterung der Gleichung zur Berechnung des Luftverhältnisses λ. Robert Bosch GmbH, Bosch Technische Berichte 56, Germany, 1994 pp 30–45.

[24] Simone, M.; Barontini, F.; Nicolella, C.; Tognotti, L.: Gasification of pelletized biomass in a pilot scale downdraft gasifier. Bioresource Technology, vol. 116, 2012. pp. 403–412. https://doi.org/10.1016/j.biortech.2012.03.119.

[25] Lehmann, A. K.; Stellwagen, K.; Plohberger, D.: Einfluss der Schmierölwahl auf den Betrieb von Gasmotoren mit Biogas. WTZ (Hrsgb.); In Proc. of the 6th Dessau Gas Engine Conference, 26. - 27. March 2009. Dessau-Roßlau, Germany; pp. 144–154.

Narr Francke Attempto Verlag GmbH + Co. KG

Thermodynamic Potential and Emission Characteristics of an Oxygen-containing Sustainable Fuel fulfilling EN 590 and RE-DII-standards

Dipl.-Ing. Lukas Nenning
University of Technology, Graz, Austria

Dipl.-Ing. Gabriel Kühberger
University of Technology, Graz, Austria

Prof. Dipl.-Ing. Dr. Helmut Eichlseder
University of Technology, Graz, Austria

Dipl.-Ing. Michael Egert
AVL LIST GmbH, Graz, Austria

Dipl.-Ing. Thomas Uitz
OMV Downstream GmbH, Vienna, Austria

Summary

This study deals with the thermodynamic potential of an oxygen-containing fuel in a compression ignition (CI) engine. To fulfill future CO_2-fleet-emission targets with conventional powertrains in the EU, besides an increasing amount of hybridization of the powertrain also the efficiency of the internal combustion engine itself must be optimized. Thus, this work in hand pursues the approach to reduce CO_2 emissions by using a 100% renewable fuel on the one hand, and to exploit specific engine hardware adaptations enabled by this fuel to further increase the engine efficiency and reduce emissions. Therefore a trinary blend (HVO, ethers and alcohol) with an oxygen content of about 10%, which fulfills EN 590 and RED-II legislation, was tested thoroughly on a CI single cylinder research engine (SCRE). The oxygen-content of the fuel leads to a significant smoke reduction and thus a drastically improved NOx-smoke trade-off compared to conventional diesel. It is shown that this advantage can be successfully converted into an improved engine efficiency by applying a distinct increase of compression ratio (CR) with a redesigned combustion chamber and adapted combustion process. Furthermore, the impact of this sustainable fuel on a EU7 capable exhaust aftertreatment system (EAS) was investigated on a four-cylinder CI engine in different driving cycles.

1. Introduction

The decreasing CO_2-fleet-emission targets in the EU are a major challenge for all car manufacturers. The large share of newly registered cars with a conventional drivetrain still underlines the importance of a high powertrain efficiency with gasoline and diesel engines. Besides the amount of hybridization, the combustion efficiency must be increased to fulfill future CO_2 targets, as well. Thus, this work in hand pursues two approaches: The use of a renewable fuel with a lower CO_2 potential and fuel-specific engine hardware adaption for efficiency improvement. As shown in Fig. 1, a typical C-class passenger car (PC) in the WLTC needs a cycle-averaged effective efficiency of about 36% with conventional diesel fuel to fulfill the CO2 target with the given average vehicle mass in 2020. In order to meet the CO2 legislation in 2030 with the same drivetrain efficiency, a fuel with a lower CO2 factor must be used (1). The second option (2) to accomplish the target in 2030 with a conventional drivetrain would require a significant increase of the efficiency.
However, since these high drivetrain efficiency values are still unrealistic, this research work strives for combining the two described possibilities to achieve a significant CO_2 reduction.
Fig. 2 illustrates the CO_2 reduction potential of different fuels compared to conventional diesel fuel on the basis of the physical properties without consideration of

Narr Francke Attempto Verlag GmbH + Co. KG

production. Especially short-chain alkanes and alcohols have an appreciable potential. In contrast, oxymethylene ethers (OME) worsen this fuel parameter. This diagram suggests the conclusion that the CO_2 factor of a fuel can be significantly reduced by choosing the right blend components.

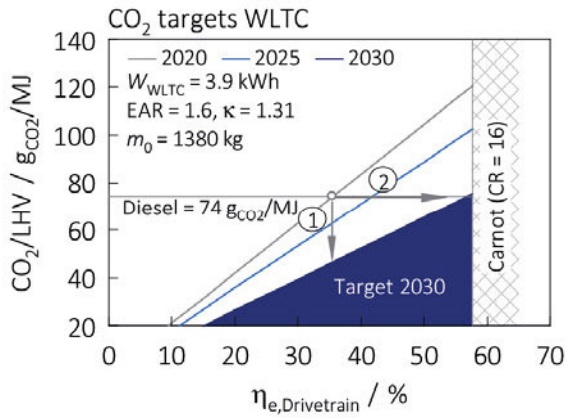

Fig. 1: Dependence of WLTC averaged drivetrain efficiency on the CO_2 factor of the fuel

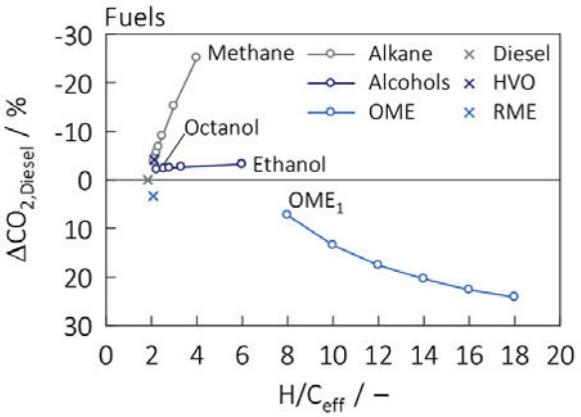

Fig. 2: Relative theoretical CO_2 potential of different hydrocarbons compared to conventional diesel fuel

2. Methodology

2.1 Fuel definition

Based on findings from the literature [1-3], which report a significant smoke reduction due to the oxygen-content in the fuel, a sustainable blend was defined. In order to ensure fleet compatibility and to fulfill future fuel legislation, this trinary blend meets the EN 590 [4] and the Renewable Energy Directive II (RED-II) legislation [5].

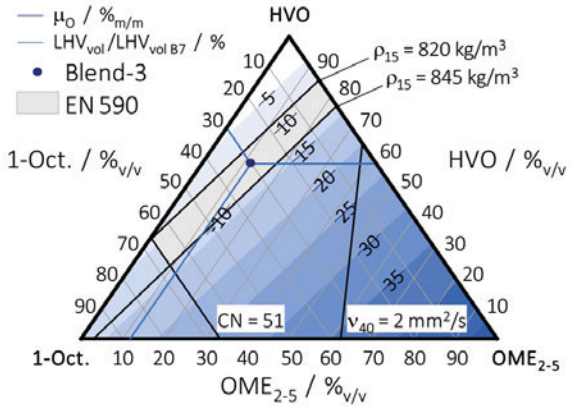

Fig. 3: Composition of Blend-3

This "Blend-3" called test fuel consists of hydrogenated vegetable oil (HVO), ethers and alcohols, which are 100% renewable components. Due to the RED-II legislation, which assigns HVO as a blend component of greater importance in the future, Blend-3 has a great share of HVO. The other two components (1-Octanol and OME_{2-5}) are mainly added for their purpose as oxygen-carriers.
Fig. 3 depicts the three-component system of Blend-3 and the blending limits due to the EN 590 legislation. Especially the narrow density limitations only allow a low admixing of the used OME mix. The minimum cetane number limits the share of 1-Octanol (1-Oct.). The maximum decrease of the volumetric lower heating value was defined with about 10% and the minimum oxygen content with 10%. Therefore, Blend-3 consists out of 58% HVO, 30% 1-Octanol and 12% OME_{2-5}. The fuel data is stated in Table 2 (Appendix).
Fig. 4 displays the distillation curves of the used commercial diesel fuel, Blend-3 and the limits of EN 590. The lower boiling points, respectively boiling ranges of the blend components of Blend-3, lead to a lower distillation curve, which nevertheless fulfills the distillation limits of the EN 590.

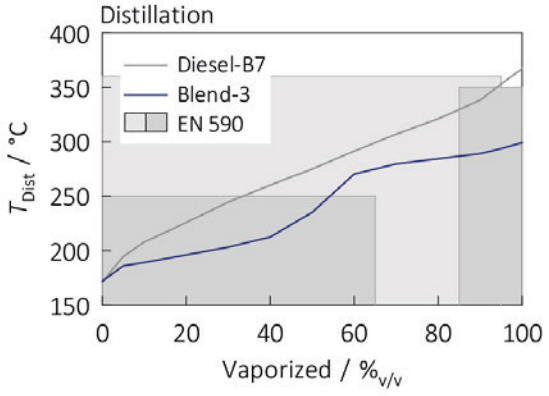

Fig. 4: Distillation curves and EN 590 limits

Narr Francke Attempto Verlag GmbH + Co. KG

2.2 Test methodology

Fig. 5 shows the comprehensive test methodology for the investigations with Blend-3 in a CI engine. Starting with the thermodynamics, the emission behavior of this fuel blend was researched with a state-of-the-art SCRE.

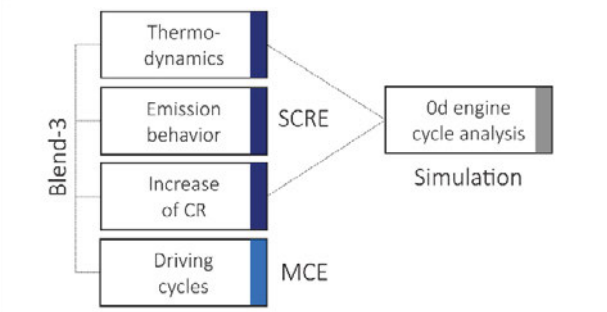

Fig. 5: Methodological approach of the investigations with Blend-3

Subsequently, the CR was increased in order to improve the combustion efficiency. Based on the afore optimized stepped-lip piston bowl with a CR of 15.5 a new combustion chamber for a CR of 20.6 was developed with a smaller bowl volume. In an upfront carried out 1d engine cycle simulation this CR was found for an engine of this cylinder size to be the most advantageous compromise between efficiency improvement and keeping maximum cylinder pressures within a reasonable limit of 200bar, assuming a similar heat release.
For the purpose of an analysis of the combustion process when using this renewable fuel blend, the experimental results were analyzed with a 0d engine cycle analysis.
In order to investigate the effects of Blend-3 on tailpipe emissions using a cutting-edge exhaust aftertreatment system (EAS) series-relevant approval cycles, such as Worldwide Harmonized Light Vehicles Test Cycles (WLTC), were carried out using a 2.0l multi-cylinder CI engine.

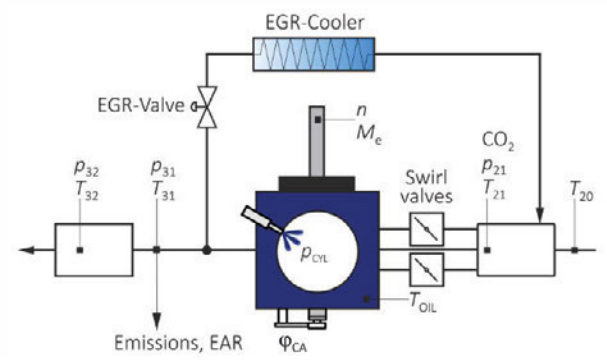

Fig. 6: Schematic of the SCRE measurement setup [6]

The major part of the experimental investigations was carried out on a SCRE, which is schematically shown in Fig. 6. The engine design allows maximum flexibility with regards to hardware modifications. The swept volume of 0.5l is very common in PC CI engines. In combination with the latest fuel injection equipment and the modern piston bowl design this combustion hardware guarantees series-relevant research results.
The technical data of the SCRE is stated in Table 1.

Table 1: SCRE specification [6]

Type	AVL 5402
Bore	85mm
Stroke	90mm
Displacement	511cm³
Compression ratio	15.5
Number of valves	4
Max. cyl. pressure	200bar
Max. speed	4200min^{-1}
Technology	Common-rail injection system
	Bosch CP4.1 fuel pump
	Bosch CRI 2-25 injector
	Stepped-lip piston bowl
	HP-EGR (cooled, with bypass)
	Variable swirl system

The wall heat loss Q_W is a significant efficiency loss in an internal combustion engine. As shown in the first law inner gas work and thus is a relevant optimization parameter of a combustion system.

$$-p\frac{dV}{d\varphi}+\frac{dQ_B}{d\varphi}-\frac{dQ_W}{d\varphi}+h_{IN}\frac{dm_{IN}}{d\varphi}-h_{EX}\frac{dm_{EX}}{d\varphi}=\frac{dU}{d\varphi}$$

Eq. 1: First law of thermodynamics for an instationary and open system

As depicted in Fig. 7, the wall heat loss is split up into three parts according to the combustion chamber walls. The piston cooling, which dissipates the main part of the wall heat loss via the piston, was used to measure an indicator of the overall wall heat loss. The temperature difference between the in- and the outflow of the piston cooling ΔT_{OIL} is proportional to the heat flux, as Eq. 2 illustrates.

Narr Francke Attempto Verlag GmbH + Co. KG

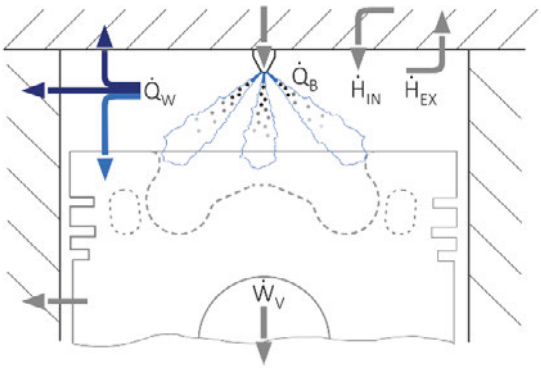

Fig. 7: Thermal energies and enthalpies in a combustion chamber according to Eq. 1

$$\dot{Q} = \dot{m}c\Delta T_{OIL} = \dot{m}c\left(T_{OIL,OUT} - T_{OIL,IN}\right)$$

Eq. 2: Heat flux in the piston cooling gallery

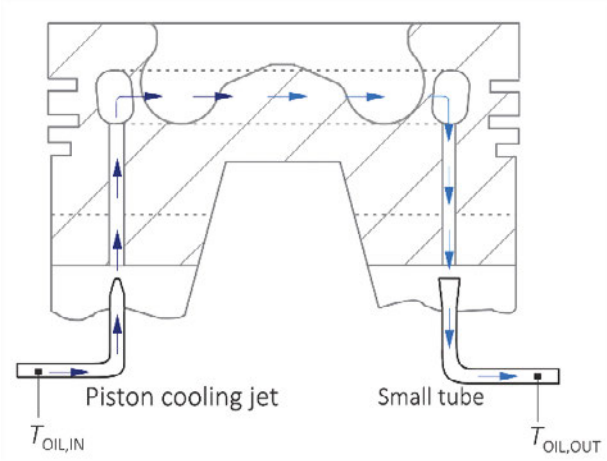

Fig. 8: Schematic of the piston cooling temperature measurement

As shown in Fig. 8, the in- and the outflow oil temperatures of the piston cooling gallery were measured. The conventional piston cooling jet was equipped with a thermocouple. In order to measure the temperature in the outflow $T_{OIL,OUT}$ a small tube was modified to collect the oil from the return-flow. Together with the temperature in the inflow $T_{OIL,IN}$ the temperature difference between these two temperatures ΔT_{OIL}, can be calculated.
In order to cover a whole engine map with a few stationary load points in the best possible way, two relevant driving cycles for PCs with different vehicle mass were simulated with AVL-CRUISE™, as shown in Fig. 9. For investigations in low engine load the load point 2000rpm and a break mean effective pressure (BMEP) of 6bar was chosen, which corresponds to an indicated mean effective pressure (IMEP) of 6.7bar (2000/6.7bar) in the referenced four-cylinder engine, stated in Table 4.

The total injection quantity in this load point with single pilot injection was 19mg, from which 18mg were used for the main injection.

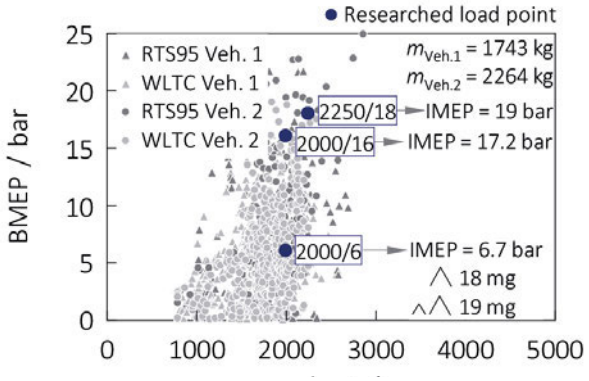

Fig. 9: Overview of the investigated load points

Investigations in high engine load were carried out at the same engine speed and a BMEP of 16bar, which requires an IMEP of 17.2bar (2000/17.2bar). The engine sweet spot with lowest BSFC in the engine map was predicted to be at 2250rpm and an IMEP of 19bar (2250/19bar) which results in a BMEP of 18bar presuming an engine friction reduction down to 1bar in this load point.

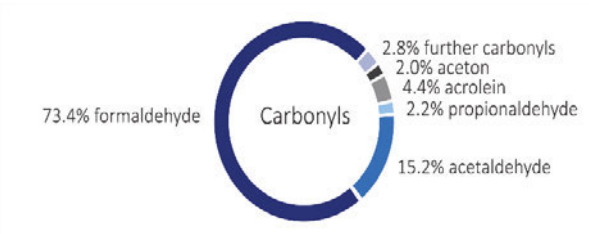

Fig. 10: Distribution of carbonyls in a Diesel exhaust gas [7]

In order to take account of future emission legislation, the emission behavior of non-limited emissions such as carbonyls was investigated as well. Formaldehyde (FA) and Acetaldehyde (AD), which together account for a share of nearly 90%, were measured (Fig. 10).
In the following results the respective injection strategy is shown in the upper right corner of the diagram by open triangles representing the main- as well as the applied number of pilot injection events (e.g.^^^)

3. Results

3.1 Thermodynamics

Fig. 11 shows the comparison of the analyzed combustion parameters using a single injection and no EGR with the researched fuels at constant center of mass fraction burned (MFB_{50}) at an engine speed of 2000rpm and an injection quantity of 18mg (2000/18mg).

Narr Francke Attempto Verlag GmbH + Co. KG

The higher cetane number of Blend-3 leads to a shorter ignition delay, resulting in an earlier rise of the rate of heat release (ROHR). It is assumed, that the oxygen content of Blend-3 is responsible for the shorter combustion duration. As a consequence, the degree of constant volume (η_{CV}) of the combustion with Blend-3 rises. The oxygen content in the fuel lowers the lower heating value (LHV). Therefore, these measurement results compare different chemical energies injected into the combustion chamber.

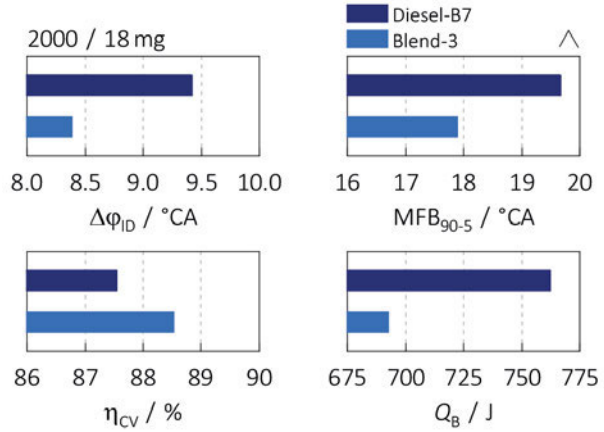

Fig. 11: Combustion parameters of the main injection without EGR

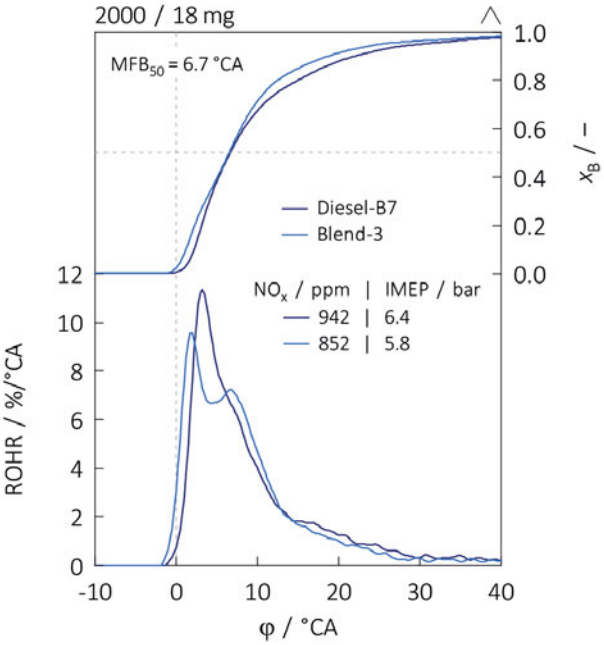

Fig. 12: Combustion analysis of a single injection without EGR

The shorter ignition delay of Blend-3 also causes a lower initial combustion rate compared to Diesel-B7, as Fig. 12 illustrates. The different nitrogen oxide (NO_x) engine-out emissions and IMEPs are a result of the different LHVs.

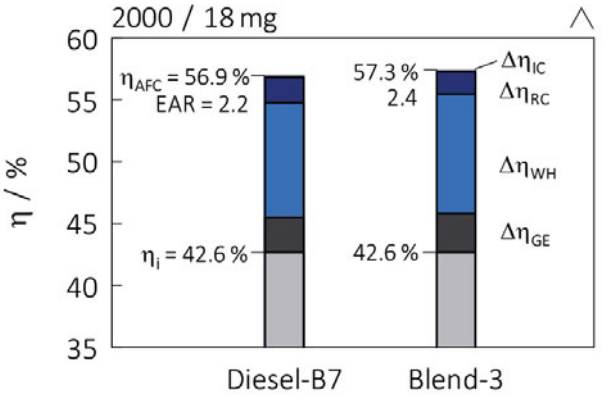

Fig. 13: Loss analyses of the single injections without EGR

The loss analyses in Fig. 13 depict the efficiency losses of the engine operated with the two fuels at a constant gas exchange. The higher excess air ratio (EAR) due to the higher oxygen content in the Blend-3 fuel leads to a higher efficiency of the standard air fuel cycle (AFC) with real charge. The loss due to incomplete combustion (IC) is negligible. The shorter combustion duration and therefore high degree of constant volume combustion leads to a lower loss due to real combustion (RC). Despite the higher EAR, the combustion of the trinary blend causes a higher wall heat loss. This result may have several causes. Both, the lower engine load with Blend-3 and a higher combustion temperature, may cause this higher efficiency loss. The gas exchange loss increases due to the measurement at constant pumping mean effective pressure (PMEP). Hence, at constant injection quantity the indicated efficiencies of the compared fuels are the same.

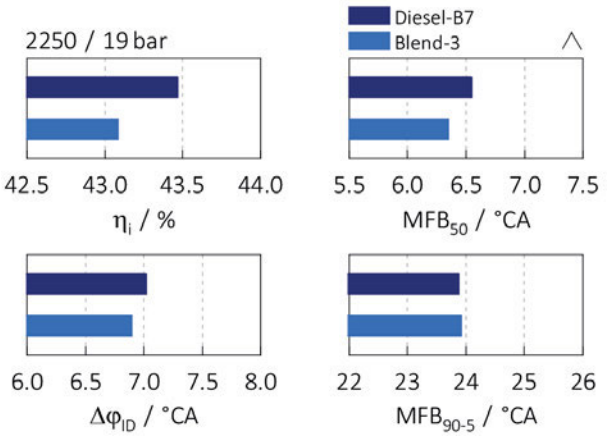

Fig. 14: Combustion parameters in the sweet spot without EGR

In the sweet spot of the engine, which was found at 2250/19bar, the indicated efficiency decreases with Blend-3, as shown in Fig. 14. The longer injection duration required to compensate the lower LHV and higher wall heat losses are the reason. In contrast to the findings in Fig. 11, the ignition delays and combustion durations

Narr Francke Attempto Verlag GmbH + Co. KG

are about the same at this high load point. Due to the high rail pressure of 2000bar, the influence of the fuel parameters on the ignition process becomes secondary.
The oil temperature measurement in the in- and outflow of the piston cooling could confirm the higher wall heat loss with Blend-3. As illustrated in Fig. 15, a significant change of the oil temperature difference over the piston in the sweet spot was measured.

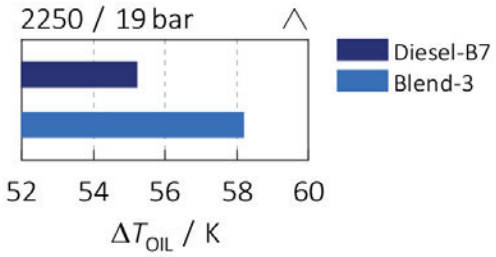

Fig. 15: Oil temperature measurement of the piston cooling in the sweet spot without EGR

3.2 Emission behavior

In addition to thermodynamics, the emphasis of the investigations with Blend-3 was laid on the emission behavior. Fig. 16 shows the combustion parameters of an EGR sweep at the selected low load point at constant IMEP and constant PMEP. As a consequence of the higher EAR and the shorter combustion duration, the trinary blend has a slightly higher indicated efficiency and a lower exhaust gas temperature. Similar to the findings in Fig. 11, Blend-3 has a shorter ignition delay, which becomes more pronounced at high EGR rates.
As shown in Fig. 17, the trinary blend reduces the exhaust emissions significantly. As a result of the higher engine efficiency and the lower CO_2 factor, the CO_2 emissions are reduced due to the use of Blend-3. Furthermore, the oxygen content of this blend causes a more complete combustion and therefore lower carbon monoxide (CO) and lower smoke emissions. Hence, the NO_x-smoke trade-off is significantly improved. As a result of the higher cetane number and the shorter ignition delay, the combustion noise level (CNL) is improved as well. With Blend-3 the FA emissions increase slightly, but due to the low level the FA emissions are negligible.
In the high load point without EGR the use of Blend-3 causes no significant change in the indicated efficiency, which is illustrated in Fig. 18. At high EGR rates, hence low NO_x emissions, the more complete combustion with the sustainable blend results in a higher efficiency. Compared to the low load point in Fig. 16, the differences in ignition delay and combustion duration become smaller due to the higher rail pressure. In line with the previous results, Blend-3 improves the emission behavior in the high load point as well, as can be seen in Fig. 19. Even in those conditions, when the indicated engine efficiency is lower, the CO_2 emissions are still reduced due to the better CO_2 factor of the Blend-3 fuel. Furthermore, the NO_x-smoke trade-off is slightly improved and

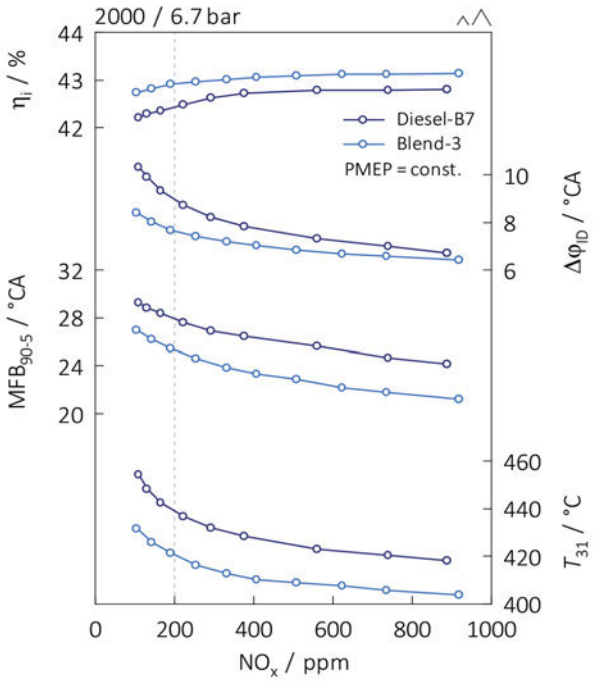

Fig. 16: Combustion parameters of the EGR sweep in a low load point

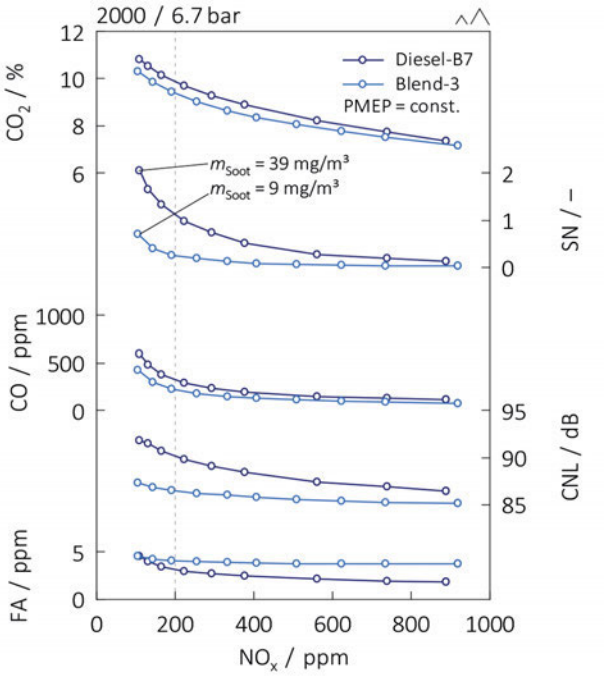

Fig. 17: Emission behavior of the EGR sweep in a low load point

Narr Francke Attempto Verlag GmbH + Co. KG

lower smoke- and/or NO_x emissions could be achieved. The CO emissions and the CNL are about the same. Again, the use of Blend-3 leads to a slight negligible increase of the FA emissions. The significant improvements found in the NOx-smoke trade-off leading to very low smoke levels enable as a next step the increase of the compression ratio (CR). This measure is a well-known way to improve the engine efficiency, however,

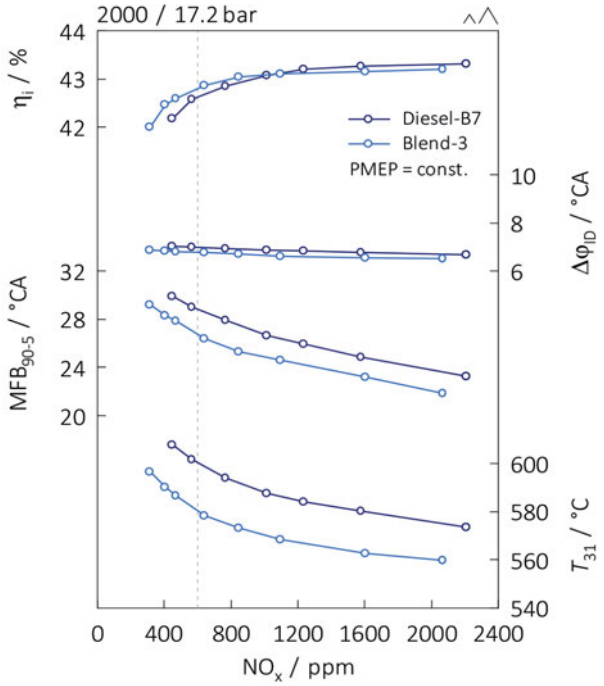

Fig. 18: Combustion parameters of the EGR sweep in a high load point

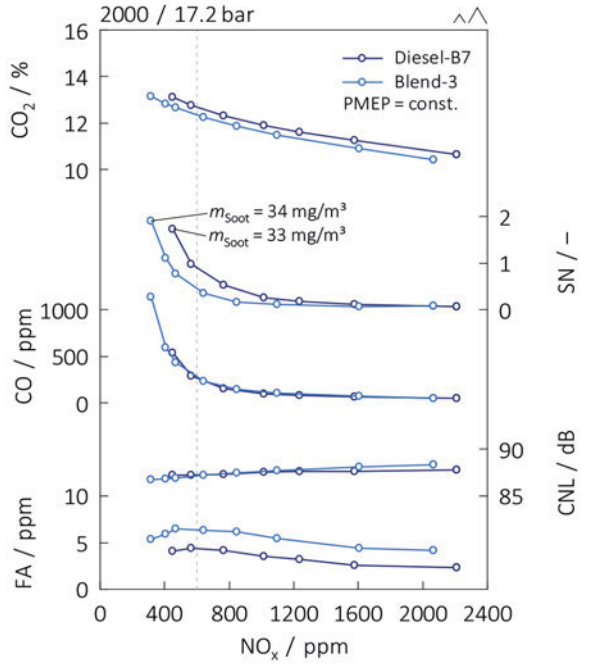

Fig. 19: Emission behavior of the EGR sweep in a high load point

a high CR also deteriorates on the other hand the NOx-smoke trade-off [5, 6].

3.3 Increase of the CR

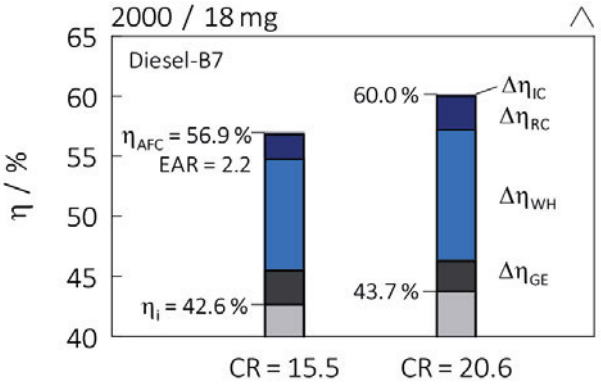

Fig. 20: Loss analyses of different compression ratios without EGR

Fig. 20 illustrates the loss analyses of the different CRs at constant EAR. The increase of the CR causes a higher efficiency of the AFC with real charge. As a consequence of the higher pressure at the end of the compression stroke and therefore shorter ignition delay, the combustion duration increases and deteriorates the real combustion loss. The higher pressure level during the combustion leads also to a higher wall heat loss. But due to the constant PMEP the gas exchange loss decreases with increased CR. Consequently, as a sum of these effects, a higher CR improves the indicated efficiency.

Narr Francke Attempto Verlag GmbH + Co. KG

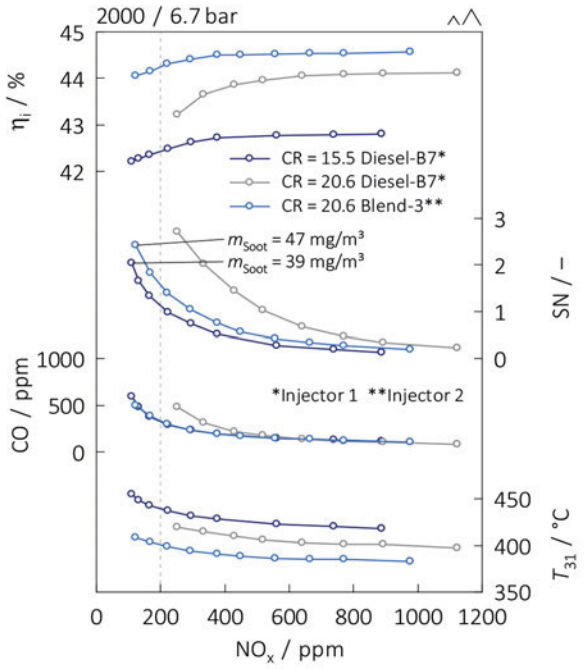

Fig. 21: Comparison of different CRs in a low load point

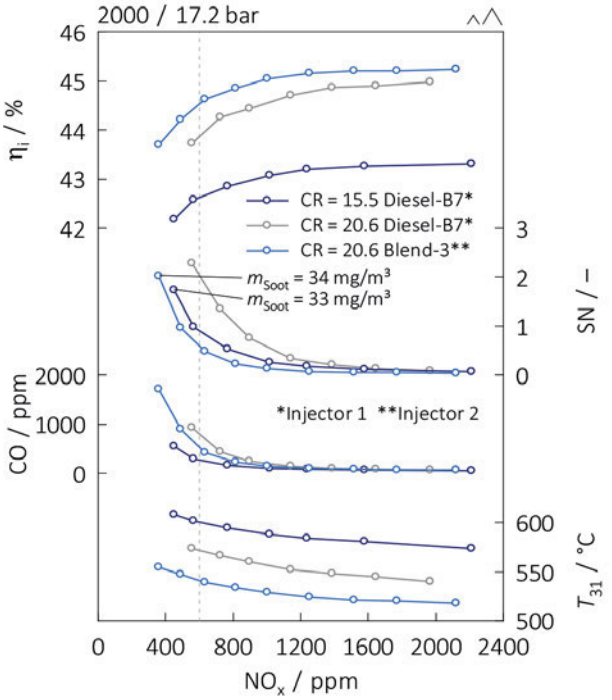

Fig. 22: Comparison of different CRs in a high load point

Fig. 21 depicts the EGR-sweep results with an increased CR with Diesel-B7 and Blend-3 in the low load point. In order to compensate the lower LHV of Blend-3 on the one hand, but also to take advantage of shortening the combustion duration to further improve efficiency at higher loads, the related test runs with Blend-3 were carried out with an injector nozzle having a 45% increased hydraulic flow rate, which is stated in Table 3.
With conventional diesel fuel the higher CR leads to a higher indicated engine efficiency due to the higher efficiency of the AFC and therefore a lower exhaust gas temperature. The shorter ignition delay due to the higher pressure at the end of the compression stroke causes a worsened initial fuel preparation and hence higher smoke emissions. Likewise, the shorter free fuel jet length deteriorates the mixture preparation as well. This is also reflected by the increase of the CO emissions, which are an indicator of an incomplete combustion.
Compared to the results with Diesel-B7, Blend-3 increases the indicated engine efficiency further due to the higher EAR and improved combustion. The oxygen content improves the NO_x-smoke trade-off significantly. With Blend-3 and the high CR the trade-off in this low load point nearly meets the one achieved with Diesel-B7 and the lower CR, while the indicated efficiency is appreciably increased.

As shown in Fig. 22, an increase of the CR with diesel fuel leads to the same effects in high load as in low load, namely a higher engine efficiency, the deterioration of the NO_x-smoke trade-off, a decreased exhaust gas temperature and higher CO emissions. The use of Blend-3 in combination with a high CR and a high flow injector at this high load point could even improve the NOx-smoke trade-off compared to Diesel-B7 with the low CR.
The key-outcome shown in these two diagrams is, that Blend-3 enables adaptations to the combustion system, such as the increase of the CR and the increase of the injector flow rate, resulting in a higher indicated efficiency at approximately the same NOx-smoke trade-off to be expected in the entire engine map.
In addition to the emission behavior, the effect of the increased CR on the sweet spot with the lowest fuel consumption in the engine map was investigated.

Narr Francke Attempto Verlag GmbH + Co. KG

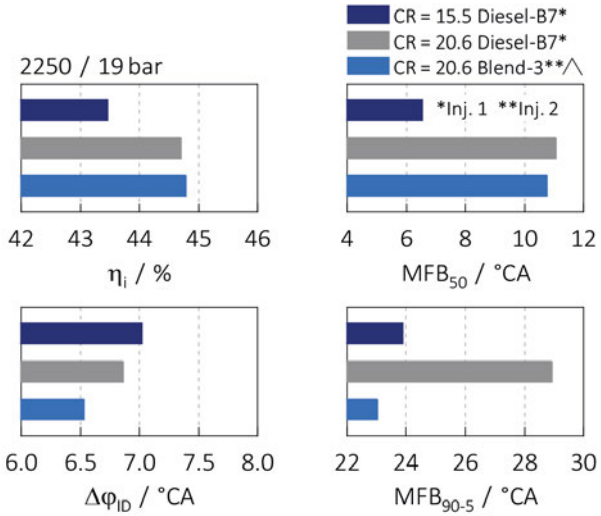

Fig. 23: Comparison of different CRs and fuels in the sweet spot

Fig. 23 shows the efficiency increase with the higher CR. The MFB_{50} needed to be retarded in order not to exceed maximum cylinder pressure. The higher cylinder pressure level and thus shorter ignition delay lead to a longer burning duration with diesel fuel. Blend-3 in combination with Inj. 2 increases the indicated efficiency due to the higher hydraulic injector flow rate and therefore shorter combustion duration. Furthermore, the influence of the higher cetane number of the trinary blend can be found as well.

3.4 Driving cycles

In order to compare the alternative blend with conventional diesel fuel in a dynamic, series-relevant approval cycle, WLTCs were carried out with a four-cylinder CI engine, whose technical data is stated in Table 4.

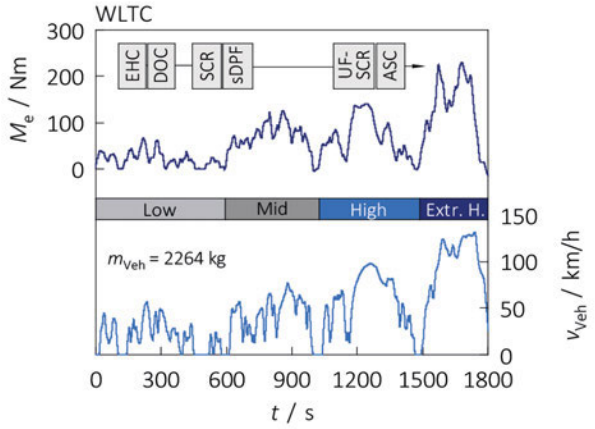

Fig. 24: Emulated WLTC with the EAS architecture

The test cycle as well as the used EU7-capable EAS are illustrated in Fig. 24. To comply with the required nitrogen oxide emission legislation limit in all driving situations, an electrically heated catalyst (EHC), located in front of the diesel oxidation catalyst, is used in addition to the loading-based SCR double dosing system. The required heating energy is recovered via load point shifting. Any possible NH_3 slip is oxidized by the ammonia slip catalyst at the end of the whole exhaust gas aftertreatment system.

To be able to run the test cycles on a dynamic test bench, the dynamic behavior of a PC was needed to be emulated. Therefore with a longitudinal dynamic simulation the target torque curve of a heavy Sport Utility Vehicle (SUV), which is among the most demanding applications for a 2.0l four-cylinder engine in terms of engine-emission, was determined and used on the test bench.

In order to counteract an undesirable shift of the engine operating point in the engine control unit maps due to the lower LHV of Blend-3 and therefore higher injection quantity, the engine maps were adapted to assure similar calibration settings.

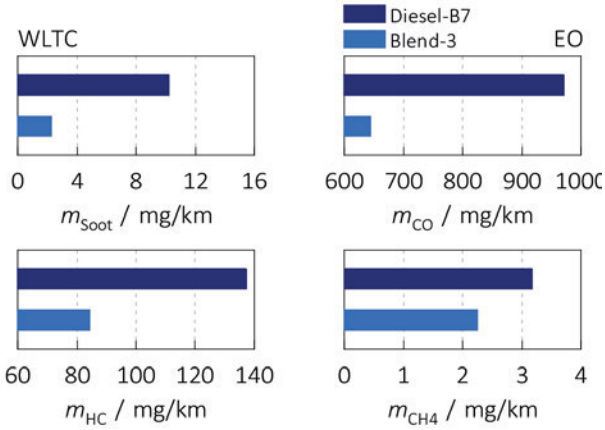

Fig. 25: Comparison of the EO emissions in the WLTC

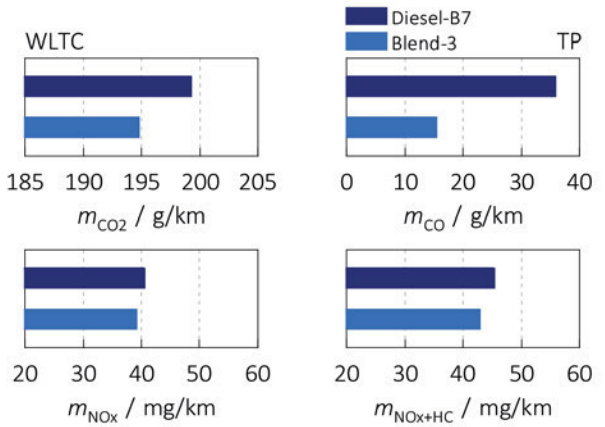

Fig. 26: Comparison of the TP emissions in the WLTC

Fig. 25 depicts the different engine-out (EO) emissions in the WLTC with the investigated fuels. Also in the cumulative cycle emissions it is obvious, that the oxygen

Narr Francke Attempto Verlag GmbH + Co. KG

content in the trinary blend causes a more complete combustion and thus significantly lower soot, CO, hydrocarbon (HC) and CH_4 emissions at approximately the same engine-out NO_x emissions.
As shown in Fig. 26, also the measured tailpipe (TP) emissions are reduced due to the use of Blend-3.
As a consequence of the lower CO_2 factor of the trinary blend, the CO_2 emissions are reduced despite a higher volumetric fuel consumption as a result of the lower LHV of Blend-3. Furthermore, the CO and HC emissions are reduced at very low NO_x (TP) emissions of about 40mg/km.
The results achieved on the multi-cylinder engine along the WLTC cycle confirm all the main findings gathered during the SCRE tests and confirmed the flawless operation of the EAS also when using the sustainable Blend-3 fuel.

4. Conclusion and outlook

The present work investigates the effects of a trinary fuel blend, fulfilling EN 590 and RED-II legislation, on thermodynamics and on the emission behavior in a CI engine of PC size. Since alternative fuels are able to make a major contribution to the decarbonization of transportation and moreover promote the achievement of the CO_2 targets car manufacturers have to fulfill, a trinary blend consisting of HVO, ethers and alcohols was defined.
This fuel blend was investigated in various test runs carried out on a state-of-the-art CI SCRE for steady state thermodynamic and emission measurements. In addition WLTC driving cycles were carried out on a four-cylinder CI engine.
The oxygen content of about 10% leads to significant NO_x-smoke trade-off improvements at low as well as high engine loads and reduces unburned exhaust gas emission components. Furthermore, the CNL is improved due to the higher cetane number. As a consequence of the oxygen content, the higher EAR and the shorter combustion duration improve the indicated engine efficiency at low load. At high load the efficiency only increases at higher EGR rates and thus low NO_x emissions due to a more complete combustion. The applied temperature measurement equipment in the piston cooling flow indicated a higher wall heat loss with Blend-3 and verified the result of the loss analysis.
The significant trade-off improvements enable adaptations to the combustion system to further improve engine efficiency and reduce CO_2 emissions. It is shown that when increasing the CR in combination with an injector with a higher hydraulic flow rate to compensate the lower LHV and reduce the combustion duration, the trinary blend increases the indicated efficiency by about two percent points at approximately the same NO_x-smoke trade-off (expected in the entire engine map) over a CI engine fueled with conventional diesel. Hence, the oxygen content in the fuel, which basically reduces smoke emissions, was successfully used to increase the efficiency via engine combustion hardware optimization.
In the WLTC Blend-3 nearly thirded the engine-out soot emissions at the same NO_x emissions, which were at a low tailpipe level of about 40mg. Besides the lower HC and CO emissions, the CO_2 emissions were decreased due to the lower CO_2 factor of this renewable blend compared to conventional diesel fuel.
Due to the high amount of OME in the fuel, it is assumed, that this fuel is not compatible with the current car fleet. Hardware adaption measures, especially sealing materials of the fuel system, are necessary for the use of the trinary blend.
Besides the afore shown tank-to-wheel considerations, a well-to-wheel analysis of this promising fuel will illustrate the importance of the production process of the renewable blend components to reduce the total CO_2 emissions even further.

5. Acknowledgements

This study is part of the research project “RC-LowCAP”, which is a publicly funded project by the Austrian Research Promotion Agency (FFG) with partners from the industry AVL, OMV (Downstream), Vitesco Technologies Emitec and Heraeus.

References

[1] Zubel, M., Bhardwaj, O. P., Heuser, B., Holderbaum, B., Doerr, S., Nuottimäki, J.: “Advanced Fuel Formulation Approach using Blends of Paraffinic and Oxygenated Biofuels:
Analysis of Emission Reduction Potential in a High Efficiency Diesel Combustion System”, SAE Technical Paper 2016-01-2179, 2016, doi:10.4271/2016-01-2179

[2] Richter, G., Zellbeck, H.: ”OME als Kraftstoffersatz im Pkw-Dieselmotor”, MTZ Motortech Z 78(12):66-73, 2017, doi:10.1007/s35146-017-0131-y

[3] Aatola, H., Larmi, M., Sarjovaara, T., Mikkonen, S.: ”Hydrotreated Vegetable Oil (HVO) as a Renewable Diesel Fuel: Trade-off between NOx , Particulate Emission, and Fuel Consumption of a Heavy Duty Engine”, SAE Technical Paper 2008-01-2500, 2008, doi:10.4271/2008-01-2500

[4] ÖNORM EN 590:2019-08-01: “Automotive fuels – Diesel – Requirements and test methods”, Austrian Standards International, Vienna, 2019

[5] Commission Regulation (EU) 2018/2001, Official Journal of the European Union L328, 2018

[6] Nenning, L., Eichlseder, H., Egert, M.: “Cold Emission Optimization of a Diesel- and alternative fuel-driven CI Engine”, unpublished manuscript submitted for publication, Automotive and Engine Technology

[5] Minamino, R., Kawabe, T., Omote, H., and Okada, S.: “The Effect of Compression Ratio on Low Soot Emission from a Small Non-Road Diesel En-

Narr Francke Attempto Verlag GmbH + Co. KG

gines", SAE Technical Paper 2013-24-0060, 2013, doi:10.4271/2013-24-0060

[6] Pellegrini, L.: "Investigation of the Effect of Compression Ratio on the Combustion Behavior and Emission Performance of HVO Blended Diesel Fuels in a Single-Cylinder Light-Duty Diesel Engine", SAE Technical Paper 2015-01-0898, 2015, doi:10.4271/2015-01-0898

[7] Merker, G., Schwarz, C., Stiesch, G., Otto, F.: "Verbrennungsmotoren, Simulation der Verbrennung und Schadstoffbildung", Vieweg+Teubner Verlag, 3. Auflage, Wiesbaden, 2006, DOI: 10.1007/978-3-8351-9069-6

6. Appendix

Table 2: Test fuel properties [6]

Fuel property	Unit	Diesel-B7	Blend-3
Cetane number	–	42	61.5
Density (15°C)	kg/m³	838.7	824.7
LHV	MJ/kg	42.66	38.72
H/C Ratio	–	1.89	2.22
Stoichiometric Air Demand	kg/kg	14.52	12.99
Carbon content	%	85.9	75.0
Hydrogen content	%	13.6	14.0
Oxygen content	%	0.9	10.7
Total aromatics content	%	19.9	0.2
Viscosity (40°C)	mm²/s	2.80	2.58
Flash point	°C	67	71
T_{10}	°C	207.2	188.4
T_{50}	°C	274.4	234.7
T_{90}	°C	338.1	287.5
CO_2 factor	g/MJ	73.8	71.0

Table 3: Diesel injectors

Abbrevation	Hole diameter	Flow rate
Injector 1	108µm	620ml/min
Injector 2	130µm	900ml/min

Table 4: Four-cylinder engine specification

Bore	84mm
Stroke	90mm
Displacement	1995cm³
Compression ratio	16.5
Number of valves	4
Max. cyl. pressure	150bar
Rated speed	4000min^{-1}

Technology	Common-rail injection system
	Bosch CP4.1 fuel pump
	Bosch CRI 2-20 injectors
	VNT turbocharger
	Variable oil pump
	HP-EGR (cooled, with bypass)
	SCR with double injection

7. Abbreviations, Symbols and Indices

AFC	Standard air fuel cycle
ASC	Ammonia slip catalyst
BMEP	Break mean effective pressure
CNL	Combustion noise level
CO	Carbon monoxide
CO_2	Carbon dioxide
CA	Crank angle
CH_4	Methane
CI	Compression ignition
CR	Compression ratio
CYL	Cylinder
DIST	Distillation
DOC	Diesel oxidation catalyst
EAR	Excess air ratio
EAS	Exhaust aftertreatment system
EGR	Exhaust gas recirculation
EHC	Electrically heated catalyst
EO	Engine-out
HC	Hydrocarbon
HP	High-pressure
HVO	Hydrated Vegetable Oil
ID	Ignition delay
IMEP	Indicated mean effective pressure
LHV	Lower heating value
MCE	Multi-cylinder engine
MFB	Mass fraction burned
NOx	Nitrogen oxide
OME	Oxymethylene ethers
PC	Passenger car
PMEP	Pumping mean effective pressure
RED	Renewable energy directive
RME	Rapeseed methyl ester
ROHR	Rate of heat release
SCR	Selective catalytic reduction
SCRE	Single cylinder research engine
sDPF	SCR-coated diesel particulate filter
SN	Smoke number
SUV	Sports Utility Vehicle
TC	Turbocharger
TP	Tailpipe
UF	Under-floor
VOL	Volumetric
WLTC	Worldwide harmonized light vehicles test cycle
c	Specific heat capacity
H, h	Enthalpy

Narr Francke Attempto Verlag GmbH + Co. KG

m	Mass
p	Pressure
Q	Energy
T	Temperature
U	Internal energy
W	Work
$\Delta\eta_{IC}$	Imperfect combustion loss
$\Delta\eta_{GE}$	Gas exchange loss
$\Delta\eta_{RC}$	Real combustion loss
$\Delta\eta_{WH}$	Wall heat loss
η	Efficiency
η_{CV}	Degree of constant volume
χ	Heat capacity ratio
λ	Stoichiometric air to fuel ratio
μ	Mass fraction
ρ	Density
φ	Angle
20	Charge air
21	Intake manifold
31	Engine-out
32	Damping vessel
e	Effective
i	Indicated

Narr Francke Attempto Verlag GmbH + Co. KG

Beyond GHG: Cradle-to-grave impact of renewable energy-fuelled mobility on water consumption and eutrophication

Victor Gordillo Zavaleta*
Aramco Fuel Research Center, Aramco Overseas BV, 232 Avenue Napoléon Bonaparte, 92500 Rueil-Malmaison, France

Alexander Stoffregen and Oliver Schuller
Sphera, Hauptstraße 111-113, 70771 Leinfelden-Echterdingen, Germany
* Corresponding author: victor.gordillo@aramcooverseas.com +31 88 262 24 99

Summary

The study focuses on the environmental impacts of a selected number of vehicles and energy propulsions at horizon 2030, in particular water consumption and freshwater eutrophication. Greenhouse gas emissions are also analysed. Powertrains include conventional internal combustion engine vehicles, battery electric vehicles and fuel cell electric vehicles. For each powertrain type, renewable energy sources like biofuels and power-to-liquid fuels are compared to conventional sources like fossil fuels and the grid electricity mix. The differences found in the study show that both the manufacturing and use phase play an important role in the life cycle impacts. Electrified solutions show higher impacts during their manufacturing stage, which are generally compensated by better engine efficiencies during their use phases, but under certain conditions conventional thermal powertrains can achieve similar results, especially for greenhouse gas emissions and water consumption. The source of energy chosen for vehicle propulsion and PtL production is critical. The study also shows the substantial impact of materials on water consumption and eutrophication, in particular for battery electric vehicles. The study concludes that for light duty vehicles, multiple parameters and criteria should be used to provide an environmental impact assessment.

1. Introduction

In recent years, renewable energy-fuelled transport solutions have increasingly gained attention because of their generally accepted potential to mitigate global warming. Liquid renewable fuels in particular are considered as a viable solution, as they can be used in the legacy fleet of road, air and marine transportation. In the particular case of drop-in liquid advanced fuels, they would also claim the advantage of minimizing the need of significant modifications in the fuel supply chain or engine retro-fitting, making them an solution well-suited during the period of energy transition.
While the discussions about the main challenges for the adoption of these mobility solutions generally include the intermittency of renewable power, direct and indirect land use, the recognition of carbon sources as sustainable, and the guarantee of origins of the renewable energy used in their production, the question of water use by these alternative pathways is vital. Impacts on water resources are present in critical steps such as electrolysis, battery and equipment manufacturing, agriculture and waste treatment processes. The present study addresses two main impacts affecting water bodies: The impact of water consumption and the eutrophication of freshwater. Both impact factors are assessed for a selected number of mobility solutions, including battery electric vehicles and internal combustion engine vehicles running on advanced renewable drop-in fuels, such as second generation biofuels and power-to-liquid (PtL) fuels. Europe in 2030 has been chosen as time and location reference for the manufacturing processes.
The analysis applies the principles of Life Cycle Assessment (LCA) on a modelling platform built on software application GaBi (licenced by Sphera). This same platform was used to carry out greenhouse gas (GHG) emission studies on vehicles in the past years [1] [2]. The present study is the first published work focusing on water and eutrophication impact categories based on this same model.

2. Scope

2.1 Methodology

For the environmental assessment, a life-cycle approach following ISO 14040:2006 [3] and ISO14044:2006 [4]

Narr Francke Attempto Verlag GmbH + Co. KG

was chosen. Data for the foreground system (carbon capture, hydrogen and syngas production, fuel synthesis, passenger vehicles and lithium-ion battery manufacturing) were taken from various literature sources. Background data, such as life-cycle inventory (LCI) data for energy (electricity, conventional fuels) and material supply were taken from Sphera's GaBi LCI databases 2021 [5]. The LCA models were created using the GaBi software system for life-cycle engineering [5].

2.2 System boundaries and cut-off

All impact categories considered are analysed on a cradle-to-grave (CTG) basis, meaning that they include direct emissions from power, fuel and vehicle manufacturing, but also plant infrastructure building and end-of-life. The methodological approach is Attributional LCA (ALCA), so all emissions are calculated as averages based on one specific life cycle inventory.
Most energy and material flows as well as emissions for the foreground system are included in the model. No specific cut-off criteria was defined for the assessment.

2.3 Allocation

In cases where several products were produced from the PtL synthesis (e.g. Methanol-to-Gasoline, Fischer-Tropsch pathways) and for conventional fuels, allocation to split-up impacts between the different products was done based on the energy content (lower heating value, LHV) of the products.

2.4 Impact categories considered

The main focus of the study are two impact categories from the EF 3.0 [6] methodology chosen for the life-cycle impact assessment (LCIA):

- **EF 3.0 Water use** (ILCD Level of recommendation III): A midpoint impact category measuring the water consumption impact as the quantity of water deprived (water scarcity), according to the model Available WAter REmaining (AWARE) [7]. This impact is recommended by the Product Environmental Footprint (PEF) initiative by the European Commission, and measured in units of cubic meters of world water-equivalent (m^3world$^-$eq).
- **EF 3.0 Freshwater eutrophication** (ILCD Level of recommendation II): A midpoint impact category measuring the excess nutrient availability in freshwater bodies, leading to phenomena such as harmful algal blooms (HABs) [8]. This impact factor is calculated according to the EUTREND model, used in LCA method ReCiPe 2008. Contrary to terrestrial or marine eutrophication, both expressed in units of nitrogen equivalent, in freshwater environments phosphorus is considered the limiting factor in pure form or in the form of phosphates and phosphoric acid. For this reason, freshwater eutrophication is measured in kg of phosphorus-equivalent (kgPO_4-eq)
- Alternatively and to provide the context of previous studies, this paper also provides figures for the impact category Climate Change, represented by its corresponding characterisation factor in EF 3.0. This impact is calculated using a baseline model of 100 years of the IPCC 2013 model [9].

3. Life Cycle Inventories

3.1 Fossil fuels

Fossil gasoline and diesel fuels are obtained via crude oil distillation and upgrading in oil refineries. Typically, the calculation of environmental impacts of a conventional fuel takes into account specific refinery configurations related to its production. For the present study and considering the variety of such configurations in Europe, impact category values come from an average European refinery production scheme and crude slate, as available in the GaBi LCI database [5]. For the calculation, direct refinery emissions were allocated based on the mass of the co-products when required. Emissions related to crude oil consumption where allocated by energy content (lower heating value) [10].

3.2 Hydrogen

Hydrogen (H_2) can be directly used as fuel-in-fuel cell electric vehicles or as feedstock, together with carbon dioxide, for PtL fuels. Although hydrogen is today predominantly produced via production routes using fossil energy, such as steam methane reforming (SMR) [11], PtL fuels as such are defined by the usage of electricity as energy input and therefore use water electrolysis to produce the hydrogen. Within the electrolysis, water is converted through an electrochemical process into hydrogen and oxygen:

= +286 kJ/mol

Several electrolysis technologies exist. Alkaline electrolysis (AE) and proton exchange membrane (PEM) electrolysis working on low temperature (70-90°C) and solid oxide electrolysis cells (SOEC) working on high temperature (650-850°C) requiring an additional heat source beside the electricity supply. Alkaline electrolysis, as the oldest and proved water electrolysis technology [12], were currently installed in industry scale with capacities up to 10 MW and proposed projects in the 100 MW [13] scale are underway.

Narr Francke Attempto Verlag GmbH + Co. KG

Table 1: Technical parameters of alk aline electrolysis

Reference year	2030
Efficiency (Low heating value) [11]	68.0%
Power consumption [kWh/kg H_2]	49.0
Water consumption [kg/kg]	15
Pressure (outlet) [bar]	30

This study assumes two types of hydrogen: Conventional hydrogen from SMR (also called grey hydrogen), and hydrogen produced from alkaline electrolysis of water and wind electricity (green hydrogen). Table 1 summarises the technical specifications of alkaline electrolysers used to produce green hydrogen.

3.3 Carbon capture

PtL fuels require a carbon source in the form of carbon dioxide (CO_2) that can be either extracted from ambient air or from flue gases or gas mixtures from which CO_2 needs to be separated. Especially for the separation of CO_2 from an industrial gas (e.g., synthesis gas from a steam methane reformer), a multitude of proven technologies for industrial scale exist [14]. These technologies include chemical absorption with amine, physical absorption with water or an organic solvent, pressure swing adsorption (PSA), membrane or cryogenic methods. Carbon sources for specific PtL plants are ideally located next to the plant to avoid CO_2 transportation.
Beyond 2030, point sources of CO_2 are expected to become scarce, and PtL plants will be probably installed in areas close to renewable electricity generation farms, usually in remote areas. In this context, direct air capture (DAC) could be a promising solution. An important difference between DAC and carbon capture from point sources is the concentration of CO_2 in the used gas (0.04% for ambient air, 3-15% for power plants and up to 100% for, e.g., ammonia plants) [15] and the related energy consumption for CO_2 separation and purification. Table 2 shows the electricity and heat demands for a low temperature DAC per kg of captured CO_2 used in this study. For the sake of comparison, in a coal power plant with 13% CO_2 concentration in its flue gas, the energy consumption by chemical absorption using amines would drop to 0.024 kWh electricity and 3.0 MJ of thermal energy per kg of captured CO2. [14]

Table 2: Technical parameters of low-temperature Direct Air Capture (DAC) unit

Power consumption [kWh/kg CO_2]	0.504
of which power for CO_2 desorption [16]	*0.40*
power for CO_2 purification [17]	*0.104*
Heat consumption [kWh/kg CO_2] [16]	**1.60**

3.4 Fischer-Tropsch diesel

Fischer-Tropsch (FT) fuels, such as synthetic diesel, gasoline or kerosene from fossil-derived syngas are proven technologies at commercial scale. Some examples are gasification of coal, like Sasol's 160,000 barrels per day Coal-to-Liquid facility in South Africa [18], and steam reforming of natural gas, like Shell's 140,000 barrels per day Pearl Gas-to-Liquid plant in Qatar [19]. So far, PtL projects using FT synthesis to produce hydrocarbons, like the Sunfire pilot plant in Dresden (Germany), are still in a demonstration/research scale with low capacities. Nordic Blue Crude together with Sunfire and Climeworks have announced their intention to build a 20 MW plant (related to electricity input) by 2022 [20].
The simplified FT reaction can be described as the following:
= -152 kJ/mol [21]
Carbon monoxide (CO) is a constituent of syngas, but in the case of PtL projects, it has to be obtained from reduction of the captured CO_2. The reverse water gas-shift reaction (RWGS) allows this conversion at high pressures (30 bar) and temperatures (800-1000 °C). The selectivity can be improved by recycling the unreacted constituents, although reducing the energy efficiency of the process [22].
= +42 kJ/mol [22]
Beside alkanes, some alkenes, alcohols and carboxylic acids are formed. For all products, the molar ratio of the syngas is approximately 2 mol H_2 to 1 mol CO. The product slate is predominantly influenced by the temperature of the FT reaction, on average resulting in lighter hydrocarbons for high temperatures FT (320-350°C) and heavier hydrocarbons for low temperatures FT (190-250°C). To maximize the yield of transport fuels (gasoline, diesel, kerosene) a low temperature FT was chosen for this study, combined with a hydrocracking step to convert the produced wax into LPG, gasoline, diesel and kerosene. This results in a product slate indicated in of 37% gasoline, 28% diesel, 32% kerosene and 3% LPG [23]. Mass balance, electricity and thermal energy inputs for the FT synthesis as well as refining/hydrocracking information are shown in Table 3.

Table 3: Technical parameters of Reverse Water Gas Shift + Fischer-Tropsch + Hydrocracking system

H_2 consumption [kg/kg_{fuel}]	0.50
CO_2 consumption [kg/kg_{fuel}]	3.80
Light ends production [kg/kg_{fuel}]	0.27
Fuel production [kg_{fuel}]	1
Water production [kg/kg_{fuel}]	3.03
Power consumption [kWh/kg_{fuel}]	0.53
Net heat production [kWh/kg_{fuel}]	2.56

Narr Francke Attempto Verlag GmbH + Co. KG

3.5 Methanol-to-Gasoline (MTG)

Synthetic methanol from electricity for the methanol-to-gasoline (MTG) synthesis can be either supplied via two-step synthesis using a synthesis gas (2-step route) or a one step process that uses CO_2 directly as feedstock (direct route). A first example of a PtL plant using the direct methanol synthesis is the George Olah plant in Iceland, run by CRI with a capacity of 4,000 t/a [24], whose material balance was used as a reference.

= -49.2 kJ/mol [24]

The methanol-to-gasoline (MTG) process was developed by Mobil in the 1970s. Commercial applications of the MTG process with capacities up to 1 Mt/a (Shanxi, China) have been realised [25]. Within the process, methanol is partially dehydrated to dimethyl ether (DME), followed by olefin and aromatic/paraffin formation using a zeolite catalyst [26]:

The overall mass and energy balances of both steps of the reaction are shown in Table 4.

Table 4: Technical parameters of Methanol synthesis + Methanol-to-Gasoline reaction

H_2 consumption [kg/kg_{fuel}]	0.47
CO_2 consumption [kg/kg_{fuel}]	3.42
Light ends production [kg/kg_{fuel}]	0.08
Fuel production [kg_{fuel}]	1
Water production [kg/kg_{fuel}]	2.81
Power consumption [kWh/kg_{fuel}]	1.26
Net heat production [kWh/kg_{fuel}]	1.44

Like for the FT pathway, the additional energy supply required for carbon capture would drop if a higher concentration point source were used instead of atmospheric CO_2.

3.6 Hydrotreated Vegetable Oil (HVO)

Hydrotreated Vegetable Oil (HVO) is a biofuel, constituted by a mix of paraffinic hydrocarbon chains obtained from hydrotreatment and hydrocracking of triglycerides of vegetable origin. Triglycerides, the main components of vegetable fats, are esters derived from glycerol and linear carboxylic acids known as fatty acids. By the action of hydrogen, triglycerides undergo several reaction steps:

- Hydrogenation to saturate the double bonds present in the linear structure of the vegetable oils.
- Hydrocracking of the saturated triglycerides to break their esteric structure into three fatty acids and propane. The latter, along with small quantities produced of LPG and naphtha (around 5% the mass of HVO) can be used to produce electricity and steam.
- Either deoxygenation or decarboxylation of the fatty acids, which produces water or carbon dioxide respectively along with linear hydrocarbons of around 17 to 18 carbons. These molecules have similar carbon length as those of fossil diesel with a more paraffinic nature, leading to higher cetane number but lower density and poorer cold properties. Further processing (isomerisation) can be applied to improve some of these properties.

The chemical reactions are represented below:

Triglycerides are also the raw material to produce another type of biofuels known as Fatty Acid Methyl Esters (FAME). FAME is formed by a mix of esters from esterification of vegetable fats, therefore its chemical nature is different from HVO's.

We propose two types of HVO feedstock for this study: A mix of rapeseed and sunflower oil (50% of each on an energy basis) to represent first-generation (1G) biofuels, and used cooking oil (UCO) for second-generation (2G) biofuels.

In our assumptions, all raw vegetable oils as well as the used cooking oil are produced in Europe. UCO is assumed to be a burden-free waste and as such, it does not support any allocation of any impact. Hydrogen consumed in the process is assumed to come from steam methane reforming (grey hydrogen). The material and energy balances used for HVO production are taken from public data from Neste Oil [27] [28] and shown in Table 5.

Table 5: Technical parameters of HVO (2G) production

UCO consumption [kg/kg_{fuel}]	1.21
H_2 consumption [kg/kg_{fuel}]	0.04
Light ends production [kg/kg_{fuel}]	0.05
Fuel production [kg_{fuel}]	1
Water production [kg/kg_{fuel}]	0.10
Waste production [kg/kgfuel]	0.10
Power consumption [kWh/kg_{fuel}]	0.04
Heat consumption [kWh/kg_{fuel}]	0.19

The UCO supply (collection and transport) is considered to be carried out as follows:

- Feedstock collection: 50 km collection route by truck within urban area, 50% payload, 14-20 t gross vehicle weight (GVW)

Feedstock transport: 100 km distance by truck between collection location and HVO plant, 34-40 t GVW.

3.7 Passenger vehicles

The reference vehicles considered for the present study are passenger vehicles of the C-Segment (medium cars), similar to VW Golf, Ford Focus or Opel Astra.

Powertrains include 4 variants of 3 types of powertrains: Internal combustion engine vehicles (ICEV) running on either gasoline or diesel, battery electric vehicles (BEV), and fuel cell hydrogen electric vehicles (FCEV). The weights of the vehicles in 2030 are based on the JEC

Narr Francke Attempto Verlag GmbH + Co. KG

TTW report v5 [29], with some adjustments for electrified vehicles in link with the weight of the batteries.

3.8 Batteries

Lithium-ion batteries used by BEVs, PHEVs, HEVs and FCEVs were assumed to be built with chemistry technology Nickel-Manganese-Cobalt in proportions 80:10:10 respectively (NMC 811), with an energy density of 250 Wh/kg. Europe was chosen as the manufacturing location at horizon 2030. The emission factors of aluminium, electricity and thermal sources were calibrated consistently. The weights of the batteries were calculated from the life cycle inventories taken from the BatPac [30] model.

4. Model parameters

4.1 Assumptions for vehicles and batteries

The main assumptions and input parameters to calculate TTW GHG emissions are summarized in Table 2. TTW emissions are calculated based on energy consumption of vehicles in MJ per km and fuel emission factors per MJ. Vehicle energy consumptions (MJ/km in WLTP) are derived from 2025+ figures in the JEC TTW study v5 [29]. The lifetime average vehicle mileage is assumed to be 200,000 km for all vehicle types.

During the end-of-life stage of vehicles and batteries, two types of emission credits are assumed:

- Credits related to the recovery of materials such as steel, aluminium, polypropylene, copper, glass or magnesium, present mainly in the chassis and internal structure of the vehicles. Battery acid as well as fluids are also partly recovered. For batteries, this is extended to the recovery of rare materials from the cathode (lithium, cobalt) and for fuel cells, to platinum.
- Credits related to the production of energy from material incineration, mostly tyres, polymers and carbon fiber.

Table 6: Assumptions for passenger vehicles

Powertrain	WLTP Energy consumption [MJ/km]	Battery size [kWh]
ICE Gasoline	1.41 (4.4 L/100 km)	--
ICE Diesel	1.30 (3.6 L/100 km)	--
BEV (200 km range)	0.43 (11.9 kWh/100 km)	24.7
FCEV*	0.70 (0.58 kg/100 km)	1.2

*Assuming a fuel cell power of 100 kW

4.2 Assumptions for fuels and electricity

Electricity and thermal energy sources are used throughout all the processes of fuel production and vehicle manufacturing. The sources are consistent with the location chosen, Europe.
For the electricity consumed in PtL and hydrogenation processes, we assume the use of 100% renewable electricity as a default value for PtL production in this study.
By default, heat integration was active for the PtL processes, meaning that the heat produced by the exothermic reactions (typically fuel synthesis) is recovered and made available for upstream processes requiring heat (carbon capture, reverse water-gas shift) assuming an 80% recovery. Additional heat required in the process is obtained from electricity via a heat pump with an efficiency of 90% heat recovered from the electricity consumed.
Table 7 summarises the impact categories for all the sources of energy used in this study per unit of energy (MJ) of fuel.

Table 7: Assumptions for vehicle energy sources

Fuel	Fuel type	Lower heating value (LHV) [MJ/kg]	EF 3.0 Climate change factor [g CO_2-eq/MJ]	EF 3.0 Water use [Lworld-eq/MJ]	EF 3.0 Eutrophication, freshwater [mg P-eq/MJ]
Diesel	Fossil	43.1	87.7	0.2	0.02
	HVO (1G)	44.0	38.4	11.7	9.38
	HVO (2G)		12.0	~0	0.01
	e-FT diesel		9.9	1.9	0.10
Gasoline	Fossil	43.2	94.4	0.2	0.05
	e-MTG		9.6	1.9	0.10
Electricity	EU mix*	-	86.2	15.2	0.42
	Wind		2.9	0.15	0.01
Hydrogen	Grey	120.0	85.7	0.1	0.16
	Green		5.4	3.5	0.04

HVO (2G) = Second generation hydrotreated vegetable oils / FT = Fischer-Trosch / MTG = Methanol-to-Gasoline
*Assuming mix from IEA Current Policies scenario (2030)

5. Results and Discussion

5.1 Greenhouse gas emissions

The results of cumulated greenhouse gas emissions generated during the life cycle of a passenger vehicle for

Narr Francke Attempto Verlag GmbH + Co. KG

all the vehicle/fuel combinations are shown in Figure 1. Both fossil fuelled vehicles emit the largest amount of GHGs (26.4 and 30.1 t CO_2-eq for diesel and gasoline ICEVs respectively), essentially produced during the use phase. These emissions include not only tailpipe gases (representing 73-83% of the total use phase) but also emissions from the production of the fuel and crude oil extraction. A small part of the impact of this use phase (2.0-2.5%) comes from diverse operating materials consumed like fluids or tyres. Results for ICEV compared to BEVs (12.4 t CO_2-eq when using grid electricity) and FCEVs (17.4 t CO_2-eq when using grey hydrogen), show that the difference in use phase emissions largely outweighs the initial disadvantage of electrified alternatives related to their manufacturing phase emissions. This disadvantage comes from their more energy-intensive manufacturing process associated to elements such as the lithium-ion battery, the fuel cell and the compressed hydrogen tank. The carbon burden associated to these elements is quickly compensated by the combination of the higher engine efficiency and, when using cleaner sources like wind electricity or green hydrogen, a lower carbon-intensive energy source.

This apparently inherent disadvantage for ICEVs can be drastically reduced when replacing the fossil fuel with a renewable alternative, either biofuel (HVO) or PtL fuel (MTG gasoline, e-FT diesel). The GHG emissions from a conventional diesel ICEV can be almost cut by half when substituting the fossil fuel by a first generation biofuel. The reduction can be further halved if the biofuel is produced from waste (2G). These calculations are based on a specific allocation methodology applied to biofuels. Variations of this methodology could result in meaningful differences not covered by the present study but explored in a separate piece of work [2].

The benefits of switching to renewable fuels also applies to electrified transport solutions, as shown in Figure 1. The impact of the use of wind electricity in BEVs or green hydrogen produced with wind electricity for FCEV (green H_2) also lowers substantially the climate change impact of the conventional variants. When focused on the use phase of these vehicles, the reduction reaches levels close to 90% in both cases. This relative reduction is higher than in the case of ICEVs, but it does not affect the initial burden of the vehicle and battery manufacturing stage.

It is important to notice that the burden of electrified solutions running on full renewable energy are of the same order of magnitude than conventional vehicles using renewable fuels.

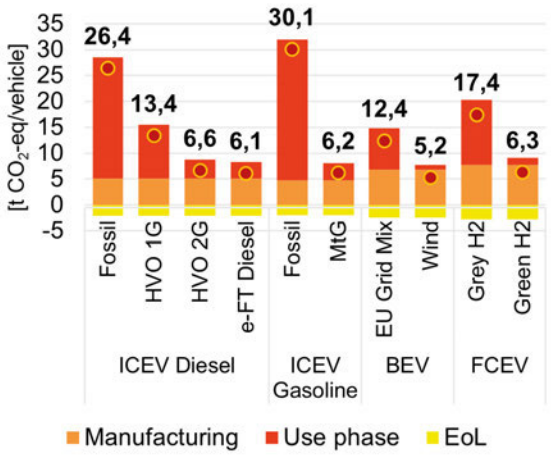

Figure 1: Cumulated GHG emissions of passenger vehicles in 2030

5.2 Water use

Figure 2 depicts the results of water use (measured according to the Water Scarcity impact category from EF 3.0) for all the transportation options analysed. Conventional fossil-fuelled ICEVs and FCEVs show similar levels of water consumption, of around 0.9 million litres of world-equivalent water per vehicle. BEVs powered with the EU Grid mix from 2030 (based on the IEA's New Policies Scenario) represent a consumption of more than 2.5 times the conventional options, with burdens coming from both the manufacturing and use phases.

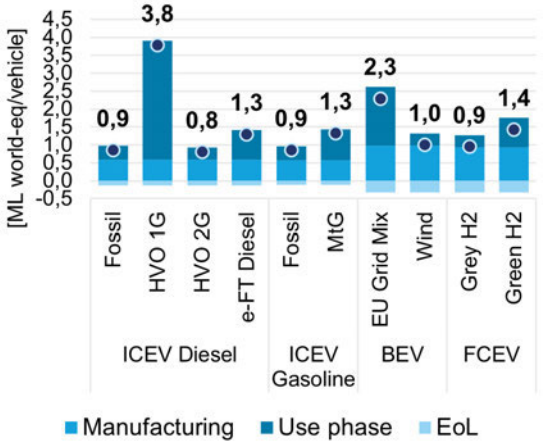

Figure 2: Cumulated water scarcity (AWARE) of passenger vehicles in 2030

Similar to the case of the Climate Change impact, the Water Scarcity level of BEVs and FCEVs of the manufacturing stage is significantly higher than their ICEV equivalents, representing an even higher difference of about 75%, although the credits from the end-of-life partially compensate this difference. Figure 3 shows a

Narr Francke Attempto Verlag GmbH + Co. KG

breakdown of the different contributions to water scarcity during the manufacturing phase. More than half of the water consumption comes from the manufacturing of the battery, and particularly of the cathode. Three main factors contribute to the impact the cathode: The energy consumption, the production of nickel and the production of lithium, which consumes substantial quantities of water. The electric engine is the third contributor (almost 11% of manufacturing water consumption), explained by the use of copper and aluminium.
Direct water utilization for vehicle manufacturing accounts for only 2.5% of the total water scarcity index. Indirect water utilization via the manufacturing process of the different materials scattered in the categories of Figure 3 account for more than 70% of the contribution, with about one third of that contribution coming from rare metals (cobalt, lithium, nickel, manganese) and plastics (water consumption during the olefins production). The rest of the contribution comes from indirect water consumptions for energy generation (heat and electricity).

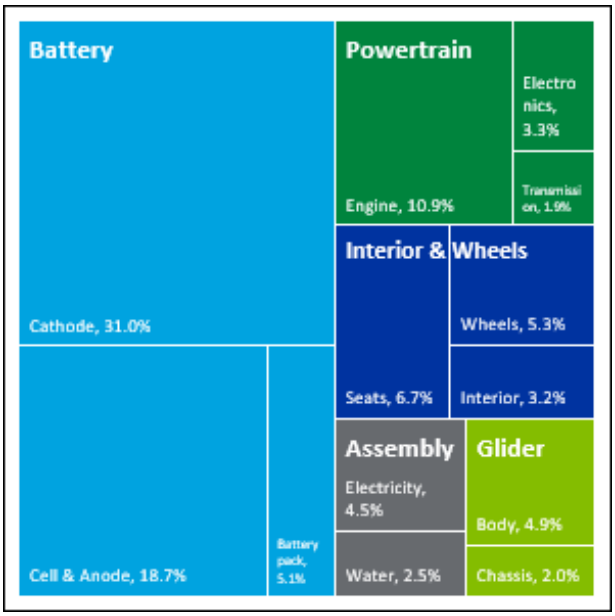

Figure 3: Breakdown of water scarcity contributions of a battery electric vehicle (manufacturing phase)

The direct use of water during the vehicle manufacturing (excluding the battery) is shown in Table 8 according to public data provided by two vehicle manufacturers. Most of the water consumed during the assembly processes comes from treated water. Almost two thirds of the water used in the processes is recovered and treated before releasing it to the environment.

Table 8: Water consumption during the vehicle manufacturing stage

[m^3 per vehicle]	BMW [31]	VW [32]
Water Input	2.32	3.56
of which Ground water	0.29	0.53
Surface water	0.00	0.10
Tap water	*2.03*	*2.93*
Water output	1.53	2.67
of which Process waste water	0.44	
Sanitary waste water	1.09	
Balance (water vapour, embodies, other losses)	**0.79**	**0.89**

The use phase of the vehicles in Figure 2 accounts for an important part to the water scarcity index. In the case of ICEVs, the impact is limited for fossil fuels due to a low net use of water during the crude oil and refining process. In the case of first generation biofuels, the impact is the most important of all the options studied, mainly because of the water required for irrigation of the rapeseed and sunflower crops required to their production. These impacts are reduced to levels comparable to fossil-fuelled ICEVs when second generation fuels are used assuming the used cooking oil feedstock does not carry any burden from its original use. ICEVs running on PtL fuels show higher water consumption levels than fossil and 2G options because of the indirect use of water for electricity generation. The water used for hydrogen production (electrolysis) is mostly recovered during the synthesis process, therefore carrying a relatively low water intensity per MJ (Table 7).
The effect of water use in electricity generation compared to a fossil source can be also observed in the case of FCEVs. The use of green hydrogen increases the impact of water use because of its water intensity. Combined with a fixed contribution from the wheels replacement, this results in the use phase water consumption for a renewable-fuelled fuel cell vehicle to be multiplied by almost 2.5 compared to another running with conventional hydrogen.
In the case of BEVs, the switch from an electricity mix to a wind electricity cuts down effectively the overall water scarcity factor of the vehicle by a factor of 2.3. The origin of the electricity plays therefore a major role in the water consumption during the use phase. The EU energy mix of 2030 is beyond 100 times more water-intensive than wind electricity.

5.3 Freshwater eutrophication

In Figure 4 we observe the impacts of the different vehicle/energy alternatives on freshwater eutrophication. The results for this environmental impact, measuring the amount of excess nutrients added to freshwater bodies,

Narr Francke Attempto Verlag GmbH + Co. KG

mostly rivers, lakes and ground reservoirs, are extremely high for the case of first-generation HVO. This is explained by the use of phosphate-based fertilizers in agriculture, directly affecting the sources of blue water. The rest of the results are less differentiated for ICEVs and FCEVs, regardless of the type of fuel consumed. BEVs stand out as a separate category of considering the impact of the vehicle manufacturing only: Freshwater eutrophication of BEV manufacturing accounts for more than twice the impact of conventional and fuel cell vehicles. The eutrophication credits from the end-of-life cycle, however, neutralise these oversized impacts to levels comparable to fuel cell electric vehicles.

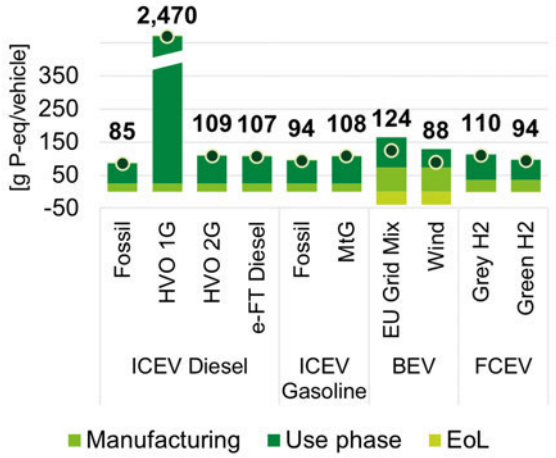

Figure 4: Cumulated freshwater eutrophication of passenger vehicles in 2030

The main impacts related to the manufacturing stage are represented in Figure 5. The biggest contributors to these impacts are the production of cobalt and lithium. For cobalt, the blasting stage has been investigated as the main responsible for causing eutrophication, because of the nitrogen oxides emitted during the blasting stage [33]. Nitrogen oxide emissions are at the origin of smog and acid rain, which in turn cause eutrophication. In the case of lithium, eutrophication comes from phosphates released in the process water used to treat spodumene, a mineral from which lithium is extracted in Australia or China (this is not the case in South America where lithium comes mainly brine). Sodium phosphates are used to precipitate lithium from alkaline solutions [34].
Another important contributor to eutrophication is the wheel manufacturing, related to the nitrogen oxide emissions during rubber manufacturing [35]. Note that the value for wheels in this graph only accounts for the initial set, so the total contribution that includes the impact from the tyres in the use phase is estimated to 5 times the value represented in this graph.
The differences in the use phase of the vehicles are not clearly distinguished. General trends can be observed, which show higher levels of eutrophication related to the use of PtL fuels. Like in the case of water consumption, the main explanation for this difference comes from the indirect pollution during the electricity generation phase. For BEVs, the change from the EU grid mix to renewable electricity represents a drop of 40% of use phase eutrophication, which is mainly explained by a reduction of 75 times the phosphorus intensity. The change of tyres included in this phase makes this difference less noticeable in the graph.

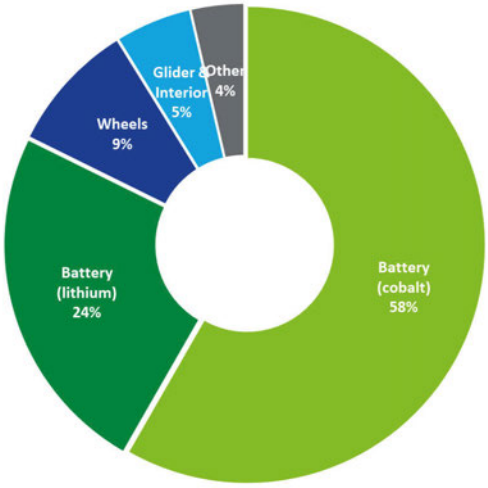

Figure 5: Breakdown of freshwater eutrophication contributions of a battery electric vehicle (manufacturing phase)

5.4 Limitations of the study

The present study is introduced as a first assessment for a limited number of powertrain combinations and only one sensitivity on fuel type per vehicle. Several parameters play a role in determining the level of pollutants:
Most of the PtL processes are still in demonstration status or do not exist at all in the assessed configuration, operational data about auxiliary consumption and especially process emissions into air and water (besides CO_2) are rather restricted, which is a limitation of the study, especially for impact categories other than climate change.
Concerning water, the results are limited to a specific regional impact. An extension of the study could include the variation of these impacts depending on the geographical zone they cover, as the water treatment standards change from country to country. Also, a more detailed breakdown of different sources of water, such as ground or desalinated seawater which could provide better insights about particular actions that can be taken to tackle the environmental effects.
Similar regionalised studies can be applied to some of the vehicle materials, in particular aluminium, copper and lithium.
Impact of second-generation biofuels is highly dependent on methodological parameters. Results can be significantly impacted if some sort of economic allocation can be applied to used cooking oil, considering its market value similar to raw oil.

Narr Francke Attempto Verlag GmbH + Co. KG

Further options potential improvements investigated:

– The impact of different sources of electricity for the production of PtL fuels, especially hydrogen. This could be extended to the hydrogen used in the biofuels production process. The utilization of blue hydrogen (produced from an SMR with an integrated carbon capture system) can also be assessed.
– The impact of the use of renewable fuels for transportation of biomass. The present study assumes fossil fuels consumed by trucks.
– The utilization of hybrid mobility solutions (hybride, plug-in electric vehicles).

6. Conclusions

The present study aimed at analysing the impact factors for passenger vehicles beyond the usual assessment of greenhouse gas emissions, including water scarcity and freshwater eutrophication. The following conclusions can be drawn from this piece of work:

- The generalisation of the use of renewable energy for transport drastically diminishes the initially clear advantage of electrified technologies with respect to internal combustion engine vehicles related to greenhouse gas emissions.
- Water use during the vehicle manufacturing phase is 70% constituted by indirect consumption to produce vehicle materials, especially aluminium, copper and lithium, but also plastics. In battery electric vehicles, this indirect use represents more than half of the consumption.
- Fossil and PtL fuels do not show significant differences in water consumption, despite the use of water for hydrogen electrolysis. Most of the water produced in the process is recovered.
- The source of electricity is critical not only for greenhouse gas emissions, but also for water use and freshwater eutrophication. With respect to wind electricity, the average electricity mix in Europe at horizon 2030 is expected to have water use and eutrophication impacts per unit of energy roughly 100 and 75 times higher respectively. This has a direct impact for BEVs but also indirect for ICEVs runnion on PtL fuels.
- First generation biofuels show relative advantages in Climate change impact with respect to fossil fuels, but they compare very poorly in water use and especially freshwater eutrophication, due to the large amounts of irrigation water and phosphate-based fertilizers used in agriculture.
- The impact of freshwater eutrophication during the manufacturing phase of a battery electric vehicle comes mainly from the Li-ion battery component, and is related to the indirect emissions from cathode components, mainly cobalt and lithium. Their impact can be reduced depending on the level of recycling targeted for these rare materials.
- Passenger vehicle technologies should not be dissociated from the source of energy when performing environmental assessments. The single impact of the energy efficiency of a given technology does not determine totally its impacts on the environment. For this purpose, Life Cycle Assessment (LCA) has proven to be a valuable tool to perform holistic comparisons between different transportation options.

References

[1] V. Gordillo et al, “Greenhouse Gas Emissions of Passenger Vehicles from a Cradle-to-Grave perspective,” in SIA Powertrains & Energy, 2020.
[2] M. Yugo, V. Gordillo, E. Shafiei and A. Megaritis, “A look into the life cycle assessment of passenger cars running on advanced fuels,” in SIA Powertrain & Power Electronics, 2021.
[3] International Organization for Standardization (ISO), “ISO 14040:2006 Environmental Management – Life Cycle Assessment: Principles and Framework,” 2006.
[4] International Organization for Standardization (ISO), “ISO 14044:2006 Environmental Management – Life Cycle Assessment: Principles and Framework,” 2006.
[5] Sphera, “GaBi 10.0 LCA Software & LCI databases v2021.1,” February 2020. [Online]. Available: http://www.gabi-software.com/international/index/.
[6] Joint Research Centre (JRC), “Supporting information to the characterisation factors of recommended EF Life Cycle Impact Assessment method,” Ispra: European Commission, 2018.
[7] A.-M. Boulay et al., “The WULCA consensus characterization model for water scarcity footprints: assessing impacts of water consumption based on available water remaining (AWARE),” The International Journal of Life Cycle Assessment, vol. 23, p. 368–378, 2018.
[8] B. Morelli et al., “Critical review of eutrophication models for life cycle assessment,” Environmental Science & Technology, vol. 17, no. 52, p. 9562–9578, 2018.
[9] Intergovernmental Panel on Climate Change (IPCC), “Climate Change 2013: The Physical Science Basis - Contribution to the Fifth Assessment Report of the IPCC,” 2013.
[10] O. Schuller, “The GaBi LCI Refinery Model 2021,” 2021. [Online]. Available: https://sphera.com/wp-content/uploads/2020/04/The-GaBi-LCA-Refinery-Model.pdf.
[11] Fuel Cell and Hydrogen 2 Joint Undertaking (FCH JU), “Hydrogen Roadmap Europe – A sustainabi-

Narr Francke Attempto Verlag GmbH + Co. KG

lity pathway for the European energy transition," 2019. [Online]. Available: https://www.fch.europa.eu/publications/hydrogen-roadmap-europe-sustainable-pathway-european-energy-transition.
[12] P. Millet et al., "Chapter 2 - Water Electrolysis Technologies," in Renewable Hydrogen Technologies, 2013, pp. 19-41.
[13] International Energy Agency (IEA), "IEA Hydrogen Project Database," 2019.
[14] Intergovernmental Panel on Climate Change (IPCC), "Special Report on Carbon Dioxide Capture and Storage," 2005.
[15] N. von der Assen, "Selecting CO2 Sources for CO2 Utilization by Environmental-Merit-Order Curves," Environmental Science & Technolgy, 2016.
[16] C. Beuttler et al., "The Role of Direct Air Capture in Mitigation of Anthropogenic Greenhouse Gas Emissions (Frontiers in Climate)," Frontiers in Climate, 2019.
[17] Element Energy, "Shipping CO2 - UK Cost Estimation Study: Final report for Business, Energy & Industrial Strategy Deparment," 2018.
[18] Sasol, "Coal Gasification and Liquefaction – SA Experiences and Opportunities," 2012. [Online].
[19] Shell, "Knowledge Guide: GTL Fuel - Synthetic Technology for Cleaner Air v2.0," 2016.
[20] A. Winther Mortensen, "Nordic GTL – a pre-feasibility study on sustainable aviation fuel from biogas, hydrogen and CO2," 2019.
[21] D. H. König, „Techno-ökonomische Prozessbewertung der Herstellung synthetischen Flugturbinentreibstoffes aus CO2 und H2," Universität Stuttgart, 2016.
[22] R. Detz, "CO production via reverse water gas shift," 2019.
[23] A. De Klerk, "Fischer-Tropsch Process," in Kirk-Othmer Encyclopedia of Chemical Technology, 2013.
[24] Carbon Recycling International (CRI), "Power and CO2 emissions to methanol," European Methanol Policy Forum Brussels, 2015.
[25] ExxonMobil, "ExxonMobil methanol to gasoline (MTG)," in Syngas Technology Conference, Colorado Springs, 2017.
[26] S. J. a. Y. Zhu, "Techno-economic analysis for the conversion of lignocellulosic biomass to gasoline via the methanol-to-gasoline (MTG) process," U.S. Department of Energy, 2009.
[27] S. Nikander, "Greenhouse gas and energy intensity of product chain: Case transport biofuel," Helsinki University of Technology, 2008.
[28] Neste Oil, "NExBTL Renewable Diesel Singapore Plant - North American Technical Corn Oil Pathways Description," 2014.
[29] JEC, "JEC Tank-to-Wheel report v5: Passenger cars," Publications Office of the EU, Luxembourg, 2020.
[30] Argonne National Laboratory (ANL), "BatPaC: Battery Manufacturing Cost Estimation," 2019. [Online]. Available: https://www.anl.gov/ tcp/batpac-battery-manufacturing-cost-estimation.
[31] BMW Group, "Sustainable Value Report 2020," 2020. [Online]. Available: https://www.bmwgroup.com/content/dam/grpw/websites/bmwgroup_com/responsibility/downloads/en/2020/2020-BMW-Group-SVR-2019-Englisch.pdf.
[32] Volkswagen Corporation, "Sustainability Report," 2020. [Online]. Available: https://www.volkswagenag.com/presence/nachhaltigkeit/documents/sustainability-report/2020/Nonfinancial_Report_2020_e.pdf.
[33] S.-H. Farjana et al., "Life cycle assessment of cobalt extraction process," Journal of Sustainable Mining, 2019.
[34] Y. Song et al., "A promising approach for directly extracting lithium from α-spodumene by alkaline digestion and precipitation as phosphate," Hydrometallurgy, 2019.
[35] K. Piotrowska et al., "Assessment of the Environmental Impact of a Car Tire throughout Its Lifecycle Using the LCA Method," Materials, 2019.
[36] JEC, "JEC Well-to-Tank report v5," Publications Office of the European Union, Luxembourg, 2020.
[37] International Energy Agency, "The Future of Hydrogen," 2019. [Online]. Available: https://www.iea.org/reports/the-future-of-hydrogen.

Narr Francke Attempto Verlag GmbH + Co. KG

E-fuels for the Energy Transition in the Transport Sector – Properties and Application: Current State of Research

Sandra Richter
German Aerospace Center (DLR) / Institute of Combustion Technology, Stuttgart, Germany
Sandra.Richter@dlr.de

Karl Planke
German Aerospace Center (DLR) / Institute of Combustion Technology, Stuttgart, Germany

Ines Österle
German Aerospace Center (DLR) / Institute of Vehicle Concepts, Stuttgart, Germany

Marina Braun-Unkhoff
German Aerospace Center (DLR) / Institute of Combustion Technology, Stuttgart, Germany

Juliane Prause
German Aerospace Center (DLR) / Institute of Combustion Technology, Bremen, Germany

Manfred Aigner
German Aerospace Center (DLR) / Institute of Combustion Technology, Stuttgart, Germany

Summery

The defossilization of the transport sector is of crucial importance to reduce climate effects, while emissions of soot particles and NO_x are harmful to environment and human health. Sustainable fuels offer the chance of addressing both: Reducing climate impact and improving local air quality. Among alternative fuels, E-fuels are considered to become a game player. Using Power-to-Liquid (PtL) technologies they will be produced from CO_2 and green hydrogen based on (excess) renewable energy, such as wind or solar power. This study provides an overview on the variety of E-fuels, including OME, DME, and methanol as well as synthetic gasoline, diesel, and kerosene produced via Fischer-Tropsch synthesis. Important fuel properties are analyzed to assess the technical applicability as well as their usage as drop-in and neat fuels by considering fuel regulations and the compatibility with existing technology. This study is part of our ongoing work within "Begleitforschung Energiewende im Verkehr" (BEniVer), a research project accompanying the funding initiative "Energy transition in transport" of the German Federal Ministry of Economic Affairs and Energy (BMWi).

1. Introduction

Carbon dioxide (CO_2) is the main anthropogenic greenhouse gas causing global warming [1]. The emissions originate from energy supply, transport and industrial processes. According to the report of the Intergovernmental Panel on Climate Change (IPCC), human made global warming reached an increase of 1 °C in 2017 compared to the pre-industrial period increasing currently by about 0.2 °C per decade [1]. Consequences of climate change are observed all over the world with drastic impacts on human and environment: Extreme heat (waves not only) in summer, aridity, forest fires, more heavy storms, floods, hurricanes, glacier melting, and raising sea level, besides others. To reduce impacts from climate change, the Paris Agreement was adopted by the United Nations in 2015 [2] with the aim to keep global warming well below 2 °C and step up efforts to keep the limit to 1.5 °C. To achieve this goal within the European Union, the European Climate Law was proposed with the target of net zero greenhouse gas emissions by 2050 [3]. On the path to climate-neutrality, the greenhouse gas emissions shall be reduced to at least 55 % by 2030 compared to 1990 [4]. In Germany, the updated climate change act aims for a CO_2 reduction of 65 % by 2030 and climate-neutrality in 2045 [5].
As part of the European 2030 Climate Target Plan, the share of renewable energy should increase to 24 % in the transport sector [6]. Here, *advanced biofuels* and *low*

Narr Francke Attempto Verlag GmbH + Co. KG

carbon fuels are named as central pillars, among others, to reach this goal. Besides the reduction of CO_2 emissions, the deployment of sustainable (advanced, low-carbon) fuels aims to reduce further also the emissions of nitrogen oxides (NO_x) and soot particles since they are harmful to human health and the environment.

Among sustainable fuels, E-fuels became of high importance within the past few years, with the focus put on research, besides of application aspects. They can be produced based on the Power-to-Liquid (PtL) technology using renewable energy such as wind or solar power as illustrated in Figure 1. First, hydrogen (H_2) is produced via electrolysis of water whereas CO_2 originating from industrial processes, direct air capture (DAC), or biogas is converted into carbon monoxide (CO). Biomass can be used as carbon source as well. The specific composition of the resulting syngas, i.e. a mixture of H_2 and CO, in detail the specific ratio between H_2 and CO, depends on the further process chain. For the fuel production from syngas, two main paths are considered within this study: (I) direct fuel synthesis via the Fischer-Tropsch (FT) process, and (II) synthesis of methanol (CH_3OH) being further converted to the fuel of interest.

Based on the design of the production process, different types of fuels can be produced which then can be applied across the different transport sectors: Road, rail, aviation as well as maritime shipping. Whereas the variety of sustainable aviation fuels (SAFs) is limited due to strong global regulation and requirements [7-9], the road, rail, and maritime sectors offer more possibilities for the usage of alternative fuels.

Within this work, the technical applicability and capability for the usage as drop-in or neat fuel is evaluated for different kinds of synthetic fuels based on their chemical and physical properties. This includes the characterization of E-fuels, a comparison of selected fuel properties of E-fuels with fossil fuels (depending on the considered sector), the analyses of combustion properties and emissions, as well as the preparation of an overview on the current state of research. This study is part of our ongoing work within BEniVer (*Begleitforschung Energiewende im Verkehr*), the accompanying research on the funding initiative "Energy transition in transport" of the German Federal Ministry of Economic Affairs and Energy (BMWi).

2. Classification of alternative fuels

This study distinguishes the following classes of alternative fuels: (I) Synthetic diesel, (II) synthetic gasoline, (III) synthetic kerosene, (IV) dimethyl ether and oxy-methylene ethers, (V) methanol and higher alcohols, (VI) further oxygenated fuels, and (VII) methane and hydrogen. Table 1 gives an overview of the different alternative fuels as studied within the research initiative "Energy transition in transport" (methane and hydrogen are leave out in Tab. 1 since they are not comparable to the other fuels). Here, these E-fuels are primarily considered as alternatives in road transport; however, they are, in general, possible candidates for the substitution of conventional maritime fuels as well. In addition, Tab. 1 includes synthetic kerosene for application in the aviation sector. The table illustrates relevant fuel properties and existing standards. Moreover, it summarizes their possibility to use as neat fuel or blend component and drop-in fuel or near-drop-in fuel.

Figure 1 illustrates the classification of the different kinds of E-fuels according to their production route via the FT process or methanol path. The FT process yields a mixture of mainly linear hydrocarbons (known as paraffins) differing in the number of carbon (C-) atoms and separated by distillation according to their boiling range. Gasoline contains the lightest hydrocarbons with carbon chains of about C_5 to C_{10}. Next, kerosene covers a C-number-range from C_8 to C_{16}. The heaviest fuel is diesel with C_{10} to C_{20} or even longer.

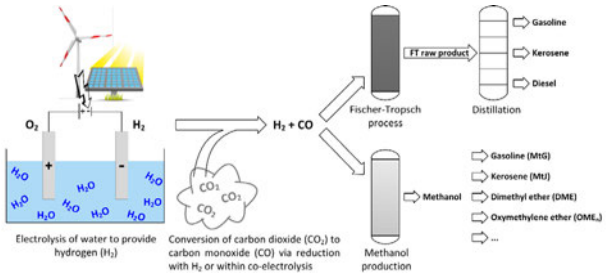

Fig. 1 Illustration of E-fuel production via the Power-to-Liquid (PtL) process including (I) water electrolysis, (II) syngas production, and (III) fuel production via the Fischer-Tropsch (FT) process or methanol production. Methanol can be processed to further sustainable fuels. Abbreviations: MtG – Methanol-to-Gasoline, MtJ – Methanol-to-Jet

Tab. 1 Overview of alternative fuels considered within BEniVer. Abbreviations: (I) Fuels: DMC – dimethyl carbonate, DME – dimethyl ether, FT – Fischer-Tropsch, MeFo – methyl formiate, MtG – Methanol-to-Gasoline, MtJ – Methanol-to-Jet, OME2-5 – oxymethylene ether (for explanation of the subscript "2-5" the reader is referred to section 3); (II) properties: CN – cetane number, FBP – final boiling point, FP – flash point, Hu – lower heating value, (M/R)ON – (motor/research) octane number, Tb – boiling temperature, Tf – freezing point, ρ – liquid density at 15 °C and 1 bar.

Narr Francke Attempto Verlag GmbH + Co. KG

	Synthetic diesel	Synthetic gasoline		Synthetic kerosene		Ether		Alcohol		Other oxygenated fuels	
	FT diesel	**FT gasoline**	**MtG**	**FT kerosene**	**MtJ**	**DME**	**OME2-5**	**methanol**	**higher alcohol**	**DMC**	**MeFo**
	Neat fuel	Neat fuel		Blend		Neat fuel	Neat fuel, Blend	Neat fuel, Blend	Blend	Blend	
	Drop-in	Drop-in		Drop-in up to 50 %(v/v)		Near-Drop-in		Near-Drop-in	Drop-in up to 50 %(v/v)a)	Near-Drop-in	
standard	EN 15940 (EN 590)	EN 228		ASTM D7566	--	ISO 16861b)	--	ASTM D5797c)	ASTM D7862c),d)	--	--
Tb (°C)	85...360e)	210e) (FBP)		205...300e)	g)	-24.8e)	105...280h)	65f)	99.5... 117.7d),e)	90f)	32f)
Tf (°C)	-40...6f)	-90.5...-95.4f)		≤ -40e)	g)	≈ -140h)	-70... 48h)	-98f)	-89.5... -114.7d),e)	5f)	-100f)
ρ (kg/m³)	765-810e) (800-845e))	720-775e)		730-770e)	g)	gas	961-1100h)	792h)	801-810d),e),j)	1007f) (20 °C)	970f) (20 °C)
FP (°C)	≥ 55e)	≤ -35f)		≥ 38e)	g)	-42.2f)	54-115h)	9f)	24...35d),e)	14f)	-27f)
CN	≥ 51e)	--		--	--	> 55e)	63-100h)	5h)	17-25d),h)	--	--
ON	--	≥ 95e) (RON) ≥ 85e) (MON)		--	--	--	--	109i) (RON) 89i) (MON)	96-113d),e) (RON) 78-94d),e) (MON)	--	--
Hu (MJ/kg)	≈ 44h)	--		≥ 42.8e)	g)	27.60h)	17.5-20.3h)	--	--	--	--
Hu (MJ/l)	--	30-33i)		--	g)	18.44h)	19.5-19.7h)	15.8i)	26-27d),i) 31.1a),i)	--	--

[a] refers to 1-octanol (n-octanol)
[b] deals with physical properties and does not give any requirements for application
[c] US standard being not valid in Germany or the European Union
[d] refers to 1-butanol (n-butanol), 2-butanol (sec-butanol), and 2-methyl-1-propanol (iso-butanol)
[e] taken from standard mentioned in table
[f] taken from [18]
[g] no information available but properties expected to be similar with FT kerosene
[h] from [19]
[i] from [20]
[j] temperature not specified in ASTM D7862 [16]

2.1 Neat fuel vs. blend / Drop-in vs. Near-Drop-in

As written in Tab. 1, the E-fuels considered in this study can be used both as neat fuels and as blend components. This depends on various aspects, including fuel composition, compatibility with current vehicle technology as well as regulations and standards, the modification or further development of power unit concepts, and the sector being of interest for specific fuel application.
The differentiation between drop-in and near-drop-in fuels describes originally the compatibility of synthetic blend components with (addition to) fossil fuels. In theory, blending of drop-in or near-drop-in fuels with synthetic fuels,

Narr Francke Attempto Verlag GmbH + Co. KG

being identical with fossil fuels, would be possible as well. Drop-in / near-drop-in fuels differ in the need of (minor) modifications of the (engine) components or of the used material. Classical neat fuels are pure gasoline and diesel, for example, whereas the typically used fuels E10 and B7 are blends containing 10 %(v/v) ethanol and 7 %(v/v) fatty acid methyl ester, respectively. With the advanced development of engine technology, also oxygenated fuels (having O atoms, besides H and C atoms) such as methanol and dimethyl ether (DME), being different from fossil fuels, became of interest as 'new' neat fuels.
Thus, the differentiation between drop-in and near-drop-in fuels is applied to neat fuels as well. In general, fuels being compatible with the existing technology (no modifications necessary) and directly usable in transport are defined as drop-in fuels. For the use of near-drop-in fuels, modifications or even new motor components are necessary.
Regarding higher alcohols, the limit of max. 50 %(v/v) (see Tab. 1) relates to the *technical compatibility* of the admixture of 1-octanol to diesel [10]. However, the resulting fuel mixture does not meet today's requirements as defined in the *relevant standard*, here EN 590 for diesel [11], i.e. using 1-octanol in road transport diesel is currently not allowed. The technical limit of alcohols as possible blending components for gasoline is likewise lower, e.g., for 2-butanol it amounts to about 15 %(v/v).
The 50 %(v/v) limit of blending synthetic kerosene is defined by the standard ASTM D7566 [9]. Note that depending on the type of a specific SAF, the technical compatibility would allow the usage higher blends up to the usage of SAF as neat fuel [12].

2.2 Regulations and standards

The fuel standards listed in Tab. 1 specify the requirements existing for the use of those E-Fuels considered in this study. Of these standards, EN 228 for gasoline [13], EN 590 for diesel [11], and EN 15940 for paraffinic diesel [14] are valid in the European Union. EN 228 and EN 590 define the requirements as well as fuel properties for gasoline and diesel for their usage in road transport. According to these specifications, synthetic fuels can be added to the fossil ones as long as the properties of the "final" fuel meets the requirements [11,13]. Currently, EN 15940 is the only standard defining a fully synthetic fuel, i.e. allowing its use as 100 % neat fuel. Due to its composition, paraffinic diesel has a lower density compared to fossil diesel. Therefore, paraffinic diesel is not identical with fossil diesel as defined within EN 590. As a result, synthetic diesel can be blended up to 30 %(v/v) with fossil diesel and according to EN 15940 [14] used as neat paraffinic diesel in automobiles approved by the manufacturer.
The ASTM D5797 standard for the use of methanol as blend component for gasoline between 51 %(v/v) and 85 %(v/v) [15] as well as ASTM D7862 for butanol as gasoline component up to 12.5 %(v/v) [16] are not valid in Europe.
Since aviation is a global business the standard specification for synthetic kerosene ASTM D7566 is valid almost all over the world. Here, different types of SAFs are defined as blending components for fossil-based kerosene (Jet A-1) up to 50 %(v/v) [9]. Whereas FT-based kerosene is certified as SAF, the Methanol-to-Jet route has no approval yet. Alcohol-to-Jet (AtJ) is a specific SAF already certified which is produced using ethanol or iso-butanol.
In contrast to the regulations mentioned before, the standard ISO 16861 for DME specifies solely fuel properties [17] and made no requirements regarding the use as alternative fuel for the transport sector.
To sell synthetic fuels in Germany it is also required that the trade with the fuel is permitted by law, in detail by the 10th Federal Emission Control Directive (10. BImSchV) [21]. This directive contains requirements not only on road transport fuels but also on maritime fuels and heating oil.

3. E-Fuels in transport

3.1 Synthetic diesel

The synthetic diesel studied within projects as part of the funding initiative "Energy transition in transport" (EiV) is produced almost exclusively via Fischer-Tropsch (FT) processes from syngas yielding FT-diesel. A further production process uses esters and fatty acids from vegetable or used cooking oils. According to the raw material, the product is called HVO (hydrogenated vegetable oil) or HEFA (hydrogenated esters and fatty acids). In contrast to FT-diesel, the production of HVO has already reached industrial scale being available in the U.S. and Europe, with Neste as largest producer [22,23].
The product of both process routes is a pure paraffinic diesel being suitable as drop-in fuel in diesel engines of light- and heavy-duty vehicles as well as of ships. At present, paraffinic diesel is the only synthetic fuel with a European standard (EN 15940) [14] for the (neat) use in the automobile sector. Indeed, most of the fuel properties are nearly identical with fossil diesel. However, the density of synthetic diesel is lower than the density of its fossil counterpart (see Tab. 2), which is due to the absence of aromatic compounds. Therefore, the manufacturer has to prove if the motor vehicle can be, fueled up with neat paraffinic diesel, i.e. without any drawbacks [14]. For blending paraffinic diesel with fossil diesel, EN 590 defines no percentage limit but requires that the properties of the mixture have to comply with all the requirements being specified in the standard [11].
On the other hand, the absence of aromatic compounds has a positive effect on the emissions of particulate matter. In general, aromatic compounds are precursors for the formation of soot. Indeed, soot is formed during combustion of synthetic diesel as well – but without aromatics, the emissions of soot and particulate matter, respectively, are considerably reduced. This offers the additional possibility that the exhaust catalyst can reduce NO_x emissions more effectively.

Narr Francke Attempto Verlag GmbH + Co. KG

3.2 Synthetic gasoline

As presented in Tab. 1 there are two different kinds of synthetic gasoline being processed via the PtL technology. The first, FT gasoline, will be produced together with diesel and kerosene (see section 3.3) from syngas. Following the synthesis unit, the FT product is separated via distillation. Apart from gaseous products, the lightest fraction contains hydrocarbons with a carbon size distribution similar to the one of gasoline (components). The raw product from the FT synthesis are mainly linear paraffins, being beneficial for a diesel fuel since the cetane number of linear hydrocarbons is higher than the ones of branched hydrocarbons. To achieve a high octane number, as required for gasoline, further refinement processes like isomerization and alkylation are necessary within the upgrading of the FT crude oil.
The production of the second type of a synthetic gasoline considered, the Methanol-to-Gasoline (MtG), is based on syngas, too. Due to the gasoline production from methanol, the extent of additional refinement processes depends on the used catalyst and the process control.
Independent of the production route, the development of synthetic gasoline generally tends to meet the requirements specified in EN 228. This means, synthetic gasoline can be used as neat fuel without any adjustments of the engine, engine components, or materials. Regarding the usage, synthetic gasoline differs from synthetic diesel or oxygenated fuels, both being of interest in different transport sectors. Since diesel engines dominate heavy-duty transport, including the maritime sector, the development of synthetic gasoline focuses on the application in passenger cars.

3.3 Synthetic kerosene

As of May 2021, a total of seven different alternative jet fuels have been approved for the usage as drop-in fuel in blends with fossil jet fuel, up to 50 %(v/v) [9]. The mixing limit results not only from the specification of fuel properties but also from the share of aromatics being natural (historic) fuel components due to their occurrence in fossil oil. Without using any aromatization and cyclization processes, specific SAFs consist of linear and / or branched paraffins only. However, the aromatics lead to the appropriate swelling of seals, i.e. without aromatics in the jet fuel the risk of leakages cannot totally be ruled out. Hence, a number of aromatics of min. 8 %(v/v) [9] is required within the specification; therefore, blending with fossil jet fuel is unavoidable at present. Nevertheless, test flights with 100 % SAF have recently demonstrated that also the use of neat paraffinic kerosene is feasible [12]. As a consequence, it is not to be excluded that future specifications might allow the use of completely non-aromatic jet fuels. Thus, additional benefits in terms of reducing non-CO_2 effects might be realized due to the reduced emission of particles.
Paraffinic FT kerosene belongs to the certified SAFs and is called FT-SPK (synthetic paraffinic kerosene). As mentioned earlier, the raw FT product can be separated in three different fractions – gasoline, diesel, and kerosene being in the middle distillation range compared to the other fuels.
A new synthetic kerosene under development, thus being not yet approved as SAF, is Methanol-to-Jet (MtJ). MtJ is produced by the oligomerization of methanol, similar to MtG, leading likewise to a paraffinic kerosene, without any aromatics. Even though at present not included in ASTM D7566, the MtJ kerosene resembles the certified Alcohol-to-Jet (AtJ) being produced from ethanol or iso-butanol.
In contrast to road transport and maritime fuels, oxygenated fuels are out of question for the use as SAFs since C-O bonds are expected to come along with a lower storage stability and an increased risk of water contamination due to hygroscopicity. Therefore, a drastic reduction of soot emissions is only achievable by keeping the amount of aromatics within the jet fuel as low as possible.

3.4 Dimethyl ether and oxymethylene ethers

Dimethyl ether (DME, H_3COCH_3) and oxymethylene ether (OME_n: $H_3CO(H_2CO)_nCH_3$ with $n \geq 1$) are of high importance as alternative fuel compounds for diesel engines in road transport as well as maritime shipping for several reasons. (I) Due to the absence of any C-C bonds within the fuel, even fuel rich mixtures show nearly no soot formation – compared not only to fossil diesel but also to synthetic diesel or other oxygenated fuels like alcohols or even to conventional biodiesel, consisting of fatty acid methyl esters. Hence, the use of DME or OME_n as a near-drop-in fuel not only promises a substantially stronger reduction of soot emission but, even more, an escape from the trade-off between soot and nitrogen oxides (NO_x). (II) DME and OME_n can be produced from renewable sources using methanol as the intermediate product – either via the Power-to-Liquid (PtL) process but also from sustainable resources (biomass) via gasification or fermentation. This means, the use of DME or OME_n will help to achieve CO_2 neutrality. (III) Although OME_n do not have any C-C bonds, they are fully miscible with conventional hydrocarbon fuels; especially higher OME_n ($n \geq 2$) are in line with important diesel fuel properties like cetane number, boiling temperature, freezing point (besides OME_5), and flash point, as shown in Tab. 2.
On the other hand, the liquid density as well as the viscosity, both properties characterizing the fluidity of a fuel, are outside of the parameter range for a diesel fuel. The high oxygen content of these fuels has a beneficial effect on reduced soot and NO_x emissions; but, on the other hand, this may cause increased emissions of new harmful substances like aldehydes and ketones, lead to a reduced heating value, and might also adhere the risk of material incompatibility. For these reasons, adjustments or even new developments of the engine system are unavoidable in case neat DME or OME_n is fueled [24,25]. For the use in blends with diesel, the degree of modifications depends on the amount of OME_n in the fuel mixture. According to Avolio et al. [26] even mixtures up to 15 %(v/v) might be compatible with

Narr Francke Attempto Verlag GmbH + Co. KG

the current vehicle technology. On the other hand, OME_n requires different sealing materials due to the oxygen in the molecule [25] to ensure that even the use of blends with small amounts of OMEn may not lead to leakages in long-term use.

Concerning the effect of OME_n on the combustion behavior when blended in diesel, it was found that 30 %(m/m) could be added without any significant change in the laminar burning velocity, being an important fundamental combustion property and a measure for heat release as well as reactivity of any fuel. Figure 2 shows the comparison of the laminar burning velocity of: (I) neat OME_4, (II) a diesel surrogate (50 %(n/n) n-dodecane + 30 %(n/n) farnesane (2,6,10-trimethyldodecane) + 20 %(n/n) 1methylnaphthalene), and (III) a mixture of the diesel surrogate + 30 %(m/m) OME_4; all data were reported at 200 °C and 1 bar. With a maximum of about 108 cm/s, OME_4 yields a distinctly higher laminar burning velocity than the diesel surrogate with a maximum of about 83 cm/s. Interestingly, the mixture of the diesel surrogate + 30 %(m/m) OME_4 shows a maximum being only slightly higher than the pure diesel surrogate. According to these results, OME_4 can be added to diesel in high amounts without having any influence on heat release or reactivity [27]. This is assumed to be true for OME_n in general as well.

Tab. 2 Overview of important physical properties of dimethyl ether (DME) and oxymethylene ethers (OMEn) compared to fossil diesel. Abbreviations: CN – cetane number, FP – flash point, Hu – lower heating value, Tb – boiling temperature, Tf – freezing point, v – viscosity, ρ – liquid density (at 1 bar).

	Diesel	DME	Oxymethylene ether (OMEn)				
			OME_1	OME_2	OME_3	OME_4	OME_5
T_b (°C)	85...360[a]	-24.8[e]	42[f]	105[f]	156[f]	201[f]	242[f]
T_f (°C)	-40...6[b]	≈ -140 [f]	-105[f]	-70...-65[f]	-43...-41[f]	-10...-7[f]	≈ 18.4[f]
ρ (kg/m³)$_{15°C}$	820-845[a] 800-840[a),c)]	gas	850-867[f]	961[f]	1021[f]	1059[f]	1100[f]
v (mm²/s)$_{40°C}$	2.0-4.5[a] 1.5-4.0[a),c)]	gas	0.32-0.33[f]	0.64[f]	1.05[f]	1.75[f]	2.63[f),g)]
FP (°C)	≥ 55[a]	-42.2[b]	-32[f]	12[h]	54[f]	88[f]	115[f]
CN	≥ 51[a]	> 55[e]	29-37.6[f]	63[f]	70-78[f]	90[f]	100[f]
H_u (MJ/kg)	≈ 43[f]	27.60[f]	22.44[f]	20.32[f]	19.14[f]	18.38[f]	17.86[f]
H_u (MJ/l)	≈ 35[f]	18.44[f]	19.30[f]	19.53[f]	19.54[f]	19.47[f]	19.64[f]

[a] data taken from [11]
[b] data taken from [18]
[c] values belong to winter diesel
[d] data taken from [20]
[e] data taken from [17]
[f] data taken from [19]
[g] at 25 °C
[h] data taken from [24]

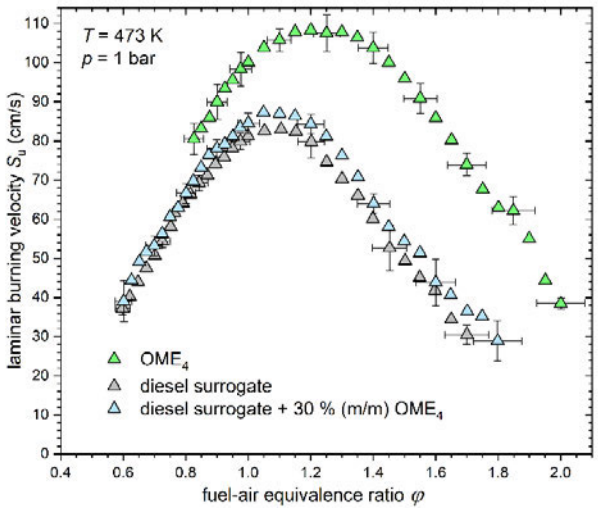

Fig. 2: Comparison of experimentally determined laminar burning velocities of: (I) neat OME4, (II) a diesel surrogate (50 %(n/n) n-dodecane + 30 %(n/n) farnesane (2,6,10-trimethyldodecane) + 20 %(n/n) 1methylnaphthalene), and (III) a mixture of the diesel surrogate + 30 %(m/m) OME4. All data are measured at 200 °C and 1 bar [27].

3.5 Methanol and higher alcohols

For the energy transition in the transport sector, methanol is a key molecule due to several reasons: (I) As already mentioned previously, methanol is a platform molecule as it is an important intermediate product for the production of several specific E-fuels. (II) Methanol offers the possibility for a flexible usage since it is of interest as alternative fuel for light- and heavy-duty vehicles as well as for the maritime sector. (III) Current research activities focus on the usage of methanol both as neat fuel and as blending component.

Narr Francke Attempto Verlag GmbH + Co. KG

Regarding dominant relevant fuel properties (see Tab. 3) methanol is an ideal blending component for gasoline with the benefit to increase the octane number. In the USA methanol gasoline blends are specified for the use in spark-ignition engines according to ASTM D5797 [15]. Here, the amount of methanol ranges from 51 %(v/v) to 85 %(v/v). The oxygen content leads to a cleaner combustion regarding soot emissions. In transport sectors (heavy-duty loading and shipping), where diesel engines are dominant, this advantage is of high importance within the consideration for the application. However, due to several unfavorable properties of methanol compared to diesel fuel (e.g., density, cetane number, and heating vale are (too) low), modifications of the engine, components, and / or material are to be expected for the use in blends and, to an even larger extent, for the use as neat fuel.
The higher alcohols being in focus within the energy transition are 2-butanol (also named sec-butanol) and 1octanol (n-octanol). For the sake of completeness, in Tab. 3 are also listed ethanol, 1-butanol (n-butanol), and tert-butanol. Ethanol is already a standard blending component for gasoline (depending on percentage of admixture named as E5 and E10) being not produced via the PtL-path but from fermentation ("bioethanol").
Regarding the C_4-alcohols, not only 2-butanol might be considered as synthetic fuel component for gasoline but also 1-butanol and iso-butanol. Even though their densities are higher, their boiling temperatures and octane numbers are within the specification for gasoline and, compared to ethanol, the heating values are closer to gasoline as well. Similar to methanol, these butanols are specified as blending components up to 12.5 %(v/v) in the USA following the standard ASTM D7862 [16]. The fourth mentioned C_4 alcohol, tert-butanol, is out of consideration due to its physical properties such as the high melting point of about 26 °C.
Based on the physical properties, 1-octanol appears as an ideal blending component to diesel fuel aiming for the reduction of the emissions of soot and particulate matter, respectively. Although not yet specified as fuel component, it was already shown by Zubel et al. [10] that an admixture of up to 50 %(v/v) is feasible from a technical perspective. In contrast to other E-fuels considered for the application in diesel engines of road transport vehicles as well as maritime shipping, 1-octanaol is currently only of interest for light-duty vehicles.

3.6 Further oxygenated fuels

Further oxygenated E-fuels considered (Tab. 1) are dimethyl carbonate (DMC, $H_3C\text{-}COO\text{-}CH_3$) and methyl formiate (MeFo, $HCOO\text{-}CH_3$) both being produced from methanol; they are of interest for the usage in spark-ignition engines due to their high octane numbers [28]. Similar to DME or OME_n no C-C bonds exist within the molecular structures, i.e. the emission of soot is significantly reduced when burned in blends with gasoline. Even if the boiling temperature is within the range of gasoline, the density is distinctly higher. For these reasons, modifications on the engine and / or engine components are assumed to be required.

3.7 Methane and hydrogen

As gaseous E-fuels, renewably produced methane (CH_4) and mixtures of renewable methane and hydrogen (H_2) are considered. Whereas H_2 stems directly from electrolysis, CH_4 is produced from syngas similar to the FT fuels. In road transport as well as in shipping, gas engines using methane as fuel are well-established. Irrespective of whether the engine runs on CNG (compressed natural gas) or LNG (liquified natural gas), the PtL based methane can be used directly with almost no modifications. According to the specification EN 16723-2 [29], the amount of H_2 is limited to 2 %(v/v) in natural gas vehicles while it is mentioned that a H_2 content of 10 %(v/v) could be applicable in gas engines with an advanced control system. Besides the currently existing regulations, also the technology has to be adjusted for the use of $CH_4 + H_2$ mixtures. For example, due to the low gas density of about 0.084 kg/m³ for H_2 (at 15 °C and 1 bar) compared to 0.671 kg/m³ for CH_4 [18], higher pressures in the fuel tank (for storage) and the engine (during operation) are necessary. What comes along is the small size of the hydrogen molecule as well as the hydrogen embrittlement, important regarding material compatibility. In detail, the diffusivity of H_2 and the degradation of the material due to embrittlement have to be respected. Furthermore, H_2 leads to higher combustion temperatures causing higher NO_x emissions. On the other hand, H_2 shows higher burning velocities which enables the combustion of lean mixtures. This offers the possibility to reduce the fuel consumption as well as the combustion temperature and therefore the NO_x emissions. Due to these reasons, the engine design and materials used require modifications respectively when the amount of H_2 exceeds 25 %(v/v) [30].
Besides in transport, the gaseous fuels are of interest in the energy sector as well. Here, the PtL based CH_4 is usable without difficulty. The use of mixtures with H_2 is possible in modern gas turbines up to 15 %(v/v) H_2.

Narr Francke Attempto Verlag GmbH + Co. KG

Tab. 3 Overview of important physical properties of different alcohols compared to fossil diesel and gasoline. Abbreviations: CN – cetane number, FP – flash point, Hu – lower heating value, (M/R)ON – (motor/research) octane number, Tb – boiling temperature, Tf – freezing point, v – viscosity (at 40 °C), ρ – liquid density (at 15 °C and 1 bar).

	Diesel	**Gasoline**	**Alcohols**						
			Methanol	Ethanol	1-Butanol	2-Butanol	iso-Butanol	tert-Butanol	1-Octanol
	$C_{14}H_{30}$ [g]	**C_8H_{15}** [g]	**CH_3OH**	**C_2H_5OH**	**nC_4H_9OH**	**sC_4H_9OH**	**iC_4H_9OH**	**tC_4H_9OH**	**$nC_8H_{17}OH$**
T_b (°C)	85...360[a]	210[e] (FBP)	65[b]	78[f]	117.7[h]	99.5[h]	108[h]	83[b]	195[b]
T_f (°C)	-40...6[b]	-90.5... -95.4[b]	-98[b]	-114[b]	-89.5[h]	-114.7[h]	-108[h]	26[b]	-16[b]
ρ (kg/m³)	820-845[a] 800-840[a),c]	720-775[e]	792[d]	785[d]	810[d]	806.3[h),i]	801.8[h),i]	790[b] (20 °C)	830[b] (20 °C)
v (mm²/s)	2.0-4.5[a] 1.5-4.0[a),c]		0.75[d]	1.5[d]	2.63-3.7[d]				
FP (°C)	≥ 55[a]	≤ -35[b]	9[b]	12[b]	35[h]	24[h]	28[h]	11[b]	84[b]
CN	≥ 51[a]	--	5[d]	8[d]	17-25[d]	--	--	--	--
RON	--	≥ 95[e]	109[f]	109[f]	96[h] 98[f]	101[h] 105[f]	113[h] 105[f]	107[f]	28[i]
MON	--	≥ 85[e]	89[f]	90[f]	78[h] 85[f]	82[h] 93[f]	94[h] 90[f]	94[f]	27[f]
H_u (MJ/l)	≈ 35[d]	30-33[f]	15.8[f]	21.4[f]	26.9[f]	26.7[f]	26.6[f]	25.7[f]	31.1[f]

a) data taken from [11]
b) data taken from [18]
c) values belong to winter diesel
d) data taken from [19]
e) data taken from [13]
f) data taken from [20]
g) average formula, taken from [20]
h) data taken from ASTM D7862 [16]
i) temperature not specified in ASTM D7862 [16]

4. Conclusions

This paper provides an overview on a range of E-fuels being of interest for the energy transition in the transport sector. Based on syngas stemming from electrolysis, hydrocarbon fuels (gasolines, diesel, kerosene) and oxygenated fuels (like alcohols or ethers) as well as gaseous fuels can be produced. Besides synthetic methane, being applicable like natural gas, synthetic gasoline, diesel and kerosene can be used as long as the required fuel properties comply with the corresponding standards. From a technical point of view, the oxygenated fuels are usable in blends with small or even no modifications to engine, engine components and / or materials. However, specifications and standards being valid in Europe are still missing.

Despite many research and development projects in progress, the PtL technology has not yet reached an industrial scale. To achieve CO_2 neutrality by 2045 in Germany, not only the PtL technology has to be promoted in order to become mature and vivid; in addition, further CO_2 saving technologies need to be implemented as well as the optimization of combustion engines regarding their efficiency and infrastructures.

References

[1] Intergovernmental Panel on Climate Change (IPCC): Global Warming of 1.5 °C (2018), https://www.ipcc.ch/sr15/ (access 11th May 2021)
[2] European Commission: European Climate Law (2020), https://ec.europa.eu/clima/policies/international/negotiations/paris_en (access 11th May 2021)
[3] European Commission: Paris Agreement, https://ec.europa.eu/clima/policies/eu-climate-action/law_en (access 11th May 2021)
[4] European Commission: 2030 Climate Target Plan (2020), https://ec.europa.eu/clima/policies/eu-climate-action/2030_ctp_en (access 11th May 2021)
[5] German Federal Government: Climate Change Act 2021 – Intergenerational contract for the climate, https://www.bundesregierung.de/breg-de/themen/klimaschutz/climate-change-act-2021-1913970 (access 1st June 2021)
[6] European Commission: Stepping up Europe's 2030 climate ambition – Investing in a climate-neutral future for the benefit of our people (2020), https://eur-lex.europa.eu/legal-content/EN/TXT/PDF/?uri=CELEX:52020DC0562&from=EN (access 11th May 2021)

Narr Francke Attempto Verlag GmbH + Co. KG

[7] Commercial Aviation Alternative Fuels Initiative (CAAFI): Fuel Qualification, https://www.caafi.org/focus_areas/fuel_qualification.html (access 11th May 2021)
[8] ASTM D4054-20c: Standard Practice for Qualification and Approval of New Aviation Turbine Fuels and Fuel Additives (2020), https://www.astm.org/ (access 11th May 2021)
[9] ASTM D7566-20c: Standard Specification for Aviation Turbine Fuel Containing Synthesized Hydrocarbons (2020), https://www.astm.org/ (access 11th May 2021)
[10] Zubel, M., Heuser, B., Pischinger, S.: 1-Octanol Tailor-made Fuel for Lower Soot Emissions. MTZ worldwide, 78 (2017) 3
[11] EN 590: Automotive fuels – Diesel – Requirements and test methods; German version EN 590:2013+A1:2017
[12] Airbus: An A350 fuelled by 100% SAF just took off (2021), https://www.airbus.com/newsroom/stories/A350-fuelled-by-100-percent-SAF-just-took-off.html (access 11th May 2021)
[13] EN 228: Automotive fuels – Unleaded petrol – Requirements and test methods; German version EN 228:2012+A1:2017
[14] EN 15940: Automotive fuels – Paraffinic diesel fuel from synthesis or hydrotreatment – Requirements and test methods; German version EN 15940:2016+A1:2018+AC:2019
[15] ASTM D5797-18: Standard Specification for Methanol Fuel Blends (M51-M85) for Methanol-Capable Automotive Spark-Ignition Engines (2018), https://www.astm.org/ (access 11th May 2021)
[16] ASTM D7862-21: Standard Specification for Butanol for Blending with Gasoline for Use as Automotive Spark-Ignition Engine Fuel (2021) https://www.astm.org/ (access 11th May 2021)
[17] ISO 16861:2015(E): Petroleum products – Fuels (class F) – Specification of dimethyl ether (DME) (2015)
[18] GESTIS Substance Database, www.dguv.de/ifa/gestis-database (access 11th May 2021)
[19] Schemme, S., Samsun, R.C., Peters, R. Stolten, D.: Power-to-fuel as a key to sustainable transport systems – An analysis of diesel fuels produced from CO2 and renewable electricity. Fuel, 205 (2017), 198-221
[20] Sarathy, S.M., Oßwald, P., Hansen, N., Kohse-Höinghaus, K.: Alcohol Combustion Chemistry. Progr. Energy Combust. Sci., 44 (2014), 40-102
[21] Zehnte Verordnung zur Durchführung des Bundes-Immissionsschutzgesetzes (Verordnung über die Beschaffenheitund die Auszeichnung der Qualitäten von Kraft- und Brennstoffen -10. BImSchV), https://www.gesetze-im-internet.de/bimschv_10_2010/ (access 1st June 2021)
[22] Neste: Neste Renewable Diesel Handbook. 2020, https://www.neste.com/sites/neste.com/files/attachments/neste_renewable_diesel_handbook.pdf (access 20th May 2021)
[23] Neste: NEXBTL Technology. https://www.neste.com/about-neste/innovation/nexbtl-technology (access 20th May 2021)
[24] Omari, A., Heuser, B., Pischinger, S., Rüdinger, C.: Potential of long-chain oxymethylene ether and oxymethylene ether-diesel blends for ultra-low emission engines. *Applied Energy*, 239 (2019), 1242-1249
[25] Pélerin, D., Gaukel, K., Härtl, M., Jacob, E., Wachtmeister, G.: Potentials to simplify the engine system using the alternative diesel fuels oxymethylene ether OME_1 and OME_{3-6} on a heavy-duty engine. Fuel, 259 (2020), 116231
[26] Avolio, G., Rösel, G., Maiwald, O.: Super Clean Electrified Diesel. MTZ worldwide, 78 (2017) 11
[27] Richter, S., Kathrotia, T., Braun-Unkhoff, M., Naumann, C., Köhler, M.: Study on the influence of oxymethylene ethers (OME_n) blending a diesel surrogate. 10th European Combustion Meeting, April 14-15, 2021, virtual
[28] Maier, T., Härtl, M. Jacob, E., Wachtmeister, G.: Dimethyl carbonate (DMC) and Methyl Formate (MeFo): Emission characteristics of novel, clean and potentially CO_2-neutral fuels including PMP and sub-23 nm nanoparticle-emission characteristics on a spark-ignition DI-engine. Fuel, 256 (2019), 115925
[29] EN 16723-2: Natural gas and biomethane for use in transport and biomethane for injection in the natural gas network – Part 2: Automotive fuels specification; German version EN 16723-2:2017
[30] Mehraa, R.K., Duan, H., Juknelevičius, R., Ma, F., Junyin, L.: Progress in hydrogen enriched compressed natural gas (HCNG) internal combustion engines – A comprehensive review. Renewable and Sustainable Energy Reviews, 80 (2017), 1458–1498

Acknowledgment

The authors thank the German Federal Ministry of Economic Affairs and Energy (BMWi) for funding.

Narr Francke Attempto Verlag GmbH + Co. KG

Additional lectures from the poster session

Narr Francke Attempto Verlag GmbH + Co. KG

Fast-Ageing method BigOxy for the examination of Fuel Blends

Karin Brendel
OWI Science for Fuels gGmbH

Nina Mebus
OWI Science for Fuels gGmbH

Summary

Though fuel ageing is a well-known phenomenon, there are still open questions concerning chemical reaction pathways and influence of environmental conditions. To examine the process of fuel ageing, especially considering new alternative fuel components, a fast-ageing method has been developed at OWI which has since been used in multiple applications. The method, called BigOxy, is based on the analytical oxidation stability measurement according to DIN 16091. Different fuel blends have been aged and consequently analyzed with various laboratory methods, and thus the course of ageing can be observed. The blends that have been examined include heating oils, diesel fuel, gasoline, heavy fuel oil, various alcohols, and alternative components like hydrogenated vegetable oil, fatty acid methyl esters and synthetic fuels. Results show that the method can successfully compress the natural ageing during storage into a much shorter time scale (down to 72 h). Possible side-effects that could occur during ageing in blends with new components can be found quicker and countermeasures can be enacted. The goal of this test is the prediction of long-term behavior of fuels.

1. Introduction

Ageing in fuels is a long-known phenomenon. The first patent for an additive to prevent ageing was filed as early as 1927 [1]. A lot of research has been conducted to assess fuel quality, prevent ageing, and better understand the underlying reactions. This has proven to be difficult due to the great complexity of mineral oils, which can contain hundreds of thousands of different substances [2]. Due to recent improvements in efficiency of both vehicles and heating systems, and development of new technologies like hybrid electric vehicles, storage times for liquid fuels have increased. Additionally, the complexity of fuel is increased by the introduction of new alternative components like hydrogenated vegetable oil (HVO), used cooking oil methyl ester (UCOME) or synthetic fuels (X to liquid, XtL, where X can be various carbon sources). Thus, the need to assess correctly and quickly not only the current fuel quality, but also the future behaviour of fuels and their ageing grows more important. Yet, no quick method exists that allows a prediction of ageing behaviour. The test rig presented in this article is an attempt to develop such a method.

1.1 Ageing processes in fuels

Various chemical reactions can happen in fuels during ageing. They range from oxidations to polymerizations and produce a variety of ageing products from aldehydes, ketones and acids to polymers. A good overview over prevalent reactions and previously done research into fuel ageing is presented by Biernat [3] in a review, especially in the subsections by Owczuk [4]. Most of the ageing reactions happen only in the presence of oxygen and are very slow at usual storage conditions. They can be accelerated by influences like temperature, pressure, and catalysts like non-ferrous metal surfaces. Prevention of ageing is usually done using additives, which can stop the peroxide radicals that are essential for most ageing reactions.
Fuel ageing changes some of the fuels properties, ranging from viscosity increase due to polymer formation [5], density increase due to evaporation of volatile components [6], over conductivity changes due to oxygenate formation [7], to turbidity due to water increase and deposit formation [6]. All these effects can be measured and quantified with various methods.

1.2 Fast-ageing methods

Many methods to accelerate ageing exist. All of them use a combination of the accelerating influences like increasing temperature, pressure, contact with non-ferrous metals, irradiation as well as direct contact with oxygen. Of these methods, a lot are standardized, like various methods that measure oxidation stability in some way

Narr Francke Attempto Verlag GmbH + Co. KG

[8–15]. Most of these methods are designed to measure one comparable parameter that can be used to assess the current stability of a fuel. Some measure the sediments formed under defined conditions, some measure oxygen uptake or detect formed oxygenated products in some way. Only a few methods have been developed expressly to study the ageing process itself, and to conduct measurements over the ageing time, but some of the norm methods have been adapted to this purpose. Järviste et al. have used a similar method to the Rancimat method (DIN 15751) [16], and the method described in this article is derived from the PetroOxy method (DIN 16901). The difference apart from the reactor volume is that the PetroOxy test is conducted with pure oxygen, not with air as in the BigOxy test.

1.3 Sensors

The ageing reactions happening in fuels cause changes to physical properties which can be measured with suitable sensors. Table 1 shows an overview of the changes that can happen during ageing, and sensor parameters that correlate to these changes.

Table 1: Sensor parameters and their correlation to changes of fuel properties during ageing.

Parameter	Changes in the sample
Water content / relative Humidity	Water from condensation, from air, water formation as a reaction product
Density	Evaporation of volatile components, reactions influencing intermolecular forces
Viscosity	Evaporation of volatile components, changed interactions of molecules due to polymerization and higher polarity
Electrical conductivity	Formation of polar components and ions, water
Permittivity	Increase of polarity through oxidation reactions, changed mobility of molecules due to changes in density
Turbidity	Formation of sediments and emulsions
Infrared	Reactions with oxygen, water

Due to the conditions in the used ageing method (closed reactor, high temperature), several of these possible sensor parameters cannot be used in the setup. The ones that are left include electrical conductivity and permittivity, as well as viscosity.

2. Methods

2.1 BigOxy method

The BigOxy test method is derived from the PetroOxy method. Figure 1 shows a flow diagram of the test rig. Four reactors are filled with 500 mL each of the samples and are then closed airtight. A pressure of air is applied (4.8 bar for middle distillates and heavy fuel oil, 3 bar for gasoline) and the pressure checked for ten minutes. If no changes occur, the test rig is then heated up to the desired test temperature (standard parameter is 105 °C) and the test runs over a predefined length of time (usually between 8 and 72 h). At the end of the run time, the reactors are cooled down and the samples can then be taken out. Further analysis with laboratory methods is possible, as well as deposit formation tests and many more.

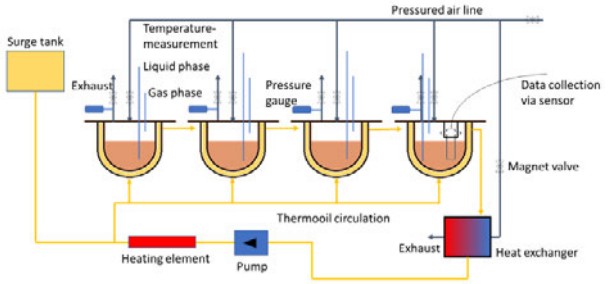

Figure 1: Flow diagram of the BigOxy test rig.

2.2 Analytics

Various analytical methods have been applied to samples that were aged using the method described in section 2.1. The results discussed in this paper have usually been obtained using norm methods, which will not be described here in detail, but referenced in Table 2 so they can be looked up.

Table 2: Short description of laboratory methods for fuel analysis and the corresponding norm numbers.

Method name and number	Short description
PetroOxy DIN 16091	Measures oxidation stability using increased pressure and temperature, determines time scale of oxygen uptake
Rancimat DIN EN 15751	Measures oxidation stability using increased temperature and oxygen flow, measures the formation of volatile conductive components

Narr Francke Attempto Verlag GmbH + Co. KG

Acid number DIN EN 14104	Measures the total acid amount in a sample, using a titration
Total contamination DIN 12662:1998	Measures the amount of sediment in a sample by filtration
Water content DIN EN ISO 12937	Measures the water content using a titration method developed by Karl Fischer
Density DIN EN ISO 12185	Density is measured using the vibration of a u-tube. The frequency relates to the weight, and for a known volume, the density of the sample.

2.3 Long term storage

To compare the ageing processes in the test rig to ageing in more realistic storage conditions, long term storage tests have been conducted. For this, fuel samples were filled in bottles with 1 L or 2 L content, and a copper spiral was added as a catalyst for ageing reactions. In addition to that, the bottles were stored open to allow contact with oxygen and humidity in the air. The copper spiral is identical to the ones used in the thermal stability test according to DIN 51371. Every one to three months, depending on the project, bottles were taken out and the fuel analysed thoroughly as described in 2.2.

3. Results

3.1 Correlations between test rig and long term storage

In a completed previous research project, a correlation between the analysis data from the BigOxy test rig and long term storage data for conventional and some alternative heating oil was found [17].
Various test parameters were tried with temperatures ranging from 90 °C to 140 °C before it was found that the best results could be gained at 105 °C. Higher temperatures accelerated ageing speed so much that a good differentiation became difficult, and the reproducibility suffered due to the long time it takes for the whole sample to reach the desired temperature. Lower temperatures increased the necessary time the sample had to spend in the test rig, so the 105 °C were a good compromise and showed the best correlation to long term storage.
To achieve a good comparison between test rig data and long term data, a stability parameter was calculated from multiple analysis results and the fuels were then ordered according to their stability parameters. This method achieved almost the same order for the long term storage as it did for the test rig, meaning the differentiation according to stability is comparable.
Another result from the tests was the calculation of time lapse factors. To do this, criteria that defined the fuels as 'aged' were empirically determined or taken from the norm (20 min in PetroOxy, 20 h in Rancimat, 200 mg/kg water content, 0,25 mg kOH/g acid number, and 24 mg/kg total contamination). The analytical data over time was then fitted to a linear function to determine the time at which these limits were reached. Since this was done for both the long term storage data as well as the test rig data, the time lapse factor between the two could be determined. Since the linear function is only a very basic approximation of the analytical data over time, a newer project is currently running to improve on this model. The time lapse factors calculated with this method differed between the various tested fuels and ranged from about 60 for 20 % rape seed methyl ester in heating oil to 250 for pure heating oil. A time lapse factor of 250 means that one hour of ageing in the test rig equals 250 h in real time, so a typical run time of 16 hours equals about five and a half months.

3.2 Sensor data in the test rig

One critical point of the previously described evaluation was the low number of data points over time. While the number was seven for the long term storage, there were only four data points in case of the test rig data. To solve this problem, a sensor has been integrated in the test rig to measure continuously during the ageing process, and in shorter intervals during the long term storage. The inclusion in the test rig necessitated several constructional changes, the reactor top had to be First tests with the sensor in the BigOxy have yielded continuous data, but due to the very temperature sensitive nature, the full evaluation is still pending. Overall results were that a slight increase of viscosity could be observed during the 64 h runtime in the reactor, and a slight decrease of the conductivity was measured over time. The data from the long term storage shows no certain trends yet.

3.3 Pressure curves of different fuels and alternative components

The BigOxy method can be used to age different alternative components, both gasoline and middle distillates as well as heavy fuel oils. The pressure curves differ slightly, depending on the oxygen uptake of the sample. For hydrogenated vegetable fuel (HVO), fatty acid methyl esters (FAME), paraffinic synthetic fuels (Fischer Tropsch products, FT) and conventional fuels, this works very well. It was found however that the use of oxygenated methyl ethers (OME) poses problems, because under the applied conditions, it can decompose into methanol and formaldehyde. In addition to these components being toxic, the resulting pressure increase is also undesirable since the reactors are only tested up to 10 bar. All other components show typical pressure curves, which increase in the beginning due to the temperature increase, and later start decreasing due to oxygen uptake. The maximum pressure achieved during the test run and the time of the oxygen uptake depend on the sample properties.

Narr Francke Attempto Verlag GmbH + Co. KG

In Figure 2, several different pressure curves are shown. The differences between the samples originate both from the composition and the fuel stability. It must be noted that the pressure can only fall by about 20 % since that is the oxygen content of air. Any additional pressure drop stems either from dissolved other gases, or slight leaking of the reactor. The presented fuels include heating oil and diesel, octanol as a pure substance and as a mixture with diesel, and ethanol and butanol in a synthetic methanol-to-gasoline fuel (MtG).

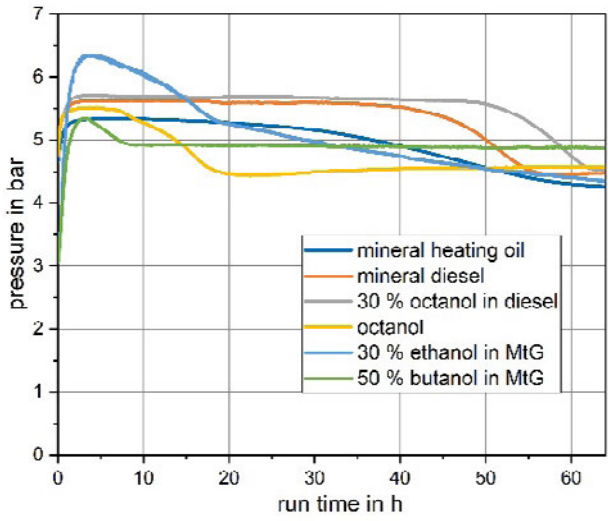

Figure 2: Pressure curves over a run time of 64 h for different fuels and blends.

3.4 Conclusion

The developed method allows a good approximation of real ageing behaviour, and thus can be used to investigate effects of ageing in various fuel components. Additive reactions in aged fuels can be examined, and deposit formation observed. This is especially interesting regarding the many new candidates for alternative fuels, as they can be tested in a short time, and especially mixing and ageing interactions can be observed. The method will be used in further research projects to examine new fuel components and investigate ageing behaviour of mixtures. Additive testing is also a possible application, especially the effectiveness testing for stability additives can be done using the test rig.

References

[1] W. W. Evans, Oil composition, etc.: Patentschrift (1927), US1752946A. https://patentimages.storage.googleapis.com/57/08/94/bd0a47b4e05835/US1752946.pdf.

[2] S. K. Panda, J. T. Andersson, and W. Schrader, Angewandte Chemie (International ed. in English) 48, 10 (2009).

[3] Storage Stability of Fuels, Ed. by K. Biernat (InTechOpen, 2015).

[4] M. Owczuk and K. Kołodziejczyk, in Storage Stability of Fuels, Ed. by K. Biernat (InTechOpen, 2015).

[5] A. Agoston, C. Ötsch, and B. Jakoby, Sensors and Actuators A: Physical 121, 2 (2005).

[6] K. Brendel and A. Duchowny, DGMK Forschungsbericht, Vol. 778: Untersuchung zur Vermeidung von höhermolekularen Alterungsprodukten in Mitteldestillaten mit alternativen Komponenten unter anwendungstechnischen Randbedingungen (DGMK, Hamburg, 2020).

[7] S.-I. Moon, K.-K. Paek, Y.-H. Lee, J.-K. Kim, S.-W. Kim, and B.-K. Ju, Electrochemical and Solid-State Letters 9, 8 (2006).

[8] ASTM, Standard Test Method for Oxidation Stability of Distillate Fuel Oil (Accelerated Method) (2014), ASTM D2274.

[9] ASTM, Assessing Middle Distillate Fuel Storage Stability by Oxygen Overpressure (2015), ASTM 5304.

[10] ASTM, Standard Test Method for Middle Distillate Fuel Storage Stability at 43 °C (2016), ASTM 4625 - 16.

[11] ASTM, Oxidation Stability of Aviation Fuels (Potential Residue Method) (2018), ASTM D873 - 12.

[12] DIN EN 16091, Flüssige Mineralölerzeugnisse – Mitteldestillat- und Fettsäuremethylesterkraftstoffe und Mischungen – Bestimmung der Oxidationsstabilität mit beschleunigtem Verfahren und kleiner Probenmenge ICS 75.160.20.

[13] DIN 15751, Kraftstoffe für Kraftfahrzeuge – Kraftstoff Fettsäuremethylester (FAME) und Mischungen mit Dieselkraftstoff – Bestimmung der Oxidationsstabilität (beschleunigtes Oxidationsverfahren) ICS 75.160.20.

[14] DIN 51471, Flüssige Mineralölerzeugnisse – Bestimmung der Lagerstabilität von Heizöl EL ICS 75.160.20.

[15] DIN 51371, Flüssige Brennstoffe – Bestimmung der thermischen Stabilität von Heizöl EL ICS 75.160.20.

[16] R. T. Järviste, R. T. Muoni, J. H. Soone, H. J. Riisalu, and A. L. Zaidentsal', Soil Fuel Chem. 42, 2 (2008).

[17] W. Koch, S. Eiden, S. Feldhoff, and D. Diarra, DGMK-Forschungsbericht, Vol. 763: Entwicklung einer neuen Prüfmethode zur Bewertung der Stabilität von Heizölen mit biogenen Anteilen: Development of a new stability test method for bio heating oils (DGMK Deutsche Wissenschaftliche Gesellschaft für Erdöl Erdgas und Kohle e.V, Hamburg, 2017) [ger].

Narr Francke Attempto Verlag GmbH + Co. KG

TAE Technische Akademie Esslingen
Ihr Partner für Weiterbildung

TOP ANBIETER FÜR WEITERBILDUNG 2021
FOCUS WEITERBILDUNGS-ANBIETER IM VERGLEICH
FOCUS-BUSINESS 03 | 2020

TRIBOLOGIE – REIBUNG, VERSCHLEISS UND SCHMIERUNG

Besuchen Sie unsere Seminare, Lehrgänge und Fachtagungen.

Bis zu 70 % Förderung möglich!

ESF Chancen fördern – Europäischer Sozialfonds in Baden-Württemberg
EUROPÄISCHE UNION

Ein Großteil unserer Seminare wird unterstützt durch das Ministerium für Wirtschaft, Arbeit und Tourismus Baden-Württemberg aus Mitteln des Europäischen Sozialfonds. Profitieren Sie von der ESF-Fachkursförderung und sichern Sie sich bis zu 70 % Zuschuss auf Ihre Teilnahmegebühr. Alle Infos zur Förderfähigkeit unter **www.tae.de/foerdermoeglichkeiten**

SEMINARE, LEHRGÄNGE, FACHTAGUNGEN

- Reibung, Verschleiß und Schmierung
- Schmierstoffe und Betriebsflüssigkeit
- Schmierungstechnik
- Geschmierte Maschinenelemente

Infos und Anmeldung: www.tae.de/go/tribologie

Narr Francke Attempto Verlag GmbH + Co. KG

Appendix

Scientific-Technical Board – International Colloquium Fuels

The programme committee for the International Colloquium Fuels is composed of recognised experts from research and development, industry and practice. Its tasks include formulating the objectives and determining the main topics of the colloquium, reviewing and selecting the submitted lecture proposals for the conference programme and providing expert advice to the organiser.

Chairman

Dipl.-Ing. J. N. Schubert
OMV Downstream GmbH, Schwechat, Austria

Members

Dr.-Ing. J. Beeckmann
RWTH Aachen University, Germany

Dr. T. Garbe
Volkswagen Aktiengesellschaft, Wolfsburg, Germany

Dr. G. Jungmeier
JOANNEUM RESEARCH Forschungsgesellschaft mbH, Graz, Austria

Dr.-Ing. H. Krämer
Audi AG, Ingolstadt, Germany

Dr.-Ing. L. Menger
BMW Group, München, Germany

Dr. O. Toedter
KIT (IFKM) Karlsruhe, Germany

Dr. J. Ullmann
Robert Bosch GmbH, Stuttgart, Germany

Narr Francke Attempto Verlag GmbH + Co. KG

Index of Authors

Narr Francke Attempto Verlag GmbH + Co. KG

With the signing of the Paris Agreement in December 2015 the United Nations explained their willingness to limit the GHG Emissions and contribute to the measures against the global warming effect. In 2019 the European Commission proposed the Green Deal and as a consequence the target to be climate neutral in 2050. In consequence the fossil based energy system has to transform into a climate-neutral energy system with renewable and sustainable energy carriers. Research on and development of alternative fuels and new production processes are ongoing to provide the technical solution. Political actions are needed to provide the economic framework for the introduction of such alternative fuel solutions.

The fulfilment of the European CO2 reduction targets until 2050 needs realistic technical solutions including backwards compatible approaches for existing vehicle fleets. An economic and sustainable development towards climate neutral mobility requires a holistic view based on life cycle assessments for the different mobility approaches including the economic impacts as well as financing options.

A synergetic discussion of solutions for future fuels and powertrain technologies is needed to develop an economic pathway to a sustainable and affordable mobility of tomorrow.

The challenging goal for mobility can only be achieved through an international cooperation of universities, the automobile industry, energy producers, the oil industry and the legislative bodies of the member states.

The international colloquium aims to contribute to the development of a climate-neutral mobility by exchanging views on and discussing all aspects connected with the "powertrain/fuel/environment" system, including the necessary political regulations.

Main Topics

- Perspectives on Renewable Fuels
- Renewable Fuels Production
- Fuels Quality Research
- Application of Renewable Fuels

The present volume contains the contributions submitted in advance for the lectures and shows the potentials and challenges of CO_2-reduced mobility.

Target Group

- Specialists and executives in
- OEM's
- Tier 1
- Companies in the mineral oil industry
- Engineering firms
- Technology companies
- Research facilities
- Municipalities
- Start-ups in the field of future mobility

TAE Technische Akademie Esslingen
Ihr Partner für Weiterbildung
www.tae.de

expert

ISBN 978-3-8169-3539-1
9 783816 935391

Narr Francke Attempto Verlag GmbH + Co. KG